

USBM Grant No. G133023
THRU-THE-EARTH ELECTROMAGNETICS WORKSHOP

Richard G. Geyer

USBM CONTRACT FINAL REPORT
(Contract/Grant No. G133023)

Date: December 31, 1973

DEPARTMENT OF THE INTERIOR
BUREAU OF MINES
WASHINGTON, D. C.

DISCLAIMER NOTICE

The views and conclusions contained in this document are those of the author(s) and should not be interpreted as necessarily representing the official policies of the Interior Department's Bureau of Mines or the U. S. Government.

PROCEEDINGS OF
THRU-THE-EARTH ELECTROMAGNETICS WORKSHOP

August 15 - 17, 1973

Colorado School of Mines

Sponsored By

United States Bureau of Mines

Edited By Richard G. Geyer

FOREWORD

This report was prepared by Richard G. Geyer under USBM Contract/Grant No. G133023. The grant was initiated under the Coal Mine Health and Safety Research Program. It was administered under the technical direction of the Pittsburgh Mining and Safety Research Center with Mr. Howard E. Parkinson acting as the technical project officer. Mr. A. L. Metheney was the contract administrator for the Bureau of Mines.

This report is a summary of the work recently completed as part of this grant during the period April 1, 1973 to December 31, 1973. This report was submitted by the author on December 31, 1973.

Conference Chairman:

Richard G. Geyer

Research Associate, Geophysics
Department, Colorado School of
Mines

Advisory Committee:

James R. Wait

Director, Environmental Research
Laboratories, NOAA; Consultant,
Institute of Telecommunication
Sciences

Howard E. Parkinson

Supervisory Electrical Research
Engineer, Industrial Hazards and
Safety Research Center, U. S.
Bureau of Mines

James Powell

Staff Research Engineer,
Mining Research Center, U. S.
Bureau of Mines

Session Chairmen:

Richard G. Geyer

Research Associate, Geophysics
Department, Colorado School of
Mines

James Powell

Staff Research Engineer,
Mining Research Center, U. S.
Bureau of Mines

David A. Hill

Research Scientist, Institute of
Telecommunication Sciences,
Boulder, Colorado

John Murphy

Supervisory Electrical Research
Engineer, Industrial Hazards
and Safety Research Center,
U. S. Bureau of Mines

James R. Wait

Director, Environmental Research
Laboratories, Boulder, Colorado

Group Chairmen:

Electromagnetic Noise
Environment

John W. Adams, National
Bureau of Standards

Location and Direction-
Finding

Arnie J. Farstad, Westinghouse
Georesearch Laboratory

Uplink and Downlink
Communications

Robert L. Lagace,
Arthur D. Little, Inc.

Operational Communications

Martyn F. Roetter,
Arthur D. Little, Inc.

TABLE OF CONTENTS

	Page
Preface	viii
Objectives and Constraints of Through-the-Earth Electromagnetic Communication Systems Howard E. Parkinson	1
State of Knowledge of Analytical Techniques for Thru-the- Earth Electromagnetic Wave Problems Relevant to Mine Rescue James R. Wait	9
Electromagnetic Field Solutions for Infinite and Finite Cables for Conducting Half-Space Models -- Both Frequency- and Time-Domain David A. Hill	15
Theory and Experiments Relating to Electromagnetic Fields of Buried Sources with Consequences to Communication and Location Richard G. Geyer	20
Electromagnetic Direction Finding Experiments for Location of Trapped Miners R. G. Olsen and A. J. Farstad	34
Theory of Propagation of UHF Radio Waves in Coal Mine Tunnels Alfred G. Emslie, Robert L. Lagace, and Peter F. Strong	38
Guided Propagation of Radio Waves P. Delogne, L. Deryck, and R. Liegeois	49
Radio Propagation Measurements in Coal Mines at UHF and VLF Arthur E. Goddard	54
Performance of Manpack Electromagnetic Location Equipment in Trapped Miner Location Tests A. J. Farstad	62

	Page
Fields of a Magnetic Dipole Excited Buried Cylinder Allen Q. Howard, Jr.	73
The Electromagnetic Response of a Buried Sphere for Buried Dipole Excitation D. A. Hill and J. R. Wait	81
The Perturbation of Alternating Electromagnetic Fields by Three-Dimensional Bodies F. W. Jones	86
A Discussion on the Three-Dimensional Boundary Value Problem for Electromagnetic Fields David Rankin	92
Reply to: "A Discussion on the Three-Dimensional Boundary Value Problem for Electromagnetic Fields" (David Rankin) F. W. Jones	95
Use of Zonal Harmonic Series for Obtaining Numerical Solutions to Electromagnetic Boundary Value Problems Richard L. Lewis	98
Application of Lebedev-Kontorovich Transforms for Describing Electromagnetic Wave Propagation in an Inhomogeneous Earth Richard G. Geyer	104
Subsurface Applications of Periodic Electromagnetic Video Pulse Signals David L. Moffatt	112
Electromagnetic Survey Method Applicable to Underground Quarries R. Gabillard, J. P. Dubus, F. Cherpereel	121
Feasibility of a Radio Communication in Mine Galleries by Means of a Coaxial Cable Having a High Coupling Impedance J. Fontaine, B. Demoulin, P. Degauque, and R. Gabillard	130

	Page
Electromagnetic Transmission and Detection at Deep Depths D. B. Starkey	140
Admittance and Effective Height of Buried Antennas Giorgio Franceschetti	149
Spectrum Measurements of Electromagnetic Noise in Coal Mines W. D. Bensema and J. W. Adams	151
Amplitude Statistics of Electromagnetic Noise in Coal Mines M. Kanda and J. W. Adams	156
Design of an ELF Noise Processor J. E. Evans and A. S. Griffiths	161
Experimental Comparison of Buried and Elevated ELF Transmitting Antennas Peter R. Bannister, Frederick J. Williams, J. Robert Katan, and John R. Ball	162
An Underground Electromagnetic Sounder Experiment Lambert Dolphin, Jr., Robert Bollen, and George Oetzel	168
Summary Report on Electromagnetic Noise Measurement Program John W. Adams	169
Summary Report of Electromagnetic Location Techniques Working Group Arnold J. Farstad	171
Summary Report of Uplink and Downlink Communications Working Group Robert L. Lagace	178
Summary Report of Operational Communications Working Group Martyn F. Roetter	202
List of Attendees	214

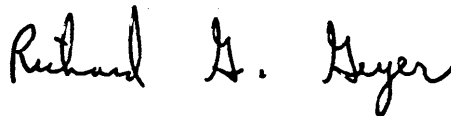
PREFACE

Over the past several years the United States Bureau of Mines has supported various research programs oriented toward the development of basic data applicable to the design of electromagnetic communications systems. Such systems would provide rescue communication links during emergencies. They might also serve as monitors of the mine environment, as well as special communication links for increasing the day-to-day efficiency of the mine operations.

Therefore research programs have been involved with experimental and theoretical investigations of wireless signal transmission through the earth. Experimental studies revolve about the identification of the electrical properties of rocks over coal mines insofar as the propagation of communications signals would depend on such properties, on the ambient electromagnetic noise fields over and in coal mines insofar as such noise would limit the detectability of communications signals, and on the effect of mine structures on the transmission of communications signals. Active theoretical work has consisted of the analysis of a variety of techniques for thru-the-earth communications and of a number of approaches for location of trapped miners. To name but a few techniques, either loops or grounded wire may be used for the subsurface or surface antenna. Each may be oriented in a variety of ways. Each may be excited with an impulsive signal or a continuous-wave signal.

In short, a need arose to assemble individuals who have been active in current research on the topic so that the problem of how information may be conveyed by electromagnetic waves propagating through rock media without the benefit of lines and cables may be better understood. Furthermore, some of the limitations and scope of such schemes needed to be identified.

Thus a "Thru-the-Earth Electromagnetics Workshop" was sponsored by the United States Bureau of Mines. This workshop was held at Colorado School of Mines on August 15-17, 1973. The papers which follow are representative of the topics discussed at that workshop.



Richard G. Geyer, General Workshop Chairman

OBJECTIVES AND CONSTRAINTS OF THROUGH-THE-EARTH ELECTROMAGNETIC COMMUNICATION SYSTEMS

by

Howard E. Parkinson¹

ABSTRACT

In 1969, new coal mine health and safety legislation was enacted in the United States. As a result of this legislation, the Department of Interior, Bureau of Mines has carried out communications research aimed at developing whole mine communications for increased safety and efficient operation. The research has advanced and many promising results are now being demonstrated to the mining industry. However, there remains a challenge to further improve wireless communications within the mine workings, and through the overburden above the workings. The objectives for future research and development will be discussed, together with the physical and operational constraints that new mine communication systems must face.

INTRODUCTION

The involvement of the U.S. Bureau of Mines, Department of the Interior, with electromagnetic (EM) communications dates back fifty years. Recently, as a result of legislation enacted by the Federal Government in 1969 concerning Coal Mine Health and Safety, the Bureau has entered into a new and promising era of communications research. As part of this effort, the Bureau is endeavoring to exploit the promise of through-the-earth communication by means of EM fields.

The program of the Bureau of Mines is unique. This program is a cooperative effort under the direction of the Bureau. Through contracts and grants, the Bureau purchases the technical efforts of universities, private communications companies – both manufacturers and consultants – and other governmental agencies, and coordinates the participants into a team. Through cooperative cost-sharing agreements with mine operators, research is performed in the working mines, where extensive demonstrations are made of new concepts under actual operating conditions in the mine.

The Bureau's philosophy is to develop day-to-day-operational communications systems that can adequately meet communications requirements for making mining safer on a

1. Supervisory Electrical Research Engineer, Industrial Hazards and Communications, Pittsburgh Mining and Safety Research Center, U.S. Bureau of Mines.

day-to-day basis, improving the efficiency of mining operations, and remaining fully operational and ready to provide essential communication needs in an emergency.

THE OBJECTIVES OF MINE COMMUNICATIONS SYSTEMS

Fundamentally, the Bureau has three objectives for communications systems:

- (1) To be a silent partner monitoring the mines, watching over the environment to ensure that the mine is providing a healthy and safe working environment;
- (2) To provide reliable rescue communication links during emergencies; and
- (3) To ensure efficient day-to-day mine operations.

The communications systems designed to achieve these objectives must satisfy the following requirements:

- (1) The silent partner monitoring the mine environment must be highly reliable, and is required to work even when there is a loss of power and a loss of wire channels to transmit signals;
- (2) The rescue communications system must be able to function under the most adverse conditions, and be able to:
 - Allow live miners to notify the surface of their presence in the mine;
 - Supply sufficient data to determine the position of the live miners;
 - Provide communication with the live miners to assist in their rescue.
- (3) The day-to-day operational communication system must be able to report automatically the status of major factors of production; additionally, communication must be extended from fixed locations and vehicles to roving miners, so that a miner working on the face can trouble-shoot equipment directly with his surface supervisor without having to leave the immediate work site at the face.

CONSTRAINTS OF THE MINE ENVIRONMENT

The environment for communications systems in a mine is a severe one, both under normal operating conditions and in emergency situations. This environment, which includes the miner himself as well as his surroundings, poses several major constraints and/or specifications to which the communications equipment must conform.

General Environmental Characteristics

(1) Through-the-earth EM communications systems must operate in the face of the conductivity and depth of the earth overburden. We have chosen values of 10^{-2} mhos per meter and 1,000 feet, respectively, as nominal design values for these parameters. The vast majority of U.S. mines fall within these limits. While higher values do exist, these are difficult to cope with while remaining within reasonable limitations of power, weight, and size for the communications equipment.

(2) The effectiveness of communication is a function of the signal-to-noise ratio. Although we have not accurately determined what the limits on usable signal-to-noise ratio can be, these limits bind us in both the operational and emergency modes. During normal operations, the most adverse noise that we have experienced to date in a mine has been in an all DC mine using 600 volt haulage and face equipment. During emergencies, through-the-earth emergency communications must be received in the face of ambient surface noise of both man-made and natural origin. Examples of performance estimates based on early noise data are shown in Figures 1-3.

Emergency Environmental Characteristics

(3) During a mine disaster tremendous flame pressure fronts are often experienced. The communications gear must be rugged enough to remain workable despite the stresses to which it is subjected. For example, the Bureau has developed special equipment that has endured pressures in excess of 25 psi at temperatures of greater than $1,800^{\circ}\text{F}$ for 30 seconds.

(4) During an emergency the mine must be assumed to be gassy, and this imposes severe intrinsic safety restrictions² on the communications equipment. There are three major restrictions to consider:

- (a) The minimum ignition current for a particular value of capacitance in the output of the communications gear;
- (b) The minimum ignition current for a particular value of inductance in the communications gear;
- (c) The minimum ignition current at the voltage being impressed on the circuit at a particular instant.

2. R.J. Redding, "Intrinsic Safety, The Safe Use of Electronics in Hazardous Locations, McGraw-Hill, London, 1971.

Characteristics of a Miner

(5) As a source of power for the communications equipment we have placed strong emphasis on the miner's cap lamp battery, and what we call the surplus energy, the energy available after an 8-hour shift, as shown in Figure 4. The cap lamp consumes 1-1.2 amperes, and the cap lamp cord is designed for this low current. Excessive loss would occur if we were to draw five to six times that current, as might be required by some types of emergency EM transmitter. Critical design constraints are therefore placed on the selection of components used in EM transmitters, and receivers, as well as circuit configurations, to enable the maximum magnetic moment to be developed in the most efficient manner for the desired period of operation.

(6) All equipment must be practical for day-to-day operational use. This will ensure that the miners know how to operate the equipment, and that the equipment is in working order should an emergency develop.

(7) The weight limitations chart (Figure 5) shows the weight of the items now carried by miners. We wish to limit the communications gear carried by the miner to no more than a 5% increase in the weight of the items that he now carries. The section foreman in particular is a key individual in this respect.

(8) The cost of the communications gear must, of course, remain within reasonable limits. The cost chart (Figure 6) shows the selling prices of various equipment often carried by miners. We have estimated what we think should be the cost of simple special communications gear; namely, about \$65 for a CW transmitter for locating trapped miners, and about \$130 for a call alert/emergency voice receiver such as that shown in Figure 7.

CONCLUDING REMARKS

We have had remarkable success with many of our communications experiments; however, our approaches still need to be refined. You will be hearing about many of these experiments, both with regard to EM propagation and EM noise measurements. This is a workshop seminar. Its output is anticipated to be at least two position papers that will summarize the present state of the Bureau of Mines through-the-earth wireless communications program and progress as you see it, and then define a short- and long-term research effort that you as researchers and equipment developers can participate in to improve these wireless communications capabilities. This definition of research efforts should include estimates of what the dollar cost might be as well as the time necessary to complete each of the suggested projects.

We are indeed grateful for the efforts of each participant and we sincerely hope this seminar will be beneficial to you, as well as to us. We hope that you will go away with a clearer vision of our needs, and that the Bureau, through your eyes, will see more clearly what next steps should be taken in our continuing efforts to improve mine health and safety.

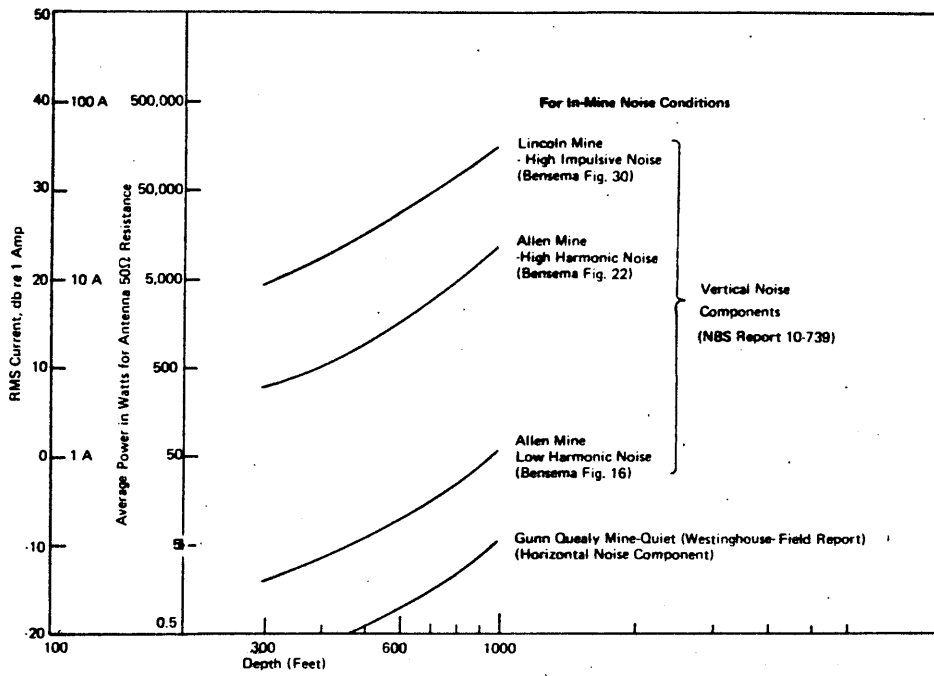


FIGURE 1 DOWNLINK AVERAGE POWER AND RMS ANTENNA CURRENT FOR 12db S/N RATIO OVER THE VOICE BAND 500 - 3000 Hz for $\sigma = 10^{-2}$ mhos/meter and Long Wire Transmit Antenna

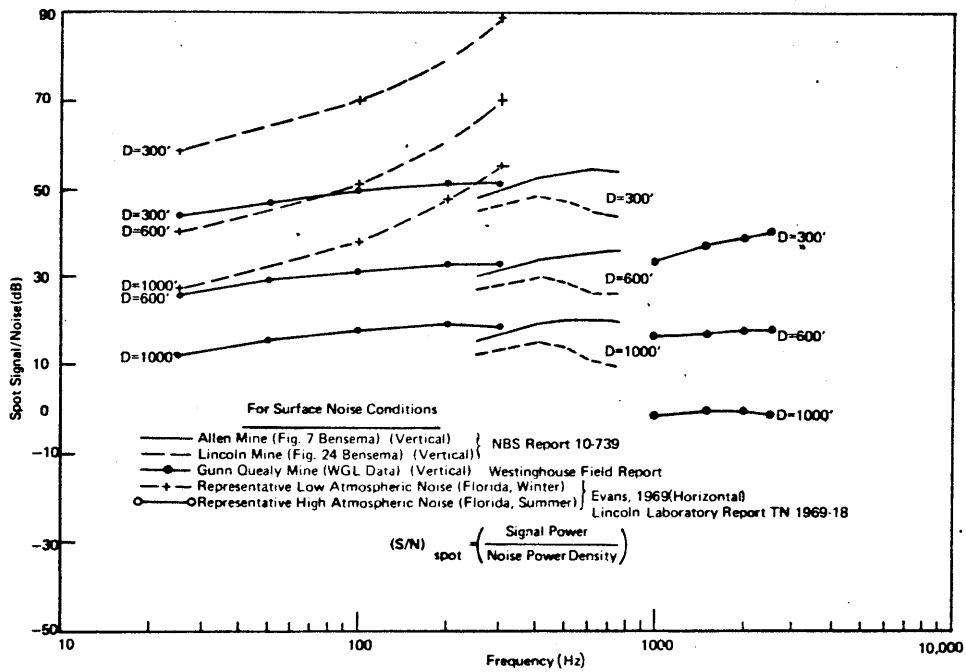


FIGURE 2 UPLINK SIGNAL-TO-NOISE RATIO FOR LOOP TRANSMIT ANTENNA, OVERBURDEN CONDUCTIVITY $\sigma = 10^{-2}$ mho/meter, LOOP MOMENT NAI = 1460 Amp-meter²

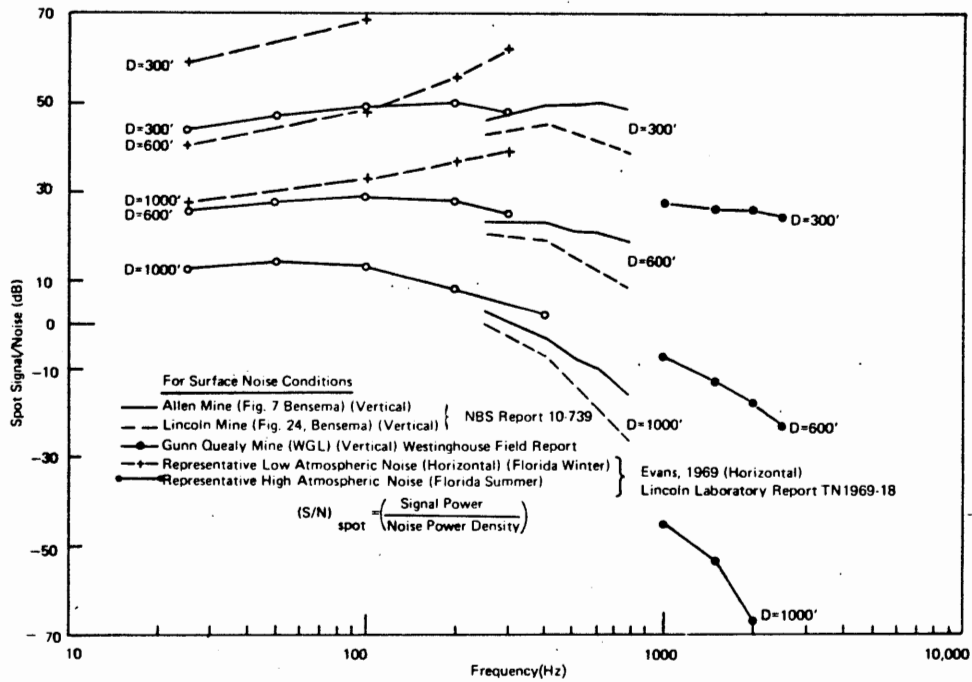


FIGURE 3 UPLINK SIGNAL-TO-NOISE RATIO FOR LOOP TRANSMIT ANTENNA, OVERBURDEN CONDUCTIVITY $\sigma = 10^{-1}$ mho/meter, LOOP MOMENT $NAI = 1460$ Amp-meter²

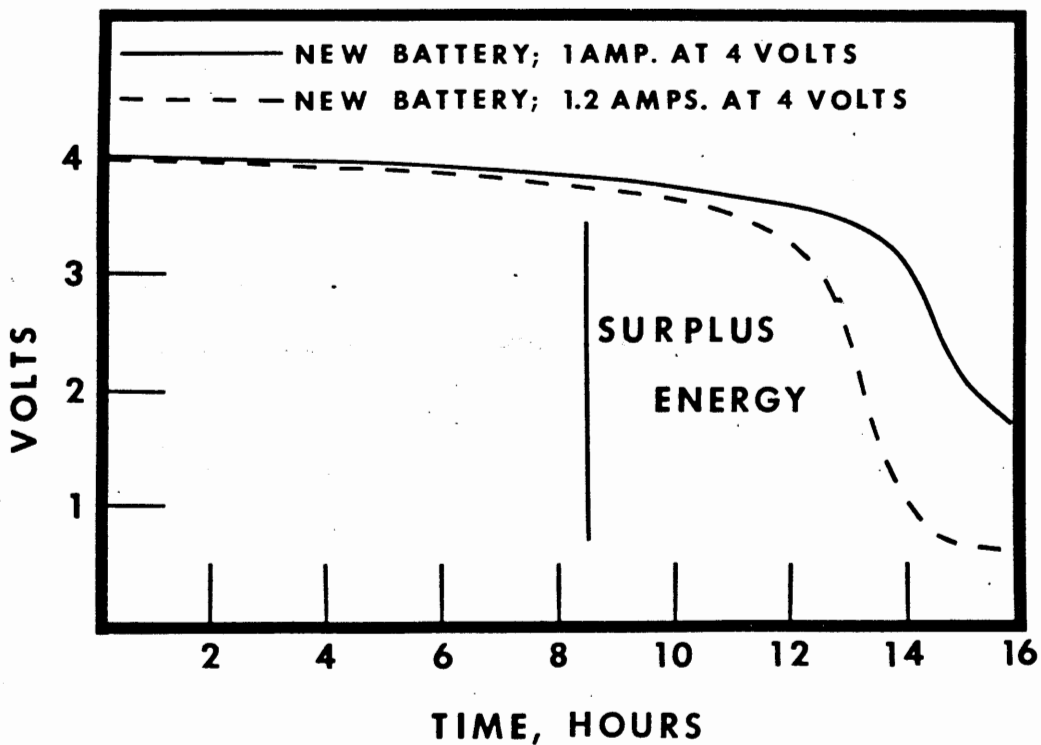


Figure 4 Voltage Curves for Miner's Cap Lamp Battery

Figure 5
TYPICAL EQUIPMENT WEIGHTS

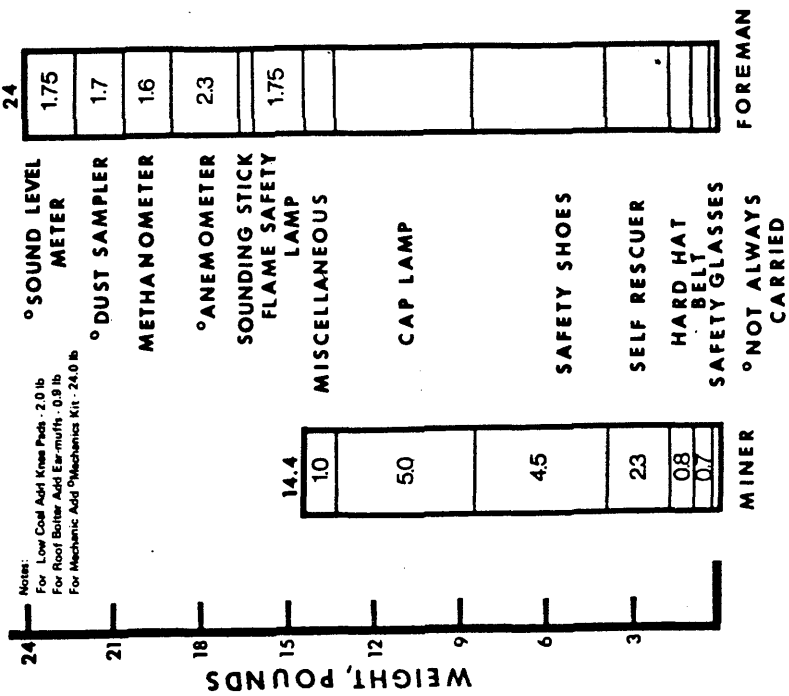


Figure 6
TYPICAL EQUIPMENT COST

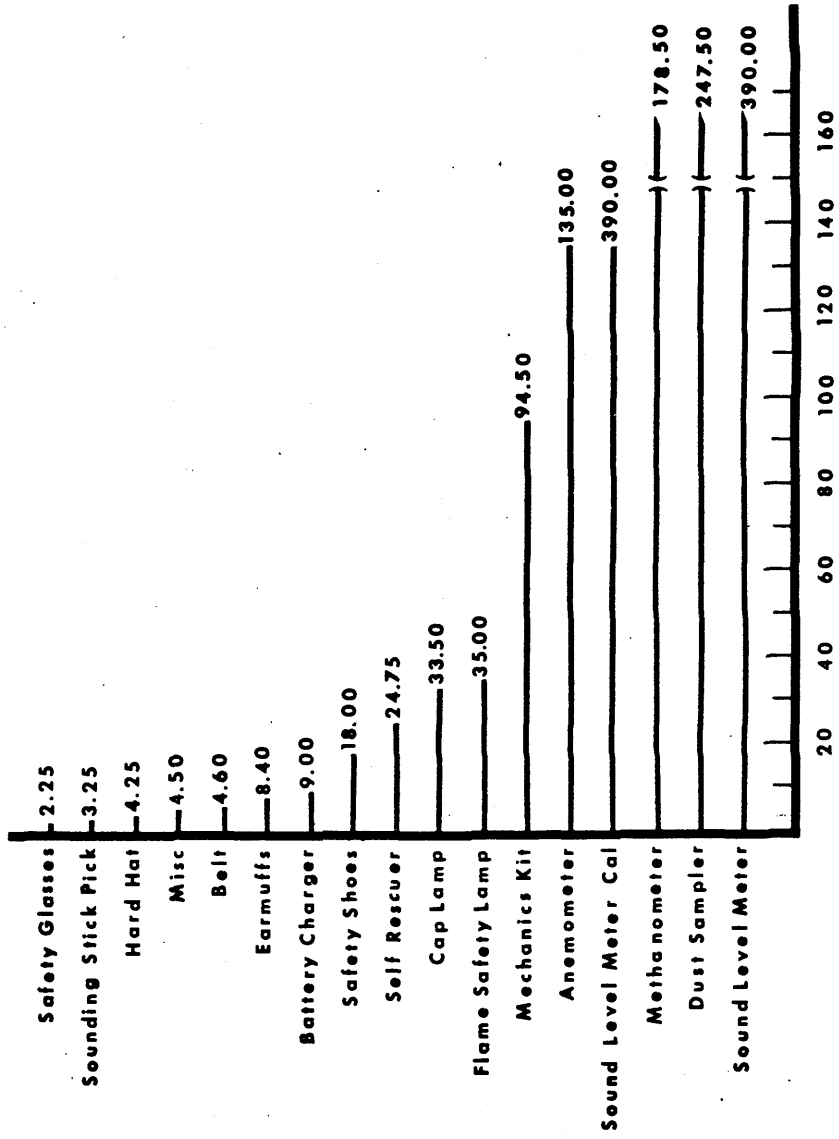
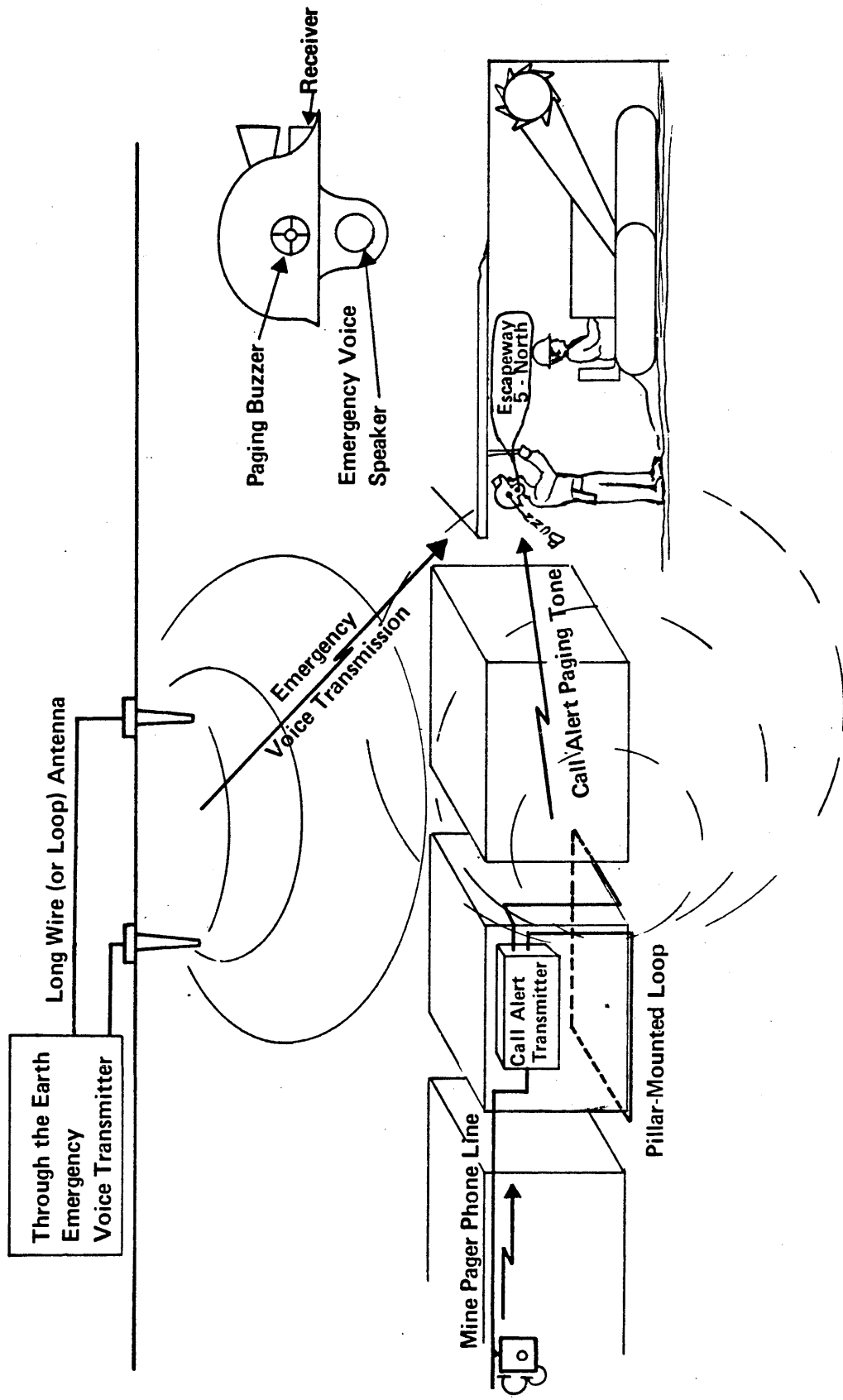


FIGURE 7
OPERATIONAL CALL ALERT/EMERGENCY THROUGH THE EARTH VOICE RECEIVER



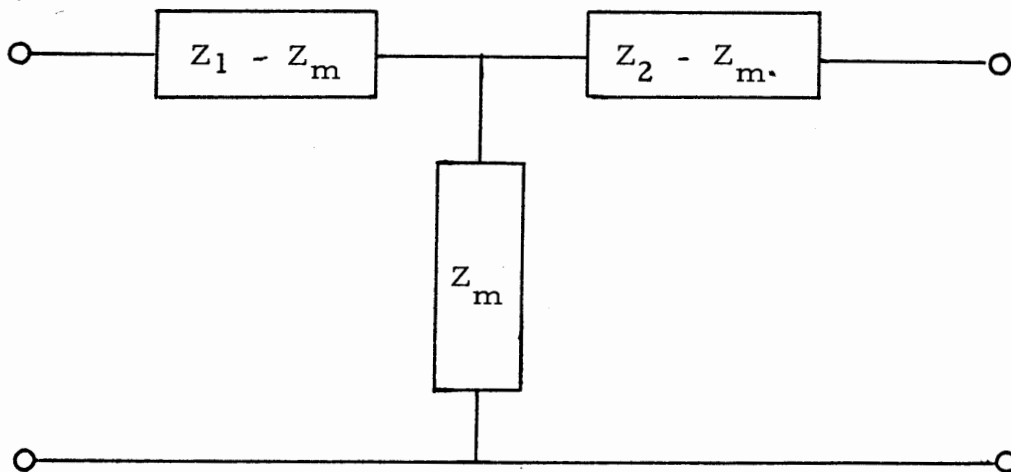
STATE OF KNOWLEDGE OF ANALYTICAL TECHNIQUES
FOR THRU-THE-EARTH ELECTROMAGNETIC WAVE
PROBLEMS RELEVANT TO MINE RESCUE

James R. Wait
U. S. Dept. of Commerce
Office of Telecommunications
Institute for Telecommunication Sciences
Boulder, Colorado 80302

It is the purpose of this paper to review theoretical model concepts in through-the-earth transmission of electromagnetic waves. While the subject is very broad in its defined scope, we will be conscious of the specific applications to mine rescue and emergency telecommunications in coal mine environments.

The plan of the paper is to outline previous theoretical efforts without attempting to attach names or organizations to the specific developments. However, we include a guide to the literature as an appendix. Without pretending to be entirely impartial we include a critique of the limitations of the available analytical models.

As I see it the central problem is to calculate the steady state mutual impedance of a four-terminal network that is the black box characterizing the through-the-earth path. Problems of secondary importance include the determination of the input impedances of the two pairs of terminals and the associated transient responses.



The simple equivalent circuit given tells us a lot about the problem that we are seeking a solution for. The mutual impedance Z_m describes the propagation phenomena involved in the transmission from input (source) to the output (receiver). Z_1 and Z_2 , on the other hand, are the input impedances. Clearly the latter are needed in a total systems study since we have only a finite amount of power available at the source and the receiver must be matched in some sense to the output terminals of the receiving antenna.

Most of the past literature deals with the calculation or merely the derivation of the mutual impedance Z_m for some highly idealized geometrical configuration. For example, the source for an ungrounded loop is a magnetic dipole that is assigned a fixed magnetic moment. In the most extreme case this magnetic dipole is an infinitesimally small loop (of area dA) with a total circulating current of I amps. The moment is IdA ! Now we can still use this concept for a multi turn loop if I is the total azimuthal current and provided the uniform current assumption is valid. Also, of course, we recognize that the finite size of the loop needs to be accounted for in some cases.

In some of the earliest work the fields of this dipole were calculated as if the conduction currents in the earth were negligible. Of course, this is a useful beginning. The next refinement was to correct these magneto-static fields by assuming that we need only multiply them by $\exp(-s/\delta)$ where s was the transmission range and δ was the skin-depth in the earth for the operating frequency being adopted. With the benefit of hindsight we can criticize this correction as being grossly pessimistic for many cases of interest to mine rescue or to communication to a receiving station above or below the source loop.

By using the correct electrodynamic forms of the magnetic dipole fields in an homogeneous conductive medium of infinite extent, we can obtain a better estimate of the relevant value of Z_m . For example, if we are transmitting between two small coaxial loops, we can easily show that

$$Z_m = Z_0(1 + \Gamma s)e^{-\Gamma s}$$

where $\Gamma = (1 + i)\delta^{-1}$ and Z_0 is the static or D.C. coupling limit.

Now usually the transmission takes place from the earth's surface to a buried receiving terminal. Or the converse situation

may exist if we are dealing with up-link communication. In both cases the air-earth interface must be considered. Here we can immediately call attention to the classical formulation of Arnold Sommerfeld that dates back to 1909 in its earliest version. This was used as the basis of much analysis in later years but the interest was mainly for the case where the range exceeded a free-space wavelength. Here we are interested in the near zone where the significant distances are small compared with the wavelength in the air but such distances (i. e., depth or offset) may be comparable with the wavelength in the earth. This is quasi-statics in the vernacular of the current workers. To obtain field estimates we now have to "do" some integrations. Fortunately it was found that identities in Bessel function theory, recognized by mathematicians of the late 19th century were ripe for the picking. Thus some closed form field expressions were obtained and published in the 1950's for a fairly broad class of such problems. Numerical results required the manipulation of modified Bessel functions whose arguments were complex. Fortunately for cases of interest, the phase angles were near $\pi/4$ radians or 45° so that the tabulated Thomson's functions could be used. These are sometimes called the Kelvin functions and denoted ber, bei, kei, etc. (Note William Thomson became Lord Kelvin who was also noted for his work on laying the first Trans-Atlantic cable.)

With the ready availability of high speed computers, the use of intricate closed form field formulas is giving way to direct numerical integration of the Sommerfeld integrals. This is OK provided the programmer has some limiting checks or if he can refer back to some of the earlier work where the more elegant closed-form expressions in terms of special functions are used. Also, as has been shown quite recently, in the treatment of a finite-length source elements the special function representations for the dipole source is a convenient starting point. Otherwise double numerical integration is needed!

As we have indicated above, the air-earth interface problem is treated by regarding the overburden as a homogeneous half-space. A rather straightforward extension is the stratified half-space wherein the intermediate interfaces are plane and parallel to the air-earth interface. Further extensions involve electric dipoles rather than magnetic dipoles. These are appropriate when dealing with grounded electrodes connected by insulated cables. No new basic difficulties are encountered here.

In the class of problems discussed above, all three of the impedance elements Z_m , Z_1 , and Z_2 are determinable. Thus, in principle, a complete determination or prediction of the system performance is possible. This includes down-link and up-link communication efficiency and estimates of source location accuracy for the models assumed.

Traditionally, the source current is assumed to vary harmonically in time. For dealing with transient excitation or in estimating signalling rate we need to understand the time-domain behavior of the system. Formally this is obtained by Fourier or Laplace transform inversion of the preceding transfer functions. In general, this is not a trivial task. However, some rather interesting closed-form results can be obtained if the original spatial wavenumber integration can be deferred until after the Laplace transforms are inverted.

Now that the homogeneous and stratified half-space models have been exhausted it is appropriate to consider more realistic situations. For example, the earth's surface is not always flat. One approach to allow for this situation was to adapt cylindrical and spherical boundaries. In such cases, the local radius of curvature was chosen to (more-or-less) match the local topography. Results of calculations from such models indicated that transmission ranges were not markedly affected but that source location errors could be significant. An even simpler method conceptually was to retain the uniform half-space model but to allow the plane interface to be tilted at such an angle that the local slope of the terrain was matched. Further analytical work on such models is justified since much insight can be gained without excessive numerical effort. Unfortunately, formally exact solutions for such models are strictly limited. One class of boundary that could be treated for line source excitation is a parabolic or hyperbolic interface. The three dimensional version involving dipoles in the presence of a paraboloidal interface is extremely intricate but it may be worth doing also.

One must clearly recognize that the overburden is not a homogeneous slab whether it be bounded by plane or uniformly curved interfaces. Thus, the influence of omni-present inhomogeneities needs to be understood. An extreme case is when metallic tracks and pipes are in the vicinity of the normal transmission path. To treat such configurations, two dimensional models have been used. An example is the line source excited buried cylinder of infinite length. This is not a trivial problem if one considers the interactions

between the buried cylindrical inhomogeneity and the air-earth interface. Two specific analytical techniques have been used to get numerical results for this problem. One is essentially a perturbation procedure that involves successive reflections between the cylinder and the plane interface while the other is a sophisticated integral equation procedure. The results between those methods agree in a common region of validity. The extension to three dimensional versions of these problems is nontrivial. Some progress has been made, however, in using perturbation procedures. An example is the buried sphere in the presence of a surface based dipole source. Some work has also been done on cylinders of finite length where certain assumptions were made about the nature of the axial induced current flow at the ends of the cylinder. Among other things this analysis showed that predictions based on infinite cylinders may be quite misleading.

Within the scope of these analytical techniques, we encompass both active and passive location concepts. In the active method, of course, the unknown source is energized by the to-be-rescued party. On the other hand, in the passive method, the target to be located is typically a loop of wire or a similar configuration. Various geometries, for such problems, have been considered in both the frequency and the time domain.

The foregoing account of theoretical analyses of electromagnetic induction problems is, by no means, claimed to be exhaustive. The selection has been based mainly on work that the author is familiar with.

APPENDIX

A rather brief "guide" to the literature is as follows:

E. D. Sunde - Earth Conduction Effects in Transmission Systems - Dover Publications, New York, 1968 - (Comprehensive review of much of the early work in the 1930-1940 period carried out at Bell Telephone Labs. - includes many useful formulations for mutual impedances of grounded circuits relevant to coupling between power and communication circuits).

D. B. Large, L. Ball, and A. J. Farstad - Radio Transmission from Underground Coal Mines - Theory and measurement trans. IEEE Comm. 21, 194-10204, 1973 (good recent account of Westinghouse's investigations).

R. E. Collin and F. J. Zucker (editors) - Antenna Theory Part II - McGraw-Hill, 1969 - (Chap. 24 by J. R. Wait gives a basic account of the theory for sources in conducting media - also an extensive bibliography is included).

L. L. Vanyan - Electromagnetic Depth Soundings (edited and translated by G. V. Keller) - Plenum Press, 1967 - (An authoritative review of Russian work on electromagnetic induction in the earth).

Also see recent volumes of the Journal Radio Science, IEEE Transactions on Antennas and Propagation, Journal of Applied Physics, and Geophysics.

ELECTROMAGNETIC FIELD SOLUTIONS FOR INFINITE AND
FINITE CABLES FOR CONDUCTING HALF-SPACE MODELS-
BOTH FREQUENCY - AND TIME-DOMAIN*

D. A. Hill

U. S. Department of Commerce
Office of Telecommunications
Institute for Telecommunication Sciences
Boulder, Colorado 80302

Introduction

The fields of an infinite line source in the presence of a conducting half-space have been examined by Wait and Spies (1971). In any real communication link using a current-carrying cable for the transmitting antenna, the cable is of finite length. Here we examine the fields of a finite length cable carrying a constant current in the presence of a homogeneous conducting half-space. The constant current assumption is valid at sufficiently low frequencies when an insulated cable is grounded at the end points (Wait, 1952; Sunde, 1968).

Here we examine both surface and buried cables since both downlink and uplink communication links are of interest. Also, we examine both frequency and time solutions since either CW or pulsed communications may be used. Finally, it is necessary to include both magnetic and electric field solutions since reception could be with either loops or dipoles.

Since the finite cable solution is more complicated than both the infinite line source and the short dipole solutions, we explore under what conditions a cable appears to be either infinitely long or very short. Some special cases, such as the low frequency limit, permit analytical solutions which exhibit the dependence on various parameters, such as cable length, quite clearly.

Frequency Domain Subsurface Fields

The geometry of a line source of length $2l$ located on a conducting half-space with the observer in the half-space is shown in Figure 1. The fields

*The research reported here was supported by the U.S. Bureau of Mines, Pittsburgh Mining and Safety Research Center.

of an incremental source can be derived from x and y components of a Hertz vector which are expressed in terms of Sommerfeld type integrals (Wait, 1961; Banos, 1966). If we assume that the frequency is sufficiently low that displacement currents can be neglected, then the Sommerfeld type integrals can be evaluated in closed form. The electric and magnetic field components then involve partial derivatives in x , y , and z . The details of the procedure are given by Hill and Wait (1973a).

To obtain the fields of the finite cable, the field components of the incremental source must be integrated over the cable length 2ℓ . Some of the field components can be integrated in closed form, but others must be integrated numerically. For an observer at a depth h , field components were computed as a function of ℓ . For an ℓ/h ratio of about 2 or greater, the results agree well with those of the infinite line source. For an ℓ/h ratio less than 0.3, the results approximate those of a short dipole. In the intermediate range, only the finite cable formulation is valid. For the zero frequency limit, the expressions simplify, and all quantities can be expressed in closed form.

Transient Subsurface Fields

Transient waveforms are of interest in pulsed communications. The transient subsurface electric field of an infinite line source at the surface has been examined by Wait (1971). From Maxwell's equations, the time derivative of the magnetic field can be determined. This is the quantity of interest when reception is with a loop antenna. Results have been computed which illustrate pulse attenuation and dispersion as a function of observer position (Hill and Wait, 1973b).

The transient subsurface fields of a finite cable are more complicated, but the frequency domain results of the previous section are useful. The necessary inverse Fourier transform can be done in closed form for some of the field components, but a numerical inversion is required for others. Details of the procedures plus various numerical results are available (Hill and Wait, 1973c), and related transient problems have been treated by Wait (1960).

Surface Fields of a Buried Cable

In the uplink application where the transmitting antenna may be in a coal mine environment, the cable is not necessarily level. Even if it is level,

the earth surface may not be. Consequently, the geometry with a tilted cable shown in Figure 2 was examined. Results simplify if the observer is on the surface ($z = 0$), and the necessary Sommerfeld type integrals can again be integrated in closed form if the quasi-static assumption is made. We are primarily interested in the magnetic field components since reception at the surface is normally with loop antennas.

Since the additional complication of an arbitrary cable angle α has been included, the source integration along the cable must in general be done numerically. The details of the formulation along with various numerical results are available (Hill, 1973). Again there is a wide range where the cable can be approximated by neither the short dipole nor the infinite line source.

REFERENCES

- Banos, A., 1966, Dipole radiation in the presence of a conducting half-space: Oxford, Pergamon Press.
- Hill, D. A., 1973, Electromagnetic surface fields of an inclined buried cable of finite length, Preliminary Report to U. S. Bureau of Mines.
- Hill, D. A., and Wait, J. R., 1973a, Subsurface electromagnetic fields of a grounded cable of finite length, Preliminary Report to U. S. Bureau of Mines.
- Hill, D. A., and Wait, J. R., 1973b, Diffusion of electromagnetic pulses into the earth from a line source, Preliminary Report to U. S. Bureau of Mines.
- Hill, D. A., and Wait, J. R., 1973c, Subsurface electric fields of a grounded cable of finite length for both frequency and time domain, Preliminary Report to U. S. Bureau of Mines.
- Sunde, E. C., 1968, Earth conduction effects in transmission systems: New York, Dover Publications, Chapt. V.
- Wait, J. R., 1952, Electromagnetic fields of current-carrying wires in a conducting medium, Can. J. Phys., v. 30, p. 512-523.

Wait, J.R., 1960, Propagation of electromagnetic pulses in a homogeneous conducting earth, Appl. Sci, Res., B., v. 8, p. 213-253.

Wait, J.R., 1961, The electromagnetic fields of horizontal dipole in the presence of a conducting half-space, Can. J. Phys., v. 39, p. 1017-1028.

Wait, J.R., 1971, Transient excitation of the earth by a line source of current, Proc. IEEE, v. 59, p. 1287-1288.

Wait, J.R. and Spies, K.P., 1971, Subsurface electromagnetic fields of a line source on a conducting half-space, Radio Sci., v. 6, p. 781-786.

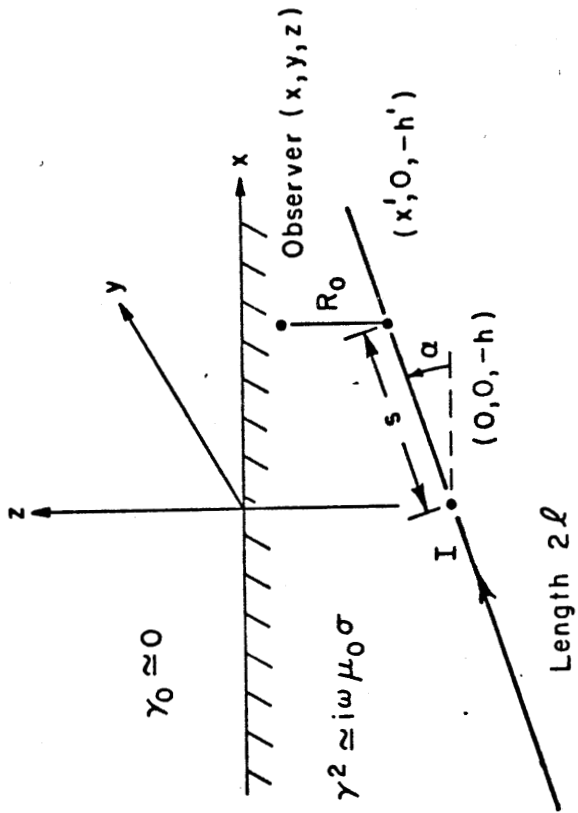


FIGURE 2. Tilted cable in a homogeneous half-space.

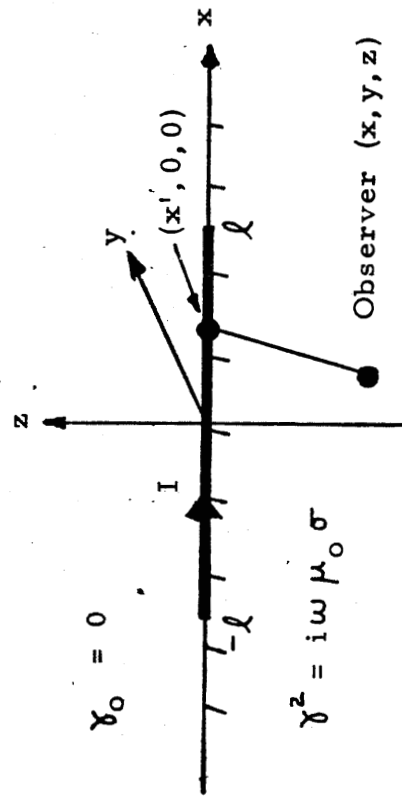


FIGURE 1. Finite length cable on a homogeneous half-space.

THEORY AND EXPERIMENTS RELATING TO ELECTROMAGNETIC FIELDS OF BURIED SOURCES WITH CONSEQUENCES TO COMMUNICATION AND LOCATION*

Richard G. Geyer, Consultant
3973 Baumberger Rd.
Stow, Ohio 44224

Abstract

One aspect of a program to improve the chances of survival following coal mine disasters is the development of a communications system which will allow surviving miners to make their circumstances known to rescue teams. Various communications techniques can be considered, including electromagnetic systems, acoustic systems, and hybrid systems. The electromagnetic and acoustic systems would be independent of existing mine communications systems and set up specifically for use in emergencies. Hybrid systems might use a short emergency link to existing telephone systems in the mine. Many variations are technically possible, and the primary task is in evaluating the relative merits of each, so that the most workable system can be selected.

Introduction

The problems related to the development of an emergency communications system are only partly technical in nature; to a large part, the choice of an optimum system will depend on human engineering factors which are sometimes difficult to formalize. Basically, the problem is that of providing the miner underground with a communications system which he may count on using if other means of communication are interrupted by some mishap or disaster in the mine working.

One important aspect of a communications system is the amount of information that can be transmitted over it per unit time. Generally, for human voice transmission, data rates as great as 3000 bits per second are desired, but rates as low as 1 bit per second are usable for beacon transmission if nothing better is available. A second important property of a communications system is whether it is one-way or two-way. One can conceive of simple communications systems which would allow the buried miner to make his presence known to people on the surface, but which would not allow communication from the surface to underground (e.g., hammer tapping). In an emergency it is of prime importance that up-link communications, from the miner to the surface, be established first so that rescue teams may

*The research reported here was supported by the U.S. Bureau of Mines, Pittsburgh Mining and Safety Research Center.

know if there is anyone alive underground and where they may be. However, it is also important to have a down-link so that information can be passed to the buried miner. Such information might advise him as to the wisest course of action to ensure survival, or would assure him that rescue attempts were proceeding, and so, prevent him from taking unwise actions on his own. Of particular interest is the possibility that the up-link and the down-link would not need to be symmetrical with respect to data rate. It would be quite reasonable to use a low-data-rate up-link system if a high-data-rate down-link system were available. In this way, specific questions along with instructions for a simply coded reply could be transmitted downward.

In order to design an optimum electromagnetic communications system coordinating both technical requirements and human engineering, it becomes necessary to know a variety of design parameters which may be grouped into three classes as follows:

- (1) the electrical properties of the rock overlying mine workings, which determine the relationship between the amount of energy or power applied to the transmitter and the strength of the signal as it propagates through the ground
- (2) the ambient background electromagnetic noise levels at receiver locations, which determine the minimum level of signal strength that can be recognized
- (3) the effect of mine workings and structures on the behavior of the communications signal

To some extent, the above design parameters may be unique for every mine so that for ultimate optimization of emergency communications systems, it would be necessary to have this parameter information for every drift of every mine working. This may be feasible in the future if conductorless communications systems are used for routine mine communications, but it is probably not feasible for an emergency system. Rather, we must settle for near-optimization based on the idea that similar mines in similar geological settings will be characterized by narrow ranges for design parameters, and that these ranges may be determined with reasonable statistical reliability by making measurements only over selected mines.

Electrical Properties Studies

The electrical properties of the earth affect signal strength in a way which is determined by the wavenumber for the medium or

media through which propagation takes place, the wavenumber being defined as

$$\delta = (2\pi i \mu \sigma f - 4\pi^2 \mu \epsilon f^2)^{\frac{1}{2}}$$

where f is the frequency used, μ is the magnetic permeability of the medium, σ is the electrical conductivity, and ϵ is the dielectric constant. Only one of these quantities, the frequency, is a design parameter. In order to specify values for the wavenumber in theoretical studies, we need values for the other three quantities, possibly as a function of frequency, if any of the factors should be frequency dependent.

Thus, knowledge of the electrical properties of the geologic section overlying a mine working is important for ensuring the best possible transmitter-receiver electromagnetic coupling for either emergency or routine communication purposes.

Both galvanic and induction surface-based techniques for measuring the electrical properties of the rock sections overlying a number of coal mine workings in various mining provinces were used and the results have been reported (Geyer, 1971b; Geyer, 1972b). A typical resistivity section observed at the Montour No. 4 Mine, Pa. is shown in Figure 1.

Ambient Electromagnetic Noise Environment Studies

Studies of ambient electromagnetic noise statistics are complementary to investigations of the overburden electrical transmission properties and are necessary for proper design of any subsurface-surface electromagnetic communications system. Ambient electromagnetic noise levels from 20 Hz to 10 kHz have been characterized in a number of mining provinces as a function of time of day by amplitude histograms (Geyer, 1971b).

In so doing, the signal from either an electric field sensor or magnetic field sensor is first passed through a filter which strongly rejects below some lower frequency limit and above some upper frequency limit. Then, within these frequency bands, the number of times ambient noise events occur which exceed specified levels is determined. An example of noise level histograms obtained with an electric-field sensor is shown in Figure 2, with the time of day noted for each curve. The advantage of this approach is that it provides information on the design of a high-sensitivity receiver

system not readily available in the more conventional spectral approach. For example, optimum noise rejection could be incorporated into an uplink receiver system by setting thresholds for signal detection just above the median or maximum percent noise level.

Thus, the noise amplitude density functions presented (Geyer, 1971b) may be used in conjunction with measured resistivity data to design and implement a practical operating beacon electromagnetic communications system in which an adequate source strength is determined which will yield a specified signal/noise ratio at the surface. Actual examples of the use of the electrical properties data together with electromagnetic noise environment data for systems design considerations have been given for a loop-loop source-receiver configuration (Geyer, 1971a) and a line-line source-receiver configuration (Geyer, 1971b).

Field Transmission Tests

Numerous transmission tests, both uplink and downlink, and both of the C.W. type and pulsed type, were performed with a grounded line transmitter and a vertical-axis loop transmitter and either electric or magnetic field receiving sensors (Geyer, 1972a; Geyer, 1972c; Geyer, 1973a; Geyer, 1973b).

The various source-receiver configurations considered for downlink pulse communications are shown in Figure 3. Generally, for impulsive excitation of a line current source, coupling transients for all field components decay less rapidly and positive signal peaks for the electric field occur later in time as the horizontal source-receiver offset distance becomes larger. Furthermore, all coupling transient responses increase as the square of the resistivity of the earth.

The results of numerous uplink C.W. field transmission tests (see Figures 4 and 5), on the other hand, which were made over a broad range in frequency and at several geographic receiving sites, show, in general, good agreement with theoretical considerations (see Figure 6) and several features of the produced surface magnetic field from a buried vertical-axis transmitting loop could be used for beacon location criteria. One criterion would be in the surface mapping of the maximum in the vertical magnetic field directly over the vertical-axis loop transmitter and the associated null in the

vertical magnetic field (for extremely low frequencies) at a horizontal offset distance which is about 1.4 times the depth of burial of the transmitter (see Figure 7). Another criterion would lie in the surface mapping of the null in the horizontal magnetic field directly over the vertical-axis beacon and the associated maximum in the horizontal magnetic field at an offset distance from the transmitter axis of half the depth of burial of the loop transmitter. In the first case, the size effect of the transmitter loop must be taken into consideration when the separation distances between the transmitter and receiving sensor are less than ten times the effective radius of the source loop; increasing the size of the transmitting source relative to the source-receiver separation distance shifts the null in the vertical magnetic field to greater offsets. In both cases care should be exercised in ascertaining that measured nulls and maxima are along radials through the axis of the source loop.

For the main part, coupling experiments show that ambient electromagnetic noise in coal mining districts is less of a problem above 1000 Hertz, although secondary and perhaps undesirable maxima and null phenomena (as well as possible penetration problems) would occur in many coal mine provinces in the behavior of the surface horizontal magnetic field if transmission frequencies as high as 10 kHz were used.

Summary

Field measurements and tests, together with theoretical considerations, enable us, on a practical basis, to make some qualified remarks on which source-receiver configuration might be best to use under a given set of circumstances or under a given set of constraints defining the objectives of a through-the-earth beacon electromagnetic communications system. Provided the overburden is relatively conductive (< 100 ohm-meters) and contact resistance at the current electrodes is no problem, it is often more convenient to put current directly into the ground by a line source. This type of transmitting source, although yielding a very adequate means for communication, is more sensitive to conductivity inhomogeneities and for a receiving surface electric-field sensor does not seem to provide as convenient a means for location as does a loop-loop source-receiver configuration (Geyer, 1973a). Thus, received magnetic-field signals in the ELF range are less sensitive in general to secondary scattering sources in the overburden than are electric-field signals.

On the other hand, for general communication purposes, some of the secondary nulls in the produced surface magnetic field from a buried vertical-axis loop antenna may make a horizontal grounded electric-current line a more desirable transmitting source. Of course, the electrical properties of the overburden must always be taken into account, for in the case of a highly resistive overburden (which, although not found usually over coal mines, is frequently found over hard-rock mines), it may not be practically feasible to use an electric line source for communication or location purposes at all, simply because of the difficulty in putting current into the ground. Thus, for the case where a resistive overburden is present, it may necessarily be advantageous to use a loop source antenna.

References

- Geyer, R. G., 1971b, Research on the transmission of acoustic and electromagnetic signals between mine workings and the surface: Quart. Tech. Rpt. for period Oct. 1, 1971 to Dec. 30, 1971 for U. S. Bureau of Mines, 106 p.
- Geyer, R. G., 1971a, Research related to the development of emergency mine communications systems: Quart. Tech. Rpt. for period July 1, 1971 to Sept. 30, 1971 for U. S. Bureau of Mines, 42 p.
- Geyer, R. G., 1972a, Evaluation of an impulsively driven line current source at the surface for downlink communications to mine workings: Quart. Tech. Rpt. for period Jan. 1, 1972 to March 30, 1972 for U. S. Bureau of Mines, 51 p.
- Geyer, R. G., 1972b, Research on the transmission of electromagnetic signals between mine workings and the surface: Annual Summary Rpt. for period June 16, 1971 to June 15, 1972 for U. S. Bureau of Mines, 49 p.
- Geyer, R. G., 1972c, Research on the transmission of electromagnetic signals between mine workings and the surface - Passive detection of a buried loop from the surface, Downlink pulse signalling to underground mine workings, Downlink C.W. signalling to underground mine workings: Quart. Tech. Rpt. for the period July 15, 1972 to Sept. 30, 1972 for the U. S. Bureau of Mines, 35 p.

Geyer, R. G., 1973a, Research on the transmission of electromagnetic signals between mine workings and the surface - uplink field transmission tests using a vertical-axis loop source: Quart. Tech. Rpt. for the period Oct. 1, 1972 to Dec. 31, 1972 for the U. S. Bureau of Mines, 52 p.

Geyer, R. G., 1973b, Uplink field transmission tests using a grounded buried horizontal electric line source antenna: Quart. Tech. Rpt. for the period Jan. 1, 1973 to April 15, 1973 for the U. S. Bureau of Mines, 17 p.

Wait, J. R., and Spies, K. P., 1971a, Subsurface electromagnetic fields of a circular loop of current located above ground: Informal Rpt. to U. S. Bureau of Mines (Nov. 15, 1971), 16 p.

NW - SE RESISTIVITY SECTION AT MONTGOMERY
 NO. 4 COAL MINE, PA.

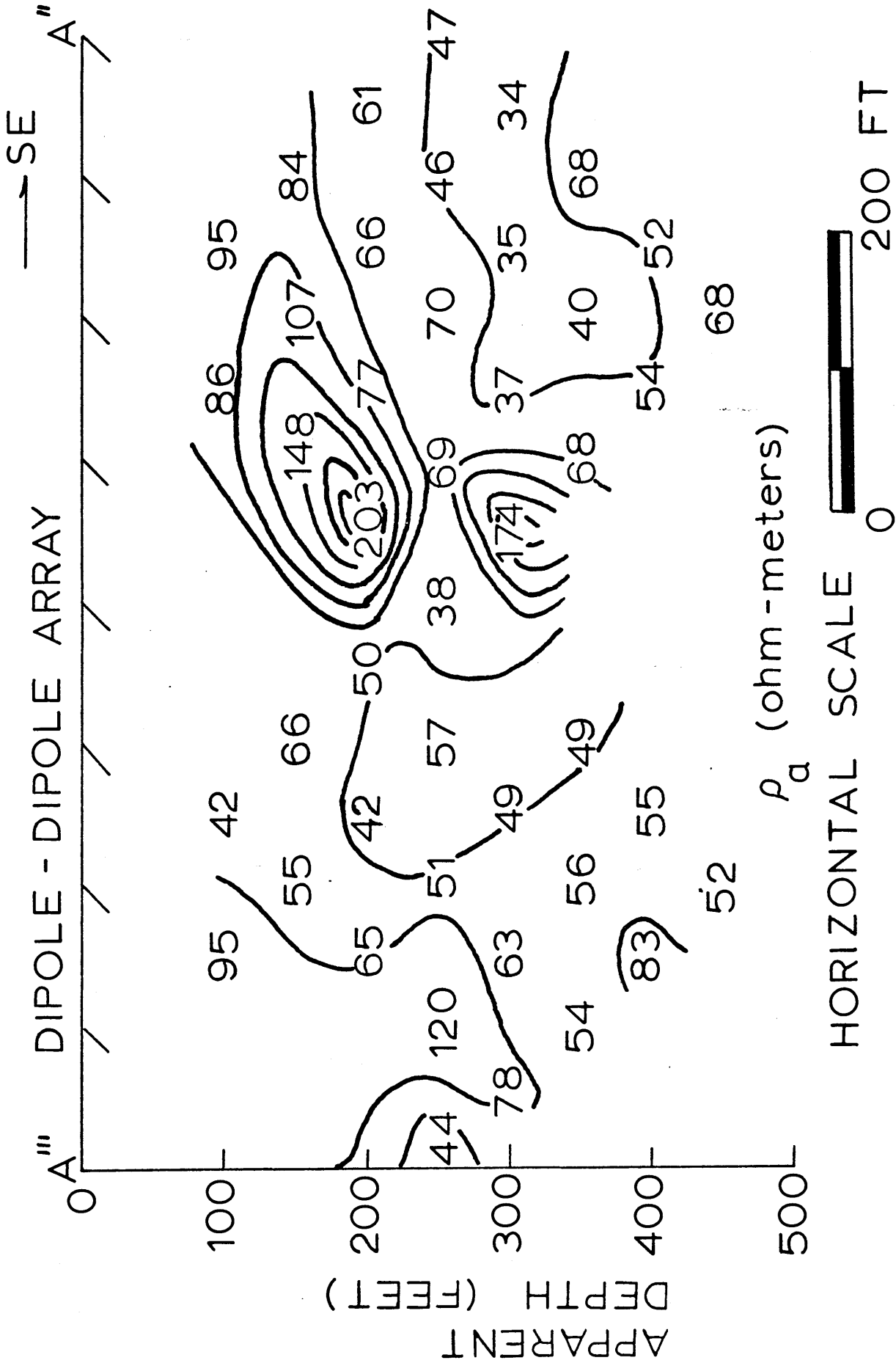


Figure 1.

NE-SW HORIZONTAL ELECTRIC FIELD NOISE

GARY NO. 14 COAL MINE W. VA.

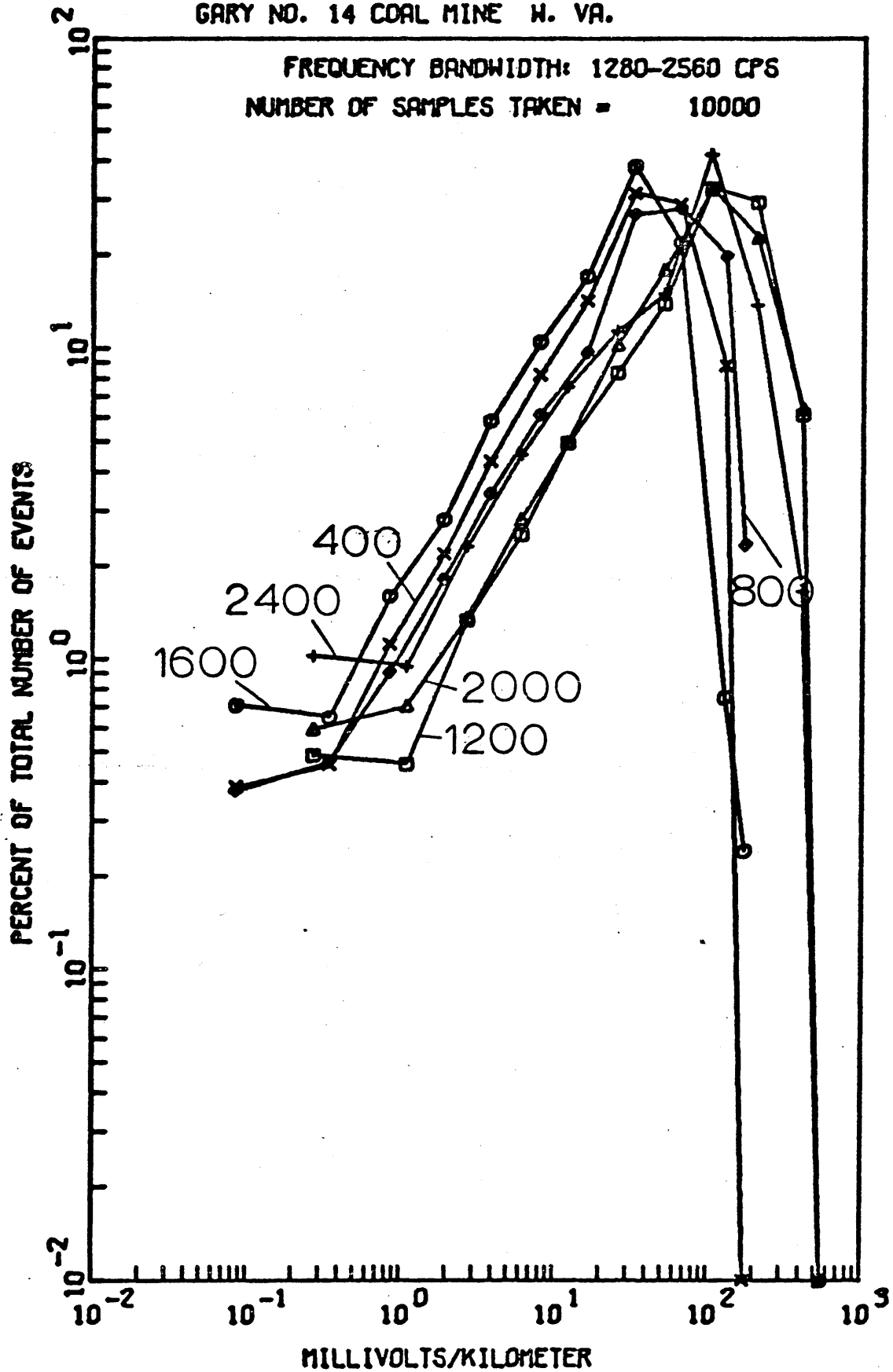


Fig. 2.

DOWNLINK SOURCE - RECEIVER SENSOR CONFIGURATIONS

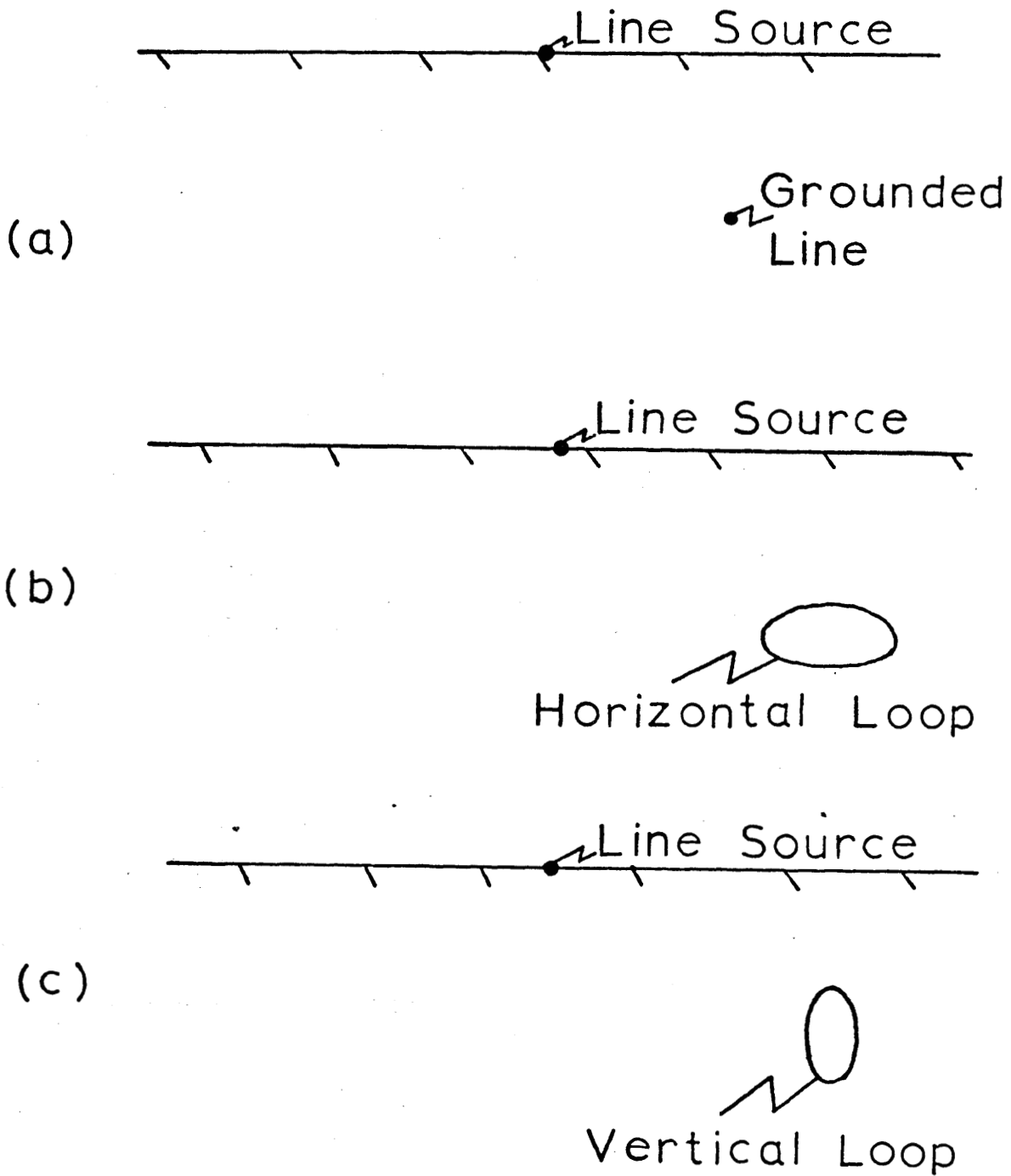


Figure 3.

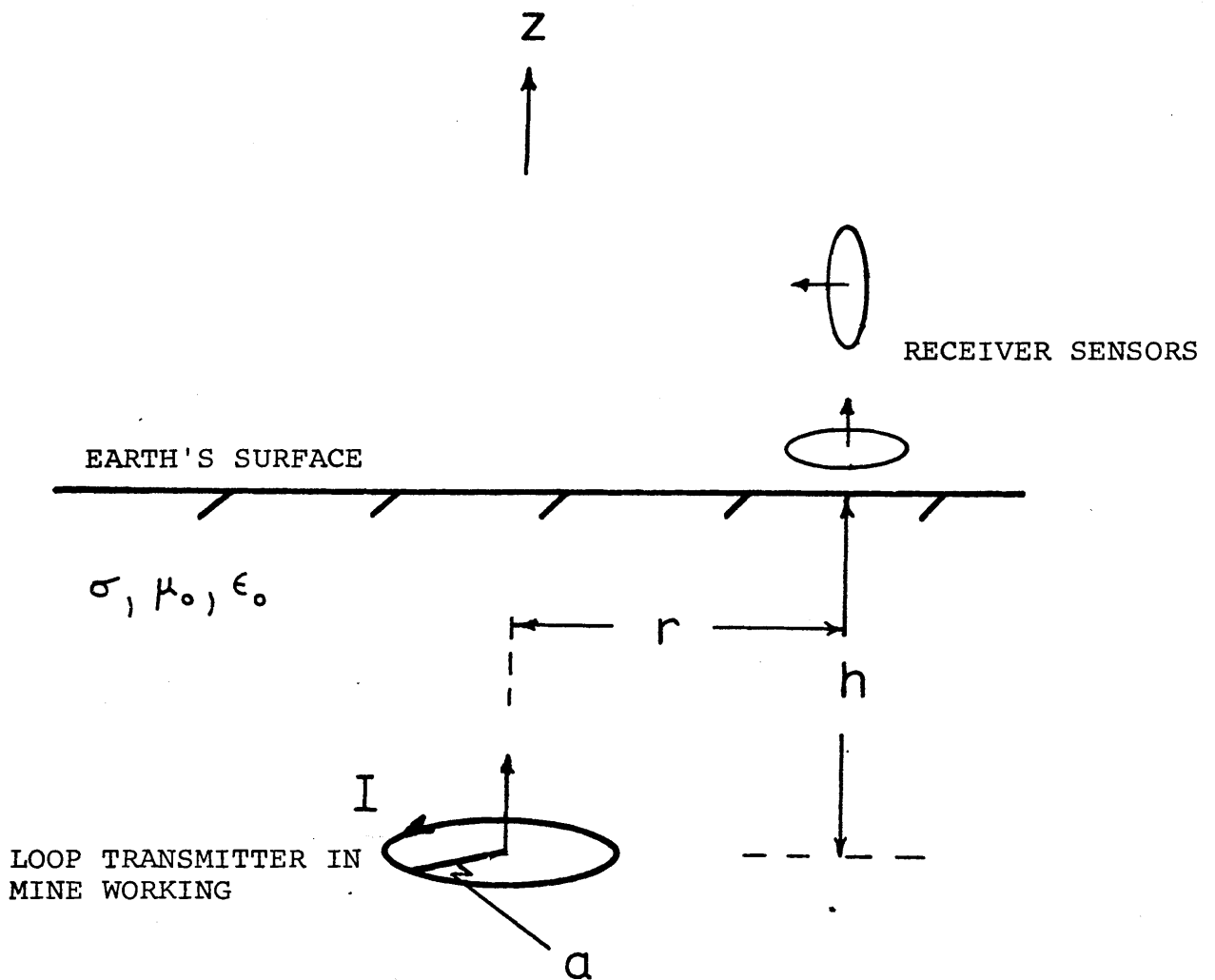


Fig. 4. Vertical-axis loop transmitter antenna and induction loop receiving sensors for uplink C.W. transmission.

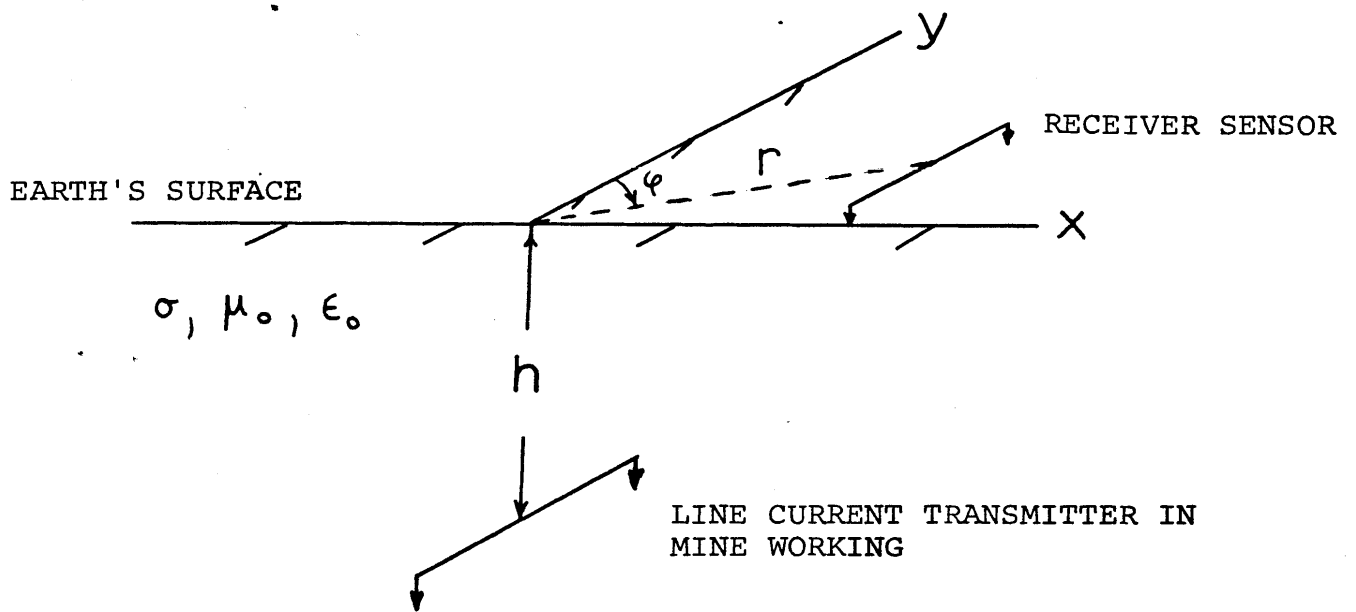
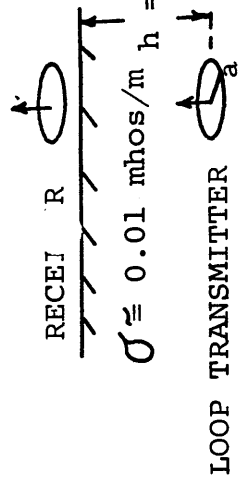


Fig. 5. Three-dimensional view of transmitter antenna and receiver sensor under consideration for uplink C.W. transmission.

JPLINK C.W. TRANSMISSION TEST

U.S. BUREAU OF MINES EXP.

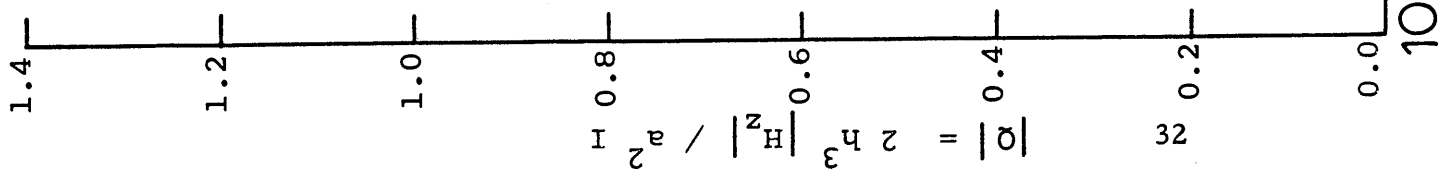
MINE, PA.



$A = a/h \approx 0.39$

$D = \rho/h \approx 0.0$

STATION 1



● FIELD DATA

△ THEORETICAL
(After Wait and Spies, 1971a)

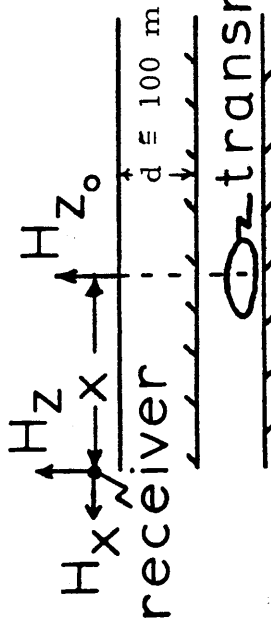
FREQUENCY (Hz)

Figure 6.

PEABODY NO. 10 MINE, ILL.

$f = 310 \text{ HZ}$

+ Data Points



transmitter

receiver

$d = 100 \text{ m}$

H_z / H_{z_0}

H_x / H_{z_0}

1 SKIN DEPTH

1000

100

10

1

OFFSET DISTANCE FROM BURIED LOOP
TRANSMITTER (meters)

Figure 7.

ELECTROMAGNETIC DIRECTION FINDING EXPERIMENTS FOR LOCATION OF TRAPPED MINERS

R. G. Olsen and A. J. Farstad
Westinghouse Electric Corporation
Georesearch Laboratory
8401 Baseline Road
Boulder, Colorado 80303

The Coal Mine Health and Safety Act of 1969, passed by Congress in the wake of the disaster at Farmington, West Virginia, led to an extensive study by the National Academy of Engineering of the problems involved in coal mine safety.¹ One of the results of this report and subsequent research conducted by the U.S. Bureau of Mines has been the investigation of electromagnetic techniques for the location of trapped miners after a mine emergency. The Westinghouse Georesearch Laboratory has been involved in both the theoretical and field studies relating to this problem².

A compact personal beacon transmitter has been developed which can be attached to and powered by a miner's lamp battery. A compatible lightweight loop antenna package has also been developed which can be easily carried on a miner's belt. This antenna can be quickly deployed on the mine tunnel floor. For the purpose of calculating its electromagnetic fields on the earth's surface, the loop can be considered to be a magnetic dipole buried in the earth. (The earth is assumed to be homogeneous and to have a conductivity of σ mhos/m.) The surface of the earth is assumed to be uniformly sloping and the transmitter dipole oriented as in Figure 1. The fields on the earth's surface can be computed³ by using a superposition of the fields of a vertical magnetic dipole³ and of a horizontal magnetic dipole⁴ in proportions which depend on the slope of the terrain.

In the case of level terrain a null in the horizontal magnetic field occurs on the surface directly above the dipole⁵. This null is designated as the apparent source location and is the criterion by which the source is located. The criterion was tested at two hardrock mines and two coal mines in the fall of 1972. The apparent source locations were compared to actual locations determined by conventional surveying techniques. It was found that due to nonlevel terrain the apparent and actual source locations differed by up to 13 meters. This discrepancy can be resolved by an examination of the fields of a source beneath uniformly sloping terrain.

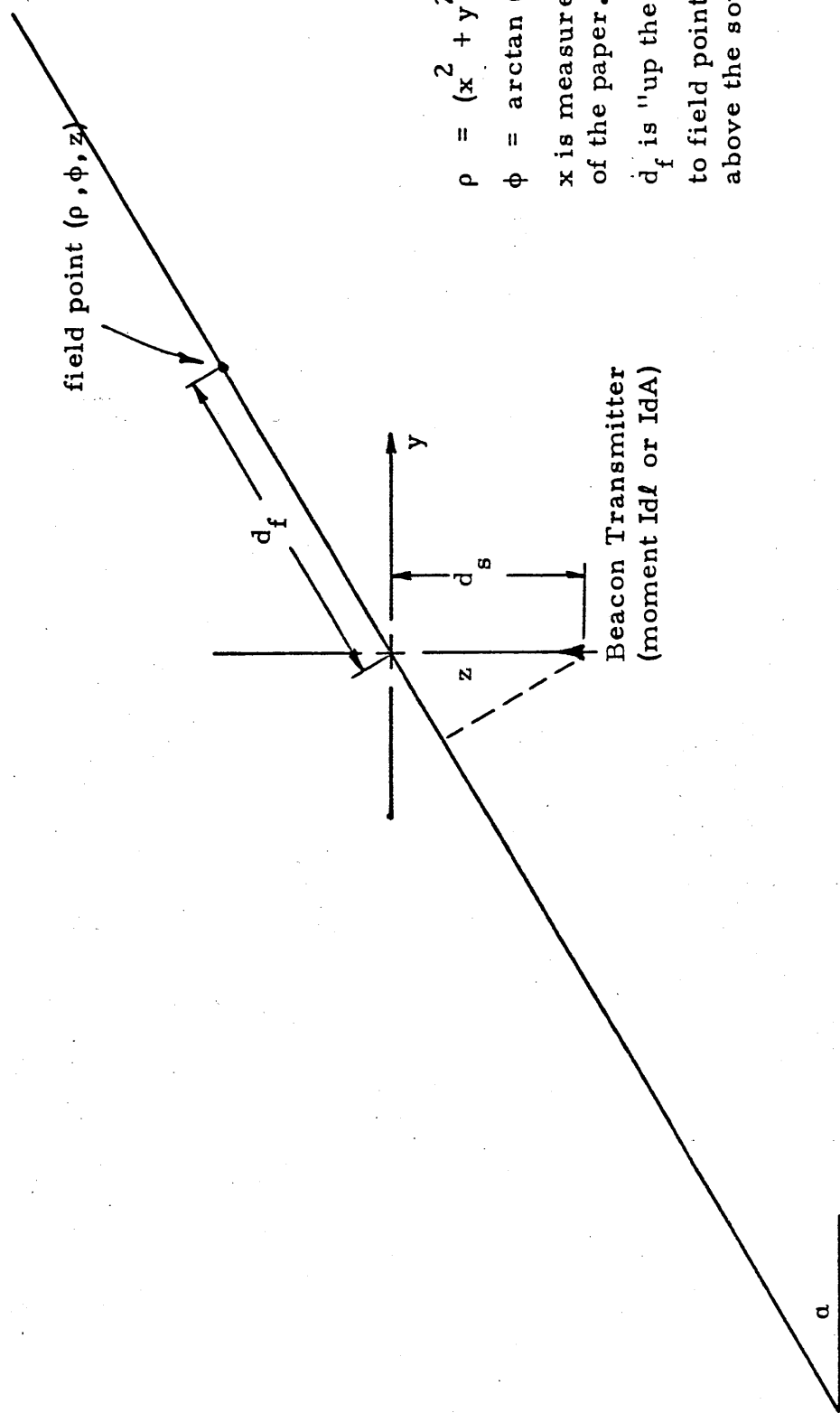
Figure 2 shows the experimental and theoretical results for a

case where the hill slope is 15° (H_ρ is the horizontal field, and H_z is the vertical field.) The null is displaced downhill by an amount which depends on the depth of the source, the ground conductivity, and the hill slope.

These results can be used to improve the location technique. If the apparent source location is known along with the ground conductivity, hill slope, and approximate source depth, the theoretical null offset can be used to obtain the actual source location.

References

1. G. Meloy, et al (1969 Mine Rescue and Survival, Nat. Acad. Eng.)
2. D. B. Large, L. Ball and A. J. Farstad (1973 IEEE Trans. Comm. Tech., vol. COM-21, No. 3, p. 194-202).
3. J. R. Wait (1971 Proc. IEEE, v. 59, n. 6, p. 1033-1035).
4. A. K. Sinha and P. K. Bhattacharya (1966 Radio Science, v. 1 (New Series), n. 3, p. 379-395).
5. J. R. Wait and L. L. Campbell (1953 Jour. Geophysics Res., v. 58, n. 2, p. 167-178).



$\rho = \sqrt{x^2 + y^2}$
 $\phi = \arctan(y/x)$
 x is measured out of the paper.
 d_f is "up the hill" distance to field point from directly above the source.

α = angle of inclination of slope

FIGURE 1 - DIPOLE LOCATED BENEATH A SLOPING INTERFACE AND COORDINATE SYSTEM IN WHICH FIELDS ARE TO BE REFERRED

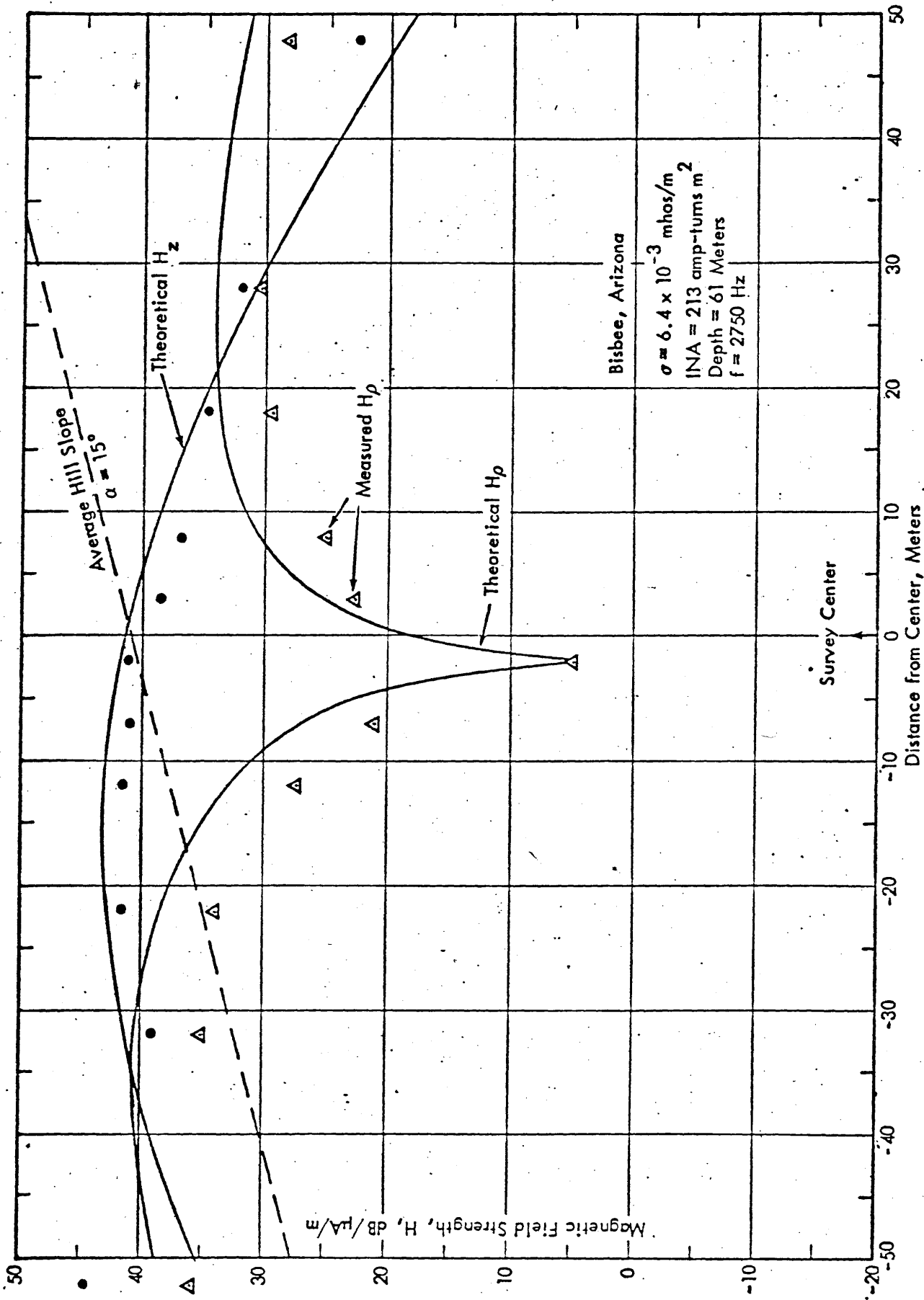


Figure 2. Electromagnetic Surface Pattern from Buried VMD (Along Hill Slope)

THEORY OF THE PROPAGATION OF UHF RADIO WAVES IN COAL MINE TUNNELS

by

Alfred G. Emslie,¹
Robert L. Lagace,² and Peter F. Strong²

ABSTRACT

This paper is concerned with the theoretical study of UHF radio communication in coal mines, with particular reference to the rate of loss of signal strength along a tunnel, and from one tunnel to another around a corner. Of prime interest are the nature of the propagation mechanism and the prediction of the radio frequency that propagates with the smallest loss. Our theoretical results are compared with measurements made by Collins Radio Co. This work was conducted as part of the Pittsburgh Mining and Safety Research Center's investigation of new ways to reach and extend two-way communications to the key individuals that are highly mobile within the sections and haulage ways of coal mines.

INTRODUCTION

At frequencies in the range of 200-4,000 MHz the rock and coal bounding a coal mine tunnel act as relatively low loss dielectrics with dielectric constants in the range 5-10. Under these conditions a reasonable hypothesis is that transmission takes the form of waveguide propagation in a tunnel, since the wavelengths of the UHF waves are smaller than the tunnel dimensions. An electromagnetic wave traveling along a rectangular tunnel in a dielectric medium can propagate in any one of a number of allowed waveguide modes. All of these modes are "lossy modes" owing to the fact that any part of the wave that impinges on a wall of the tunnel is partially refracted into the surrounding dielectric and partially reflected back into the waveguide. The refracted part propagates away from the waveguide and represents a power loss. This type of waveguide mode differs from the light-pipe modes in glass fibers in which total internal reflection occurs at the wall of the fiber, with zero power loss if the fiber and the matrix in which it is embedded are both lossless. It is to be noted that the attenuation rates of the waveguide modes studied in this paper depend almost entirely on refraction loss, both for the dominant mode and higher modes excited by scattering, rather than on ohmic loss. The effect of ohmic loss due to the small conductivity of the surrounding material is found to be negligible at the frequencies of interest here, and will not be further discussed.

The views and conclusions contained in this document are those of the authors and should not be interpreted as necessarily representing the official policies of the Interior Department's Bureau of Mines or the U.S. Government. This paper was prepared under USBM Contract No. H0122026.

1. Consultant: Formerly with Arthur D. Little, Inc. (Retired)
2. Arthur D. Little, Inc., Cambridge, Massachusetts.

The study reported here is concerned with tunnels of rectangular cross section and the theory includes the case where the dielectric constant of the material on the side walls of the tunnel is different from that on top and bottom walls. The work extends the earlier theoretical work by Marcatili and Schmeltzer⁽¹⁾ and by Glaser⁽²⁾ which applies to waveguides of circular and parallel-plate geometry in a medium of uniform dielectric constant.

In this paper we present the main features of the propagation of UHF waves in tunnels. Details of the derivations are contained in Arthur D. Little, Inc. reports.⁽³⁾

THE FUNDAMENTAL (1,1) WAVEGUIDE MODES

The propagation modes with the lowest attenuation rates in a rectangular tunnel in a dielectric medium are the two (1,1) modes which have the electric field \vec{E} polarized predominantly in the horizontal and vertical directions, respectively. We will refer to these two modes as the E_h and E_v modes.

The main field components of the E_h mode in the tunnel are

$$E_x = E_0 \cos k_x x \cos k_y y e^{-ik_z z} \quad (1)$$

$$H_y = (k_z / \omega \mu_0) E_0 \cos k_x x \cos k_y y e^{-ik_z z} \quad (2)$$

where the symbols have their customary meaning. The coordinate system is centered in the tunnel with x horizontal, y vertical, and z along the tunnel. In addition to these transverse field components there are small longitudinal components E_z and H_z and a small transverse component H_x . For the frequencies of interest here k_x and k_y are small compared with k_z which means that the wave propagation is mostly in the z -direction. From a geometrical optics point of view, the ray makes small grazing angles with the tunnel walls.

In the dielectric surrounding the tunnel the wave solution has the form of progressive waves in the transverse as well as the longitudinal directions. The propagation constant k_z for the (1,1) mode is an eigenvalue determined by the boundary conditions of continuity of the tangential components of \vec{E} and \vec{H} at the walls of the tunnel. Owing to the simple form of the wave given by (1) and (2) these conditions can be satisfied only approximately. However, a good approximation to k_z is obtained. The imaginary part of k_z , which arises owing to the leaky nature of the mode, gives the attenuation rate of the wave. The loss L_{E_h} in dB for the (1,1) E_h mode is given by

$$L_{E_h} = 4.343 \lambda^2 z \left(\frac{K_1}{d_1^3 \sqrt{K_1 - 1}} + \frac{1}{d_2^3 \sqrt{K_2 - 1}} \right) \quad (3)$$

where K_1 is the dielectric constant of the side walls and K_2 of the roof and floor of the tunnel. The corresponding result for the (1,1) E_v mode is

$$L_{E_v} = 4.343 \lambda^2 z \left(\frac{1}{d_1^3 \sqrt{K_1 - 1}} + \frac{K_2}{d_2^3 \sqrt{K_2 - 1}} \right) \quad (4)$$

These results are valid if the wavelength λ is small compared with the tunnel dimensions d_1 and d_2 . The same formulas are also obtained if one adds the attenuations for horizontal and vertical slot waveguides with dimensions d_2 and d_1 , and dielectric constants K_2 and K_1 , respectively. The losses calculated by (3) and (4) also agree closely with those calculated by a ray approach.

Figure 1 shows loss rates in dB/100 ft as functions of frequency calculated by (3) and (4) for the (1,1) E_h and E_v modes in a tunnel of width 14 ft and height 7 ft, representative of a haulage way in a seam of high coal, and for $K_1 = K_2 = 10$, corresponding to coal on all the walls of the tunnel. It is seen that the loss rate is much greater for the E_v mode. Figure 2 shows the calculated E_h loss rate for a tunnel of half the height. The higher loss rate in the low coal tunnel is due to the effect of the d_2^3 term in (3).

Two experimental values obtained by Collins Radio Co.⁽⁴⁾ for horizontal-horizontal antenna orientations are also shown in Figure 1. These values agree well with theory for the E_h mode for 415 MHz, but not so well for 1000 MHz. The departure suggests that some additional loss mechanism sets in at higher frequencies.

It is also significant that the experimental values of the loss rates for all three orientation arrangements of the transmitting and receiving dipole antennas, namely, horizontal-horizontal, vertical-horizontal, and vertical-vertical, are surprisingly close to each other. The independence of loss rate with respect to polarization is not predicted by the theory discussed so far, as seen in Figure 1 for the E_h and E_v modes. Indeed, the theory predicts no transmission at all for the VH antenna arrangement.

PROPAGATION MODEL

The higher observed loss rate at the higher frequencies relative to the calculated E_h mode values, and the independence of the loss rate on antenna orientation can both be accounted for if one allows for scattering of the dominant (1,1) E_h mode by roughness and tilt of the tunnel walls. The scattered radiation goes into many higher modes and can be regarded as a diffuse radiation component that accompanies the E_h mode. The diffuse component is in dynamical equilibrium with the E_h mode in the sense that its rate of generation by scattering of the E_h mode is balanced by its rate of loss by refraction into the surrounding dielectric. Since the diffuse component consists of contributions from the (1,1) E_v mode and many higher order waveguide modes, all of which have much higher refractive loss rates than the fundamental E_h mode, the dynamical balance point is such that the level of the diffuse component is many dB below that of the E_h mode at any point in the tunnel.

Our propagation model, comprising the (1,1) E_h mode plus an equilibrium diffuse component, explains the discrepancy between theory and experiment in Figure 1, since the loss due to scattering

of the E_h mode is greater at 1000 MHz than at 415 MHz owing to the larger effect of wall tilt at the higher frequency. The model accounts for the independence of loss rate on antenna orientation, since the loss rate is always that of the E_h mode, except for initial and final transition regions, no matter what the orientations of the two antennas may be. The transition regions, however, cause different insertion losses for the different antenna orientations.

Further strong support for the theoretical model is provided by the discovery by Collins Radio Co. that a large loss in signal strength occurs when the receiving antenna is moved around a corner into a cross tunnel; and that the signal strength around the corner is independent of receiving antenna orientation. This is exactly what our model predicts since the well collimated E_h mode in the main tunnel couples very weakly into the cross tunnel, whereas the uncollimated diffuse component couples quite efficiently. Since the diffuse radiation component is likely to be almost unpolarized, the observed independence of signal strength on receiving antenna orientation is understandable.

Another experimental result is that the initial attenuation rate in the cross tunnel is much higher than the rate in the main tunnel. This is also in accord with the model since the diffuse radiation component has a much larger loss rate than the E_h mode owing to its steeper angles of incidence on the tunnel walls.

THE DIFFUSE RADIATION COMPONENT

Scattering of the (1,1) E_h mode into other modes to generate the diffuse component occurs by two mechanisms: wall roughness and wall tilt.

Roughness is here regarded as local variations in the level of the surface relative to the mean level of the surface of a wall. For the case of a Gaussian distribution of the surface level, defined by a root mean square roughness h , the loss in dB by the E_h mode is given by the formula

$$L_{\text{roughness}} = 4.343 \pi^2 h^2 \lambda (1/d_1^4 + 1/d_2^4) z. \quad (5)$$

This is also the gain by the diffuse component due to roughness.

Long range tilt of the tunnel walls relative to the mean planes which define the dimensions d_1 and d_2 of the tunnel causes radiation in the E_h mode to be deflected away from the directions defined by the phase condition for the mode. One can calculate the average coupling factor of such deflected radiation back into the E_h mode and thereby find the loss rate due to tilt. The result in dB is

$$L_{\text{tilt}} = 4.343 \pi^2 \theta^2 z/\lambda \quad (6)$$

where θ is the root mean square tilt. Eq. (6) also gives the rate at which the diffuse component gains power from the E_h mode as a result of the tilt.

It is noted from (5) and (6) that roughness is most important at low frequencies while tilt is most important at high frequencies.

Figure 3 shows the effect on the (1,1) E_h mode propagation of adding the loss rates due to roughness and tilt to the direct refraction loss given in Figure 1. The curves are calculated for a root mean square roughness of 4 inches and for various assumed values of θ . It is seen that a value $\theta = 1^\circ$ gives good agreement with the experimental values of Collins Radio Co. The effect of tilt is much greater than that of roughness in the frequency range of interest.

Having determined the value of θ , for the assumed value of h , we can now find the intensity ratio of the diffuse component to the E_h mode from the equilibrium balance equation

$$I_{d, \text{ main}} / I_{h, \text{ main}} = L_{hd} / L_d \quad (7)$$

where L_{hd} is the loss rate from the E_h mode into the diffuse component, and L_d is the loss rate of the diffuse component by refraction. To estimate L_d approximately, we take the loss rate to be that of an "average ray" of the diffuse component having direction cosines $(1/\sqrt{3}, 1/\sqrt{3}, 1/\sqrt{3})$. Then

$$L_d = 10 (z/d_1 + z/d_2) \log_{10} 1/R \quad (8)$$

where R , the Fresnel reflectance of the average ray for $K_1 = K_2 = 10$, has the value 0.28. Then for $d_1 = 14$ ft, $d_2 = 7$ ft, $z = 100$ ft, we find that $L_d = 119$ dB/100 ft. This value has to be corrected for the loss of diffuse radiation into cross tunnels which we assume have the same dimensions as the main tunnel and occur every 75 ft. From relative area considerations we find that this loss is 2 dB/100 ft. The corrected value is therefore

$$L_d = 121 \text{ dB/100 ft.} \quad (9)$$

which is independent of frequency.

The loss rate L_{hd} is shown in Table I as a function of frequency for the 14 ft x 7 ft tunnel. The values are the sum of the roughness and tilt losses calculated by (5) and (6) for $h = 4$ inches rms and $\theta = 1^\circ$ rms. The diffuse component level relative to the E_h mode, calculated by (7), is given in the fourth column of Table I. The diffuse component is larger at high frequencies owing to the increased scattering of the E_h mode by wall tilt.

PROPAGATION AROUND A CORNER

From solid angle considerations one finds that the fraction of the diffuse component in the main tunnel that enters the 14 ft x 7 ft aperture of a cross tunnel is 15% or -8.2 dB. The diffuse level just inside the aperture of the cross tunnel, relative to the E_h mode level in the main tunnel is therefore obtained by subtracting 8.2 dB from the values in column 4 of Table I. The results are shown in column 5 of the table. A dipole antenna with either horizontal or vertical orientation

placed at this point responds to one half of the diffuse radiation, and therefore gives a signal that is 3 dB less than the values in column 5 of Table I, relative to a horizontal antenna in the main tunnel.

If a horizontal antenna is moved down the cross tunnel the loss rate is initially 119 dB/100 ft (the value calculated above without correction for tunnels branching from the cross tunnel). Ultimately, however, the loss rate becomes that of the E_h mode excited in the cross tunnel by the diffuse radiation in the main tunnel. We determine the E_h level at the beginning of the cross tunnel by calculating the fraction of the diffuse radiation leaving the exit aperture of the main tunnel which lies within the solid angle of acceptance of the E_h mode in the cross tunnel. The result is

$$I_{h, \text{cross}}/I_{d, \text{main}} = \lambda^3 / 16 \pi d_1^2 d_2 \quad (10)$$

This ratio, in dB, is given in column 2 of Table II.

Column 3 of Table II is the E_h level at the beginning of the cross tunnel relative to the E_h level in the main tunnel found by adding column 2 of Table II and column 4 of Table I. We find the corresponding ratio at 100 ft down the cross tunnel by adding the E_h propagation loss rates given in Figure 3 for $\theta = 1^\circ$. The results are shown in the last column of Table II.

The foregoing theoretical results for the diffuse and E_h components in the cross tunnel allow us to plot straight lines showing the initial and final trends in signal level in the cross tunnel. These asymptotic lines are shown in Figures 4 and 5 for 415 MHz and 1000 MHz, in comparison with the cross tunnel measurements of Collins Radio Co. The agreement both in absolute level and distance dependence gives good support to the theoretical model.

EFFECT OF ANTENNA ORIENTATION

The theoretical model also allows us to predict the effect of antenna orientation when the transmitting and receiving antennas are far enough apart so that dynamical equilibrium between the E_h mode and the diffuse component is established. We start with both antennas horizontal (HH configuration) and consider this as the 0 dB reference. Then if the receiving antenna is rotated to the vertical (HV configuration) this antenna is now orthogonal to the E_h mode, and therefore responds only to one half of the diffuse component, so that the loss is 3 dB more than the values in Table I, column 4. The result is shown in Table III column 2. Now, by the principle of reciprocity, the transmission for VH is the same as for HV as shown in column 3 of Table III. We now rotate the receiving antenna to get the configuration VV. Again we incur an additional transmission loss of 3 dB more than the values in Table I, column 4. The VV values are shown in Table III, column 4.

ANTENNA INSERTION LOSS

Dipole or whip antennas are the most convenient for portable radio communications between individuals. However, a considerable loss of signal power occurs at both the transmitter and receiver when simple dipole antennas are used because of the inefficient coupling of these antennas to the waveguide mode. The insertion loss of each dipole antenna can be calculated by a standard

microwave circuit technique for computing the amount of power coupled into a waveguide mode by a probe, whereby the dipole antenna is represented as a surface current filament having a sinusoidal current distribution along its length. The result is

$$C = \lambda^2 Z_0 / \pi^2 d_1 d_2 R_r. \quad (11)$$

Z_0 is the characteristic impedance of the E_h (1,1) mode and R_r is the radiation resistance of the antenna, which are approximately 377 and 73 ohms, respectively, provided that λ is small compared with d_1 and d_2 .

Formula (11) applies to antennas placed at the center of the tunnel and gives the results shown in Table IV, where the insertion loss L_i in dB is equal to $-10 \log_{10} C$. It is seen that the insertion loss decreases rapidly with increasing wavelength, as one would expect, since the antenna size occupies a larger fraction of the width of the waveguide. The overall insertion loss, for both antennas, is twice the value given in the table. A considerable reduction in loss would result if high gain antenna systems were used.

OVERALL LOSS IN A STRAIGHT TUNNEL

The overall loss in signal strength in a straight tunnel is the sum of the propagation loss and the insertion losses of the transmitting and receiving antennas. Table V lists the component loss rates for the (1,1) E_h mode due to direct refraction, roughness, and tilt; the total propagation loss rate; the insertion loss for two half-wave antennas; and the overall loss for five different distances. The overall loss for the HH orientation is also shown in Figure 6, where it is seen that the optimum frequency for minimum overall loss is in the range 500-1000 MHz, depending on the desired communication distance.

It is also of interest to combine the results in Table V with those in Table III to obtain the overall loss versus distance for the HH, HV (or VH), and VV antenna orientations. In order to compare the theoretical values with the experimental data of Collins Radio Co., which are expressed with reference to isotropic antennas, we add 4.3 dB to the overall loss calculated for half-wave dipoles. The theoretical results for the three different antenna orientations for frequencies of 415 MHz and 1,000 MHz are compared with the experimental data in Figures 7 and 8. It is seen that the theory agrees quite well with the general trend of the data.

OVERALL LOSS ALONG A PATH WITH ONE CORNER

Table VI gives the overall E_h mode loss for a path from one tunnel to another, including the corner loss involved in re-establishing the E_h mode in the second tunnel. The loss is the sum of the corner loss, given in column 3 of Table II and repeated in Table VI, and the straight tunnel loss given in Table V for various total distances. The results in Table VI are for the case of half-wave dipole transmitting and receiving antennas and are valid when neither antenna is within about 100 ft of the corner. The overall loss is less than the values in Table VI if the receiving antenna is within this distance, owing to the presence of the rapidly attenuating diffuse component that passes

around the corner. From the principle of reciprocity, the same is true if the transmitting antenna is within 100 ft of the corner.

The results indicate that the optimum frequency lies in the range 400-1,000 MHz. However, if one installs horizontal half-wave resonant scattering dipoles with 45° azimuth in the important tunnel intersections, in order to guide the E_h mode around the corner, the optimum may shift to somewhat lower frequencies since a greater fraction of the incident E_h wave will be deflected by the longer low-frequency dipoles.

CONCLUSIONS

The kind of propagation model developed in this paper, involving the (1,1) E_h waveguide mode accompanied by a diffuse component in dynamical equilibrium with it, seems to be necessary to account for the many effects observed in the measurements of Collins Radio Company: the exponential decay of the wave; the marked polarization effects in a straight tunnel; the independence of decay rate on antenna orientation; the absence of polarization at the beginning of a cross tunnel; the two-slope decay characteristic in a cross tunnel; and overall frequency dependence. All of these effects are moderately well accounted for by the theoretical model. However, considerable refinement of the theory could be made by removing some of the present oversimplifications, such as: the assumption of perfectly diffuse scattering both in the main tunnel and immediately around a corner in a cross tunnel; the use of the "average ray" approximation; and the description of the propagation around a corner in terms of two asymptotes only.

The last item particularly deserves more attention since we have not included the conversion of the diffuse component in the transition region near the beginning of the cross tunnel into the E_h mode. For this reason we think that the good fit of the theory to the experimental data in Figures 4 and 5 may be somewhat fortuitous. More data at greater distances down a cross tunnel would be very desirable to settle this question. Data covering a wider frequency range in both main and cross tunnels would also allow a more stringent test of the theory.

REFERENCES

1. E. A. J. Marcatili and R. A. Schmeltzer, "Hollow Metallic and Dielectric Waveguides for Long Distance Optical Transmission and Lasers," *The Bell System Technical Journal*, Vol. 43, 1783, 1964.
2. J. I. Glaser, "Attenuation and Guidance of Modes in Hollow Dielectric Waveguides," *IEEE Transactions on Microwave Theory and Techniques*, March 1969, p. 173; and M.I.T. Ph.D. Thesis, "Low-Loss Waves in Hollow Dielectric Tubes," February 1967.
3. Arthur D. Little, Inc., reports to U.S. Department of the Interior, Bureau of Mines, Pittsburgh, Pa.
4. Collins Radio Company, "Coal Mine Communications Field Test Report," December 29, 1972 prepared for U.S. Department of the Interior, Bureau of Mines, Pittsburgh, Pa.

FIGURE 1
REFRACTION LOSS FOR E_h AND E_v MODES
IN HIGH COAL

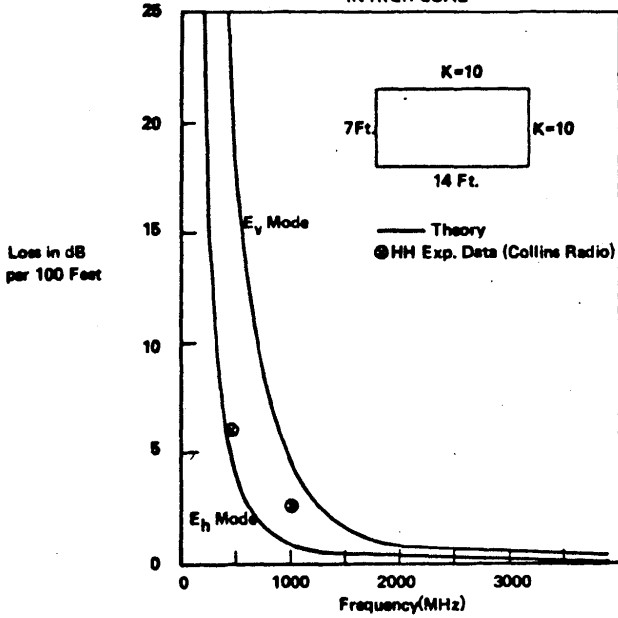


FIGURE 3
RESULTANT PROPAGATION LOSS FOR E_h MODE IN HIGH COAL
(Refraction, Wall Roughness and Tilt)

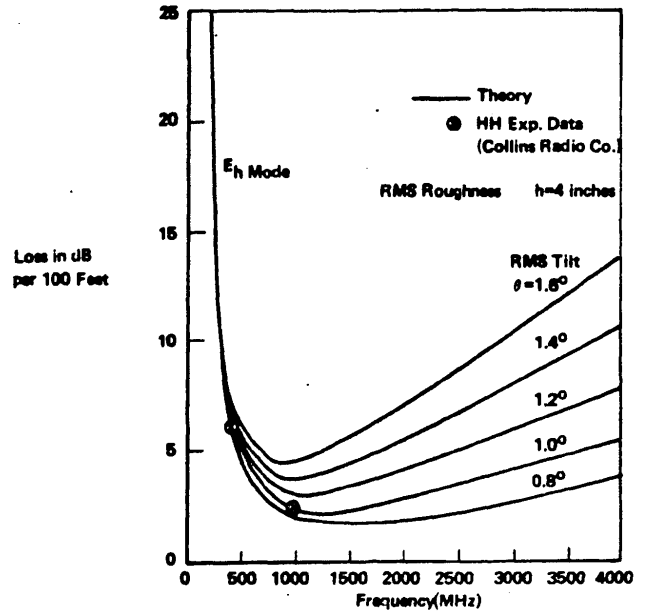


FIGURE 2
REFRACTION LOSS FOR E_h MODE IN LOW COAL

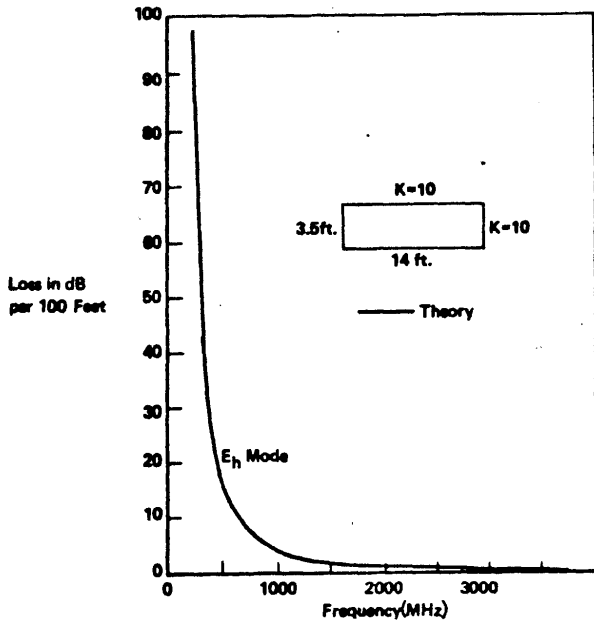


FIGURE 4
CORNER LOSS IN HIGH COAL

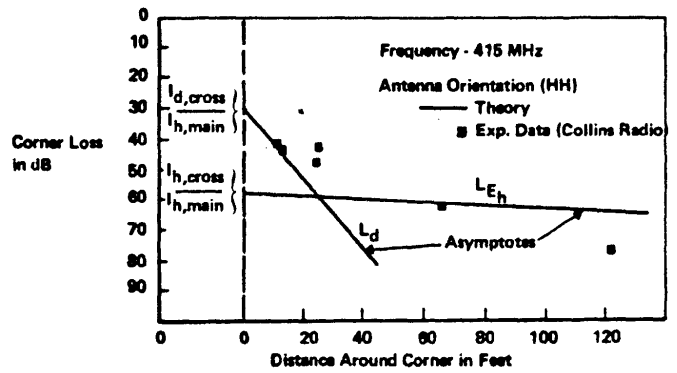


FIGURE 5
CORNER LOSS IN HIGH COAL

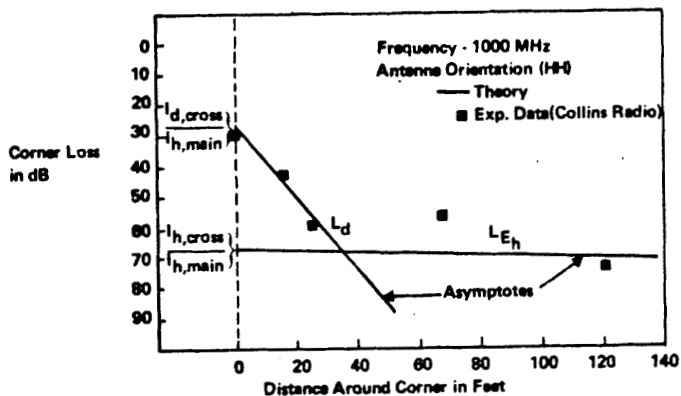


FIGURE 6

TOTAL LOSS FOR VARIOUS DISTANCES ALONG A STRAIGHT TUNNEL

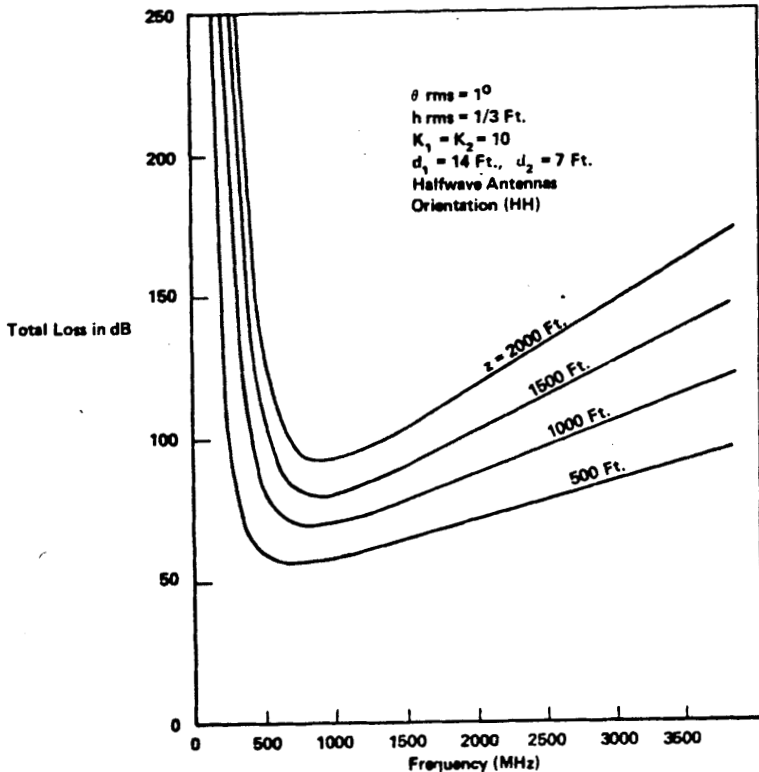


FIGURE 7

OVERALL LOSS IN A STRAIGHT TUNNEL IN HIGH COAL
(For Isotropic Antennas)

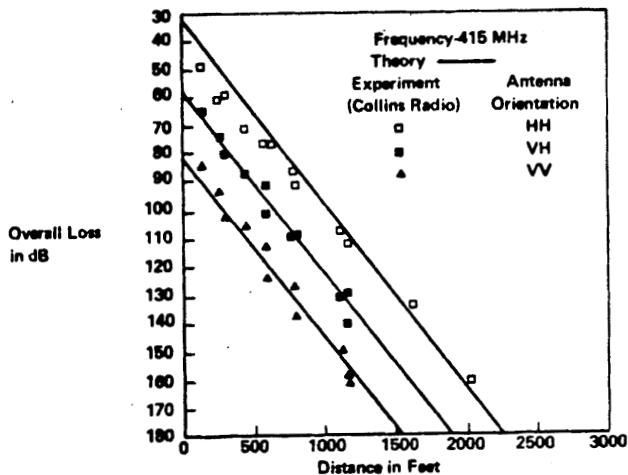


FIGURE 8

OVERALL LOSS IN A STRAIGHT TUNNEL IN HIGH COAL
(For Isotropic Antennas)

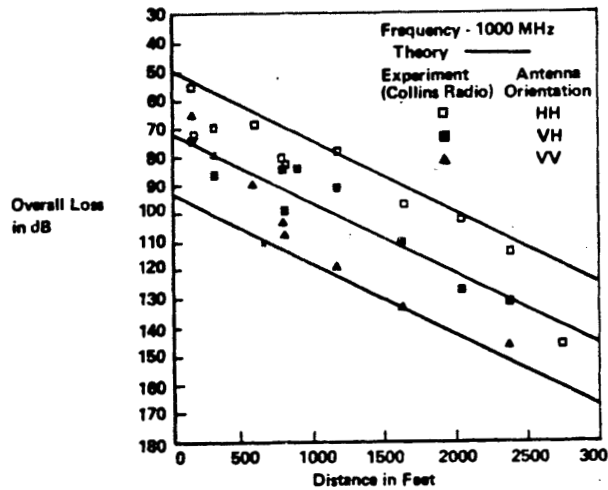


TABLE I

DIFFUSE RADIATION COMPONENT IN MAIN TUNNEL
AND AT BEGINNING OF CROSS TUNNEL

f (MHz)	λ (Ft.)	L_{hd} (dB/100 ft.)	$\frac{I_{d, main}}{I_{h, main}}$ (dB)	$\frac{I_{d, cross}}{I_{h, main}}$ (dB)
4,000	.245	5.4	-13.5	-21.7
3,000	.327	4.1	-14.7	-22.9
2,000	.49	2.8	-16.4	-24.6
1,000	.98	1.5	-19.0	-27.2
415	2.37	1.1	-20.6	-28.8
200	4.92	1.3	-19.7	-27.9

TABLE II

EXCITATION OF E_h MODE IN CROSS TUNNEL
BY DIFFUSE COMPONENT IN MAIN TUNNEL

f (MHz)	$\frac{I_{h, cross}}{I_{d, main}}$ (dB)	$\frac{I_{h, cross}}{I_{h, main}}$ (dB)	$\frac{I_{h, cross}}{I_{h, main}}/100'$ (dB)
4,000	-66.7	-80.2	85.6
3,000	-62.9	-77.6	81.8
2,000	-57.7	-74.1	77.1
1,000	-48.6	-67.6	70.1
415	-37.1	-57.7	64.1
200	-27.6	-47.3	71.6

TABLE III
EFFECT OF ANTENNA ORIENTATION

f (MHz)	HH (dB)	HV (dB)	VH (dB)	VV (dB)
1000	0	-22.0	-22.0	-44.0
415	0	-23.6	-23.6	-47.2
200	0	-22.7	-22.7	-45.4

TABLE IV
INSERTION LOSS (L_i)
(For a Half-Wave Antenna)

F (MHz)	λ (Feet)	L_i (dB)
4000	0.245	36.0
3000	0.327	32.4
2000	0.49	28.9
1000	0.98	22.9
415	2.37	15.2
200	4.92	8.9

TABLE V

CALCULATION OF OVERALL LOSS FOR E_h MODE WITH TWO HALF-WAVE DIPOLE ANTENNAS

($h = 1/3$ Ft. $\theta = 1^\circ$, $K_1 = K_2 = 10$, $d_1 = 14$ Ft., $d_2 = 7$ Ft.)

f (MHz)	$L_{refraction}$ (dB/100')	$L_{roughness}$ (dB/100')	L_{lift} (dB/100')	$L_{propagation}$ (dB/100')	$L_{insertion}$ (dB)	$L_{overall}$ (dB)				
						100'	500'	1000'	2000'	
4000	.06	.05	5.33	5.44	69.90	75	97	124	152	179
3000	.10	.07	3.99	4.16	64.88	69	86	107	127	148
2000	.23	.10	2.66	2.99	57.86	61	73	88	103	118
1000	.91	.21	1.33	2.45	45.82	48	58	70	81	93
415	5.34	.50	0.55	6.39	30.48	37	62	94	126	158
200	23.00	1.04	0.27	24.31	17.80	42	139	261	383	504
100	92.00	2.08	0.14	94.20	5.80	100	477	948	1419	1890

TABLE VI

OVERALL LOSS ALONG A PATH INCLUDING ONE CORNER
 E_h MODE WITH HALF-WAVE DIPOLE ANTENNAS

f (MHz)	E_h Loss per Corner (dB)	Overall Loss (dB)		
		500'	1000'	2000'
4000	80.2	177	206	232
3000	77.6	163	184	206
2000	74.1	147	162	177
1000	67.6	128	138	148
415	57.7	120	152	184
200	47.3	187	308	430

GUIDED PROPAGATION OF RADIO WAVES

P. DELOGNE, Université Catholique de Louvain,
L. DERYCK, Université de Liège,
R. LIEGEOIS, Institut National des Industries Extractives

Monofilar Waveguide Cable

So far as the propagation of electromagnetic waves is concerned, an underground tunnel behaves like a pipe or hollowed waveguide. Waves propagate in this tunnel with a low attenuation only if their frequency is higher than a so-called critical frequency which depends on the shape and mostly on the cross-dimensions of the tunnel and which value is in the neighbourhood of several tenths of MHz.

However, when a metallic conductor is stretched along the gallery the electromagnetic characteristics of the latter are considerably modified and the effect of the cut-off frequency disappears; this is due to the fact that the gallery equipped with such a conductor works like a coaxial cable where the conductor serves as the outward conductor and the wall of the gallery as the return conductor. This is the principle of the monofilar waveguide cable which has been perfectly studied by Cabillard.

Two main characteristics of the monofilar mode are as follows: first of all, when the cable is suspended in the middle of the cross section of the gallery, the electromagnetic field occupies all the space between the wire and the walls of the gallery. When the wire is close to the wall, the electromagnetic field tends to become concentrated between the wire and the wall, with the consequence that, with the given monofilar mode power, the aerial of a receiver standing somewhere in the tunnel will capture a weaker and weaker signal. Secondly, owing to the fact that the mode of monofilar propagation uses the ground as return conductor, its power of propagation is considerably diminished; the closer the wire is to the wall the higher the attenuation, for only a very small part of the wall is utilized as return conductor.

To cover great distances, everything else being equal, two or more conductors must be placed in the gallery. If the distance between two conductors of a cable is much smaller than the distance between one or other of the conductors and the walls; or again if one of the conductors surrounds the others and forms a screening, two sorts of modes appear : on the one

hand the monofilar mode in which the wires or the screening serve as an outward conductor and the ground as a return conductor and, on the other hand, one or several modes in which the outward and return are effected solely by wires without intervention of the earth. This new type of mode will therefore be characterized by a relatively slight attenuation of propagation : hence, the ranges will be greater. However, the electromagnetic field of these modes is concentrated in the neighbourhood of the wires or inside the screening and it may not influence the antenna of mobile sets; only the monofilar mode possesses this property. For this system to be completed, it is therefore necessary to produce energy exchanges between these two types of mode, the monofilar mode being used in as small a quantity as possible for the link with the antenna, and the other mode for long distance propagation.

Systems Based on the Use of a Coaxial Cable

The guide-cable with the greatest range is that in which the attenuation is the slightest : it consists of a coaxial cable. For purposes of clearness we shall call the coaxial mode that which is propagated between the inner conductor and the screening and the single wire mode that which is situated outside the cable. The coaxial cable has a second advantage over cables such as the bifilar twin lead cable : the coaxial mode is entirely protected against the outer environment and does not suffer at all from a prolonged stay in a damp or dusty atmosphere or from being placed against the wall of the gallery.

The INIEX/Delogne system consists of connecting along a coaxial cable, radiating multi-purpose devices including conversion of modes.

Generally speaking, any antenna could perform these functions, but there is only one which is simple, small, economic and at the same time remarkably efficient : it consists of a cutting of the screening of the cable to which concentrated elements - coils and condensers - can always be added in order to improve the working.

Theoretical and Experimental Study

To study the INIEX/Delogne radiating devices it was necessary to solve the Maxwell equations, utilise the computer and verify the theory on the small-scale model with UHF in the la-

boratory. The full study has been published in a technical review (1); we give here the most important results of this study.

From the point of view of the propagation of the coaxial mode, the complete cut of the outer conductor behaves like an impedance inserted in series between the two lips in the gap of the outer conductor. This impedance is an electrical resistance and a capacity put in parallel (fig. 1). The power that should be dissipated by the electrical resistance we imagine is exactly the one which in reality goes out of the cut of the outer conductor and this power is representative of the radiation and of the monofilar mode, and this, of course, means that there is a loss of signal for the propagation in the coaxial mode.

To reduce the impedance of the cut we may add a condenser as shunt.

We may balance the effect of the condenser by inserting in series with the inner conductor a resonating spool matched with the condenser on the working frequency.

An interesting characteristic of the radiating waves is that they are concentrated in directions situated not more than about 10 degrees further away from the axis of the cable.

While systems based on coaxial cable described by others have to take into account a coupling loss of the order of 75 to 105 dB between the coaxial mode and the input of a mobile receiver, the coupling loss is only 25 dB in the INIEX/Delogne system. Therefore it allows the greatest ranges one could obtain at present without any intermediate amplification.

The system is now operating in several mines (fig. 2). A patent has been issued in several countries and is pending in the United States.

The INIEX/Deryck System

When a bifilar cable is suspended in an underground gallery, two modes of propagation appear : the parallel mode and the anti-parallel mode (fig. 3).

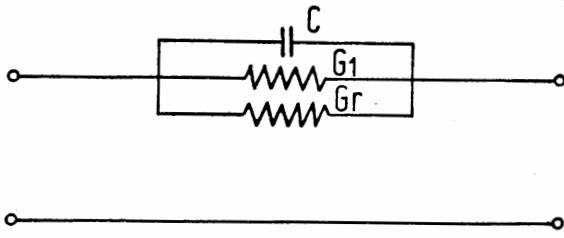
The way it works has been analysed intensively (2); it has been possible to provoke a controlled diaphony by inserting in the line devices called "mode converters" which are quadripoles with a transverse asymetry. Figure 4 shows two models of such a mode converter.

It happens that a bifilar transmission line equipped with the mode converters works in an entirely similar manner as the coaxial cable equipped with INIEX/Delogne radiating devices. Ranges are smaller because the attenuation of the bifilar line is higher than that of a coaxial cable. A bifilar line is less resistant to weathering than a coaxial cable, but it is cheaper.

REFERENCES

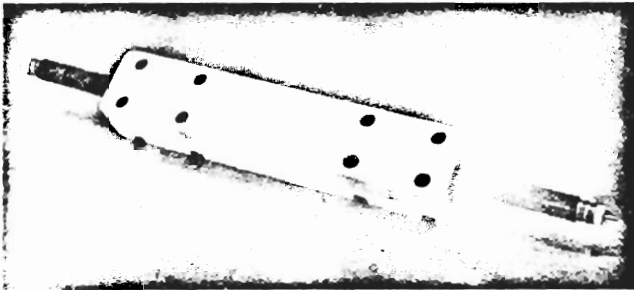
- P. DELOGNE & R. LIEGEOIS. - Ann. Tél., France, t. 26, n° 3-4, pp. 85-100, 1971, mars-avril.
- L. DERYCK. - Etude de la propagation des ondes électromagnétiques guidées dans les galeries souterraines. Thèse de doctorat en Sciences, Université de Liège, Belgique, 1973.

Fig. 1



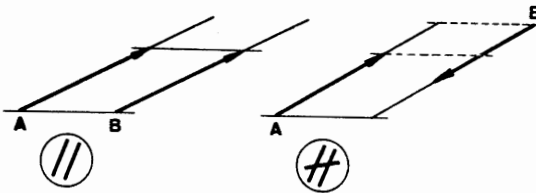
Electrical model of the cut
Schéma équivalent de la coupure

Fig. 2



Radiating device of the INIEX/Delogne system
Dispositif rayonnant du système INIEX/Delogne

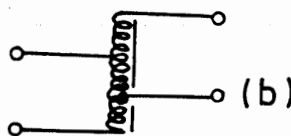
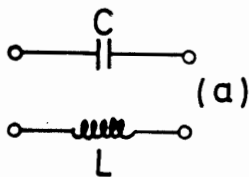
Fig. 3



"Parallel" mode, on the left;
"anti-parallel" mode, on the right

*Mode parallèle, à gauche;
mode anti-parallèle, à droite*

Fig. 4



Mode-converters
(a) narrow band
(b) wide band

*Convertisseurs de mode sélectif (a)
et à large bande (b)*

RADIO PROPAGATION MEASUREMENTS IN COAL MINES

AT UHF AND VLF *

Arthur E. Goddard
Collins Radio Company
Telecommunications Group
Cedar Rapids, Iowa

ABSTRACT

Radio propagation measurements were conducted in a coal mine at UHF (200 to 1000 MHz) and VLF (1 to 50 kHz) to characterize the transmission loss of intra-mine paths. The basic experimental parameters included frequency, polarization, path orientation and distance. Further tests evaluated the performance of roof-bolt vs. loop antennas at VLF and parasitic reflectors at UHF.

Measurement results are summarized in a series of transmission loss curves. Examples are presented to show the use of these curves in predicting the performance of radio communication systems in mines.

INTRODUCTION

This paper summarizes a coal mine communication field test project conducted by Collins Radio as part of a continuing study of coal mine communications for the Bureau of Mines. The measurement and analysis effort centers on the propagation characteristics of radio signals in a working coal mine environment. The intent of the resulting data is to provide basic propagation loss characteristics in a form convenient for establishing requirements and evaluating alternate approaches for an integrated mine communications system. The goal of such a system is to satisfy both operational and emergency communication needs in the mine.

Field testing was conducted during the last week of November, 1972, at a coal mine operated by Inland Steel Company, near Sesser, IL. The mine has a vertical shaft entry with 750 feet of overburden and is located

* This work was supported by the U. S. Department of Interior, Bureau of Mines.

" The views and conclusions contained in this document are those of the authors and should not be interpreted as necessarily representing the official policies of the Interior Department's Bureau of Mines or the U. S. Government."

in the Illinois No. 6 seam. At present, the mine is 8,000 feet North-South by 13,000 feet East-West with an ultimate size 3 miles North-South by 7.5 miles East-West. All tunnels and haulage ways are 14 feet wide by 7-8 feet high with pillars running 60 feet by 74 feet. Roof bolts are 6 to 9 feet in length and secured by expansion anchors. The roof bolts are placed on 4 foot centers throughout the mine.

The test area extended along a 4450 foot segment of the main west entry. The tunnel in which measurements were taken was the same as used for haulage of men and supplies via battery-operated, rubber tire vehicles. This tunnel also contained a 7200 VAC, 3-phase prime power cable suspended from the roof. A cross section of the tunnel is shown in figure 1. Measurements of corner attenuation were made along cross-cuts at right angles to the main tunnel. A typical corner geometry is shown in figure 2.

UHF TESTS

At UHF, transmission loss along the main tunnel and around corners was measured as a function of frequency, polarization and distance. All UHF tests utilized a 20-watt source and $\lambda/4$ ground plane antennas for transmission and standard $\lambda/2$ dipole antennas for reception. At each receiver point, a series of measurements was made to determine local signal strength variation over a range of several wavelengths. Horizontal and vertical polarization measurements were conducted to determine the extent of signal depolarization. Measurements were continued along the main tunnel and around corners at appropriate intervals determined by the rate of signal attenuation. Measurements were continued outward from the transmitter until no further signal could be detected. Transmission loss measurement accuracy is ± 2.5 dB based on receiver and antenna calibration tolerances.

The observed signal attenuation along the main tunnel is shown in figures 3, 4, and 5 for 200, 415, and 1000 MHz respectively. Attenuation is plotted as the power transfer ratio between isotropic antennas (basic transmission loss) for the indicated polarizations. Transmission loss may be combined directly with equipment parameters to establish communications performance.

Significant propagation characteristics are:

- a) Attenuation (in dB) increases nearly linearly with increasing distance.
- b) Horizontal polarization produces significantly lower transmission loss at a given distance than does vertical polarization. Cross polarization produces a loss intermediate between horizontal and vertical.
- c) Transmission loss decreases significantly at a given distance as the frequency is increased from 200 to 1000 MHz.

Linear attenuation (in dB) versus distance is a characteristic of waveguide propagation; the tunnel geometry also suggests a guided mode of propagation. From the slope of the attenuation curves, attenuation rates have been determined as shown in figures 3-5. The values for 200 MHz are considered to be very approximate because they are based on a small number of data points. For comparison, Farmer and Shephard¹ report a value of 12 dB/100' at 160 MHz for straight passageways underground and in buildings.

With the main tunnel measurements as a reference, data were also obtained around corners. Observed corner attenuation is shown in figures 6, 7, and 8 for 200, 415, and 1000 MHz, respectively. Corner attenuation is plotted in dB relative to the horizontally polarized signal level observed in the center of the main tunnel. Significant propagation characteristics are:

- a) Signal attenuation immediately around a corner is considerable at all three frequencies.
- b) Complete signal depolarization is observed around the corner.

Because of the high attenuation of a single corner, propagation around multiple corners is expected to be even more severely attenuated. Consequently, the signal existing at any point can be reasonably assumed to have followed the path including the least number of corners. The transmission loss at any point along a cross tunnel can then be estimated by adding the attenuation from the appropriate curve in figure 6, 7, or 8 to the transmission loss corresponding to the distance along the main tunnel back to the transmitter.

One possible UHF communications system consists of a 20-watt base station and 1-watt walkie-talkie. As shown in Table 1-A, the base to walkie-talkie link has a "range" of 156 dB wherein satisfactory communications can be obtained. Communications coverage can thus be determined by comparing the predicted transmission loss to the 156 dB limit.

VLF TESTS

At VLF, the transmission loss and field strength were measured as a function of frequency, distance, and antenna orientation. All VLF tests utilized a 7-watt source with roof bolt (line source) antennas for transmission and standard loop or roof bolt antennas for reception. The line source antenna was established by clamping a pair of wire leads to two roof bolt heads separated by 52 feet. At each receive point, signal strength readings were made for two orthogonal positions of the roof bolt antenna and three orthogonal positions for the loop. The entire measurement sequence was then repeated for a second orientation of the transmit antenna. Measurements were conducted at three points spaced at intervals determined by the rate of signal attenuation. Transmission loss measurement accuracy is ± 2 dB based on receiver calibration tolerance.

Observed signal attenuation for intra-mine roof bolt-to-roof bolt antennas is shown in figure 9. Attenuation is plotted as the power transfer ratio between the roof bolt antenna terminals. Transmission loss may be added directly to transmitter power to determine the received signal level (available power into matched load). Significant propagation characteristics are:

- a) Minimum transmission loss occurs for the end-to-end antenna orientation.
- b) Transmission loss is relatively flat versus frequency.
- c) The attenuation rate is approximately 5 dB/100' averaged over all frequencies and antenna orientations.

The available measurements do not fully characterize the propagation behavior. In particular, measurements over a greater range of distance, frequency and roof bolt spacing are desirable. However, the range of a roof bolt voice radio system can be estimated from measured data. For a 25-watt transmitter and other parameters as shown in Table 1B, the "range" of a typical system is 158 dB. Assuming that the curves of figure 9 extrapolate at 5 dB/100, 158 dB transmission loss then occurs at a distance of 1200 to 1400 feet, depending on antenna orientation.

Observed field strength for intra-mine roof bolt-to-loop antennas is shown in figure 10. Field strength is shown as the magnetic field intensity in dB/ μ A/m. This quantity is chosen rather than transmission loss to facilitate trade-off studies involving loop parameters such as size and weight. Field strength measurement accuracy is ± 2 dB based on receiver and loop calibration tolerances.

Significant propagation characteristics are:

- a) Maximum field strength occurs with the vertical magnetic dipole oriented along the axis of the roof bolt antenna.
- b) Field strength is relatively flat versus frequency.
- c) The attenuation rate is approximately 4 dB/100' averaged over all frequencies and antenna orientations.

The range of a roof bolt-to-loop voice bandwidth radio system can be estimated from measured data. Assuming the equipment parameters listed in table 1B and a 30-inch diameter, 20-turn loop for receiving, the required field strength is -14dB/ μ A/m at 50 kHz and +20 dB/ μ A/m at 1 kHz. Further assuming that the curves of figure 10 extrapolate at 4 dB/100', the minimum useful field strengths are reached at approximately 1500 feet at 50 kHz and 800 feet at 1 kHz when the loop is oriented as a VMD.

ACKNOWLEDGEMENT

The cooperation and assistance of management and engineering personnel at the Inland Steel Co. coal mine is gratefully acknowledged.

REFERENCES

1. Farmer, R. A., and N. H. Shephard, "Guided Radiation. . .The Key to Tunnel Talking," IEEE Transactions on Vehicular Communications, pp 93-102, March, 1965.

TABLE 1 COMMUNICATION LINK CALCULATIONS

(A) UHF, 2-WAY FM RADIO

Transmit Power,	P_t	$=$	+13 dBW
Transmit Antenna Gain,	G_t	$=$	0 dBi
Receive Antenna Gain,	G_r	$=$	0 dBi
Receive Sensitivity*,	P_r	$=$	-143 dBW

$$\begin{aligned} \text{System "Range"} &= P_t + G_t + G_r - P_r \\ &= 156 \text{ dB} \end{aligned}$$

*0.5uV for 20 dB quieting

(B) VLF, SSB RADIO

Transmit Power,	P_t	$=$	+14 dBW
External Noise,	N_e	$=$	-194 dBW/Hz
Receiver Noise,	N_r	$=$	-194 dBW/Hz
Total Noise	N_s	$=$	-191 dBW/Hz
Required SNR*	SNR_o	$=$	+47 dB-Hz

$$\begin{aligned} \text{System "Range"} &= P_t - N_s - SNR_o \\ &= 158 \text{ dB} \end{aligned}$$

* Articulation index = 0.3

DEPTH IN FEET
(NOT TO SCALE)

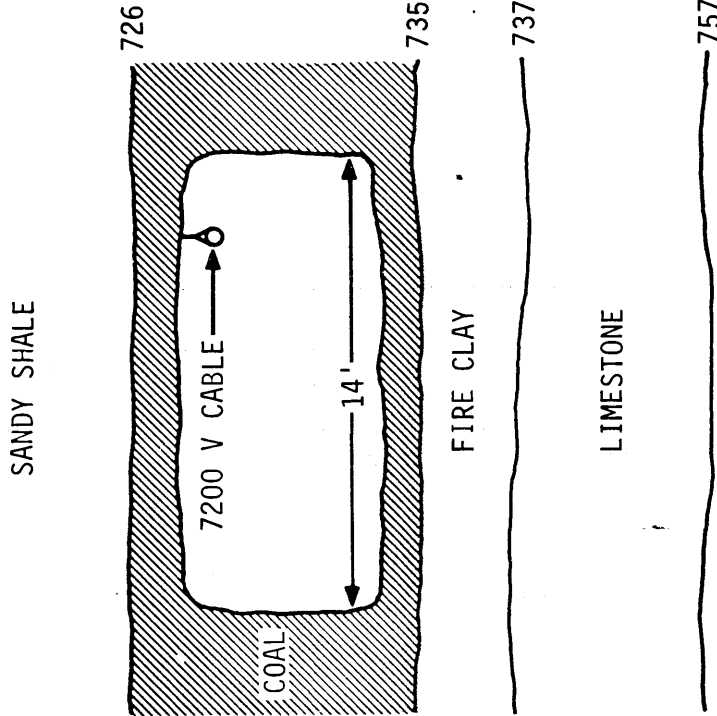
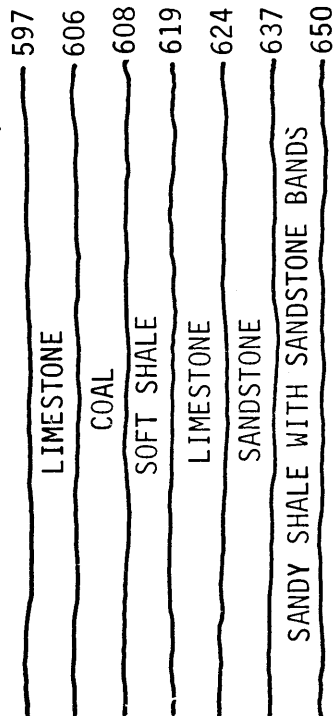
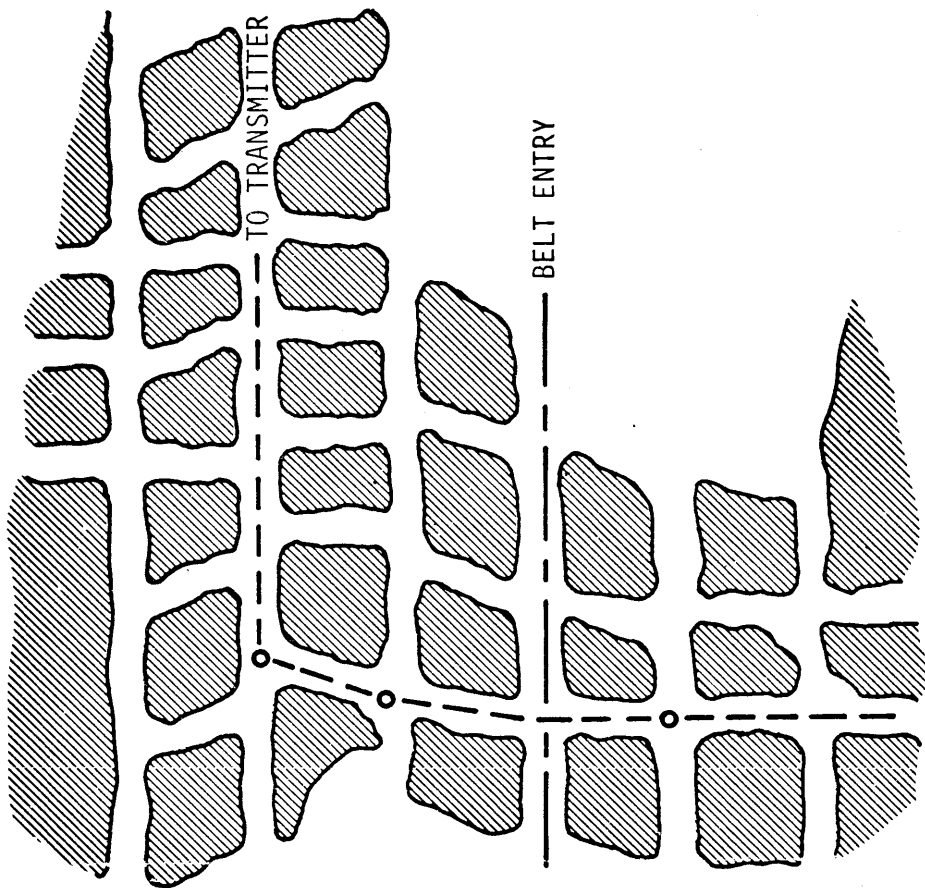


FIG. 1 - TUNNEL CROSS SECTION



○ = MEASUREMENT POINT
SCALE, 1" = 100'

FIG. 2 - TYPICAL CORNER GEOMETRY

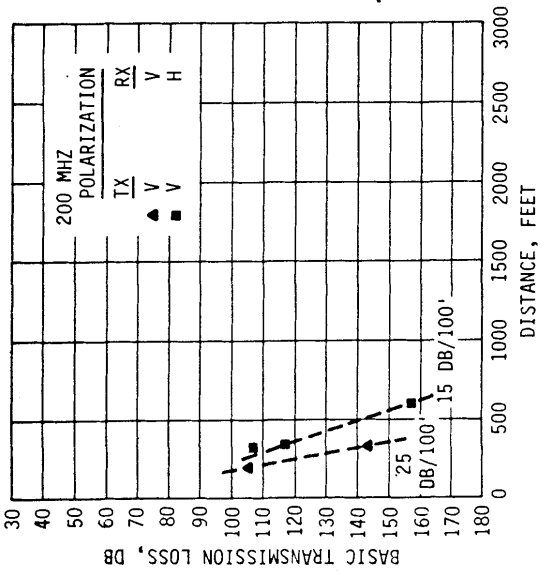


FIG. 3

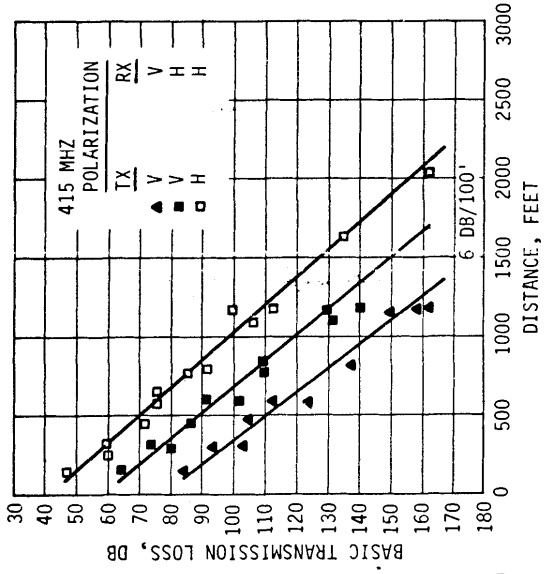


FIG. 4

UHF TRANSMISSION LOSS ALONG STRAIGHT TUNNEL

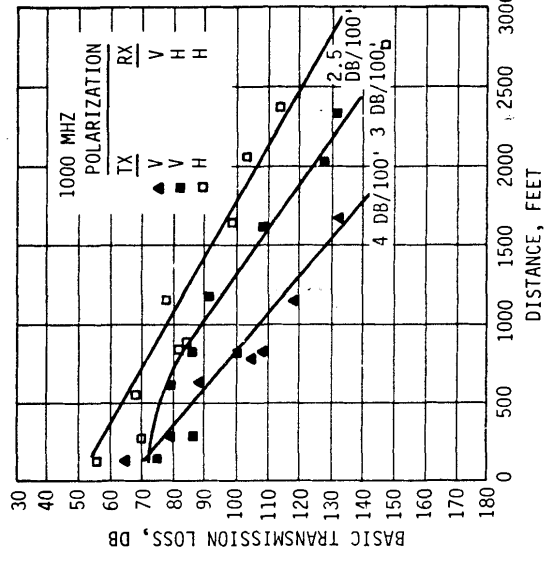


FIG. 5

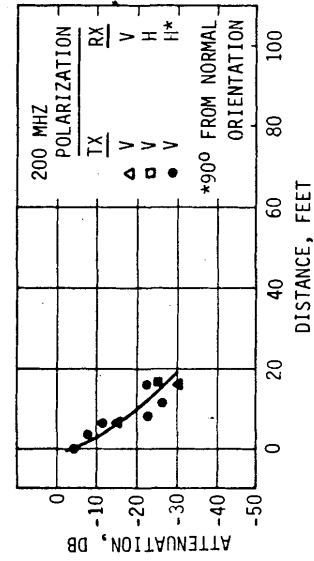


FIG. 6

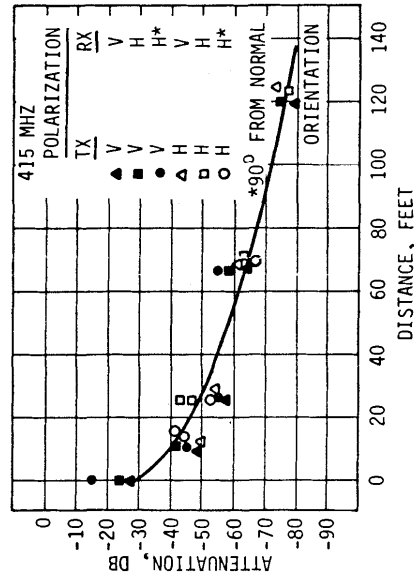


FIG. 7

UHF ATTENUATION OF SINGLE CORNER

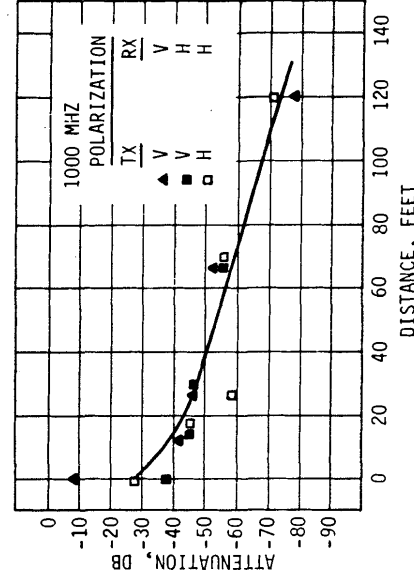


FIG. 8

- = 50 KHZ
- = 20 KHZ
- = 10 KHZ
- = 3 KHZ
- △ = 1 KHZ

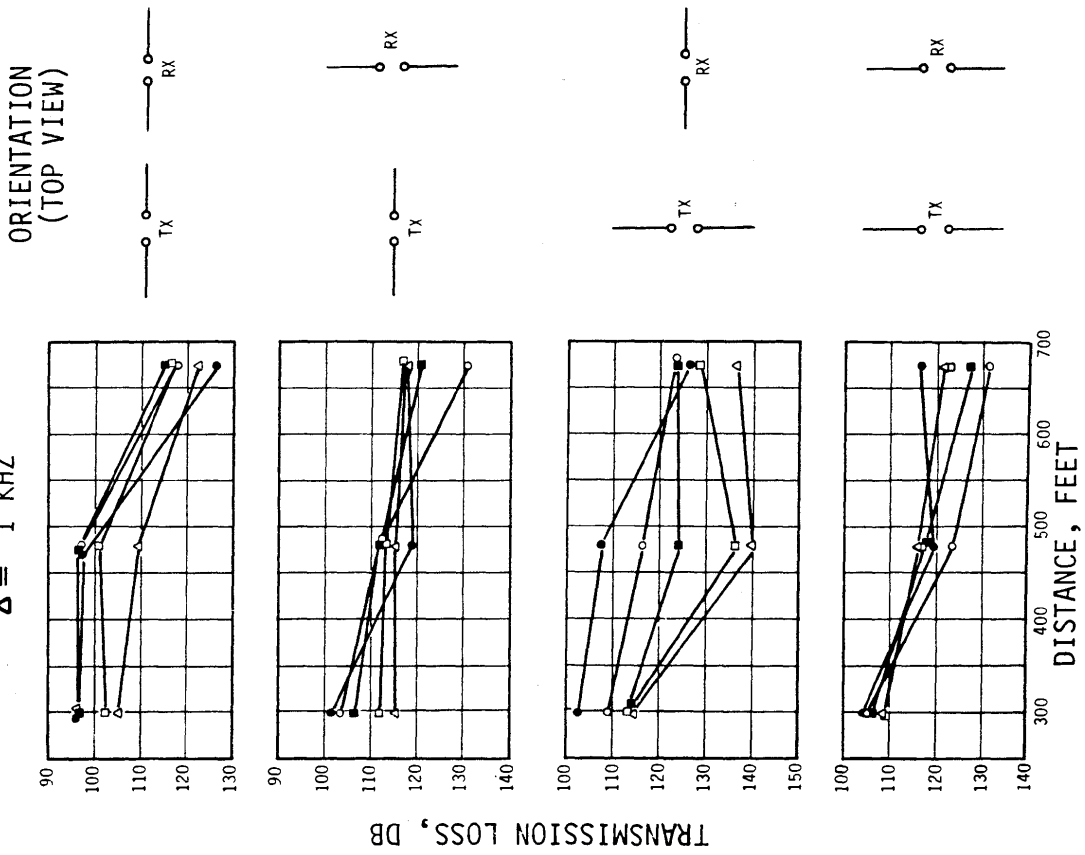


FIG. 9 - VLF TRANSMISSION LOSS FOR ROOF-BOLT ANTENNAS

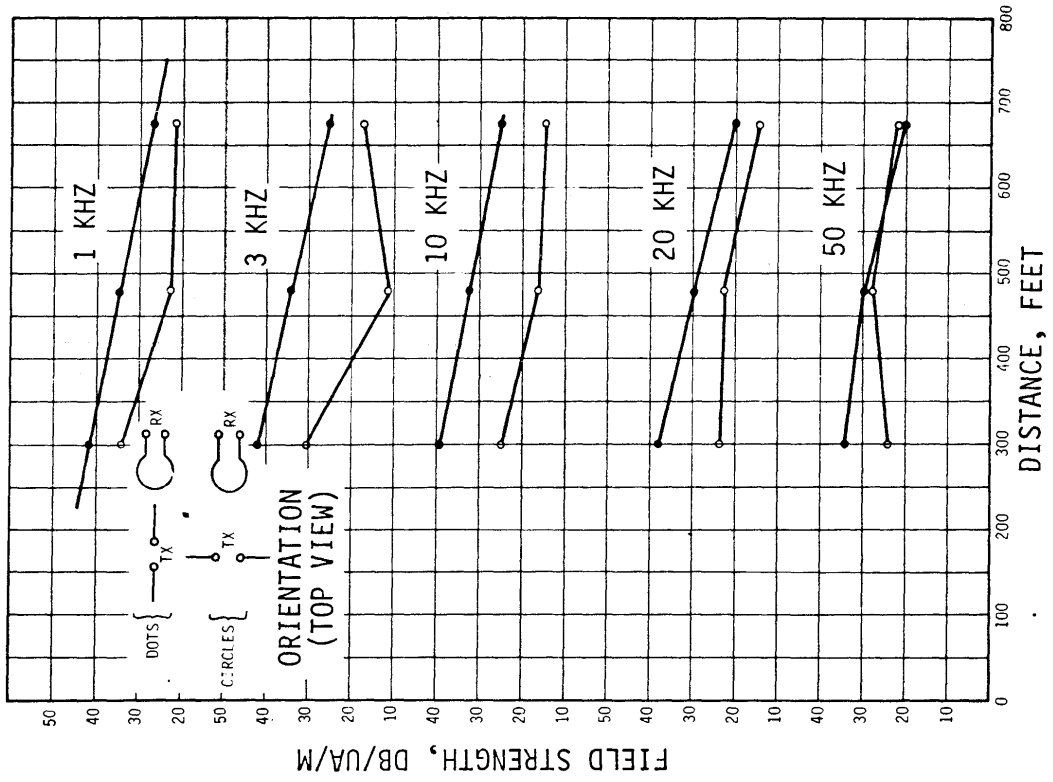


FIG. 10 - VLF FIELD STRENGTH FOR ROOF-BOLT ANTENNA

PERFORMANCE OF MANPACK ELECTROMAGNETIC LOCATION EQUIPMENT IN TRAPPED MINER LOCATION TESTS

by

A. J. Farstad

Westinghouse Georesearch Laboratory
8401 Baseline Road
Boulder, Colorado 80303

1.0 Introduction

The use of radio signals for underground communications was considered as early as the mid-1920's [1] - [4] . However, early experiments did not produce promising results with the type of equipment that was available then [5] . With advancements in solid state technology many of the schemes considered impractical in the early days suddenly became practical.

The properties of electromagnetic wave behavior in conducting media have been intensively studied by Wait [6] and others and can be utilized not only in communication with trapped miners, but also as a means of locating their position. This report deals with the development of portable electromagnetic equipment, powered by the miner's conventional lamp battery, which can be used to alert surface rescue personnel of the trapped miner's location. The Westinghouse Georesearch Laboratory (WGL) under BUMINES sponsorship initially approached the trapped miner location problem using seismic techniques. It was learned from this effort that two serious shortcomings of seismic techniques are (1) the extremely weak signals available on the surface from miner generated hammer blows, requiring long processing times at the surface receiver, and (2) the relatively slow procedure of deploying geophone arrays to sense the seismic uplink signals. By contrast, the electromagnetic techniques have proven much more practical from a deployment time standpoint and in most cases have also proven to be more accurate in determining location. Furthermore, these techniques have been successfully tested using a receiver in a helicopter for reconnaissance purposes. However, before any electromagnetic location technique can become fully operational, the miners themselves must be equipped with emergency transmitters to be carried with them on each work shift. Consequently, much emphasis has been placed on the development of extremely lightweight transmitting equipment. The performance of some of the electromagnetic location equipment developed by Westinghouse will be described in the following sections.

2.0 Basic Concepts

Theoretical concepts for locating magnetic dipoles in the earth have been treated by Wait [7] and Olsen [8] . A generalized curve for the attenuation of magnetic fields in a conducting half-space is derived from

Wait's work [7] and is shown in Figure 1. This curve applies only to fields directly above or directly beneath a transmitting source. Experimental verification of the validity of the theory is shown in Figure 2 which compares actual field measurements obtained over the Imperial Mine near Boulder, Colorado with the theoretical curve based on Wait's theory. The value of conductivity used in determining the theoretical curve was obtained from a dipole-dipole conductivity sounding taken over the Imperial Mine.

While the vertical magnetic field over vertical magnetic dipole source reaches a maximum directly over the source, the corresponding horizontal magnetic field experiences a null as shown by the example in Figure 3. This curve was obtained at the Rainbow No. 7 Mine in Rock Springs, Wyoming and depicts close agreement between the measured and calculated field profiles for both the vertical and horizontal fields. This was a relatively shallow (136 feet) mine, and the resulting signal-to-noise ratios at the surface were, in most cases, greater than 40 dB. However, the preliminary equipment used to obtain this data was not sufficient to obtain usable location data at the deeper mines of 500 feet and greater. Consequently, Westinghouse Georesearch Laboratory, under BuMines sponsorship, embarked on a development program aimed at producing portable equipment which would be operable at mine depths as great as 1500 feet. Since geometric spreading accounts for an (inverse distance)³ roll-off of field strength and increased losses in the earth at greater depths could account for up to 40 dB additional attenuation, we were faced with the problem of dealing with signal strengths as much as 100 dB down from those observed in the shallow mine tests. The equipment development and the results of the deep mine field tests are described in the following sections.

3.0 Description of Equipment

3.1 Operating Frequency

It is well known that low frequencies penetrate conductive material better than high frequencies. However, there are also other factors to consider in choosing the best frequency for an uplink electromagnetic location system, among which are (1) natural and man-made background noise, (2) availability of circuit components, (3) suitability of circuit miniaturization, and (4) permissibility restrictions in coal mines. Figure 4 shows a family of curves of expected field strength parametric in mine depth and superimposed on expected atmospheric noise levels for different seasons of the year. Based on signal-to-noise ratio alone, the optimum frequency for a 1500 foot (457 meter) mine would be on the order of 350 Hz. However, in most mining districts, there are strong harmonic interference fields from power lines which make frequencies this low difficult to use in a practical system. Consequently, to avoid the power line interference, our choice of frequencies was considerably higher, covering the band from 900 Hz to 2900 Hz.

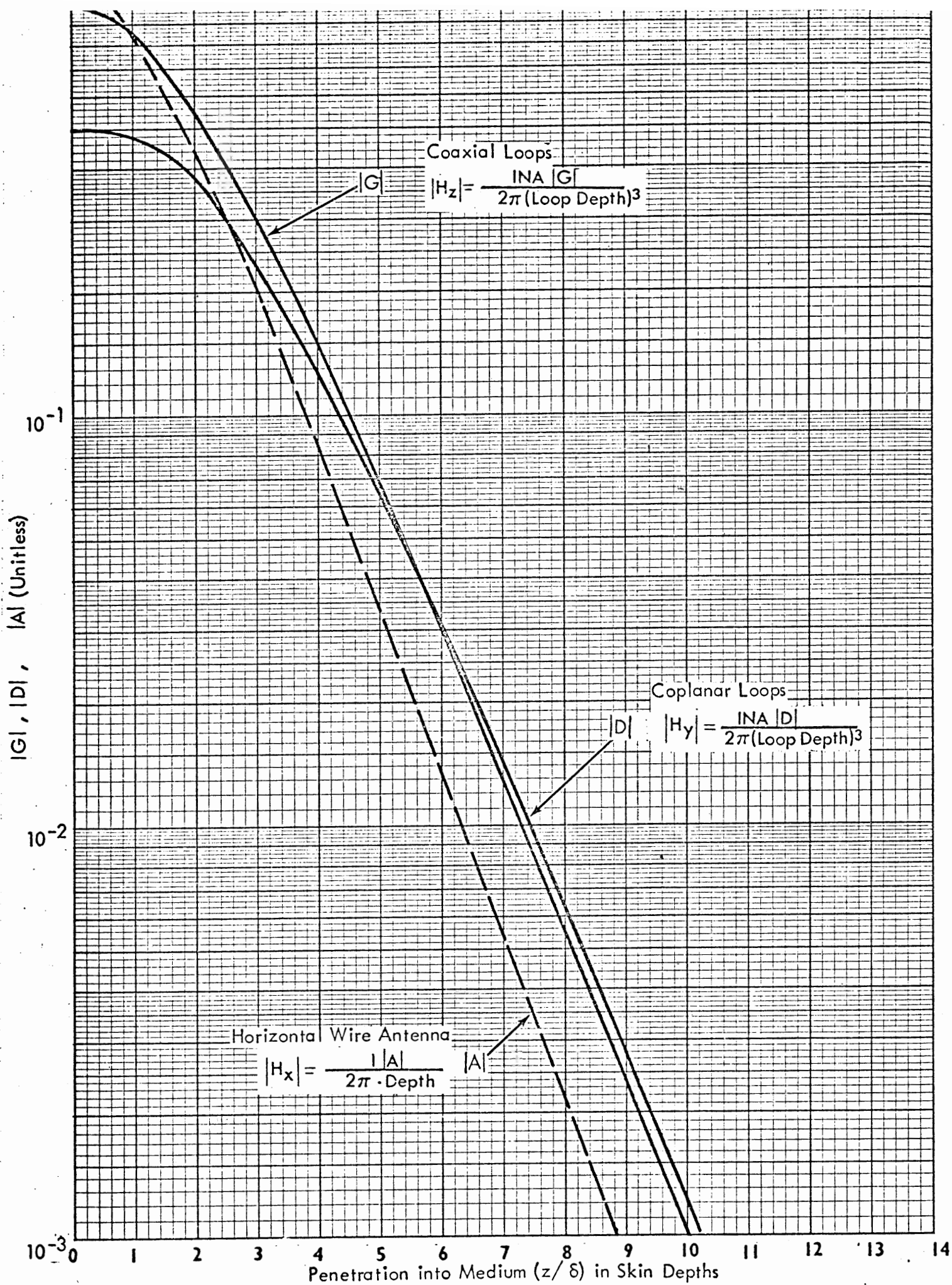


Figure 1. Loop Antenna and Horizontal Coupling Relationships

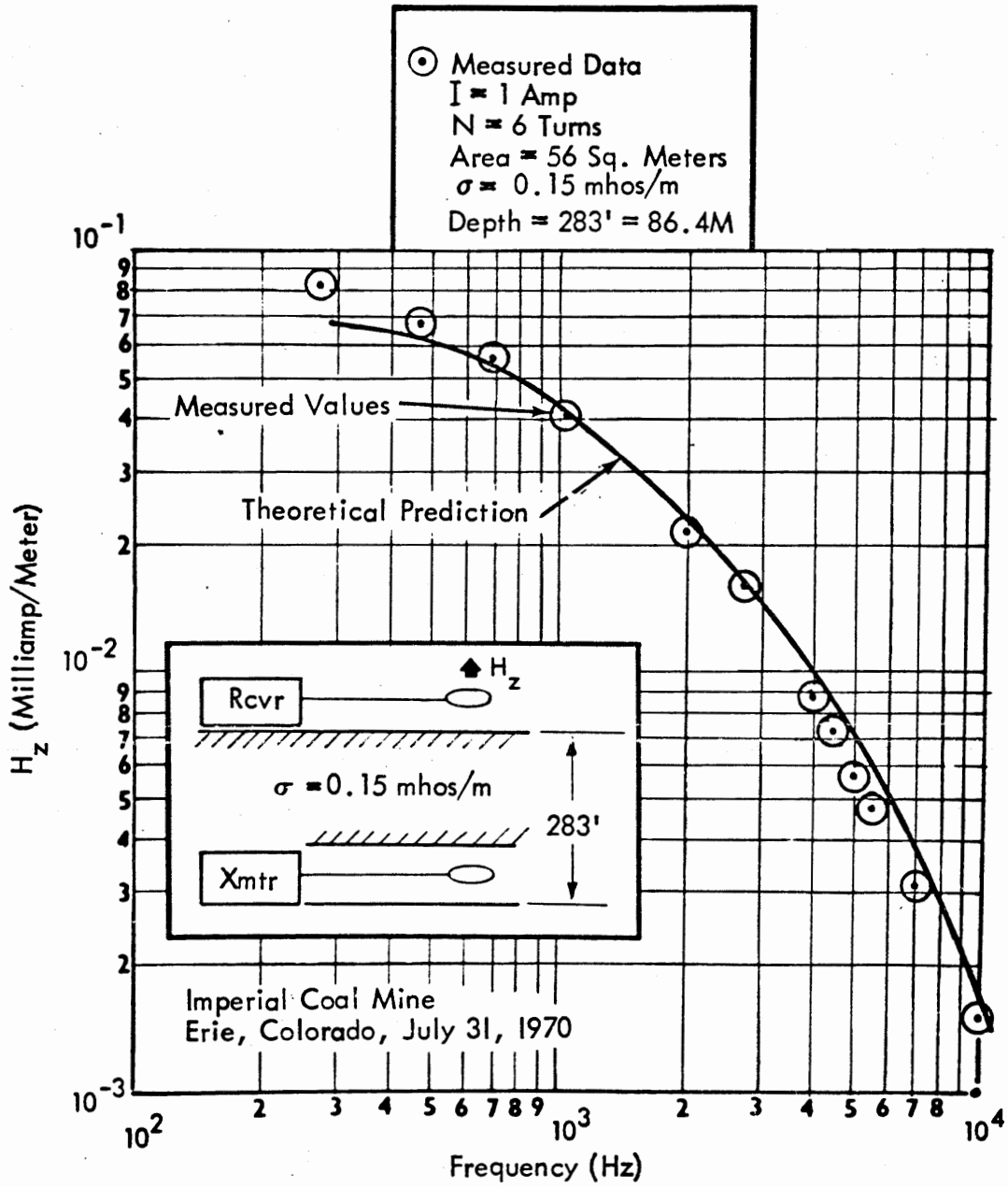


Figure 2. Comparison of Measured Magnetic Field With Theoretical Prediction for Beacon (Uplink) System

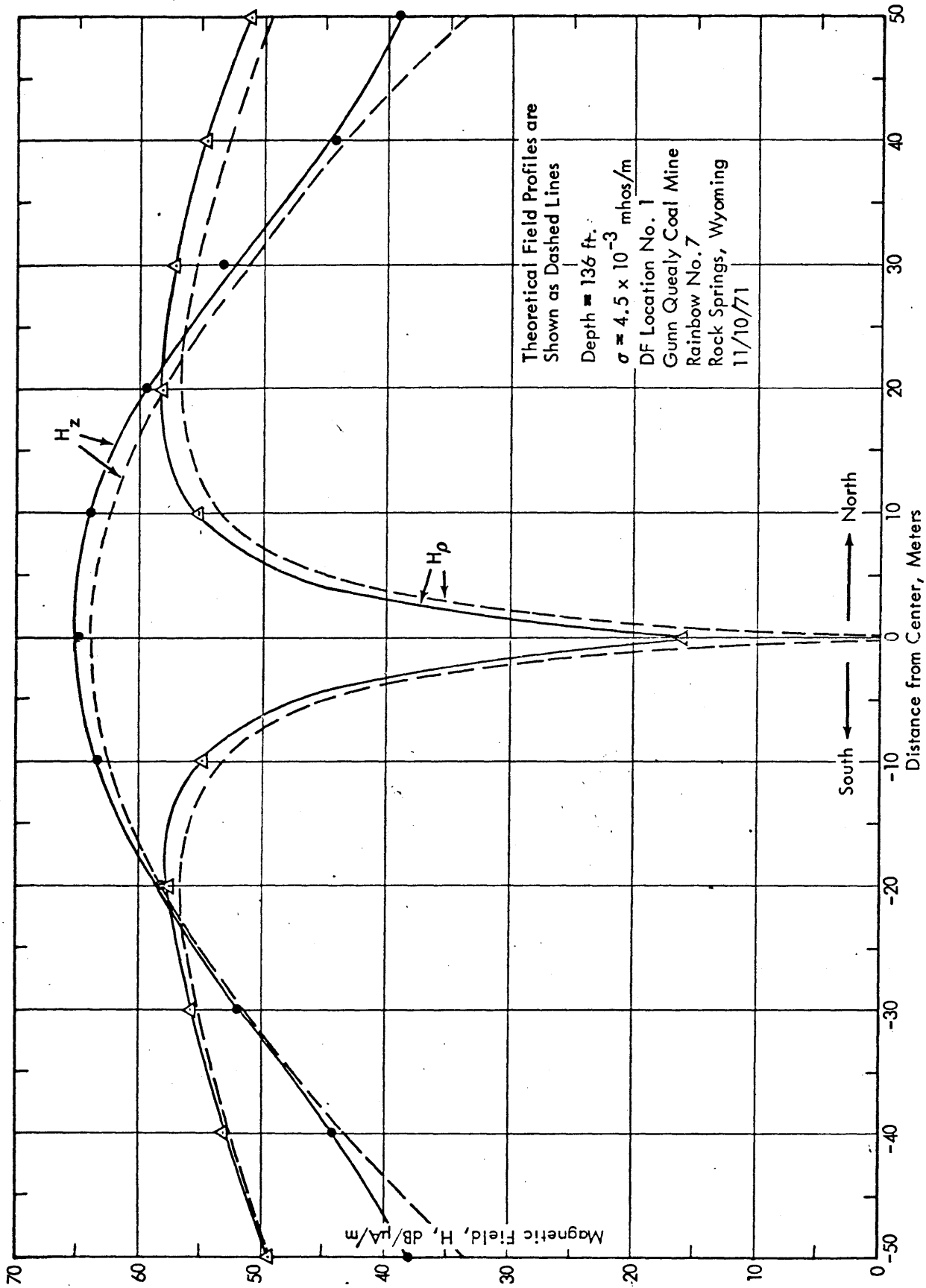
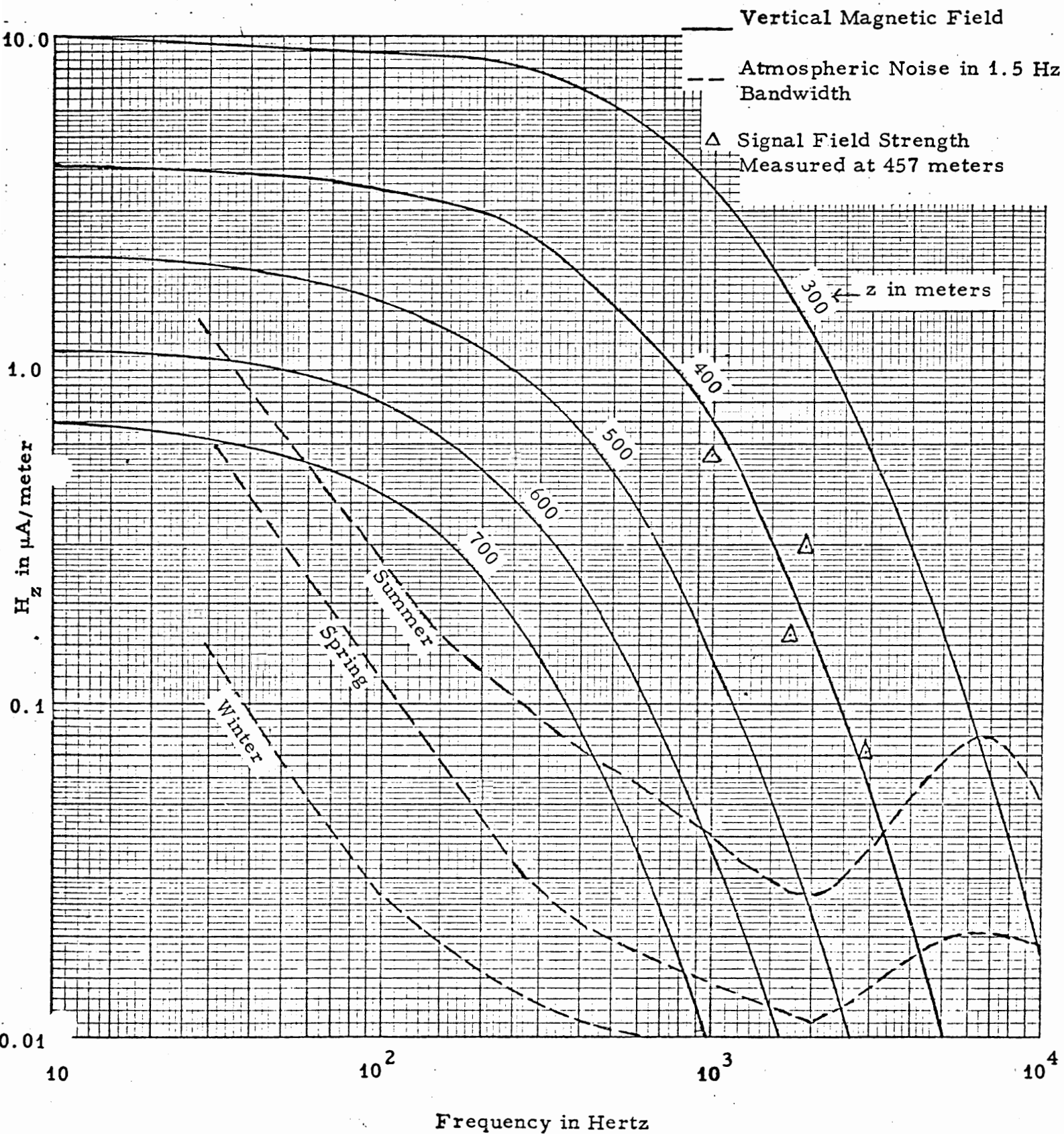


Figure 3 Electromagnetic Surface Pattern from Buried VMD
(North-South Profile)

Figure 4. Signal and Atmospheric Noise Field Estimates for Geneva Mine.
 Estimates for Geneva Mine.
 ($\sigma = 2.7 \times 10^{-2}$ mhos/meter²)
 INA = 2000 amp-turn-meters².)



3.2 Manpack Transmitter

The initial development of a manpack location transmitter resulted in a half-wave system packaged inside the miner's battery cap. The transmitting antenna consisted of a 100 foot flat ribbon conductor wound into a tape measure enclosure. Upon deployment, the two-conductor cable was laid out in the form of a circle on the mine floor and connected to the output terminals of the transmitter. Several amperes of rms current were fed into the loop antenna at a duty cycle of 200 milliseconds on and 2 seconds off. It was discovered during tests at the Robena #4 coal mine in Pennsylvania that the system would operate continuously for greater than 72 hours and still be detectable through nearly 1000 feet of overburden. A later version of this transmitter utilized essentially the same on-off duty cycle but incorporated a full-wave push-pull arrangement in the output stage during each 200 millisecond tone burst. With the full-wave transmitter, a tuning capacitor was inserted in series with the antenna at the higher frequencies (1700 Hz - 2900 Hz) giving an increase in current of up to 3 times that of the untuned equivalent. The full-wave transmitter was tested at the Geneva Mine in Dragerton, Utah and generated transmitter moments of up to 2000 ampere-turn-meters squared using a 500 foot length of No. 12 wire wound around a coal pillar as an antenna.

3.3 Manpack Locator

The portable receiver used to measure the magnetic field profiles on the surface utilizes a tuned air core receiving loop followed by a six stage tuned amplifier with a gain of approximately 105 dB and an overall sensitivity of 0.02 μ A/meter. The bandwidth of this receiver is approximately 0.2% of the tuned frequency. It has a phone jack output which can be used for hook up to earphones for null detection purposes or a portable oscilloscope for measuring field strength profiles.

3.4 Multichannel Receiver

The multichannel receiver consists of six narrowband receiver circuits tuned to different frequencies and packaged in a common enclosure. The outputs of each channel are selectively summed together in a summing amplifier to drive a set of earphones. Also, each channel is individually metered on the front panel. This receiver was designed primarily for helicopter reconnaissance work but also is useful for ground search operations. The antenna used with the multichannel receiver is a 24" square loop with 600 turns of No. 28 wire. A built-in battery operated preamp is included in the antenna enclosure to drive the 35 foot connecting cable between the antenna, towed beneath the helicopter, and the receiver in the helicopter cabin.

4.0 Test Results

4.1 Robena No. 4 Mine, Waynesburg, Pennsylvania

Table 1 outlines the results of the tests conducted at the Robena Mine No. 4 near Waynesburg, Pennsylvania. The overburden at this mine ranged from 725 feet to 990 feet at the location chosen for the tests. Comparison of surveyed locations with locations determined by the electromagnetic null were mostly in agreement within less than 50 feet. This is considered sufficient location accuracy for practical mine rescue applications. Helicopter tests were also conducted here and demonstrated a horizontal detection range of about 1000 feet while flying at an elevation of 100 feet over a location with 725 feet of overburden.

4.2 Geneva Mine, Dragerton, Utah

Tests at the Geneva Mine represented the severest test to the use of the electromagnetic location system of any coal mine visited to date. Not only was the overburden depth considerably greater than the mines in the Eastern coal region, but also the conductivity was higher ($\sigma \approx 2 \times 10^{-2}$ mhos per meter), and the terrain more rugged. The feasibility of using intrinsically safe manpack transmitters in the mine with signals detectable from a helicopter over 1500 feet of overburden was clearly demonstrated. Oscilloscope photographs of the receiver output, recorded in the helicopter, are shown in Figure 5. Location accuracies at this mine were not as good as anticipated but were in most cases within 1 or 2 coal blocks (150-300 ft) of the actual source. Some ambiguities were uncovered in the null technique when operating in extremely rugged terrain such as this. These ambiguities, which consist of secondary nulls, have been verified by comparison with theoretical profiles for the Geneva Mine conditions.

5.0 Conclusions

Results of field tests conducted under "worst case" conditions have demonstrated the feasibility of using through-the-earth electromagnetic signals for detection and location of trapped miners equipped with manpack transmitters. Furthermore, the prototype receiving equipment is lightweight and easy to operate suggesting that unskilled personnel could be used in rescue search operations. Helicopter reconnaissance using a multichannel receiver and a towed loop and preamplifier provides a rapid means of determining the existence and general location of signals emanating from the mine. Signal reception at the mine portal provides another quick method of detecting the existence of signals. Precise location of EM sources over hilly terrain is sometimes hampered by profile ambiguities and secondary nulls. Further research is needed to develop techniques for resolving these ambiguities in the field.

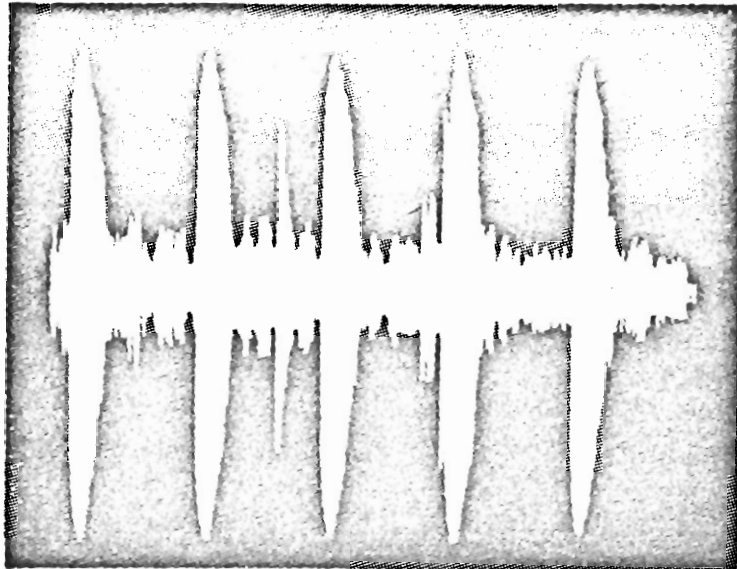
TABLE 1

Results of Robena Mine Tests

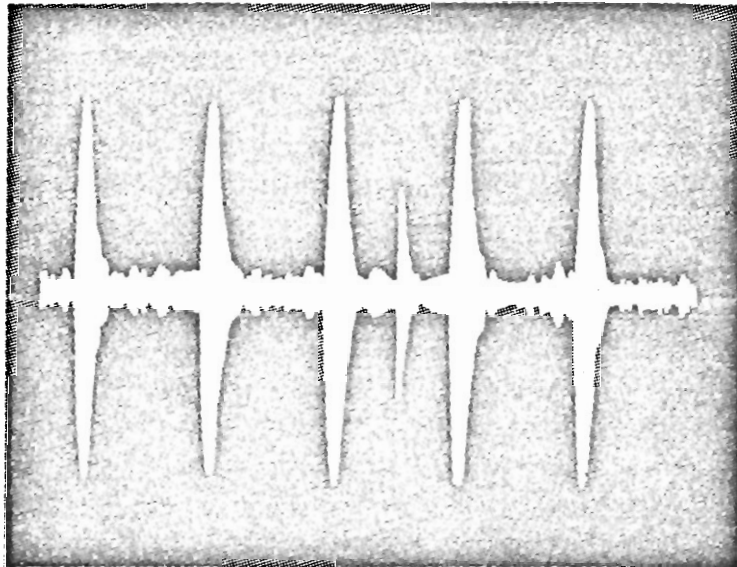
Location	f	Transmitting Antenna	Overburden	Slope	Field Strength*	Uncorrected Location Error	Horizontal Detection Range	Corrected Location Error
A	2070	#10 Wire	800 ft.	16°	-5dB/ μ A/m	18 ft.	1125 ft.	27 ft.
B	2010	4 Manpack Antennas	725 ft.	0 - 13°	-14dB/ μ A/m	27 ft.	390 ft.	27' - 3'
C	3030	#10 Wire	725 ft.	0 - 13°	-3dB/ μ A/m	50 ft.	890 ft.	50' - 2'
D	4050	4 Manpack Antennas	990 ft.	16°	-26dB/ μ A/m	8 ft.	360 ft.	67'
E	2070	#10 Wire	990 ft.	16°	-15dB/ μ A/m	17 ft.	800 ft.	58'

* Represents relative field strength indication on the output meter. For pulsed signals, this meter indication is about 20dB low.

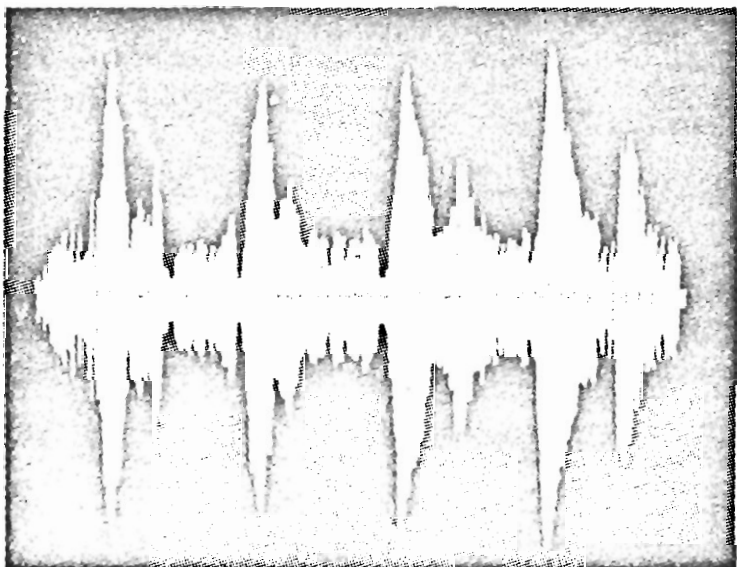
Location	Undetectable Signals	Comments
F	2010 Single Manpack Antenna	800 ft. 16° Power Line within 200 ft.
G	3030 " "	800 ft. 16°
H	4050 " "	725 ft. 13° Power Cables and metal Pipes Running up both Sides of Entry.



$f = 922.5 \text{ Hz}$
 $d = 1400 \text{ feet}$
 $\text{Alt.} = 100 \text{ feet}$



$f = 1900 \text{ Hz}$
 $d = 1150 \text{ feet}$
 $\text{Alt.} = 100 \text{ feet}$



$f = 982.5 \text{ Hz}$
 $+ 2900 \text{ Hz}$
 $d = 1500 \text{ feet}$
 $\text{Alt.} = 100 \text{ feet}$

Figure 5. Received Signals from Multichannel Receiver in Flight

6.0 Acknowledgments

The work described in this paper was prepared by Westinghouse Georesearch Laboratory, 8401 Baseline Road, Boulder, Colorado 80303 under USBM Contract No. H0220073 and H0232049. The contract was initiated under the Coal Mine Health and Safety Research Program. It was administered under the technical direction of the Pittsburgh Mining and Safety Research Center with Mr. H. E. Parkinson acting as the technical project officer. Mr. G. Honold was the contract administrator for the Bureau of Mines.

7.0 References

- [1] C. L. Colburn, C. M. Bouton, and H. B. Freeman, "Underground signaling with radio sets," U. S. Bureau of Mines, R. I. 2407, 1922.
- [2] J. J. Jakosky, "Radio as a method of underground communication in mines," U. S. Bureau of Mines, R. I. 2599, 1924.
- [3] J. J. Jakosky and D. N. Zellers, "Factors retarding transmission of radio signals underground, and some further experiments and conclusions," U. S. Bureau of Mines, R. I. 2561, 1924.
- [4] J. J. Jakosky and D. N. Zellers, "Line radio and effects of metallic conductors on underground communications," U. S. Bureau of Mines, R. I. 2682, 1925.
- [5] L. C. Ilsley, H. B. Freeman, and D. N. Zellers, "Experiments in underground communication through earth strata," U. S. Bureau of Mines, T. P. 433, 1928.
- [6] J. R. Wait, Electromagnetic Waves in Stratified Media, Pergamon Press, 1962.
- [7] J. R. Wait, "Criteria for Locating an Oscillating Magnetic Dipole Buried in the Earth," Proc. IEEE, Vol. 59, No. 6, pp. 1033-1035, June, 1971.
- [8] R. G. Olsen and A. J. Farstad, "Electromagnetic Direction Finding Experiments for Locating Trapped Miners," to be published in "IEEE Transactions on Geoscience Electronics," October, 1973.

FIELDS OF A MAGNETIC DIPOLE EXCITED BURIED CYLINDER

Allen Q. Howard, Jr.
U. S. Dept. of Commerce
Institute for Telecommunication Sciences
Office of Telecommunications
Boulder, Colorado 80302

Abstract

An approximate solution to the electromagnetic boundary value problem consisting of a horizontal cylindrical conductor buried in a lossy half-space and excited by an arbitrarily oriented magnetic dipole is found using an iterative perturbation technique in a double Fourier transform space. This model is used to gain insight into the anomalous fields due to strong scatterers such as pipes or tracks which would be in close proximity to an EM mine rescue operation. The novel three-dimensional aspect of the problem (i. e., the source) imposes the complexity that the current in the cylinder is not uniform. The field expressions are ideally suited to evaluation using FFT algorithm.

Introduction

The electromagnetic response of an inhomogeneous half-space continues to be a subject of high interest because of its direct application to EM prospecting techniques, mine rescue operations, and location of buried gas or water pipes. By in large, with the notable exceptions of D'Yakonov (1959), and Hill and Wait (1973), the theory applied to this class of problems has been restricted to two-dimensional time harmonic analyses. For example, the February '71 issue of Geophysics was devoted entirely to numerical solutions of this type. The comparatively simple sub-case consisting of an idealized buried cylindrical inhomogeneity has also received considerable attention (D'Yakonov (1959), Wait (1972), and Howard (1972)). We comment that D'Yakonov published no numerical results; the approximate iterated perturbation method due to Wait, which accounted for the interaction of the air-earth interface and the induced axial monopole current is readily evaluated. Numerical results based on Wait's method have been shown to be in complete agreement with the integral equation solution of Howard (1972). All three of these solutions are two-dimensional since the primary excitation in each case is taken to be a uniform line current parallel to the cylinder.

Herein, we consider a three-dimensional extension of these solutions. That the extension is non-trivial is attested by the effort involved in considering such problems in the absence of the air-earth

interface (Wait, 1960). Thus, the uniform line source is replaced by a more realistic arbitrarily oriented magnetic dipole in the earth. This introduces several complications. The most serious are that we now need a two-dimensional transform representation and the problem is now intrinsically vector. The vector nature requires either the introduction of both electric and magnetic potentials (Wait (1958), Weaver (1970)) or the appropriate Green's function dyadic (Tai (1971)). For an arbitrary cylinder, the relevant two-dimensional Fourier integral dyadic can be used with a vector integral equation formalism. It is, under certain conditions, permissible and much simpler to by-pass the integral equation technique and use a perturbation analysis.

Thus, to keep the problem tractable, we will assume that the cylinder is perfectly conducting and electrically small so that only an axial surface current density has appreciable excitation. This allows us to perform a perturbation analysis similar to that of Hill (1970) and Wait (1972) to obtain an iterated approximant of the axial surface current. Note that in so doing, the features of an air-earth interface and an arbitrarily oriented magnetic dipole are not compromised. Hence, the problem remains three-dimensional; however, the simplifying assumptions divide the problem into three almost completely independent parts - each one of which is a well-defined boundary value problem.

As an overview, we give in section two a two-dimensional Fourier integral representation of the magnetic loop in a half-space. With an eye to the application of this "incident" field, we represent the resulting interface fields in terms of magnetic and electric vector potentials parallel to the cylinder axis which is introduced in the following step. In the third section, we obtain the zeroth order surface current on the cylinder which includes the "over and down" mode coupling. This is done for one spectral component of the incident field - i. e., an arbitrarily polarized plane wave constituent.

Then, in the fourth section, we obtain the interface dependent potentials for a given axial surface current. It then becomes a straightforward matter to iterate the correction to the surface current starting with the zeroth order current obtained in the previous section. The anomalous fields are, of course, written in terms of the potentials derived in section four.

II. Two-Dimensional Fourier Integral Incident Field

Here we consider the well-known problem of a magnetic dipole in a half-space. Our application, however, requires us to look at the problem afresh. The geometry is given in Figure 1.

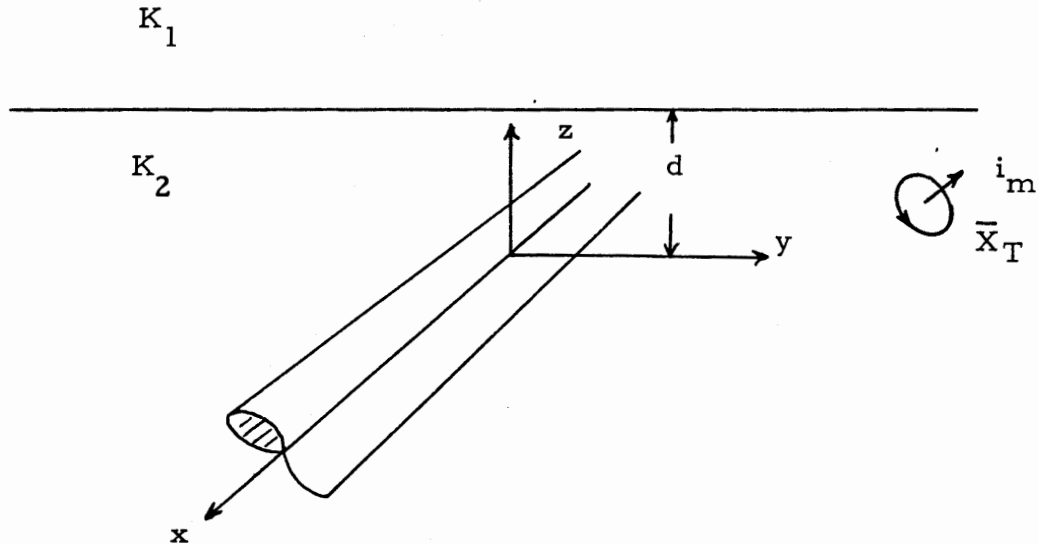


Figure 1. Scattering geometry.

Our solution is not standard in that for numerical reasons, it is preferable to use Cartesian coordinates, and the potentials are conveniently chosen parallel to the cylinder axis. We require a solution then to

$$\begin{aligned} \nabla \times \bar{H} &= -i\omega \epsilon'_2 \bar{E} & \epsilon'_2 &= \epsilon_2 + i\sigma_2/\omega \\ \nabla \times \bar{E} &= i\omega\mu_0 (\bar{H} + \bar{M}) \end{aligned} \quad (2.1)$$

by way of the potentials \bar{F} and \bar{A} , i.e.,

$$\begin{aligned} \bar{H} &= 1/\mu_0 \nabla \times \bar{A} + \frac{1}{\mu_0 K_2} \nabla \times \nabla \times \bar{F} \\ \bar{E} &= \frac{i\omega}{K_2} (\nabla \times \bar{F}) + \frac{1}{K_2} \nabla \times \nabla \times \bar{A} \end{aligned} \quad (2.2)$$

For an elementary magnetic dipole, \bar{M} is given by

$$\bar{M} = \bar{m} \delta(\bar{x} - \bar{x}_T), \quad \bar{m} = I_0 d A \bar{i}_m \quad (2.3)$$

Now for a homogeneous space $\bar{A} = 0$ and

$$\bar{F} = \bar{F}_0 = k_2 \mu_0 \bar{m} \frac{e^{ik_2 R}}{4\pi R}, \quad R = |\bar{x} - \bar{x}_T| \quad (2.4)$$

This, in the representation required, is also written

$$\bar{F}_0 = \frac{ik_2 \mu_0 \bar{m}}{8\pi^2} \int_{-\infty}^{\infty} \frac{d^2 K}{K_z^-} e^{i\bar{K} \cdot (\bar{x} - \bar{x}_T)} \quad , \quad K_z = (K_x^2 - K_y^2 - K_z^2)^{1/2} \\ \text{Im}(K_z) \geq 0 \\ z - z_T \geq 0 \quad (2.5)$$

where $d^2 K = dK_x dK_y$

To account for the interface at $z = d$, we define

$$\bar{F} = \begin{cases} \bar{F}_0 + \bar{F}^- & z \leq d \\ \bar{F}^+ & z > d \end{cases} \quad \bar{A} = \begin{cases} \bar{A}^- & z \leq d \\ \bar{A}^+ & z > d \end{cases} \quad (2.6)$$

where

$$\bar{F}^\pm = \bar{i}_x \int d^2 K f^\pm(K^\pm) e^{iK^\pm \cdot \bar{x}} \\ K^\pm = (K_x, K_y, \pm K_z^\pm) \quad (2.7)$$

The pertinent solution is

$$a^- = \frac{i e^{2iK_z^- d}}{K_z^-} \left\{ [K_z^- K_x^2 - K_z^+ K_y^2] [K_z^2 f_0^{(2)} - K_y \bar{K} \cdot \bar{f}_0] \right. \\ \left. + K_x K_y K_z^2 [K_z^- f_0^{(1)} - K_x f_0^{(3)}] + K_x K_y [(K_z^2 f_0^{(1)} - K_x \bar{K} \cdot \bar{f}_0) \right. \\ \left. (K_z^+ + K_z^-)] \right\} / [K_y^2 K_z^2 + K_z (K_x^2 K_z^- - K_z^+ K_y^2)] \quad (2.8)$$

where

$$\bar{f}_0 = \frac{ik_2 \mu_0 \bar{m}}{8\pi^2 K_z^-} e^{-i\bar{K} \cdot \bar{x}_T}$$

III. Zeroth Order Surface Current

We now consider the interaction of a plane-wave constituent of the previous section with the cylinder surface current. Basically, we require a transverse vector cylindrical wave expansion of a plane wave constituent of the "incident" field.

$$\bar{E}^{\circ} e^{i \cdot \bar{x}} = \int_{-\infty}^{\infty} d\lambda \int_{-\infty}^{\infty} dh \sum_{n=0}^{\infty} (a_n \bar{M}_{en\lambda}^{(1)} + b_n \bar{N}_{en\lambda}^{(1)}) \quad (3.1)$$

$$\bar{M}_{en\lambda}^{(j)} = \nabla \times (\psi_{en\lambda}^{(j)}(h) \hat{i}_x), \quad \bar{N}_{en\lambda}^{(j)}(h) = \frac{\nabla \times \bar{M}_{en\lambda}^{(j)}}{(\lambda^2 + h^2)^{1/2}}$$

$$\psi_{en\lambda}^{(j)}(h) = Z_n^{(j)}(\lambda \rho) \cos n \varphi e^{ihx}, \quad Z_n^{(1)}(\cdot) = J_n(\cdot), \quad Z_n^{(3)}(\cdot) = H_n^{(1)}(\cdot)$$

The M and N functions are orthogonal; it is easy to solve (3.1) for a_n and b_n . Now again we match boundary fields, this time at the cylinder surface. Thus let

$$\bar{E}_s(\bar{x}) = \sum_0^{\infty} (c_n \bar{M}_{enk\rho}^{(3)}(\mathbf{K}_x) + d_n \bar{N}_{enk\rho}^{(3)}(\mathbf{K}_x)) \quad (3.2)$$

and one finds

$$c_n = -(J_n^{(1)}(\alpha)/H_n^{(1)}(\alpha)) a_n, \quad d_n = -(J_n(\alpha)/H_n^{(1)}(\alpha)) b_n \quad (3.3)$$

$$= K_\rho a, \quad K_\rho = (k_2^2 - K_x^2)^{1/2}$$

The surface current in amperes/meter on a perfectly conducting body is proportional to the total magnetic intensity H, i.e.,

$$\hat{n} \times \bar{H} = \bar{K} \Big|_{\rho=a}, \quad \hat{n} = \hat{i}_\rho \quad (3.4)$$

This condition yields the zeroth order transformed axial surface current density

$$K_x^{\circ}(K_x, K_y) = \frac{-2 [\bar{K} \times (\bar{K} \times \bar{E}^{\circ})] \cdot \hat{i}_x}{K_\rho^2 \pi \mu_0 a H_0^{(1)}(K_\rho a)} \quad (3.5)$$

where
$$\bar{E}^{\circ} = -\frac{\omega}{K_2} \left[\bar{K} \times (\bar{f} + \bar{f}_0) + \frac{i}{K_2} \bar{K} \times (\bar{K} \times \bar{a}) \right] \quad (3.6)$$

Hence (3.5) becomes

$$\begin{aligned}
K_x^{\circ}(K_x, K_y) &= \frac{2i \{ a^- - i k_z \bar{K} \cdot (\hat{i}_x \times \bar{F}_0) \}}{\pi a \mu_0 H_0^{(1)}(K_p a) K_p^2} \\
&= K_{x2}^{\circ}(K_x, K_y) + K_{x1}^{\circ}(K_x, K_y) \quad (3.7)
\end{aligned}$$

Define

$$\begin{aligned}
K_{x1}^{\circ}(K_x) &= \int_{-\infty}^{\infty} K_{x1}^{\circ}(K_x, K_y) dK_y \\
&= \frac{k_z^2 e^{-i k_x x_T} H_0^{(1)}(K_p \rho_T) (m_y |z_T| + m_z |y_T|)}{4\pi^2 K_p a H_0^{(1)}(K_p a) \rho_T}, \quad \rho_T = (y_T^2 + z_T^2)^{1/2} \quad (3.8)
\end{aligned}$$

Note that K_{x1}° is the interface independent zeroth order axial surface current transform. The interface term $K_{x2}^{\circ}(K_x)$ is unfortunately a numerical integral.

IV. Iterated Current and Anomalous Fields

We now temporarily assume the current is known; i.e.,

$$\bar{J}(\bar{x}') = \hat{i}_x K_x(x') \delta(\rho' - a) \quad (4.1)$$

The excitation potential for this section is thus

$$\bar{A}^{\circ} = \mu_0 \int_R G_0(\bar{x}, \bar{x}') \bar{J}(\bar{x}') d^3 x' \quad (4.2)$$

Now, substituting (4.1), and G_0 as given by (2.5) into (4.2), and carrying out the spatial integrations gives

$$\bar{A}^{\circ} = \int e^{i\bar{K} \cdot \bar{x}} \bar{a}^{\circ}(\bar{K}) d^2 K, \quad \bar{a}^{\circ} = \hat{i}_x \frac{i \mu_0 a}{2 K_z^2} K^{\circ}(K_x) J_0(K_p a) \quad (4.3)$$

Again, we now introduce potentials A^{\pm} , F^{\pm} , match fields across the interface and obtain in the quasi-static approximation

$$a^-(\bar{K}) = Q(\bar{K}) a^{\circ}(-), \quad Q(\bar{K}) = e^{2i k_z d} \frac{[f(\bar{K}) - k_z^2 k_y^2]}{[f(\bar{K}) + k_z^2 k_y^2]}$$

$$f(\bar{K}) = k_z [(k_z^+ - k_z^-) k_x^2 - k_z^2 k_z^+] \quad (4.4)$$

Thus, the air-earth interface to first order modifies the potential

amplitude a^0 ; it becomes $(1 + Q) a^0$. In fact, the iteration is equivalent to a geometric series which formally can be summed to give as an infinite iterant $a^0/(1 - Q)$. Thus, the corrected potential \bar{A} is given by

$$\bar{A} = \int d^2K \frac{a^0}{1 - Q} \left\{ e^{i\bar{K}\uparrow \cdot \bar{x}} + Q e^{i\bar{K}\downarrow \cdot \bar{x}} \right\} \quad (4.5)$$

and the surface current is, from (3.4),

$$K_x(x) = 1/\mu_0 \partial/\partial \rho \langle A \rangle \Big|_{\rho=a}, \langle A \rangle = \frac{1}{2\pi} \int_0^{2\pi} A(\bar{x}) d\varphi \quad (4.6)$$

It turns out that since Q is exponentially small for large K_y , the averaging integral and the K_y integral do not commute; hence, we first subtract out the asymptotic limit to the integral (4.5) and add it on in integrated form giving

$$K_x(K_x) = i\alpha J_0(\alpha) K_x^0(K_x) \left[J_1(\alpha) P(K_x, d) + \pi/2 H_1^{(1)}(\alpha) \right] \quad (4.7)$$

where

$$\alpha = K_\rho a, \quad P(K_x, d) = \int_{-\infty}^{\infty} dK_y \frac{Q}{K_z^- (1-Q)}$$

An important limiting case of (4.8) is when $d \rightarrow \infty$, then $P \rightarrow 0$; it can be shown that the remaining term is then identical to the exact expression in the absence of the interface. Using the key result (4.7), the anomalous magnetic field H_a in the lower half-space is given in terms of the potentials A^0 , A^a , and F^- .

$$\bar{H}_a(\bar{x}) = \bar{H}_a^0(\bar{x}) + \bar{H}_a^i \quad (4.8)$$

where H^0 depends on the interface only through the current (it corresponds to A^0 with iterated current (4.7)). In particular

$$H_{ax}^0 = 0, \quad H_{ay}^0 = -z/\rho h^0, \quad H_{az}^0 = y/\rho h^0 \quad (4.9)$$

where

$$h^0 = ia \int_0^{\infty} \cos(K_x x) K_x(K_x) J_0(K_\rho a) H_1^{(1)}(K_\rho \rho) K_\rho dK_x \quad (4.10)$$

The H_a^i term is given by A^- , F^- through (2.2). For completeness these potential coefficients are determined to be

$$a^- = \frac{i\mu_0 a}{z K_z^-} K_x(K_x) J_0(K_\rho a) Q(K)$$

$$f^- = - \frac{\mu_0 k_z a k_x k_y Q(k) k_x(k_x) J_0(k_p a)}{f(\bar{R}) + k_y^2 k_z^2}$$

(4.11)

This completes the formal solution to our problem.

References

- D'Yakonov, B. P., 1959, The diffraction of electromagnetic waves by a circular cylinder in a homogeneous half-space: Bull. Acad. Sci. U.S.S.R., Geophys. Ser., n. 9, p. 950-955.
- Hill, D. A., 1973, The electromagnetic response of a buried sphere for buried dipole excitation (to be published).
- Wait, J. R., 1972, The effect of a buried conductor on the subsurface fields for line source excitation: Radio Science, n. 7, p. 587-591.
- Howard, A. Q., Jr., 1972, The electromagnetic fields of a subterranean cylinder inhomogeneity excited by a line source: Geophysics, v. 37, n. 6, p. 975-984.
- Wait, J. R., 1959, Some solutions for electromagnetic problems involving spheroidal, spherical and cylindrical bodies, J. of Res., v. 64B, n. 1, p. 15-32.
- Hill, D. A., and Wait, J. R., 1972, Electromagnetic scattering of a small spherical obstacle near the ground, Can. J. Phys., v. 50, n. 3, p. 237-243.
- Hill, D. A., 1970, Electromagnetic scattering concepts applied to the detection of targets near the ground: Ph.D. dissertation, Ohio State University, Columbus, Ohio.
- Weaver, J. T., 1970, The general theory of electromagnetic induction in a conducting half-space: Geophysics. J. R. Astr. Soc., v. 22, p. 83-100.
- Tai, C. T., 1971, Dyadic Green's functions in electromagnetic theory: Intext Educational publishers, San Francisco, California.

Acknowledgment

This research was sponsored in part by the U.S. Bureau of Mines. The author is indebted to Dr. J. R. Wait for his help in carrying out this research.

THE ELECTROMAGNETIC RESPONSE OF A BURIED SPHERE FOR BURIED DIPOLE EXCITATION*

D. A. Hill and J. R. Wait
U. S. Department of Commerce
Office of Telecommunications
Institute for Telecommunication Sciences
Boulder, Colorado 80302

Introduction

The feasibility of locating a buried vertical magnetic dipole source (horizontal loop) from surface measurements of the vertical and horizontal magnetic field components has been investigated by Wait (1971). For sufficiently low frequencies, the magnetic fields have a simple static-like behavior, and a single observation of the ratio and relative phases of the vertical and horizontal field components is sufficient for location when the earth is homogeneous. However, when inhomogeneities are present, the surface fields will be modified, and source location may be more difficult.

In order to obtain a quantitative idea of the surface field modifications, we consider a spherical conducting zone as a perturbation to the homogeneous half-space. A rigorous solution for the buried sphere problem has been formulated by D'Yakanov (1959). Unfortunately, his solution is restricted to azimuthally symmetric excitation, and even then the solution is not in a convenient computational form. However, if the sphere is electrically small and is located at a sufficient distance from both the dipole source and the interface, the scattered fields can be identified as the secondary fields of induced dipole moments. The latter are equal to the product of the incident fields and the polarizabilities of the sphere. The details of the approach are given by Hill and Wait (1973).

Wait (1968) has used this induced dipole moment approach for scattering by a small sphere above a conducting half-space. The method has the advantage that it is easily generalized to scatterers of other shapes for which both the electric and magnetic polarizabilities are known, such as spheroids (Van de Hulst, 1957). This concept has

*The research reported here was supported by the U.S. Bureau of Mines, Pittsburgh Mining and Safety Research Center.

also been considered by Ward (1967) in the context of electromagnetic detection of massive sulfide ore bodies from airborne platforms.

Induced Dipole Moments

The geometry of the situation is shown in Figure 1. The buried sphere has radius a , conductivity σ_s , permeability μ_s , and permittivity ϵ_s .

Although the distances involved are much less than a free-space wavelength, they are not necessarily small compared with a wavelength in the lower half-space. Consequently, the induced electric dipole moment must be considered as well as the induced magnetic dipole moment. The unperturbed magnetic field has both horizontal and vertical components at the sphere center, H_x^0 and H_y^0 , and the unperturbed electric field has only a horizontal component, E_y^0 . The components can be obtained from Wait (1951; 1971), Banos (1966), or Ward (1967). The induced magnetic dipole moments, m_x and m_y , are given by the product of the magnetic polarizability and the unperturbed magnetic field (Wait, 1960; 1968). The induced electric dipole moment, p_y , is given by the product of the electric polarizability and the unperturbed electric dipole moment (Van de Hulst, 1957; Wait, 1960).

In order that higher order multipoles are not important, it is necessary that the sphere radius is small compared to both the wavelength in the lower half-space (Stratton, 1941) and the geometric mean of the source and observer distances (Wait, 1960). The sphere radius must also be small compared to the depth so that interactions between the sphere and the interface are not important. Actually, interface interaction terms have been computed for a buried cylinder (Wait, 1972), but the interaction terms are more complicated for a sphere because of coupling between the electric and magnetic dipole modes (Hill, 1970). In the static limit, the interaction has shown to be unimportant for a sphere-interface separation of at least two sphere radii (Hill and Wait, 1972).

Surface Fields

The total magnetic field at the surface is the sum of the vertical magnetic dipole source field and the reradiated fields of the dipole moments induced in the sphere. The fields of buried vertical and horizontal magnetic dipoles are given by Wait (1971; 1972), and the fields of a buried horizontal electric dipole are given by Wait (1961) and Banos (1966).

The actual calculations involve the evaluation of numerous Sommerfeld type integrals which must be done numerically. However, all of the integrals can be evaluated in closed form in the zero-frequency limit. If these limiting forms are subtracted, the convergence of the remaining integrals is significantly improved. These static limits may even be of direct interest if the frequency is sufficiently low. In the static limit the contribution from the electric dipole moment goes to zero, but the contribution from the magnetic dipole moment goes to zero only for a non-magnetic ($\mu_s = \mu_o$) sphere (Ward, 1959).

Discussion and Conclusions

A computer program was written to calculate the magnitude and phase of the ratio of the vertical and horizontal magnetic field components at the earth's surface. These are the measurable quantities which Wait (1971) has suggested for location of the vertical magnetic dipole source. For spheres of radius less than .2 times the source depth, the change in surface fields are found to be insignificant. For a sphere of radius .3 times the source depth located at half the source depth, some noticeable changes in the surface fields begin to occur. However, resultant errors in source location should still be small.

Larger errors can be expected when the sphere is either larger or closer to the source or interface, but the simplified theory presented here is not valid under such conditions. The study of such cases is a worthwhile extension.

REFERENCES

- Banos, A., 1966, Dipole radiation in the presence of a conducting half-space: Oxford, Pergamon Press.
- D'Yakonov, B. P., 1959, The diffraction of electromagnetic waves by a sphere located in a half-space: Bull. Acad. Sci. USSR, Geophys. Ser., v. 11, p. 1120-1125.
- Hill, D. A., 1970, Electromagnetic scattering concepts applied to the detection of targets near the ground: Ph.D. dissertation, Ohio State University, Columbus, Ohio.
- Hill, D. A. and Wait, J. R., 1972, Electromagnetic scattering of a small spherical obstacle near the ground: Can. J. Phys., v. 50, No. 3, p. 237-243.

- Hill, D.A. and Wait, J.R., 1973, The electromagnetic response of a buried sphere for buried dipole excitation, Preliminary Report to U.S. Bureau of Mines.
- Stratton, J.A., 1941, Electromagnetic theory: New York, McGraw-Hill Book Co., Inc.
- Van de Hulst, H.C., 1957, Light scattering by small particles: New York, John Wiley and Sons.
- Wait, J.R., 1951, The magnetic dipole over the horizontally stratified earth: Can. J. Phys., v. 29, p. 577-592.
- Wait, J.R., 1960, On the electromagnetic response of a conducting sphere to a dipole field: Geophysics, v. 25, No. 3, p. 649-658.
- Wait, J.R., 1961, The electromagnetic fields of a horizontal dipole in the presence of a conducting half-space, Can. J. Phys., v. 39, p. 1017-1028.
- Wait, J. R., 1968, Electromagnetic induction in a small conducting sphere above a resistive half-space: Radio Sci., v. 10, No. 3, p. 1030-1034.
- Wait, J.R., 1971, Criteria for locating an oscillating magnetic dipole buried in the earth: Proc. IEEE, v. 59, No. 6, p. 1033-1035.
- Wait, J. R., 1972, The effect of a buried conductor on the subsurface fields for line source excitation: Radio Sci., v. 7, No. 5, p. 587-591.
- Ward, S.H., 1959, Unique determination of conductivity, susceptibility, size, and depth in multifrequency electromagnetic exploration: Geophysics, v. 24, p. 531-546.
- Ward, S.H., 1967, Electromagnetic theory for geophysical applications: Chapt. II, Pt. A in Mining Geophysics, v. 2 (ed. by D.A. Hansen, et al): Tulsa, Oklahoma, Society of Exploration Geophysicists.

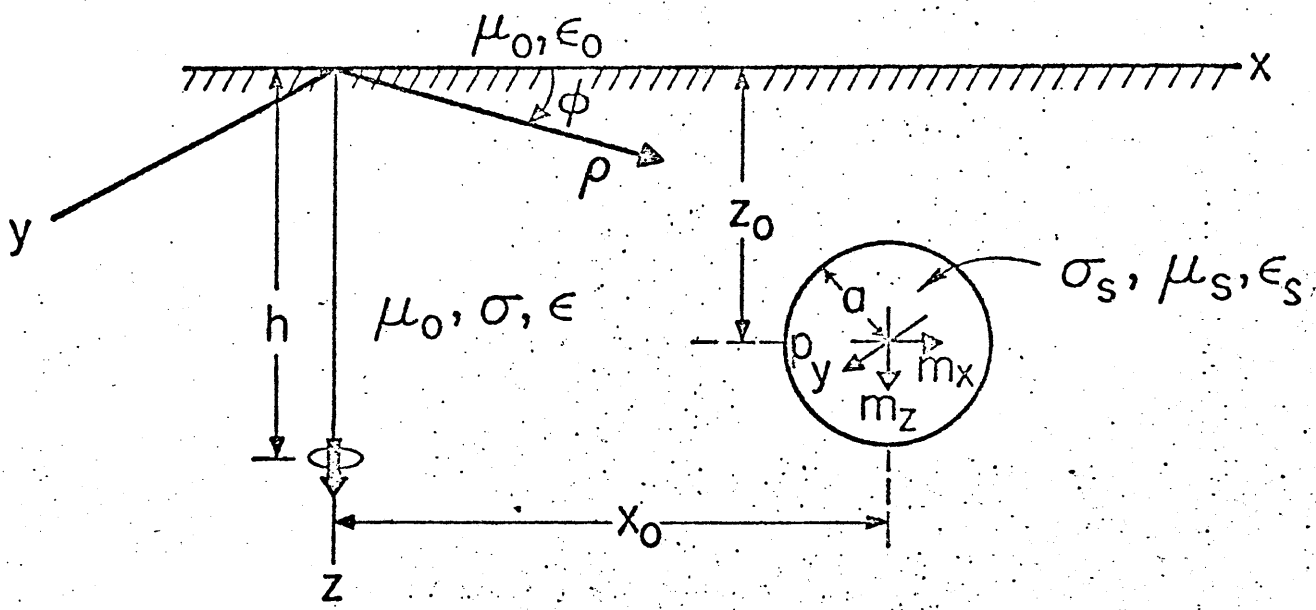


FIGURE 1. Geometry for source loop and buried sphere with induced dipole moments.

THE PERTURBATION OF ALTERNATING ELECTROMAGNETIC FIELDS BY THREE-DIMENSIONAL BODIES

F. W. Jones
Dept. of Physics and the Institute of Earth
and Planetary Physics
University of Alberta
Edmonton, Alberta, Canada

Abstract

The perturbation of alternating electromagnetic fields by three-dimensional structures is considered. The general model is that of a semi-infinite conducting half-space which consists of regions of different conductivities. A numerical method is used to obtain the solution for the equations and boundary conditions. The effects on the fields at the surface of the half-space due to the conductivity discontinuities are shown by three-dimensional amplitude and phase plots.

General Method

During the last year or so a numerical method has been developed for studying three-dimensional electromagnetic induction problems. The conductive structure of interest is defined over a three-dimensional mesh of grid points and a solution for the equations and boundary conditions is obtained by a finite iterative technique. By means of this method, the effects of buried anomalies have been studied (Jones and Pascoe, 1972) as well as islands and coastlines (Lines and Jones, 1973a,b) and cubic conductors (Jones, 1973) for uniform inducing fields.

The general method is described in detail by Lines (1972). If we neglect displacement currents as is normal for the slowly varying fields we wish to consider, and assume a time variation $\exp(i\omega t)$, we obtain from Maxwell's equations (in e. m. u.):

$$\nabla \times \nabla \times \vec{E} = -4\pi\sigma i\omega \vec{E} \quad (1)$$

or

$$\nabla^2 \vec{E} - \nabla(\nabla \cdot \vec{E}) = i\eta^2 \vec{E} \quad (2)$$

where $\eta^2 = 4\pi\sigma\omega$

Equation (2) must be solved in all regions. Also, the usual boundary conditions must be satisfied. This equation may be written as three scalar equations in Cartesian coordinates:

$$\frac{\partial^2 E_x}{\partial y^2} + \frac{\partial^2 E_x}{\partial z^2} - \frac{\partial}{\partial x} \left[\frac{\partial E_y}{\partial y} + \frac{\partial E_z}{\partial z} \right] = i\eta^2 E_x \quad (3)$$

$$\frac{\partial^2 E_y}{\partial x^2} + \frac{\partial^2 E_y}{\partial z^2} - \frac{\partial}{\partial y} \left[\frac{\partial E_x}{\partial x} + \frac{\partial E_z}{\partial z} \right] = i\eta^2 E_y \quad (4)$$

$$\frac{\partial^2 E_z}{\partial x^2} + \frac{\partial^2 E_z}{\partial y^2} - \frac{\partial}{\partial z} \left[\frac{\partial E_x}{\partial x} + \frac{\partial E_y}{\partial y} \right] = i\eta^2 E_z \quad (5)$$

In the method these equations are written in finite difference form and are solved simultaneously for E_x , E_y , and E_z at each point of the mesh by the Gauss-Seidel iteration technique.

The external boundaries of the mesh are set by assuming that the conducting half-space is uniform or uniformly layered there. That is, the external boundaries are placed far enough from any conductivity discontinuities so that the perturbations of the fields at the boundaries by such discontinuities will be negligible. Within the mesh the usual boundary conditions are employed. However, when discontinuities in conductivity are encountered, the mixed partial derivatives which arise from the $\nabla(\nabla \cdot \vec{E})$ term in (2) (and which insure the proper coupling of the three field components) are evaluated by central differences in the same manner as for the other derivatives. The component of \vec{E} normal to an abrupt boundary between conductivity regions will be discontinuous and such a discontinuity cannot be represented by a point value at the boundary. The use of a double mesh to accommodate all possible occurrences of double valued functions for the arbitrary models we wish to consider is prohibitive in computer time and cost. Therefore, at discontinuities the average of the values of the \vec{E} component normal to the boundary on either side of the discontinuity is used to represent the value at the boundary. When this is done, and the boundary conditions applied to \vec{E} , η^2 in the difference equations representing (3), (4), and (5) is replaced by $\bar{\eta}^2$, the average of η^2 for all the regions surrounding the point being considered. This implies that the conductivity discontinuity is represented by a transition zone from one conductivity region to the other. This is a reasonable approximation for geophysical situations. If the boundary is a transition zone from one conductivity region to the other, then \vec{J} ($=\sigma \vec{E}$) must be continuous, and if σ varies continuously through the transition, \vec{E} will vary as we have assumed.

After the electric field components are approximated by the Gauss-Seidel iterative technique, the magnetic field components are calculated by taking the curl of the electric field, i. e.,

$$\vec{H} = -\nabla \times \vec{E} / i\omega \quad (6)$$

A model of geophysical interest is shown in Fig. 1. This is an anomaly embedded in a half-space. This anomaly is just below the surface and $\sigma_1 = 10 \sigma_2$. The source field is such that \hat{E} is polarized in the x-direction. In Fig. 2 are shown three-dimensional plots of the amplitudes and phases of the electric field components over the surface of the conducting region. The magnetic field components are shown in Fig. 3. From these figures it is clear that the uniform fields are considerably perturbed by the presence of the buried anomaly.

References

- Jones, F. W., and Pascoe, L. J., 1972, Geophys. J.R.A.S., v. 27, p. 479-485.
- Jones, F. W., 1973, Submitted for publication.
- Lines, L. R., 1972, A numerical study of the perturbation of alternating geomagnetic fields near island and coastline structures: Thesis, Dept. of Physics, University of Alberta.
- Lines, L. R., and Jones, F. W., 1973a, Geophys. J.R.A. S., v. 32, p. 133-154.
- Lines, L. R., and Jones, F. W., 1973b, Can. J. Earth Sci., v. 10, p. 510-518.

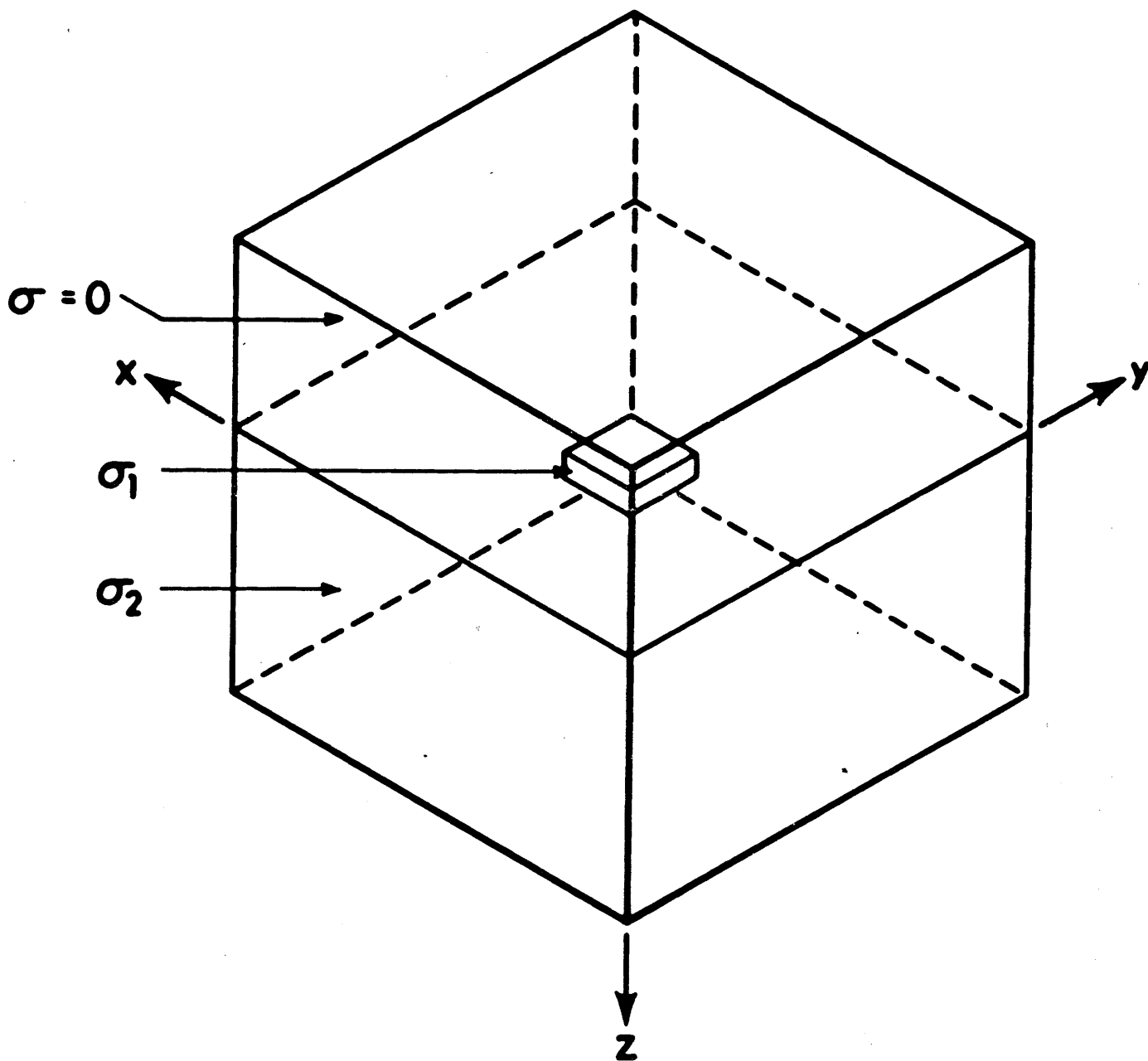
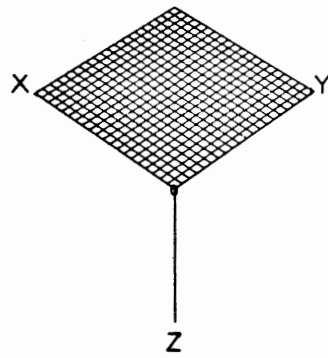
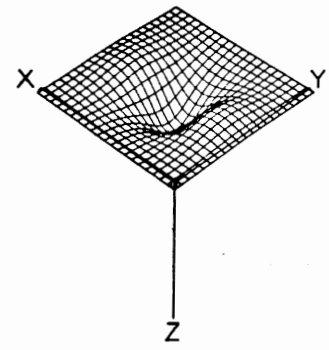


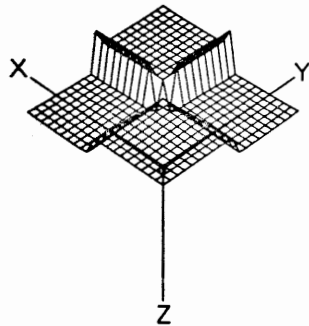
Fig. 1. The general three-dimensional model
(from Jones and Pascoe, 1972)



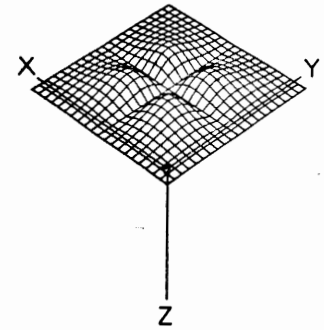
PHASE OF EX



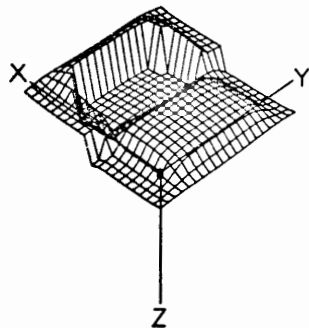
AMPLITUDE OF EX



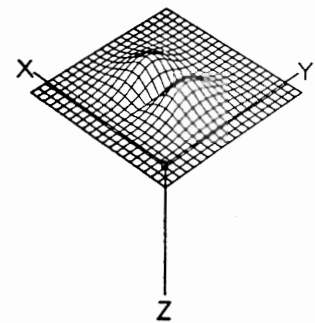
PHASE OF EY



AMPLITUDE OF EY

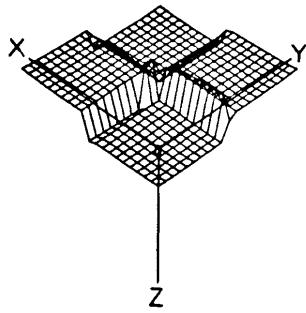


PHASE OF EZ

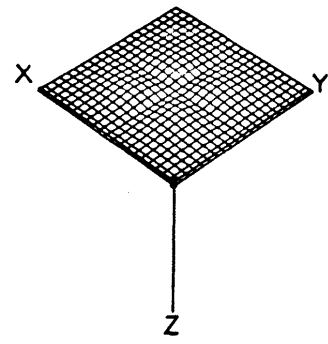


AMPLITUDE OF EZ

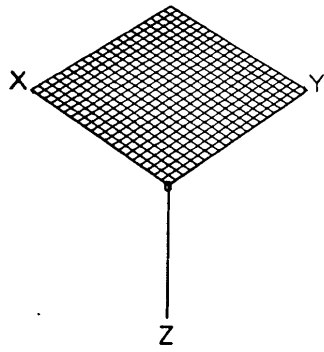
Fig. 2. Electric field component amplitudes and phases for the model as in Fig. 1, for $\sigma_1 > \sigma_2$. (From Jones and Pascoe, 1972).



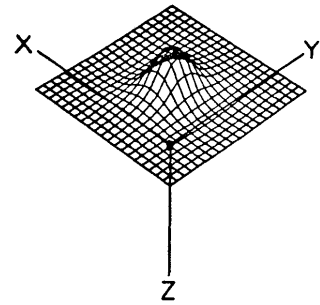
PHASE OF HX



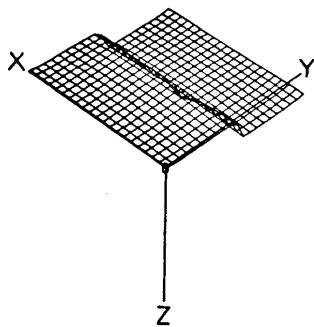
AMPLITUDE OF HX



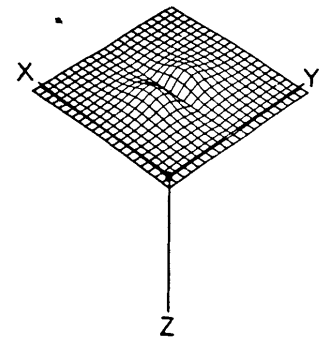
PHASE OF HY



AMPLITUDE OF HY



PHASE OF HZ



AMPLITUDE OF HZ

Fig. 3. Magnetic field component amplitudes and phases for the model as in Fig. 1. for $\sigma_1 > \sigma_2$. (From Jones and Pascoe, 1972).

A DISCUSSION ON THE THREE-DIMENSIONAL BOUNDARY VALUE PROBLEM FOR ELECTROMAGNETIC FIELDS

David Rankin
Institute of Earth and Planetary Physics
Dept. of Physics
University of Alberta
Edmonton , Alberta

Three-dimensional boundary value problems are difficult to solve. Indeed, while the separation of the scalar wave equation can be effected in 11 different coordinate systems, an analytic solution requires that the boundaries, both external and internal, possess the same symmetry as the coordinate system. Numerical methods are thus of great importance for the solution of such problems; however, despite the availability of high-speed, large memory digital computers, the solution to a significant three-dimensional problem is by no means trivial. It is unfortunate that the results reported here by Jones are invalid.

Jones discusses a model in which a three-dimensional island lies off a linear coastline where all the interfaces lie in the coordinate planes in a Cartesian system. A downward plane em wave polarized with the electric field parallel to the linear coastline, and two of the islands coast, is incident downward. This, of course, requires that the incident electric field is perpendicular to the other faces of the idealized Cartesian island.

The significant equation used by Jones for his finite difference calculations is

$$\frac{\partial^2 E_x}{\partial y^2} + \frac{\partial^2 E_x}{\partial z^2} - \frac{\partial}{\partial x} \left[\frac{\partial E_y}{\partial y} + \frac{\partial E_z}{\partial z} \right] = i\eta^2 E_x$$

where $\eta^2 = \sigma\mu\omega$. σ is the conductivity, $\mu = \mu_0$ is the permeability of the appropriate medium, and ω is the angular frequency of a Fourier component of the incident field. We see that the displacement current term is omitted, which is an excellent approximation for the parameters of interest in this model. In the similar equation for the y-component of the diffusion equation, the same considerations which we are about to discuss are equally valid.

It can be seen from the equation that the field components are related and thus any errors introduced will be propagated into all three components. The difficulty arises when E_x or E_y is perpendicular to one or other of the surfaces of discontinuity in σ . The continuity of current at the air-earth interface (upper surface), e.g., j_y , requires

that E_y is discontinuous; i.e., $j_y = \sigma_1 E_{y1} = \sigma_2 E_{y2}$. Jones uses the average value of E_y at the interface in the belief that continuity of E_y is necessary in order to calculate $\partial E_y / \partial y$ in the first equation above. The calculations are made in the finite difference approximation. The result is that all the field components and the derivatives are grossly distorted in the region about the boundary and this distortion will be propagated outward into the surrounding regions. Since the magnetic field components are deduced from the electric through Maxwell's equations, they will also suffer a distortion. Self-consistency required that the correct electric field components are themselves deducible from the magnetic, clearly impossible in this case.

Furthermore, it is also necessary that if E_y is forced to be continuous, then j_y must be discontinuous. For the values used by Jones $j_{y1}/j_{y2} = \sigma_1/\sigma_2 = 4 \times 10^3$. This would be in clear violation of the continuity condition on j which is used explicitly by Jones in his work and would in turn require that

$$\nabla \cdot \vec{j} = -\partial \rho / \partial t = j_1 - j_2 = -\nabla \cdot \vec{\Delta D} / \partial t$$

which requires a by no means negligible displacement current.

The anti-skin effect and the nonzero values of E_z which Jones obtains at the air-earth interface may be due to a computer artifact as well as the incorrect computational procedures. In any event, the incorrect procedures could have been avoided since good numerical approximations can be obtained by taking one-sided derivatives of the discontinuous functions near the interfaces. The averaging of these derivatives would, of course, be a permissible procedure.

For a complete discussion of the nature of the discontinuity in the electric field in the two-dimensional case, see D'Erceville and Kunetz (1962). The relevance to the three-dimensional case is quite clear. The subject matter discussed here by Jones appears in the publications Jones and Pascoe (1972), Lines and Jones (1973a, 1973b), and Lines (1972).

References

1. D'Erceville, I., and Kunetz, G., 1962, The effect of a fault on the Earth's natural electromagnetic field: *Geophysics*, v. 27, p. 651-665.
2. Jones, F. W., and Pascoe, L. J., 1972, The perturbation of alternating geomagnetic fields by three-dimensional conductivity inhomogeneities: *Geophys. J. R. Astr. Soc.*, v. 27, p. 479-485.

3. Lines, L. R., and Jones, F. W., 1973, The perturbation of alternating geomagnetic fields by three-dimensional island structures: *Geophys. J. R. Astr. Soc.*, v. 32, p. 133-154.
4. Lines, L. R., and Jones, F. W., 1973, The perturbation of the alternating geomagnetic fields by an island near a coastline: *Can. J. Earth Sci.*, v. 10, n. 4, p. 510-518.
5. Lines, L. R., 1973, A numerical study of the perturbation of alternating geomagnetic fields near island and coastline structures: M. Sci. Thesis, University of Alberta.

REPLY TO: "A DISCUSSION ON THE THREE-DIMENSIONAL
BOUNDARY VALUE PROBLEM FOR ELECTROMAGNETIC
FIELDS" BY D. RANKIN

F. W. Jones
Dept. of Physics
Institute of Earth and Planetary Physics
University of Alberta
Edmonton, Alberta, Canada

I do not regard the criticism by Rankin of my work as valid or even meaningful. I strongly reject the assertion by Rankin that my results are invalid.

As stated in my paper, the equation to solve (in e.m.u.) is:

$$\nabla^2 \vec{E} - \nabla (\nabla \cdot \vec{E}) = i \eta^2 \vec{E} \quad (1)$$

where $\eta^2 = 4\pi\sigma\omega$. This may be rewritten as three scalar equations in Cartesian coordinates, one of which is

$$\frac{\partial^2 E_x}{\partial y^2} + \frac{\partial^2 E_x}{\partial z^2} - \frac{\partial}{\partial x} \left[\frac{\partial E_y}{\partial y} + \frac{\partial E_z}{\partial z} \right] = i \eta^2 E_x \quad (2)$$

The equation to be solved is the diffusion equation, and it is not appropriate to consider waves in this context.

In the method a point-wise solution to the problem is approximated. As discussed in my paper the approach taken at discontinuities in conductivity is to choose the normal component of \vec{E} at the discontinuity as the average of the normal components on either side of the discontinuity. This is similar to the well-known assumption made in obtaining Fourier series representations for piecewise continuous functions (Pipes, 1958; p. 51). In the geophysical problem this means that the discontinuity is approximated by a transition zone, which is a very good approximation for such cases. By using this approach, both the values of the function and its derivatives give a good estimate for those associated with the physical situation. It is not apparent and Rankin has not shown that "all the field components and the derivatives are grossly distorted in the region about the boundary" for geophysically realistic situations. He has given no evidence to support his assertion that the results are "invalid".

Although Rankin declares that one cannot calculate the electric components from the magnetic, in his discussion he has not stated why this is so. After once calculating the magnetic components the electric components may be calculated, but one must insure that the initial solution is accurate enough to prevent significant round-off errors.

REFERENCES

- D'Erceville, I. and Kunetz, G., 1962. The effect of a fault on the Earth's natural electromagnetic field. *Geophysics* 27, p. 651-665.
- Jones, F. W., 1973. Reply to the discussion by D. Rankin of the paper: "The perturbation of alternating geomagnetic fields by an island near a coastline" by L. R. Lines and F. W. Jones (*Can. J. Earth Sci.* 10, p. 510-518). *Can. J. Earth Sci.*, in press.
- Jones, F. W. and Pascoe, L. J., 1972. The perturbation of alternating geomagnetic fields by three-dimensional conductivity inhomogeneities. *Geophys. J. R. astr. Soc.* 27, p. 479-485.
- Jones, F. W. and Price, A. T., 1970. The perturbations of alternating geomagnetic fields by conductivity anomalies. *Geophys. J. R. astr. Soc.* 20, p. 317-334.
- Lines, L. R., 1972. A numerical study of the perturbation of alternating geomagnetic fields near island and coastline structures. M.Sc. Thesis, Dept. of Physics, Univ. of Alberta.
- Lines, L. R. and Jones, F. W., 1973a. The perturbation of alternating geomagnetic fields by three-dimensional island structures. *Geophys. J. R. astr. Soc.* 32, p. 133-154.
- Lines, L. R. and Jones, F. W., 1973b. The perturbation of alternating geomagnetic fields by an island near a coastline. *Can. J. Earth Sci.* 10, p. 510-518.
- Lines, L. R. and Jones, F. W., 1973c. Reply to the discussion by E. Nyland of the paper "The perturbation of alternating geomagnetic fields by an island near a coastline" by L. R. Lines and F. W. Jones (*Can. J. Earth Sci.* 10, p. 510-518, 1973). *Can. J. Earth Sci.*, in press.
- Nyland, E., 1973. The perturbation of alternating geomagnetic fields by and island near a coastline. Discussion. *Can. J. Earth Sci.*, in press.
- Pipes, L. A., 1958. *Applied Mathematics for Engineers and Physicists*. McGraw-Hill Book Co. Inc.

USE OF THE ZONAL HARMONIC SERIES FOR OBTAINING NUMERICAL SOLUTIONS TO ELECTROMAGNETIC BOUNDARY VALUE PROBLEMS

Richard L. Lewis
Office of Telecommunications
U. S. Department of Commerce
Institute for Telecommunication Sciences
Boulder, Colorado 80302

This is a discussion of the application of the zonal harmonic series to problems involving dipole sources in the vicinity of spherical boundaries. The application of a formal zonal-harmonic series solution to directly obtain numerical results involves two distinct problems: namely, the convergence of the series solution and the accurate calculation of the special functions involved in the series solution. Some interesting techniques will be introduced which help to improve the convergence properties of the series solution.

Introduction

The numerical techniques involved will be discussed in light of two distinct problems for which numerical summation of the zonal-harmonic series is especially applicable. In the first problem, we are interested in calculating the magnetic field wave-tilt on the surface of a spherical hill due to a buried magnetic dipole orientated in a vertical direction off of the axis of symmetry, as illustrated in figure 1. This problem has application to locating the position of a buried magnetic dipole source in hilly terrain from surface measurements of the field. The major distinction of this problem is that the spherical Bessel functions involved in the formal series solution all have complex arguments, of which more will be said later. The formal solution of this problem proceeds, incidentally, by summing the zonal harmonic series solution for an inclined dipole source and then performing a rotation of coordinates to align the dipole axis with the vertical. This leads to the interesting problem of relating the spherical coordinate θ' of the rotated sphere to the horizontal distance between two surface points that grow further apart (the distance X in figure 1) such that the bearing ψ from the source to the observer remains constant. Another problem of note is to obtain the magnitude and phase of the maximum component of the field in the horizontal plane when the two component fields are not necessarily in phase.

The second problem of interest is the application of the zonal harmonic series to the calculation of the fields in the earth-ionosphere waveguide due to a dipole source on the earth's surface. In the preceding problem, the frequency range is restricted to low enough values so that the zonal harmonic series was a natural consideration, and so it is also in the case of the earth-ionosphere waveguide for frequencies in the ELF or lower part of the VLF range. Nevertheless, it is frequently felt by many that the mode series solution is preferable for physical interpretation as well as for simplicity of computation. The former point cannot be argued, but the latter point is only valid when it is possible to oversimplify the problem, say by assuming the ionosphere reflection coefficient is nearly unity. When more realistic assumptions about the upper boundary are made, a mode theory solution requires a search for modes by some sort of iterative process¹, which can be more time consuming than summing the

series solution. One interesting analytical step that is utilized by both the contour integral formulation as well as zonal harmonics is to expand the denominator for each component of the series in a geometric series and then interchange the order of summation.² This has the advantage for mode theory that the ionosphere term is removed from the residue calculation, while for zonal-harmonics the convergence of the series is greatly improved. In each case, the outer series has the physical interpretation of wave-guide hops for which the series converges rapidly for VLF frequencies on up.

In the discussion of these two applications, the convergence of the series has been alluded to numerous times. Generally speaking, adequate convergence of the amplitude of the zonal harmonic series is attained by summing $10 \times ka$ terms, where $k = \frac{2\pi f}{c}$ is the wave number and a is the radius of the spherical boundary.³ Adequate convergence of the phase usually requires a 50% increase over that number of terms. A few techniques have been utilized to make minor improvements in the speed of convergence, such as noting that the Legendre polynomial is a cyclic function of the summation index and consequently selective grouping of the terms produces partial sums which can be averaged to give some improvement. However, the major technical problem is the calculation of the special functions, using recursion formula. The Legendre polynomial is well behaved,⁴ but not so the spherical Bessel functions. One spherical Bessel function increases asymptotically with the summation index, while the other decreases asymptotically. Consequently the functions must always be paired to avoid exponential underflow or overflow problems on the machine. This can involve some additional problems in arranging the Bessel functions as components in each term of the formal series solution. For the case of the Bessel function which decreases asymptotically with the index of summation, backward rather than forward recursion must be utilized. How far backwards one must recurse is always a problem, but for the case of Bessel functions of complex argument it is of significant practical interest to note that the starting point need not be an order which exceeds the magnitude of the argument, as is necessary for Bessel functions of real argument.⁵ This is of particular importance for calculating the fields below the surface, since there the wave number may be much greater than the free space wave number, with the consequence that the argument of the spherical Bessel function can be quite large. Fortunately, the calculation of the Bessel functions by recursion is not only fast but produces very accurate results since, for both forward and backward recursion, the numerical process converges naturally to the desired function.

Buried Magnetic Dipole Model

Having thus introduced the range of our investigation, we can proceed with introducing explicit expressions for a buried magnetic dipole in a spherical hill.

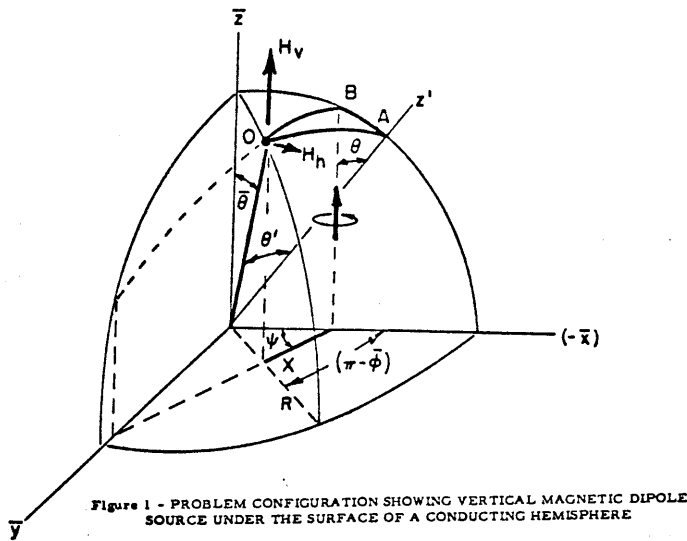


Figure 1 - PROBLEM CONFIGURATION SHOWING VERTICAL MAGNETIC DIPOLE SOURCE UNDER THE SURFACE OF A CONDUCTING HEMISPHERE

In figure 1 the z' axis forms a part of a rotated (x', y', z') coordinate system. The x' axis subtends an angle θ with the x axis, where θ is the dipole tilt angle. The y' and y axes are coincident. The corresponding spherical coordinates in the rotated coordinate system are R , θ' , and ϕ' , where the latter angle lies in a plane perpendicular to the z' axis. The formal series solution for the magnetic field components can easily be expressed in the rotated coordinate system. For convenience we introduce the abbreviations

$$\alpha = \cos \theta \quad \beta = \sin \theta$$

Thus, those terms multiplied by α denote the contribution to the fields due to the source component orientated along the z' axis, while those terms multiplied by β denote the contribution from that source component orientated parallel to the x' axis. The series solution for the component fields at the surface of the spherical hill is given by

$$\begin{aligned} H_R &= \frac{\alpha R}{R_0} \sum n(n+1)(2n+1) P_n(\cos \theta') a_n \\ &\quad - \beta \cos \phi' \sum (2n+1) P_n^1(\cos \theta') \frac{b_n}{u_n} \\ H_{\theta'} &= \frac{\alpha R}{R_0} \sum (2n+1) P_n^1(\cos \theta') a_n u_n \\ &\quad - \beta \cos \phi' \sum \frac{2n+1}{n(n+1)} \left[\frac{\partial P_n^1(\cos \theta')}{\partial \theta'} b_n + \frac{P_n^1(\cos \theta')}{\sin \theta'} c_n \right] \\ H_{\phi'} &= \beta \sin \phi' \sum \frac{2n+1}{n(n+1)} \left[\frac{P_n^1(\cos \theta')}{\sin \theta'} b_n + \frac{\partial P_n^1(\cos \theta')}{\partial \theta'} c_n \right], \quad (1) \end{aligned}$$

where R is the radius of the spherical hill (c.f. figure 1), R_0 is the radial distance to the dipole source, the index of summation is n , $P_n(X)$ is the Legendre polynomial of order n , the associated Legendre function is $P_n^1(\cos \theta) = \frac{\partial}{\partial \theta} P_n(\cos \theta)$, and we have

$$a_n = \frac{\psi_n(k_1 R_0)}{\psi_n(k_1 R)} / D_n \quad b_n = k_1 R \frac{\psi_n'(k_1 R_0)}{\psi_n(k_1 R)} \times u_n / D_n, \quad (2)$$

$$c_n = \frac{\psi_n(k_1 R_0) / \psi_n(k_1 R)}{u_n - \frac{k_2^2 R}{k_1} \ln[\psi_n(k_1 R)]} \times (k_2 R)^2, \quad (3)$$

where $D_n = u_n - k_1 R \ln[\psi_n(k_1 R)]$ (4)

$$\text{and } u_n = k_2 R \ln[\zeta_n^{(2)}(k_2 R)] = k_2 R \frac{\zeta_n^{(2)'}(k_2 R)}{\zeta_n^{(2)}(k_2 R)} \approx -n. \quad (5)$$

In the above, $\psi_n(x)$ is the spherical Bessel function of the first kind and $\zeta_n^{(2)}(x)$ is the spherical Hankel function of the second kind, the primes on the spherical Bessel functions denote differentiation with respect to the argument in parenthesis, k_1 is the complex wave number for propagation in the media inside the spherical hill, and k_2 is the free space wave-number exterior to the spherical hill. The dipole magnetic current normalization is $J_m d\ell = -j\omega\mu_0 R_0 A$, where A is the surface area of the sphere. Those terms in equations (1) containing a_n and b_n constitute contributions from the scalar magnetic potential, while those terms containing c_n are contributions from the scalar electric potential.

The summations indicated in (1) receive their maximum contribution from terms of the order of $n \approx |k_1 R|$. For orders of n much larger than this, we have $D_n \sim -2n$ and $\psi_n(k_1 R_0) / \psi_n(k_1 R) \sim (\frac{R_0}{R})^n$. Consequently, we can expect the magnitude of subsequent terms to decrease very rapidly. Moreover, if terms of order very much less than $|k_1 R|$ are removed from the summation there is negligible effect on the summation value. This, in conjunction with the fact that $k_2 R$ is quite small in most problems of interest, leads to the validity of the approximation in (5). Moreover, the contribution from the scalar electric potential term (3) can be expected to be small, so that to a first approximation the only term involving frequency in the expressions for the field is $k_1 R$. Consequently, it can be anticipated that the ratio of the source depth to skin depth, $H = \sqrt{\omega\mu_0 \sigma} \times d$, where d is the depth below point B to the source, is a significant parameter of the problem.

We can introduce the following asymptotic formula for the Legendre function,

$$P_n(\cos \theta) \sim \frac{2 \cos[(n + \frac{1}{2})\theta - \pi/4]}{[2\pi(n+1) \sin \theta]^{\frac{1}{2}}}, \quad (6)$$

which provides us with a suggestive means for grouping terms of the summation in order to improve the convergence properties of the series.³ Viewed as a function of the summation index n , equation (6) is nearly periodic of period $\frac{2\pi}{\theta}$. Consequently, terminating successive partial sums when the Legendre function changes sign and averaging only even numbers of such partial sums is equivalent to integrating (6) with respect to n over the period.

The practical question to be answered is how many terms are required for graphical accuracy. This is obviously a function of the ratio R_0/R as well as the value of $|k_1 R|$. Assuming that R_0/R is nearly unity and that the elevation angle of the observation point θ' lies well away from the extreme positions zero or pi, then the summation can be truncated at $n \approx 10 |k_1 R|$ with negligible effect on the value of the summation from the neglected terms. It should be pointed out, however, that for very small angles θ' the number of terms required for convergence increases drastically (unless the ratio R_0/R is much less than unity).

The calculation of the special functions involved in the summation proceeds by invoking the recursion formula for each special function required. Thus the series summation and the special function calculation are able to proceed rapidly together. The recursion formula for the Legendre polynomial is

$$P_{n+1}(x) = \frac{(2n+1)xP_n(x) - nP_{n-1}(x)}{n+1}$$

$$P_0(x) = 1 \text{ and } P_1(x) = x \quad (7)$$

This recursion process, as well as related formulas for the derivatives of the Legendre function, absolutely converges to the required functional values. The calculation of the logarithmic derivative of the spherical Hankel function is also readily accomplished using forward recursion. The spherical Bessel function of the first kind, however, requires use of a backwards recursion formula and careful attention to the problem of computer underflow. The backwards recursion relation for the logarithmic derivative is

$$\frac{\psi'_n(x)}{\psi_n(x)} = \frac{n}{x} - \frac{1}{\frac{n}{x} + \frac{\psi'_n(x)}{\psi_n(x)}}, \quad n \leq n_s \quad (8)$$

The starting value of the index n_s need only be slightly larger than the value of the index n required in the series summation when $n \geq |z|$. For n significantly less than $|z|$, where the argument of z is large, then a starting value $n_s \approx \frac{|z|}{2}$, say, would be sufficient to generate functional values when $n \leq \frac{|z|}{5}$, $|z| \geq 1000$. On the other hand, if z is real, then a starting value $n_s > z$ is required at all times. The initial value of the logarithmic derivative is arbitrarily chosen to be zero for the backward recursion process.

Using the value of the logarithmic derivative, the ratios of two spherical Bessel functions of the first kind with different arguments can be obtained from the relations

$$\frac{\psi'_n(x)}{\psi_n(x)} = \frac{n}{x} + \frac{\psi'_{n-1}(x)}{\psi_{n-1}(x)} \quad (9)$$

and

$$\frac{\psi_n(x)}{\psi_n(y)} = \frac{\psi_n(x)}{\psi_{n-1}(x)} \times \frac{\psi_{n-1}(x)}{\psi_{n-1}(y)} \times \frac{\psi_{n-1}(y)}{\psi_n(y)} \quad (10)$$

The starting value for (10) is given by

$$\frac{\psi_0(x)}{\psi_0(y)} = \frac{\sin x}{\sin y} \quad (11)$$

Thus, by restricting our calculations to the ratios of the Bessel functions, we have avoided the numerical underflow problem.

The wave tilt of the magnetic-field at an observation point on the surface of the spherical hill is defined as the ratio of the maximum horizontal field component to the vertical field component, where the vertical direction coincides with the direction of the magnetic dipole current moment. Two complex components in the horizontal plane combine to form the maximum horizontal component, which lies at some unknown angle γ in the horizontal $\bar{x} - \bar{y}$ plane. The unknown angle can be found by setting to zero the derivative with respect to γ of

$$H_h = H_{\bar{x}} \cos \gamma + H_{\bar{y}} \sin \gamma \quad (12)$$

resulting in

$$\tan 2\gamma = \frac{2 \operatorname{Re}(H_{\bar{y}}/H_{\bar{x}})}{1 - |H_{\bar{y}}/H_{\bar{x}}|^2} \quad (13)$$

From (13) and the trigonometric half angle formulas, we are able to obtain an expression for $\tan \gamma$ which enables us to determine the angle γ within π radians. Finally, artificially interchanging $H_{\bar{x}}$ and $H_{\bar{y}}$ in (13) whenever the former is smaller in magnitude than the latter enables us, after some ado, to keep track of the sign ambiguity in (12) and so resolve it.

Explicit expressions for the field components $H_{\bar{x}}$, $H_{\bar{y}}$, and H_z , orientated along the axes of the Cartesian coordinate system of figure 1, are obtained by applying well-known coordinate transformation formulas to the field components given by equations (1). The resulting formulation is lengthy and will not be reproduced here.

The magnetic field components (1) can be calculated independently of both θ and ϕ' , this being the slowest computer operation, and then combined in a subsequent program to produce plots of the wave tilt versus the horizontal distance X (figure 1). Since the component calculation routine must have specified sequential values of θ' , and since the spherical coordinate transformation requires both θ' and ϕ' to locate a point in the unrotated (R, θ, ϕ) coordinate system, we need to determine a relationship which will enable us to obtain ϕ' as a function of θ' , θ , and ψ if we are to hold constant the dipole tilt angle θ and the azimuthal bearing angle ψ when plotting wave tilt versus X . From simple geometrical relationships in figure (1) we have the law of cosines,

$$X^2 = (R \sin \bar{\theta})^2 + (R_0 \sin \theta)^2 + 2(R \sin \bar{\theta})(R_0 \sin \theta) \cos \bar{\phi} \quad (14)$$

and the law of sines,

$$\frac{R \sin \bar{\theta}}{\sin \psi} = \frac{X}{\sin \bar{\phi}}$$

from which we obtain

$$\sin \theta' \cos \phi' = \left\{ \cos \bar{\psi} \sqrt{(1 - \sin^2 \bar{\theta} \sin^2 \psi) \sin^2 \theta' - \left(\frac{R_0}{R} - \cos \theta'\right)^2 \sin^2 \bar{\theta} \sin^2 \psi} \right. \\ \left. - \left(\frac{R_0}{R} - \cos \theta'\right) \sin \bar{\theta} \cos \bar{\theta} \sin^2 \psi \right\} / (1 - \sin^2 \bar{\theta} \sin^2 \psi) \quad (15)$$

In utilizing (15) it is necessary to avoid specifying an angle θ' too small to meet the arc \overline{OB} . The minimum angle θ'_0 that can be used is obtained from

$$\sin \theta'_0 = \sin \frac{\overline{AB}}{R} / \sqrt{1 + \frac{1}{\tan^2 \psi \cos^2(\bar{\theta} - \overline{AB}/R)}} \quad (16)$$

Also, for angles $\psi > \frac{\pi}{2}$, for X to increase monotonically the angle θ' must decrease from its maximum value $\frac{\overline{AB}}{R}$ to θ'_0 and then start to increase. It is at this crossover point that the sign of the square root in (15) changes. Frequently θ'_0 is less than the minimum angle θ' for which it is practical to sum the series to convergence, due to the extreme increase in the number of terms required when θ' is small. In 16, we have

$$\frac{\overline{AB}}{R} = \theta - \sin^{-1} \left(\frac{R_0}{R} \sin \bar{\theta} \right)$$

As previously mentioned, the ratio H of source depth to skin depth is an important problem parameter. Equally important is the ratio $\frac{d}{R}$, where

$$d = \sqrt{(R - R_0)^2 + 2RR_0(1 - \cos \frac{\overline{AB}}{R})}$$

The graphical results can be extrapolated to encompass any desired frequency, conductivity, sphere radius, or source depth by trade off from one parameter to another, as long as H and d/R are held constant.

A sample contour plot of the magnitude of the wave tilt function is given in figure 2, where the abscissa axis corresponds to the \bar{y} axis and the ordinate axis corresponds to the \bar{x} axis, the origin locating the point of intersection of the magnetic dipole current moment. Both coordinates are normalized with respect to the source depth, d . Here, $d \approx 100$ m, the sphere radius is 400 m, and the dipole tilt angle $\theta = 20^\circ$. It is apparent in figure 2 that a great deal of symmetry exists about the current moment axis, leading to the conclusion that wave tilt measurements can lead to a determination of the source location.

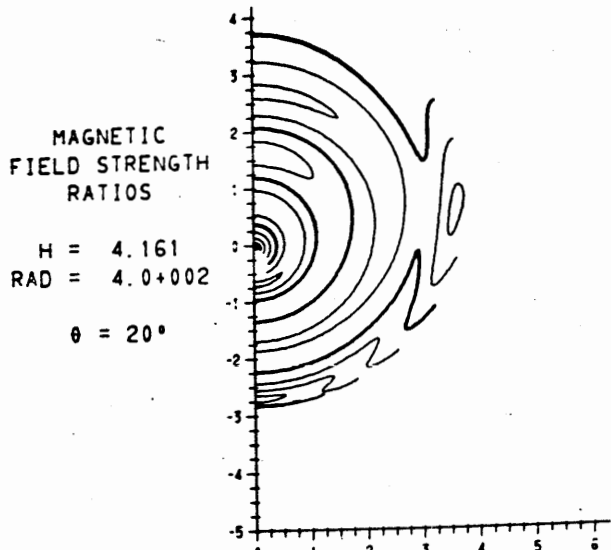


Figure 2. Wave tilt contours.

Figure 3 shows a plot of the amplitude of the wave tilt as a function of X/d , parametric in sphere radius (curve numbering refers to the increasing values of R), but with H held nearly constant ($R - R_0 = 100$ m in

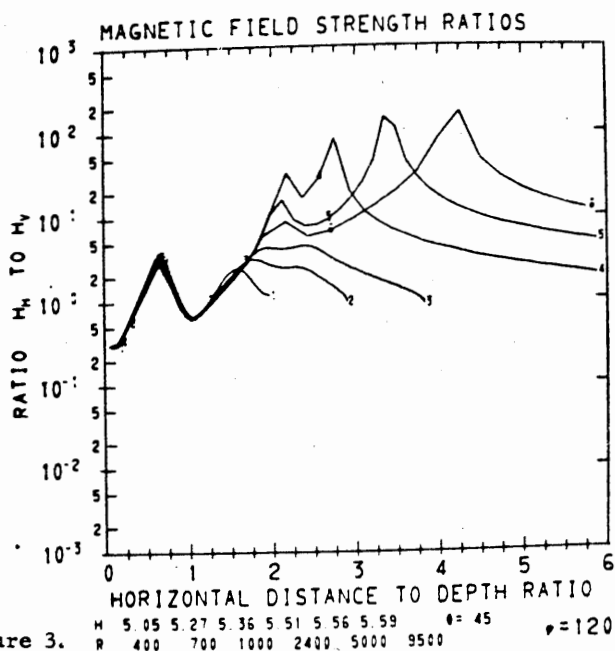


Figure 3.

figure 3). We can conclude that the wave tilt amplitude is nearly independent of sphere radius close in to the current moment axis, which in itself is a necessary requirement for a reliable source location scheme.

A comparison of the numerical results for a spherical hill with an analysis by J. R. Wait⁶ for the homogeneous half-space leads to the conclusion that the amplitude of the wave-tilt function in both analyses is capable of providing useful information for electromagnetic position determination, but in the case of the spherical hill the phase of the wave-tilt function must be considered unreliable for this purpose.

Stratified Ionosphere Model

The second problem of interest is the stratified ionosphere problem of figure (4). Here it is assumed that the source is located at a radius $r = b$, while the observation point is at radius r . The formal problem solution, obtained by requiring continuity of the tangential fields at each spherical boundary, is a straightforward procedure.³ The result is considerably simplified if it is specified that $k_1 = k_0$, which results in $R_1 = T = 0$ and $U_1 = -1$. Thus, we obtain, for the case $r > b$, the vertical electric field component

$$E_r = \frac{I_0 l \mu_0 c}{4\pi k_1^2 r^2 b^2} \sum_{n=0}^{\infty} n(n+1)(2n+1) P_n(\cos\theta) \times \frac{(\psi_{1b} - R_1 \zeta_{1b}^{(2)}) (\zeta_{1r}^{(2)} - \Gamma_1 \psi_{1r})}{1 - R_1 \Gamma_1} \quad (17)$$

The quantity Γ_1 is an effective ionosphere reflection coefficient whose value is obtained as the end result of a recursion process,

$$\Gamma_j = \frac{(1 - R_{2j} T_{2j}) - (R_{2j+1} - R_{2j} U_{2j+1}) \Gamma_{j+1}}{(T_{2j-1} - U_{2j} T_{2j}) - (T_{2j-1} R_{2j+1} - U_{2j} U_{2j+1}) \Gamma_{j+1}} \quad (18)$$

for $j = 1, 2, \dots, [\frac{P}{2}]$. The initial value for the recursion process is

$$\Gamma_{[\frac{P}{2}]+1} = \begin{cases} T_p & , p \text{ odd} \\ 0 & , p \text{ even} \end{cases} \quad (19)$$

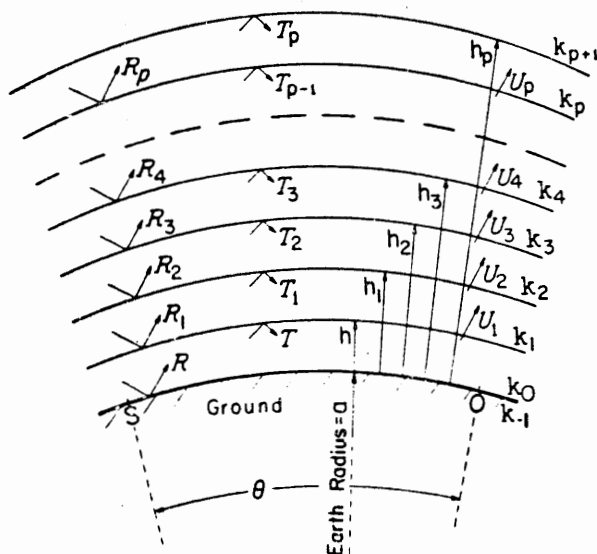


Fig. 4 Stratified ionosphere model of earth-ionosphere waveguide.

Figure (4) suggests the interpretation of R_j and T_j as the bottom and top reflection coefficients, respectively, of the j^{th} layer, while U_j has the character of a transmission coefficient for interlayer coupling. Replacing the spherical Bessel functions in R_j and T_j by the asymptotic expansions for large argument results in the Fresnel reflection coefficients⁷ multiplied times a spherical focusing factor. The specific expressions are

$$R_j = \frac{-\psi_{j-1} \zeta_{j-1}^{(2)} - \frac{\psi'_{j-1} - k_{j-1}}{k_{j-1}} \psi_{j-1} \zeta_{j-1}^{(2)'}}{\zeta_{j-1}^{(2)} - \frac{\psi'_{j-1} - k_{j-1}}{k_{j-1}} \psi_{j-1} \zeta_{j-1}^{(2)'}}$$

$$T_j = \frac{-\zeta_{j-1}^{(2)} \zeta_{j+1}^{(2)'}}{\psi_{j-1} \zeta_{j+1}^{(2)'}}$$

$$U_j = \frac{-\zeta_{j-1}^{(2)} \psi_{j+1} \zeta_{j+1}^{(2)'}}{\psi_{j-1} \zeta_{j+1}^{(2)'}}$$

In (17) and (20) we have utilized the notation $\zeta_{jr}^{(2)} = \zeta_n^{(2)}(k_j r)$, $\psi_{jr} = \psi_n(k_j r)$, $\zeta_{jr}^{(2)'} = \zeta_n^{(2)'}(k_j r)$, $g_j = a + h_j$. Finally, we have the ground reflection coefficient

$$R = -\frac{\psi_{1a}}{\zeta_{1a}^{(2)}} \times \frac{\frac{\psi'_{1a} - k_0}{k_0} \psi_{1a} \zeta_{1a}^{(2)'}}{\zeta_{1a}^{(2)} - \frac{\psi'_{1a} - k_0}{k_0} \psi_{1a} \zeta_{1a}^{(2)'}}$$

Calculation of the special functions involved in this formulation and use of the technique for grouping of terms to improve convergence proceeds in the same manner as for the spherical hill problem. Identical remarks also apply regarding the number of terms required for convergence and regarding which terms make the maximum contribution to the summation. An additional technique that is particularly useful in improving the series convergence properties is to subtract, term by term, the series expansion of the quasi-static fields of a dipole source near a perfectly conducting sphere from the summation (17).³ The asymptotic expansion of each term in (17), for n large, can be shown to equal the corresponding term of the quasi-static series expansion, with the result that the term-by-term subtraction introduces a convergence factor of $\frac{1}{n}$ into the series summation. The quasi-static fields can be added back in at the end as a closed form expression. One note of caution regarding the truncation of the infinite series applies to the calculation of the phase correction term. This is defined as

$$\varphi_c = -\psi_r - k_1 d \quad (22)$$

where $\psi_r = \arg\{E_r\}$ and $d = a\theta$. Since (22) is the difference of two very nearly equal terms (ψ_r is negative), practical experience has dictated that the accurate calculation of the phase correction may require roughly twice as many terms as is required to calculate the function amplitude.

In addition to the normal difficulties experienced in the calculation of spherical Bessel functions regarding underflow and overflow, there are also some particular problems associated with the formulation (17). Specifically, for the case $b = a$, we note that, for large n , $\frac{\zeta_{1a}^{(2)}}{\psi_{1a}} R \rightarrow 1$ if the surface impedance of the earth is large. This machine under-

flow problem can be resolved by utilizing the Wronskian relation to obtain²

$$\psi_{1a} - R \zeta_{1a}^{(2)} = \frac{-i}{\zeta_{1a}^{(2)'} - \frac{k_0}{k_{-1}} \frac{\psi'_{-1a}}{\psi_{-1a}} \zeta_{1a}^{(2)}} \quad (23)$$

Asymptotically it may be noted that (23) approaches zero for large n . Specific use may be made of this fact to improve the convergence properties of the series. Thus, we have^{1,8}

$$\frac{\zeta_{1r}^{(2)} - \Gamma_1 \psi_{1r}}{1 - \Gamma_1 R} = \zeta_{1r}^{(2)} - (\psi_{1r} - R \zeta_{1r}^{(2)}) \sum_{j=1}^{\infty} R^{j-1} \Gamma_1^j \quad (24)$$

Upon substitution of the first term in (24) into (17), there results simply the ground wave term, which can be calculated separately using the classical ground wave theory.⁹ Interchanging the order of summation of j and n when the second term of (24) is substituted into (17) results in the wave-hop summation,¹ illustrated in figure (5). Here, the source is at S and the observer is at O . The usefulness of this technique arises from the fact that only a few wave-hops need be summed for reasonable accuracy, while we have introduced the additional factor $\psi_{1r} - R \zeta_{1r}^{(2)}$ which can be treated in similar fashion to (23). Thus, only a few terms beyond $n \approx k_1 a$ need be summed for the summation over n to converge.² This technique is used at VLF and LF frequencies.

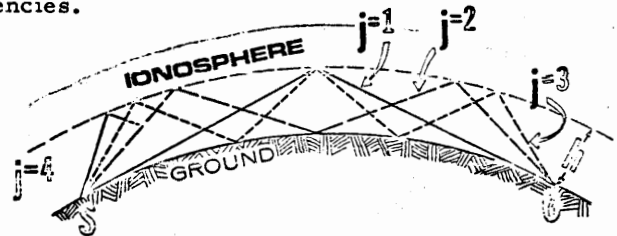


Figure 5. The wave hop fields.

An example of the capability of the formulation is depicted in figure 6, where we show the complicated field

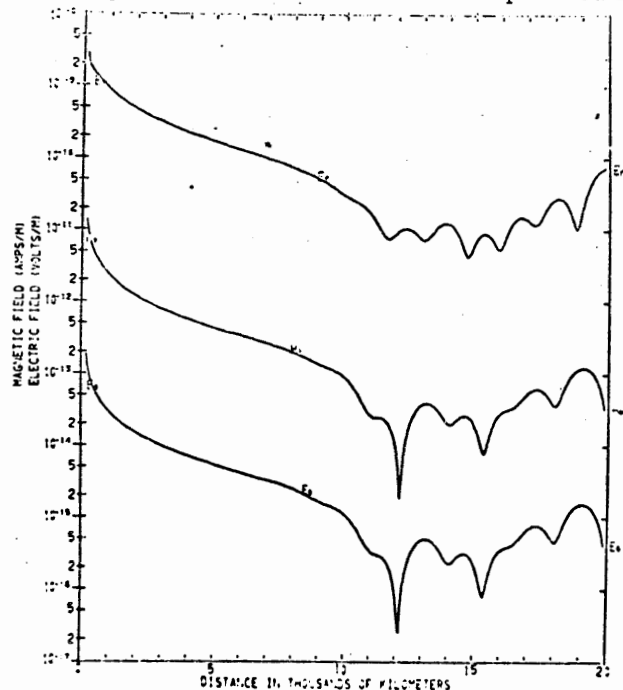


Fig. 6. Two layer ionosphere with low conductivity bottom layer.

structure produced by a two layer ionosphere in which the upper layer has a very high conductivity while the lower layer is a moderately lossy dielectric. Thus, the two layer "ionosphere" functions as a dielectric coated conductor which guides a surface wave completely around the spherical wave-guide, leading to the standing-wave pattern shown. The upper trace is the E_r field, while below that are the H_{θ} and E_{θ} fields. The lowest layer, at a height of 70 km, was taken to be $1\frac{1}{2}$ km thick, while the excitation frequency is 100 Hz.

In figure 7, we show the effect of increasing the conductivity of the lowest layer by an order of magnitude. Here, the standing wave structure is greatly enhanced. Finally, in figure 8, we have decreased the conductivity of the lowest layer by an order of magnitude from the value used in figure 6. Figure 8, incidentally, is identical with the result obtained for a single layer or sharply bounded ionosphere commonly used when the conductivity of lower layers is simply ignored.

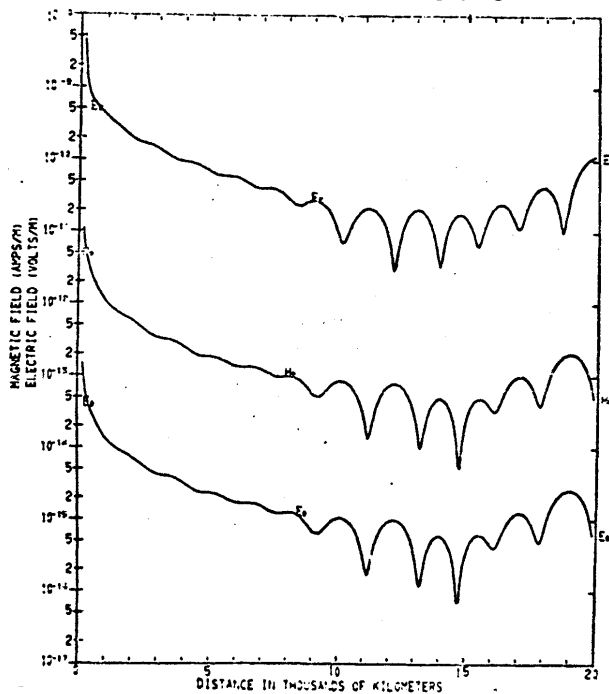


Fig. 7. Two layer ionosphere with moderate conductivity bottom layer.

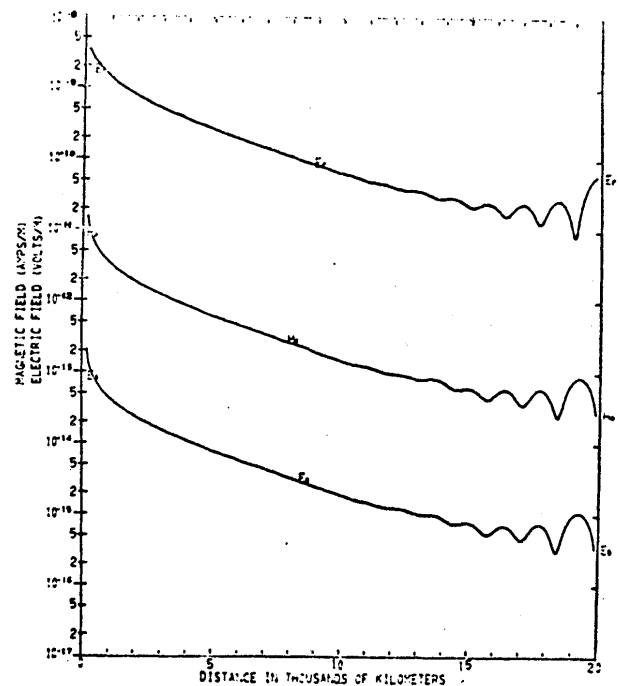


Fig. 8. Two layer ionosphere with extremely low conductivity bottom layer.

In conclusion, it might be worthwhile to contrast the zonal-harmonic series summation with the more conventional mode theory approach. Although either formulation is equally valid, it must be noted that the latter approach requires a time consuming search for modes, possibly involving a very complicated modal equation. Especially this would be true for the treatment of a spherically layered model. Furthermore, it should be pointed out that more than one mode may be required to fully explain a complicated field structure such as is shown in figure 6, even at the low frequency of 100 Hz. Consequently, although the determination of the field strength can proceed extremely rapidly once the modes are known, I submit that the necessary mode determination could be a deterring factor from considering a mode theory approach. The zonal-harmonics summation, on the other hand, can be extremely rapid, particularly when $|k_1 a|$ is not too large, although some physical insight may be sacrificed by its use.

- ¹Richard L. Lewis, "The wave-hop fields for an inclined dipole over a spherical earth with an anisotropic ionosphere", Telecommunication Research Report OT/ITS 5, U.S. Dept. of Commerce, Oct. 1970.
- ²J. Ralph Johler, "Spherical wave theory for MF, LF, and VLF propagation", Radio Science 5, 12, pp. 1429-1443, Dec. 1970.
- ³J. Ralph Johler and Richard L. Lewis, "Extra low-frequency terrestrial radio-wave field calculations with the zonal-harmonic series", Journal of Geophysical Research 74, 10, pp. 2459-2470, May 15, 1969.
- ⁴Walter Gautschi, "Computational Aspects of Three-Term Recurrence Relations", SIAM Review 9, 1, pp. 24-82, January 1967.
- ⁵Richard L. Lewis, "Recursion Formula for the Logarithmic Derivatives of Spherical Bessel Functions in the Complex Plane", ESSA Technical Report ERL 151-ITS-99, U. S. Dept. of Commerce, January 1970.
- ⁶J. R. Wait, "Electromagnetic Sources in Lossy Media," Chapter 24 in *Antenna Theory*, pt. II, Ed. by Collin & Zucker, McGraw Hill 1969, cf. also: J. R. Wait, "Influence of earth's curvature on the subsurface fields of a line source," Electronics Letters 7, 23, pp. 697-699, Nov. 1971.
- ⁷J. R. Wait, *Electromagnetic Waves in Stratified Media*, Pergamon Press 1970, c.f. also: J. Ralph Johler, "Zonal harmonics in low frequency terrestrial radio wave propagation, NBS Tech note 335, U. S. Dept. of Commerce, April 13, 1966.
- ⁸J. Ralph Johler, "Concerning limitations and further corrections to geometric-optical theory for LF, VLF propagation between the ionosphere and the ground.", Radio Science 68D, 1, pp. 67-78, January 1964.
- ⁹Johler, J. R., and J. C. Morgenstern, "Propagation of the ground wave electromagnetic signal with particular reference to a pulse of nuclear origin", Proc. IEEE 53, 12, pp. 2043-2053, 1965.

Theory

A general analytical solution of the effect of an inclined contact separating two media of differing electrical properties on a normally incident plane electromagnetic field has been given (Geyer, 1972). These solutions for the electromagnetic response at any observation point $P(r, \varphi)$ are given in the form of inverse Lebedev-Kontorovich transforms. Two modes of excitation are considered: (1) case where current density flows across strike of the contact separating the media of differing electrical properties (only E_r , E_φ , and H_x differ from zero) and (2) case where current density flows along strike (only H_r , H_φ , and E_x differ from zero). The electromagnetic fields in the frequency range of interest and for the rock conductivities under consideration are quasi-static in nature so that to a first-order approximation the horizontal magnetic field at the surface of the earth is constant and continuous across the discrete discontinuity in resistivity for case (1) above, and so that the tangential derivative of the horizontal electric field at the surface of the earth is constant and continuous across the discrete discontinuity for case (2) above. Of course, it is well known that where large horizontal gradients in conductivity exist, there also exists large anomalous components of the vertical magnetic field (Weaver, 1963). The recognition of such anomalous components and their magnitudes due to the presence of lateral resistivity changes in the overburden becomes very important in any wavetilt type measurement which may be used to locate a miner.

When the lateral change in resistivity becomes quite large, the integral solutions (expressed as Lebedev-Kontorovich transforms) simplify considerably and allow ready numerical evaluation. Examples of the amplitude and phase responses of the radial electric, horizontal electric, and vertical magnetic field in the vicinity of the contrast in resistivity are shown in Figures 2, 3, and 4. Of particular significance is the fact that the anomalous vertical magnetic field is three orders of magnitude larger near the contact than far from the contact. This fact implies that where large resistivity contrasts do occur in the rocks overlying mine workings, that significant errors may be present in wavetilt measurements as used above for location criteria! Another observation insofar as the anomalous vertical magnetic field is concerned is the linear variation of phase as one proceeds away from strike in induction number (increased distance or frequency). For a pulse-excited communications system this phenomena would have a bearing on where the zero crossings would occur (i. e., 'pulse breadth') in the transient coupling between any given source-receiver configuration and at any given receiver site.

Summary

Application of Lebedev-Kontorovich transforms together with the imposition of the quasi-static condition on the electromagnetic field at the air-earth interface have led to analytic integral solutions for the electric and magnetic fields inside two regions separated by a sloping interface where the normally incident fields were plane waves. In the derivation of the solutions the assumed boundary conditions were that the horizontal magnetic field (H polarization) and vertical derivative of the horizontal electric field (E polarization) are continuous and constant across the interface. Therefore the results are correct to $O(\omega\epsilon/\sigma_n)^{\frac{1}{2}}$. These solutions may be used to compute a correction term to the field in the air above the lateral resistivity contrast (and thus along the surface) which, in turn, might be used to evaluate field solutions on either side of the dipping contact to $O(\omega\epsilon/\sigma_n)$. This type of iteration may be continued indefinitely with each step improving the order of accuracy of the solutions in the quantity $(\omega\epsilon/\sigma_n)^{\frac{1}{2}}$.

The integral solutions obtained simplify considerably where large resistivity contrasts occur. By use of saddle-point techniques it is possible to evaluate the fields for $\pi/4 < \delta < 3\pi/4$ and at the same time to estimate the error involved in the asymptotic expansions in terms of the proximity to the interface separating the two regions of contrasting resistivity.

The numerical results indicate that one must exercise caution in wavelit schemes for the location of a miner, especially in those regions where the presence of lateral resistivity contrasts in the rock overlying mine workings may affect the positioning of maxima and null phenomena in the surface magnetic fields produced by a buried loop antenna.

References

- Clemmow, P. C., 1953, Plane wave spectrum representation of electromagnetic fields.
- Geyer, R. G., 1971, Research on the transmission of electromagnetic signals between mine workings and the surface: Quart. Tech. Rpt. for period Oct. 1, 1971 to Dec. 30, 1971 for U.S. Bureau of Mines, 106 p.
- Geyer, R. G., 1972, The effect of a dipping contact on the behavior of the electromagnetic field: Geophysics, v. 37, n. 2, p. 337-350.

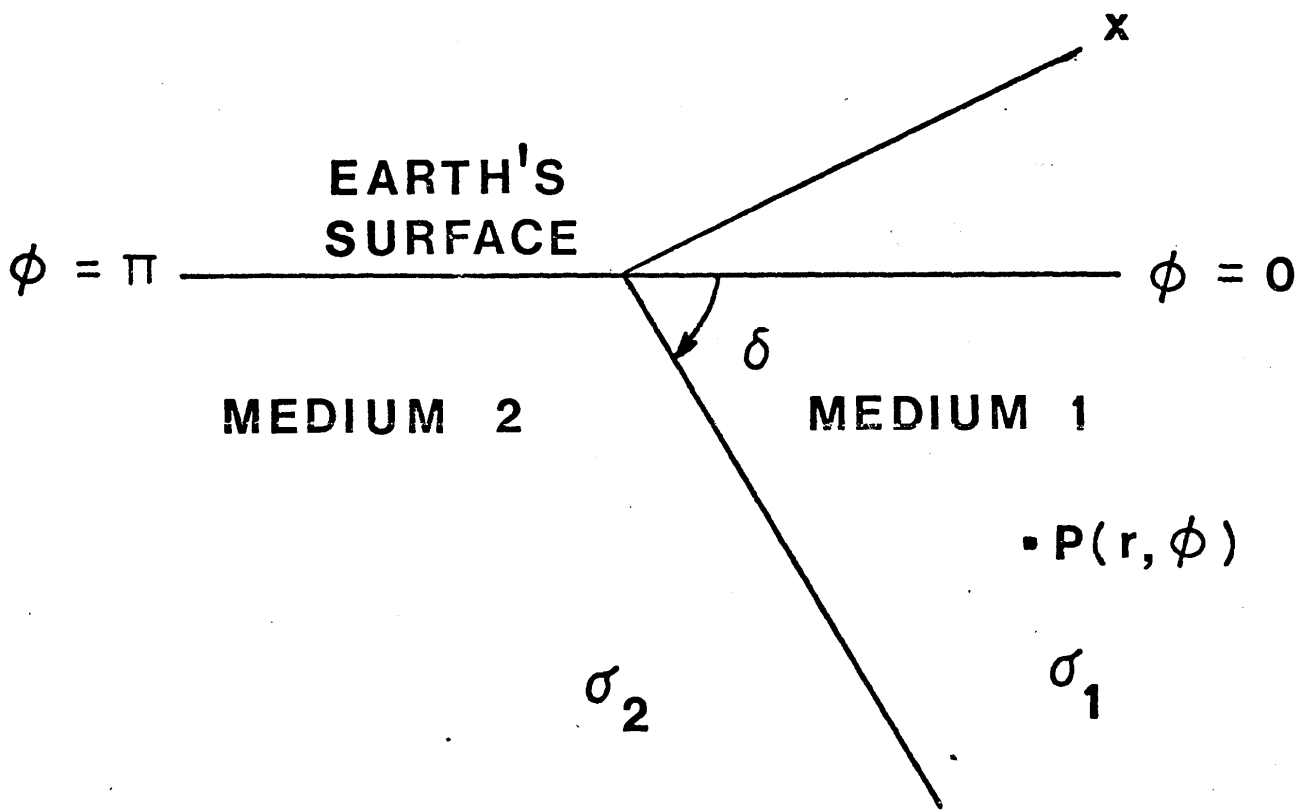


Fig. 1. Geometry of model where discrete contrasts in electrical properties occur.

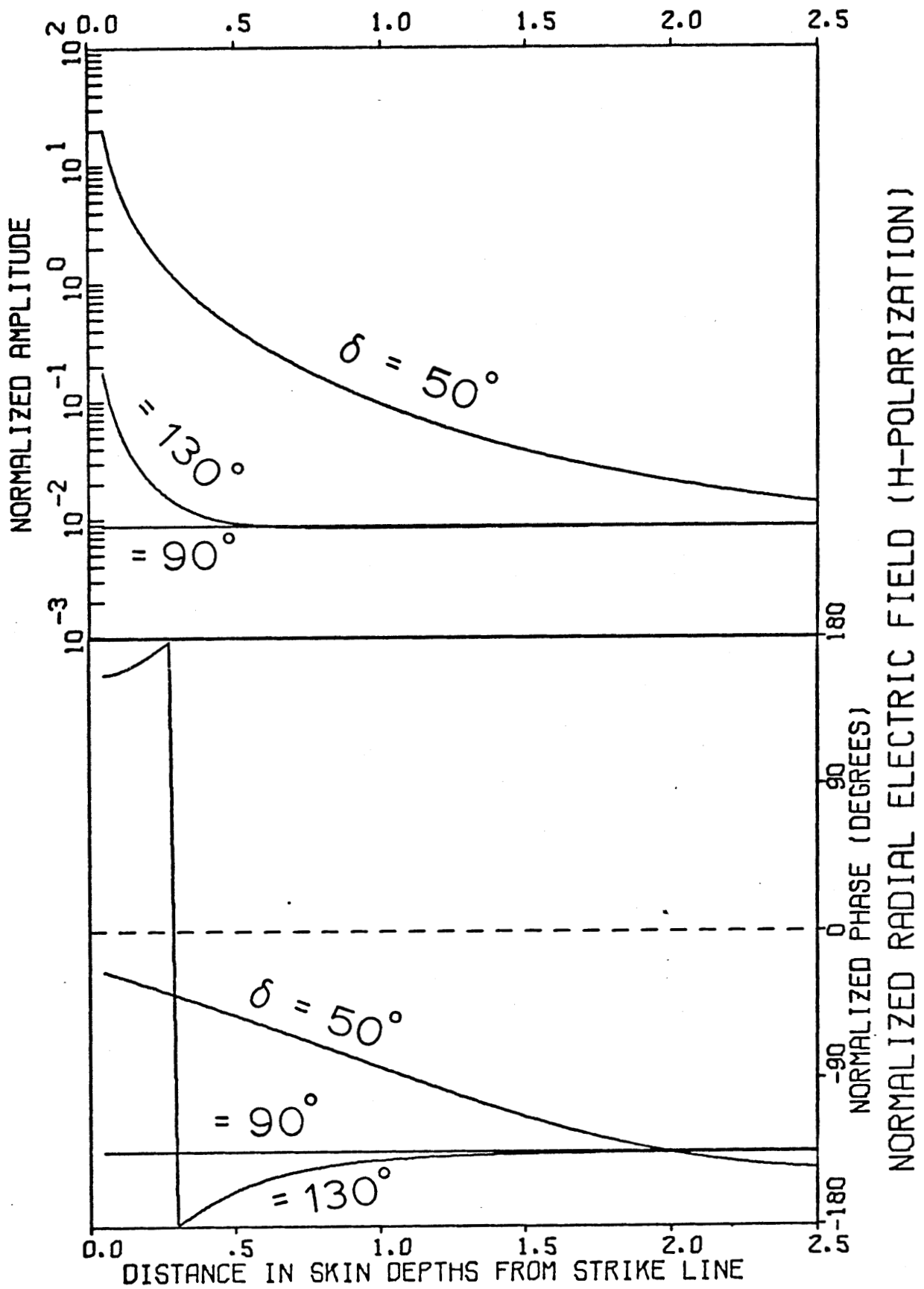


Fig. 2. Normalized radial electric field response over poorly conducting region for several dip angles of the interface (H-polarization).

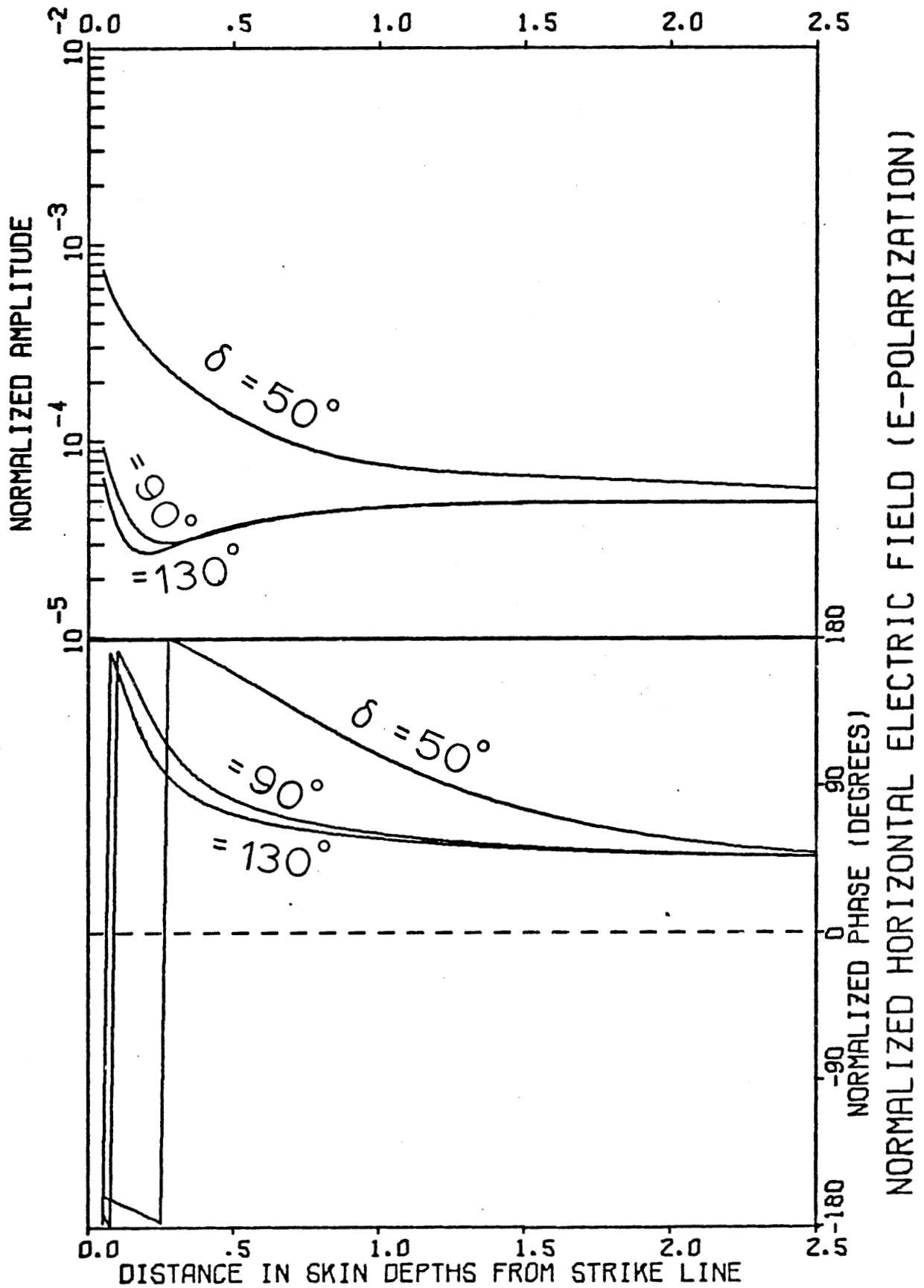


Fig. 3. Normalized horizontal electric field response over poorly conducting region for several dip angles of the interface (E-polarization).

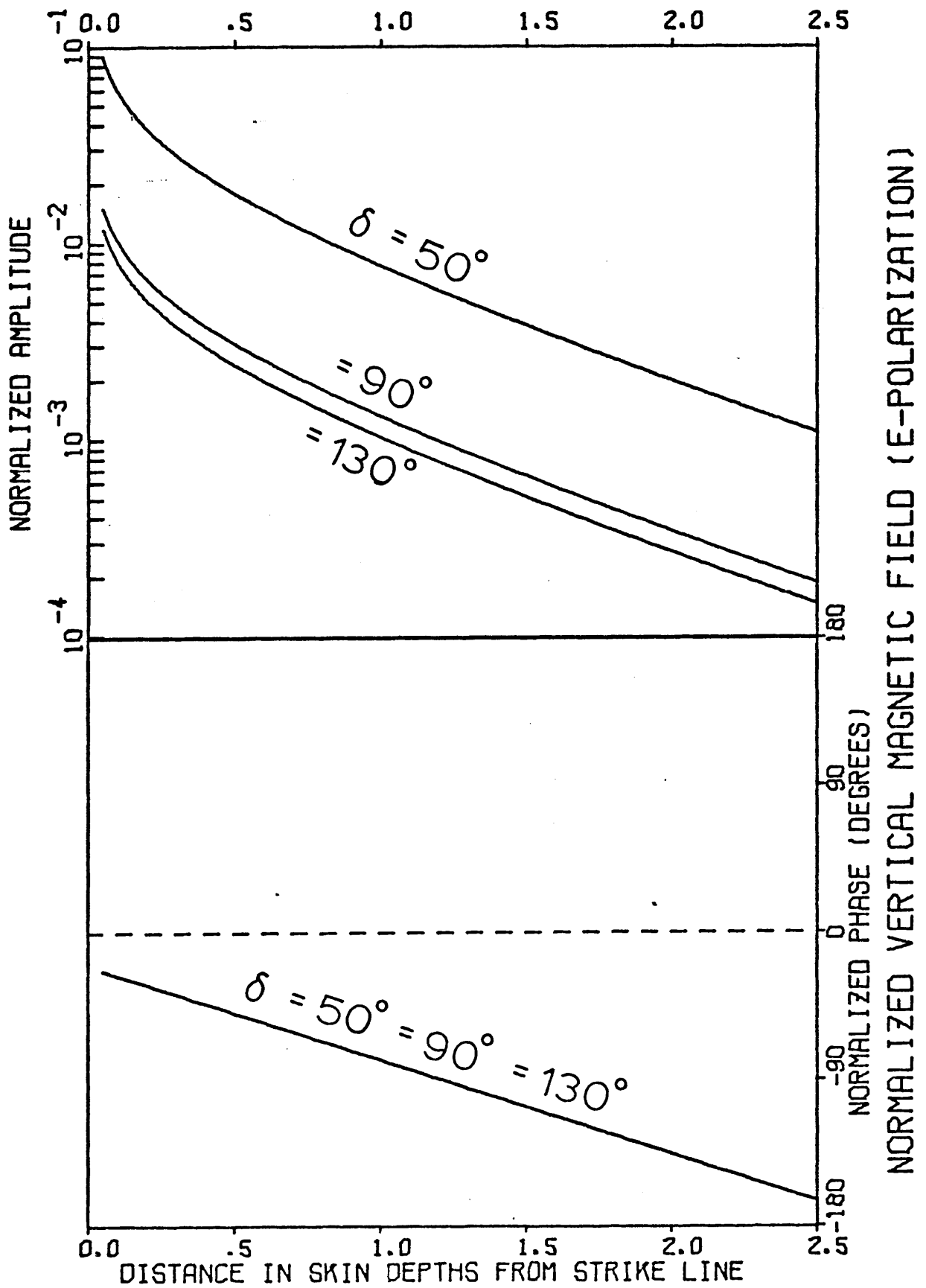


Fig. 4. Normalized anomalous vertical magnetic field over poorly conducting region for several dip angles (E-polarization).

SUBSURFACE APPLICATIONS OF PERIODIC ELECTROMAGNETIC VIDEO PULSE SIGNALS

David L. Moffatt
The ElectroScience Laboratory
Department of Electrical Engineering
The Ohio State University
Columbus, Ohio 43212

Introduction

Considerable current interest is evident[1,2] in the use of transient electromagnetic methods for subsurface remote sensing. A transient method is discussed which uses a periodic video-type pulse containing a wide frequency range. A video pulse is used as an interrogating signal both for "target" identification and detection for relatively short depth (< 20 meters) applications in soil and soft rock media. If the medium is favorable, e.g., hard rock, greater depth applications appear to be feasible. The same procedures would be applicable for deep geological exploration but would require a substantial reduction in frequency and increase in target size. It should be noted that video pulse generators with 35 kv peak voltage and nanoseconds base widths are now within the state-of-the-art, thus significant power over broad spectral ranges is possible.

In the design of a video pulse sounding system, 5 main problem areas can be identified; 1) selection of the pulse shape or spectral content of the video pulse, 2) design of a radiating structure which effectively couples such a pulse into the medium, 3) isolation of the radiating and receiving mechanisms, 4) realistically accounting for the dispersion and attenuation of the medium and the air-medium interface, and 5) interpretation or processing of the received signal waveform. Each of these problem areas will be discussed and illustrated with experimental and/or theoretical results.

The Video Pulse

Selection of the proper video pulse signal is dictated by 3 considerations, the maximum desired depth of penetration, the attenuation of the medium and the required resolution and size of the target. For a lossy medium, penetration and resolution are clearly at cross purposes and a compromise is necessary. The exact nature of the compromise is dictated by the application, but the spectrum of the video pulse should not contain any frequencies higher than the predicted cut-off, i.e., that frequency which is attenuated to the threshold level of the receiver. As a practical matter, it may be necessary to select 1 or 2 video pulses reasonably suited

for a variety of applications. For example, the experimental data presented here were obtained using 2 video pulse signals - a 1,000 volt peak picoseconds base width with a spectrum essentially flat to the GHz range and a 50 volt peak nanoseconds base with significant spectrum to roughly 60 MHz. With current technology, the video pulse can be tailored to an individual application. It is stressed however that for a diagnostic capability, all frequencies which can realistically be observed must be included in the pulse spectrum. Geological exploration would involve larger targets at greater depths but pulses with lower frequency content would be used.

The Antenna

Required is a structure which when oriented on or above a given medium effectively couples energy into the medium over a broad range of frequencies. The broadband requirement precludes achieving significant gain. For the video pulse sounding system, a dipole antenna is used with each dipole arm made up of two linear conductors in a V arrangement. The angle of the V is adjusted to control, in situ, the characteristic impedance of the dipole at the feed point. In the time domain the objective is to minimize sequentially and individually each reflection along the feed system and antenna. This is most simply done experimentally using a fast rise time pulse with a very long period and viewing the feed system and antenna as a transmission line with changing characteristic impedance along its length. Assuming a well selected feed system, the major sources of reflection are the antenna feed point and the ends of the dipole arms. Feed point reflections are minimized by adjusting the angle of the V arms. End reflections are controlled by 3 different mechanisms. In soil media, adjustable depth grounding rods at the end of each dipole arm element effectively controls the reflection. Often, if the soil has a vegetative cover, the attenuation of the vegetation is sufficient for control. On rock media, the large dipole (28 feed) has 8 foot long solid metal sheets at the end of each arm. For the small dipole, a thin layer of absorber material (Hairflex) is inserted between the antenna and the medium. When the local geometry permits, the most effective method of end reflection control is simply to extend the arms such that end reflections are beyond the "time window," i.e., would return to the feed point at times later than those from the target. Successful end reflection control using these mechanisms have been documented with experimental measurements [3,4].

Isolation

With video pulse systems, the receiver is usually a sampling oscilloscope. In a direct or monostatic mode where a single antenna is used for both transmission and reception the antenna can be switched between generator and sampler or alternatively a limiter to protect the sampler is provided and the entire time history is viewed. This direct

mode of operation has the advantage of using same polarization transmission and reception. A major disadvantage is that a strong reflection from the air-medium interface can be anticipated. In addition, the ringing associated with horizontally stratified media would always be present which may or may not be desirable depending upon the application. The video pulse sounder can be operated in the direct mode (with limiter) but measurements indicate a need for faster diodes in the limiter for high power operation. Isolation via bistatic mode operation with two antennas (one for transmission one for reception) arrayed side by side with some horizontal separation is also possible. With dipole antennas on rock and soil media it was found that a surface wave component bound to the lower impedance medium resulted in a strong direct coupling which would be difficult to control.

The video pulse sounder is operated principally in an orthogonal mode using again two dipoles on the medium surface but oriented orthogonally with the feed points in very close proximity. In this case the direct coupling is a substantially reduced replica of the pulse delivered to the input feed point and therefore has a very brief time duration therefore permitting a clean time window. Orthogonal mode operation has the disadvantage (assuming only partial depolarization) of using the depolarized component of the scattered field. Note however that in this mode the sounder does not respond to targets which are symmetric to a vertical axis through the feed points. Thus the air-medium interface and other horizontal stratifications are not seen.

Attenuation, Dispersion, Interface

To properly process video pulse soundings it is desirable to remove from the received transient signal spectrum the effects of the antennas in situ, the feed system, and the medium. The effects of the feed system can be accurately measured. While certain locations and media offer geometries whereby the antenna in situ and medium effects can be measured, a theoretical capability is highly desirable.

An analysis and computer programs have been developed employing piecewise-sinusoidal expansion functions and Galerkin's method to formulate a solution for an arbitrary thin-wire antenna configuration in an infinite, homogeneous, isotropic, conducting medium[5]. The solution determines the current distribution, impedance, radiation efficiency, gain and both near zone fields and far-field patterns. As a first order approximation to account for the half-space, 3 possible modifications have been added. Note that the goal is a simple modification of an existing state-of-the-art computer program for an infinite medium which yields reasonable results in the vicinity of broadside for the same antenna on a half-space. One modification is an image-type using a plane wave reflection coefficient most appropriate if the antenna were immersed

in the half-space. A second modification takes the wavenumber for the current flowing on the dipole to be the geometric mean of the wavenumbers for air and the half-space. A third modification combines the first 2. An example of the results is shown in Fig. 1, where the result of each modification is shown and compared to the result for an infinite medium. The antenna is a 6 foot V dipole with an included V angle of 30° . The frequency and half-space parameters are shown in the figure. Similar results for this antenna and half-space spanning 100 KHz to 100 MHz are given in reference 4. At 100 KHz (Fig. 1), none of the modifications alter the θ -dependence of the fields. At higher frequencies [4], the θ -dependence does change. In the broadside region ($\theta = 0^\circ$) and at low frequencies, both the image and current modifications alone are roughly compatible with results given by Wait [6] for an infinitesimal dipole under the quasi-static approximation. At this point, no claim is made as to the appropriateness of these modifications but the versatility of the available programs dictate an attempt at simple corrections. That only simple corrections may be needed near broadside is illustrated in Fig. 2 where a comparison of measured and calculated pulses transmitted through 20 feet of limestone is shown. The calculated pulse was obtained without any modification of the infinite medium program. The agreement between calculated and measured pulse shape is excellent. The magnitude error is partially accounted for by the fact that in the measurements, the thin absorber layer described previously was used on both the transmitting and receiving dipoles. The absorber was not taken into account in the calculations.

Attenuation and dispersion may also be calculated using the program. In Fig. 3, calculated received pulses are shown for transmission between 2 identical dipoles (Fig. 1) over 2 different path lengths. The antennas are broadside to each other, the transmitted signal is a 45 volt peak 50 nanosecond base width pulse, and the electrical properties of the medium have the assumed linear frequency dependence given in Fig. 3. A linear frequency dependence may not be realistic, but because the calculated pulses are obtained via transforms of frequency domain calculations, any frequency dependence can be used.

Processing

The processing scheme presently being utilized is to obtain from the measured orthogonal mode signal the band-limited impulse response of the target. In this approach, a given signal in the "time window" is isolated in time by gating and then transformed to the frequency domain. This spectrum is then normalized by the spectra of the interrogating pulse, the feed system, the antennas and the medium. The resultant spectrum is then inverse transformed to the time domain. In Fig. 4, the band-limited impulse response of a large cylindrical void (road tunnel) in limestone at a depth of 20 feet is shown. The specular-type impulse

response in Fig. 4 is reasonable considering the size (\approx 25 foot diameter) of the tunnel.

Conclusions

In applications where either the medium or required penetration depth make the use of video pulse signals feasible the electromagnetic video pulse sounder offers a new capability. Such applications as plastic and metal pipe detection in soil, overburden profiling, hazard detection in hard rock tunneling, route selections for subsurface installations, volumetric mapping of abandoned and hazardous drift coal mines, backfill analysis of pipe installations in permafrost, etc., would appear to be within the capabilities of the present system. Again, deep probing would require much different pulses and larger targets. The present system has also been used to experimentally record the responses of geological features such as joints, faults and a lithologic contrast in a dolomite medium.

References

1. Wait, J.R., "On the Theory of Electromagnetic Sounding Over a Stratified Earth," Canadian Journal of Physics, Vol. 50, No. 11, 1972.
2. Vanyan, L.L., Electromagnetic Depth Soundings, Translated from the Russian by G.V. Keller, Consultant Bureau, 1967.
3. L. Peters, Jr., and D.L. Moffatt, "Electromagnetic Pulse Sounding for Geological Surveying with Application in Rock Mechanics and Rapid Excavation Program," Report 3190-2, September 1972, ElectroScience Laboratory, Department of Electrical Engineering, The Ohio State University; prepared under Contract No. H0210042 for Bureau of Mines, Department of Interior (ARPA), Denver, Colorado.
4. Moffatt, D.L., R.J. Puskar, and L. Peters, Jr., "Electromagnetic Pulse Sounding for Geological Surveying with Application in Rock Mechanics and the Rapid Excavation Program," Report 3408-2 (in preparation), ElectroScience Laboratory, Department of Electrical Engineering, The Ohio State University; prepared under Contract No. H0230009 for Bureau of Mines, Department of Interior (ARPA), Denver, Colorado.
5. Richmond, J.H., "Radiation and Scattering by Thin-Wire Structures in the Complex Frequency Domain," Report 2902-10, July 1973, ElectroScience Laboratory, Department of Electrical Engineering, The Ohio State University; prepared under Grant No. NGL 36-008-138 for National Aeronautics and Space Administration, Washington, D.C.
6. Wait, J.R., "Theory of Wave Propagation Along a Thin Wire Parallel to an Interface," Radio Science, Vol. 7, No. 6, June 1972.

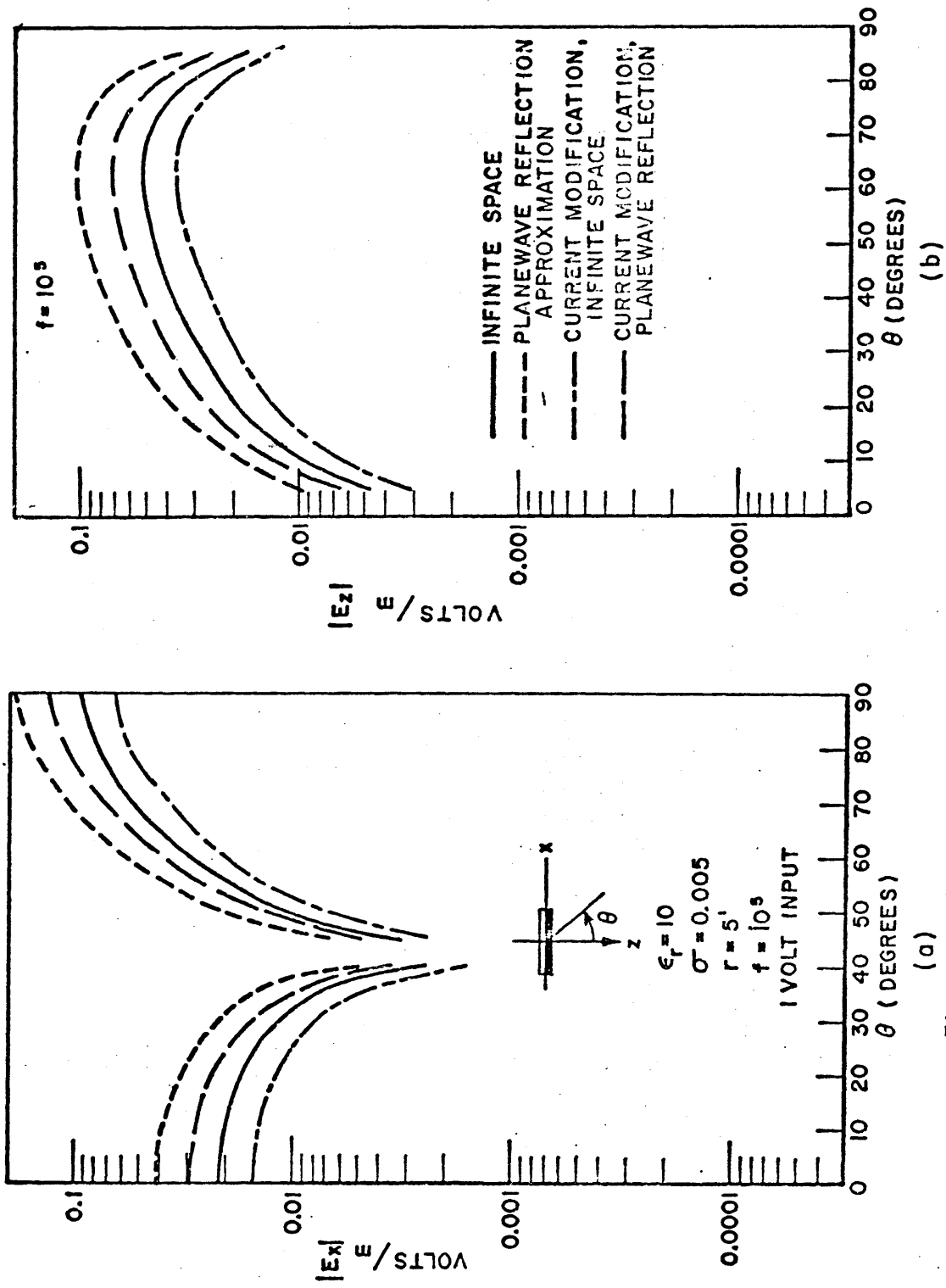


Fig. 1. Subsurface fields of 6 foot dipole, 100 KHz.
 (a) x-component (b) z-component.

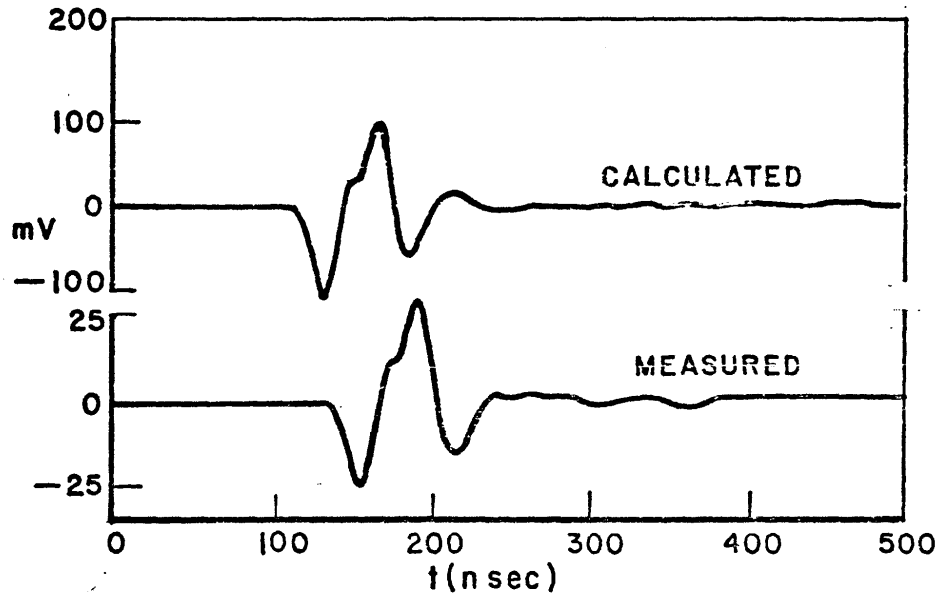


Fig. 2 Comparison of measured and calculated pulse transmission waveforms

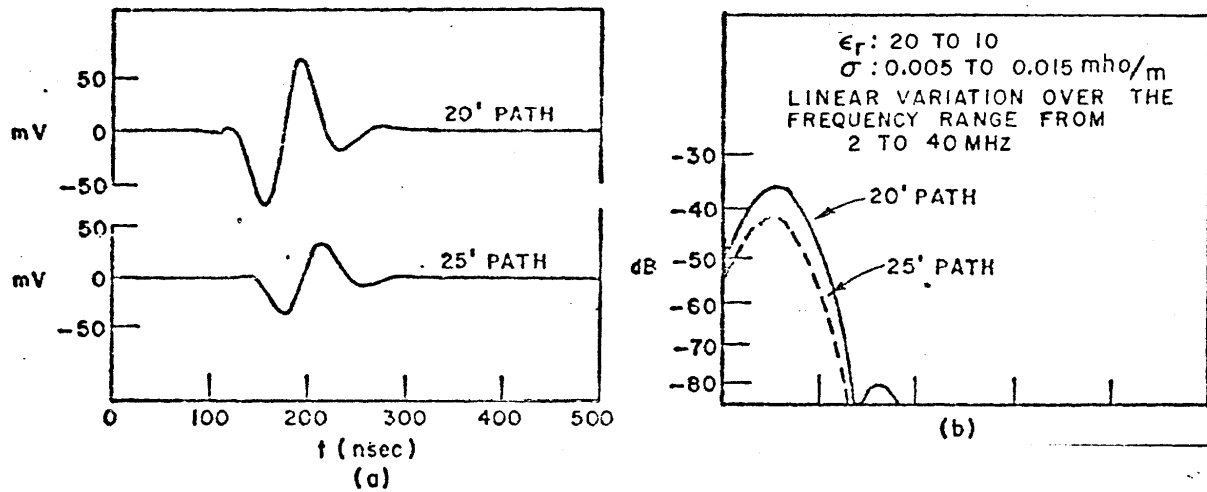


Fig. 3 Effect of dispersion on pulse propagation.
 (a) time domain waveform
 (b) amplitude spectra

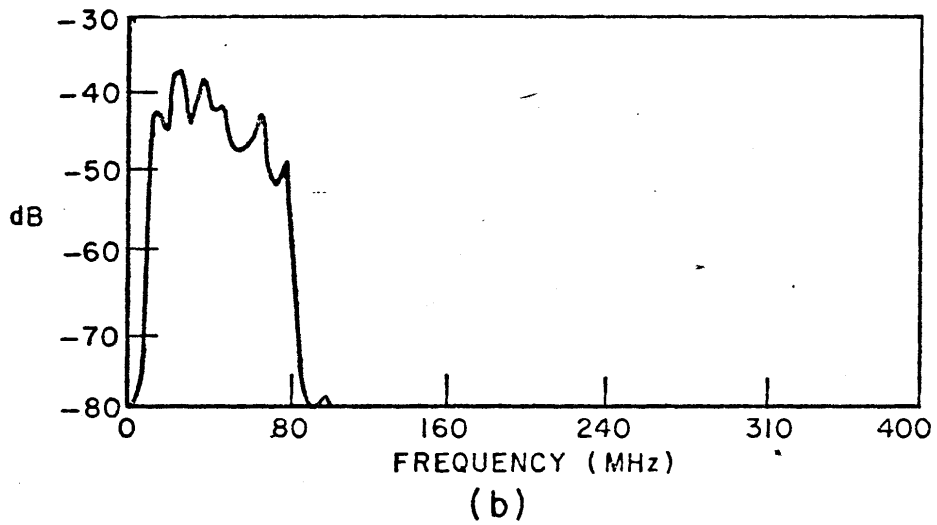
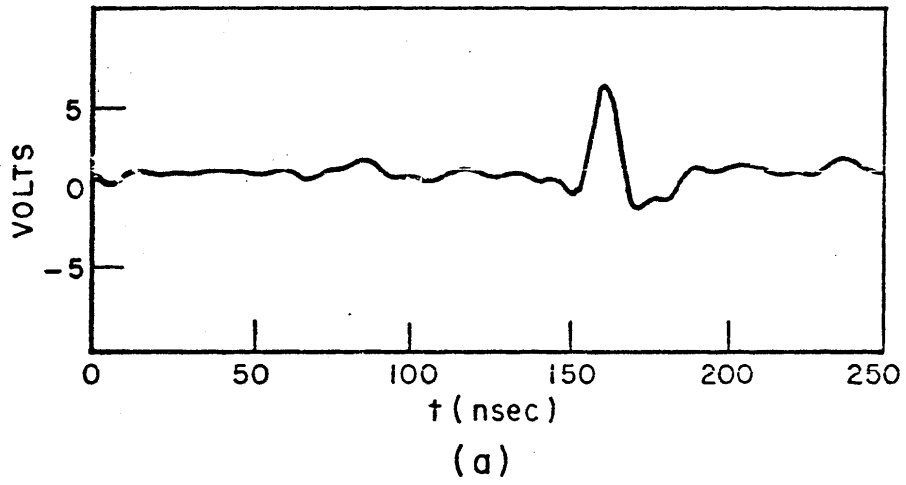


Fig. 4 Processed measurements over the tunnel.
(a) time domain waveform
(b) amplitude spectra.

ELECTROMAGNETIC SURVEY METHOD APPLICABLE TO UNDERGROUND QUARRIES

R. Gabillard, J. P. Dubus, F. Cherpereel
Electronics Department
University of Lille - 59650
Villeneuve d'Ascq
France

Abstract

We present an electromagnetic method taken from the well known radiogoniometer that allows us to locate at the surface of the ground the vertical axis of a magnetic antenna transmitter buried at a depth h in the earth.

The method and the equipment achieved are called R. E. P. E. (Relevé Electromagnétique de Points Enterrés). They are daily used to accurately survey old quarries by using triangulation instruments at the surface of the earth rather than in galleries where the setting difficulties considerably reduce their accuracy and increase the work length.

The results of several surveys allow us to give the optimum working conditions of the instruments and show that, when the transmitter is at a 20 meters depth, its position is known at the surface with an error lower than 1 centimeter. The power transmitter is of about 8 watts and we can find its location with an error smaller than 1 meter when buried at a depth of about 100 meters.

This equipment may be successfully used for location of subsurface miners. The space surrounding the transmitter must then be free from ferromagnetic bodies.

Principle of the Method

The principle of the method is illustrated in Fig. 1. We put on the ground (for example, in a mine galery) a small emitter; this emitter has an antenna that we consider as a vertical magnetic dipole. If the signal frequency is low enough, the discontinuities of the mine galleries and the surface of the ground do not deform the magnetic field ^{(1), (2)} produced by the emitter. Under these conditions the magnetic field is symmetrically distributed around the vertical axis of the antenna.

For determining the position of the vertical axis of the antenna, it is sufficient, on two different stations at the surface of the ground, to practice - with a magnetic antenna receiver - two sightings in the direction of the horizontal component of the magnetic field. The

position of the vertical axis of the emitter antenna is then at the intersection of the two sightings.

Description of the Equipment

The equipment consists of:

- an emitter set in the mine galleries
- a magnetic receiver operating at the surface of the ground
- and a pair of radiophones allowing to the workers to communicate through the earth.

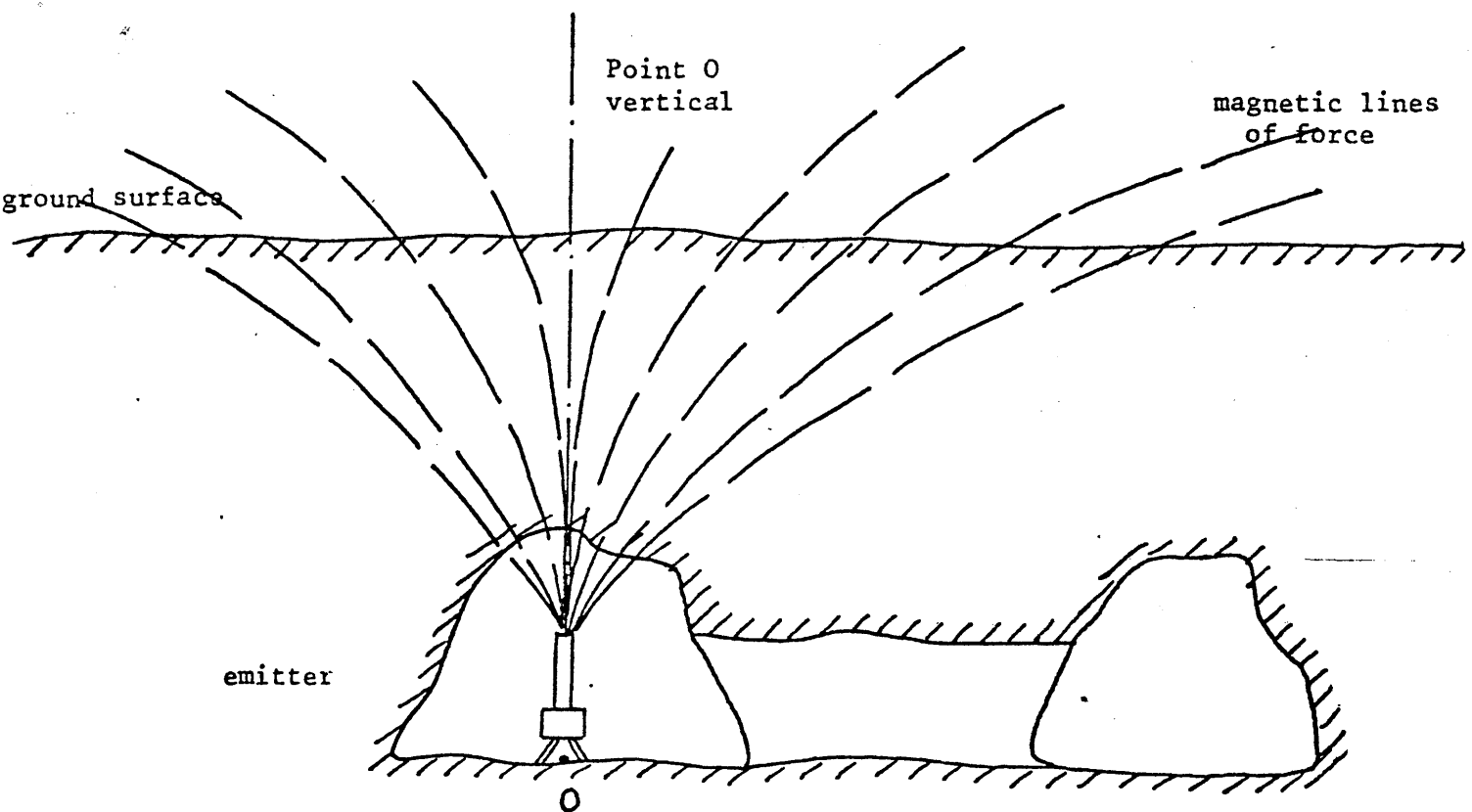


fig.1.

The Emitter

The block diagram of the emitter is presented in Fig. 2. The signal frequency radiated is about 1 kHz and the power produced by the emitter is of about 8 watts.

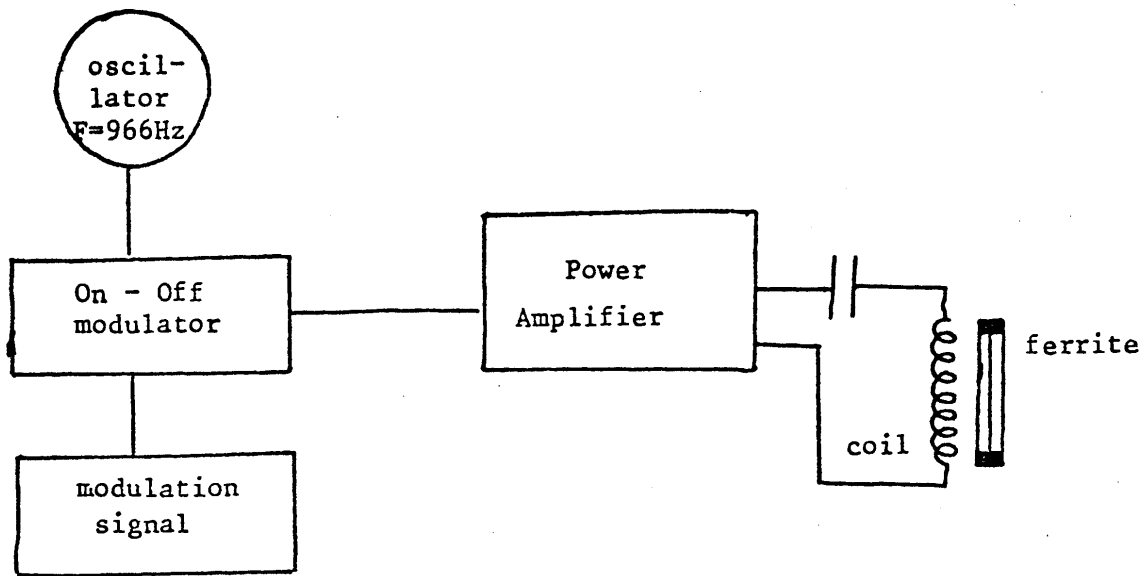


fig.2.

The antenna is constituted by a coil wound around a small bar of ferrite half a meter long. Figure 3 shows the photo of the emitter. The apparatus is mounted on the embase of a theodolite Wild to maintain the verticality of the coil axis.

The Receiver

The receiver, as shown in Fig. 4, is made of two perpendicular coils and of electronic amplifier and filters. This receiver can operate either as an amplitude detector or as an angle detector.

Amplitude Detector Operation

When the receiver is connected (Fig. 5) as an amplitude detector, we only use the coil A. The signal appearing at the ends of the coil A is amplified and simultaneously heard by a headphone and read on the dial of a voltmeter.

To determine the direction of the horizontal component of the magnetic fields, one turns the axis of the coil A in a horizontal plane until one finds a minimum deviation on the dial. Then the direction of the horizontal field component corresponds to the coil B axis.

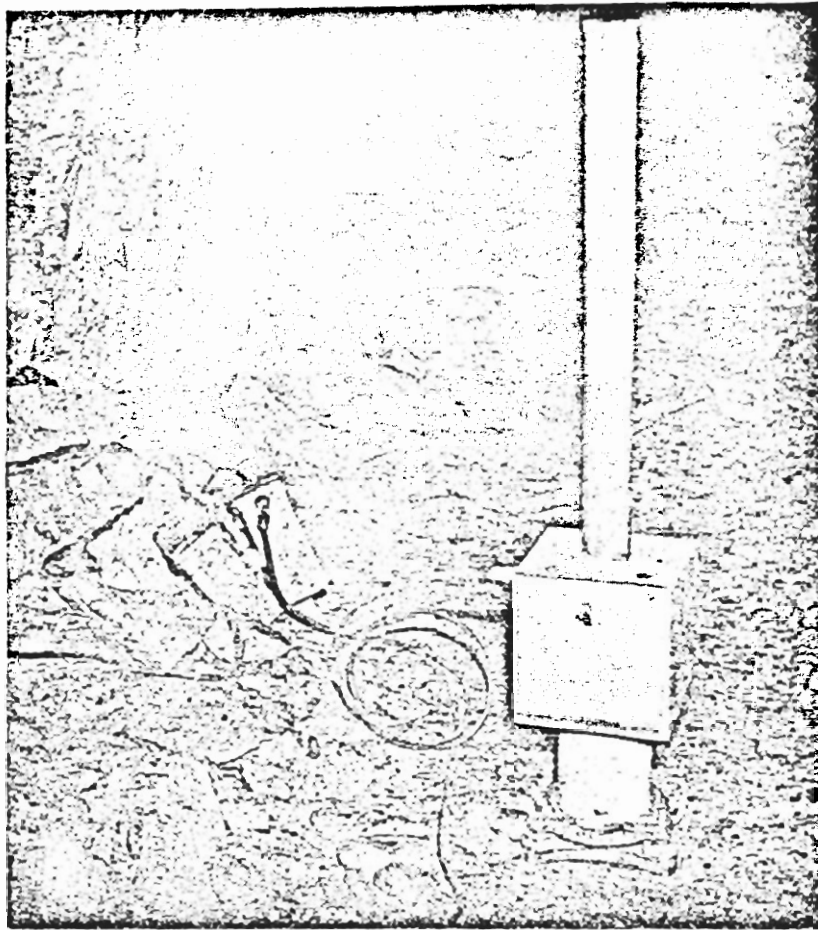


fig.3.

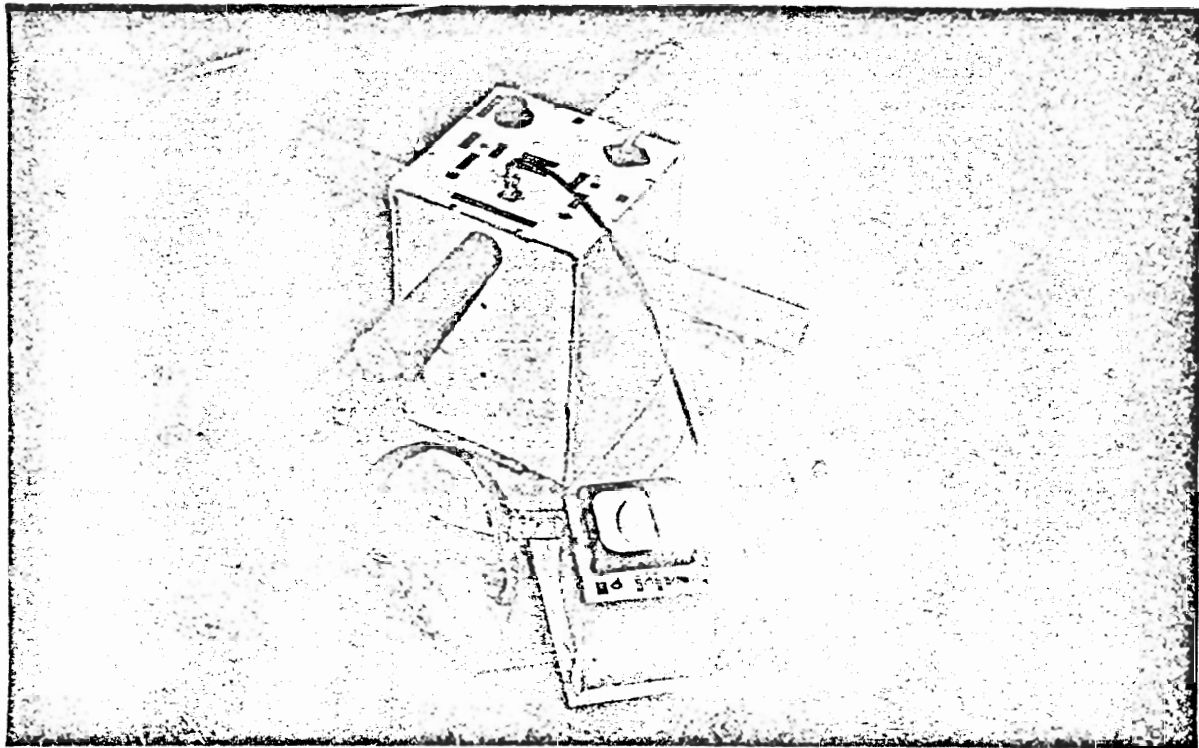


fig.4.

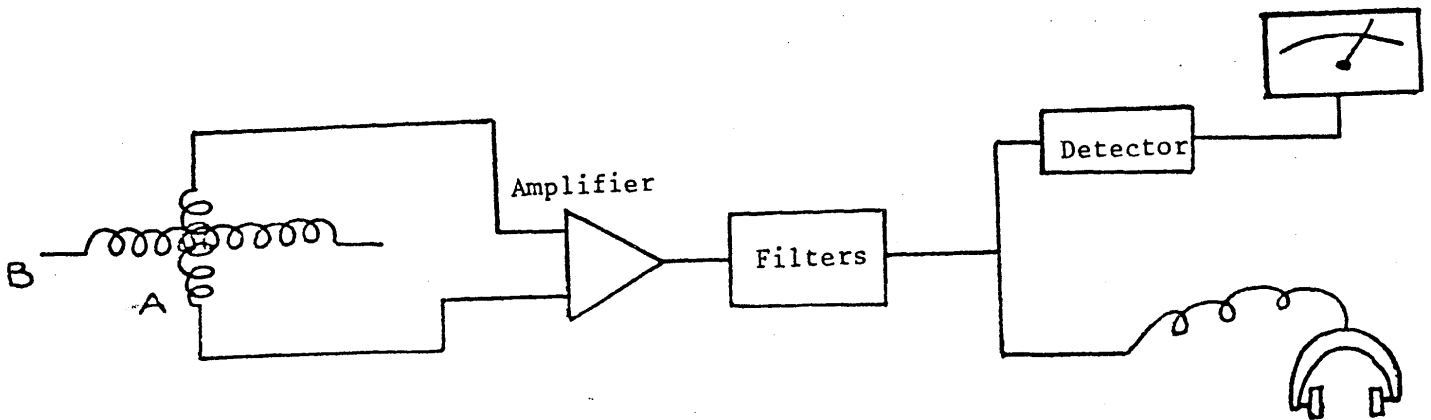


fig.5.

Angle Detector Operation

In this case the coils A and B are both used and the receiver acts as shown in Fig. 6. It detects the phase difference between the signals issued from the coils A and B.

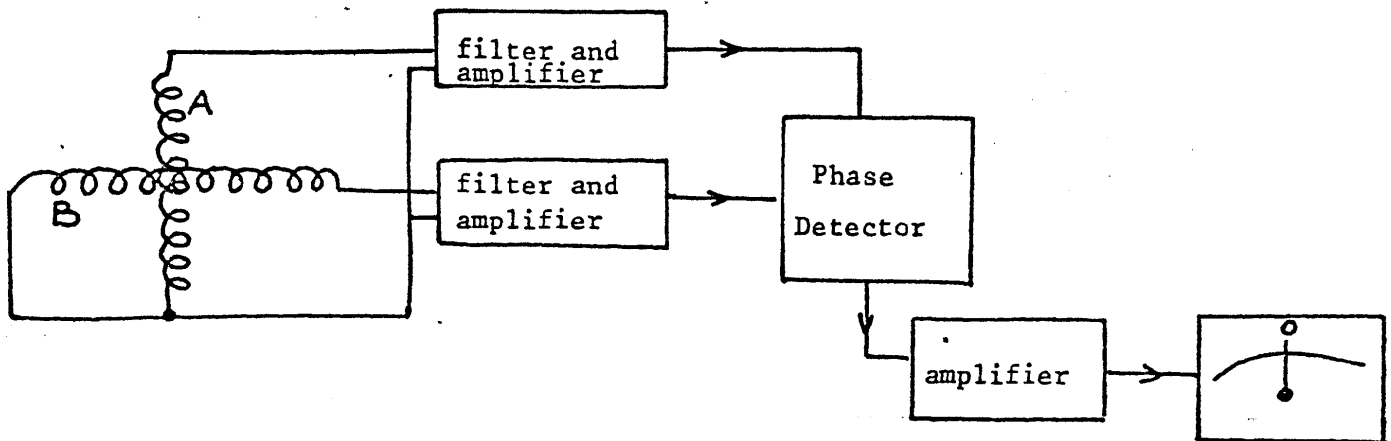


fig.6.

As is shown in Fig. 7, when the phase difference is $\pi/2$, the coil A or the coil B are in the emitter direction. When one of them is in the emitter direction a system of control allows us to verify the coil A is found in the right direction. The use of the receiver as an angle detector permits good accuracy when the signal/noise ratio is high.

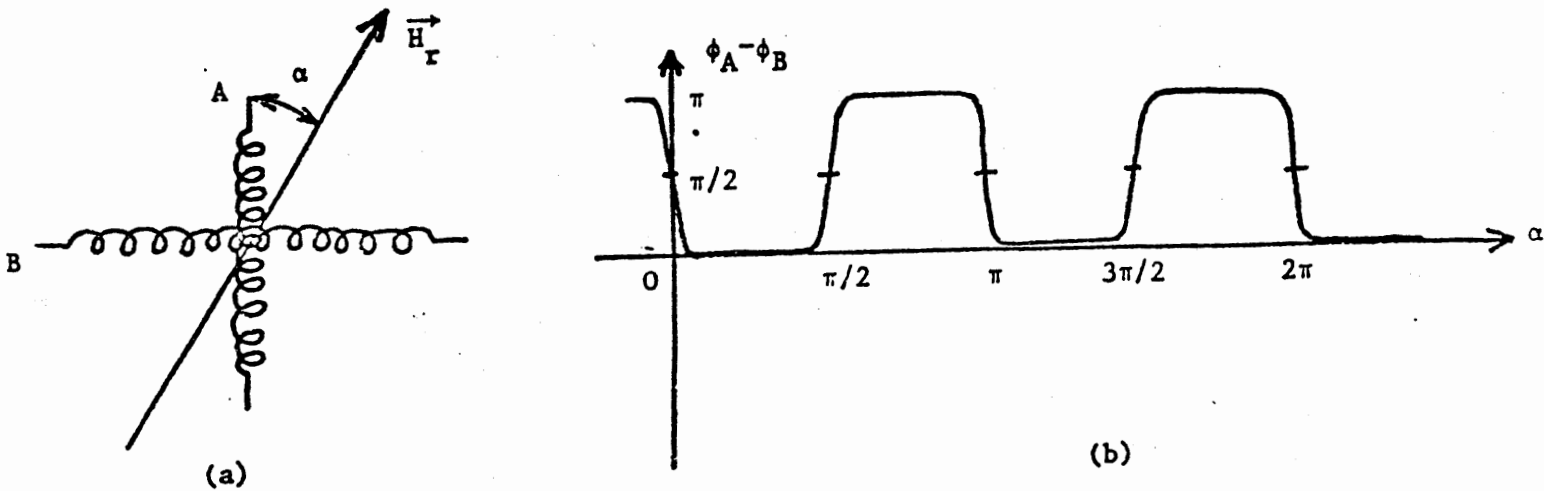


fig.7.

Radiophones

The radiophones were built to establish radio communications between the team at the surface of the earth and the team in the mine gallery. The main data are the following:

- the power supply is a 7 volt and 10 amp-hour battery
- the consumption of each radiophone is about 8 watts
- the transmission is made with a single-sideband system.

These radiophones allow communication between the surface of the ground and a station buried at a depth of about 25 meters. Figure 8 shows a radiophone set on the ground.

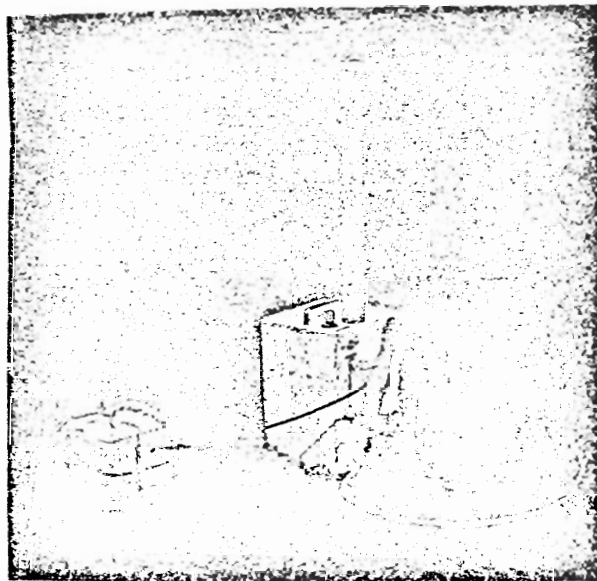


Fig. 8.

Performances of R. E. P. E.

This system has been used for three years to survey old quarries near Lille in the North of France. The experience acquired with this apparatus allows us to study the different kinds of errors made during the survey and the average of errors taking account of the working conditions.

We can distinguish four sorts of errors:

- the error due to anomalies of conductivity included in the surrounding ground of the emitter
- the error due to the verticality of the antenna emitter axis
- the error due to the horizontality of the receiver coil axis
- the error due to the noise signal acting near the receiver.

We have particularly studied the first three of them.

Anomalies of Conductivity

The magnetic lines of force are theoretically distorted by conductivity and magnetic permeability anomalies. We have chosen the signal frequency of the emitter in order to verify the relation:

$$(\sigma_a \omega \mu_0)^{\frac{1}{2}} l < 0.2$$

where σ_a = conductivity of the anomaly
 l^a = dimension of the anomaly

In these conditions we can deduce from⁽²⁾ that the magnetic lines of force are not modified by the finite conductivity and the geometry of possible anomalies.

In our case where the main anomalies are cavities, the experiment shows that the magnetic field is not disturbed when the frequency is about 1 kHz and when the depth of the emitter is about 12 meters. For larger depths it could be necessary to reduce the frequency until we verify the above equation where l represents the emitter depth. However, the magnetic lines of force are distorted by ferromagnetic bodies whatever frequency is used and, in general, it is impossible to survey near iron pipes or metallic buildings. We can consider the survey must be made according to the R. E. P. E. method for distances greater than 16 meters from iron pipes and 8 meters from metallic buildings.

Verticality of the Emitter Antenna Axis

The error of verticality of the antenna axis is mainly due to the reading of the air-level which equips the emitter. Several measure-

ments showed that this error is about 2.4 mm when the emitter is at a depth of 12 meters.

Horizontality Error of the Receiver

When the receiver is used as an amplitude detector, the principle of the determination of the emitter direction consists of the evaluation of the amplitude of the horizontal magnetic field component produced by the emitter. If the receiver coil axis does not turn in a horizontal plane, the emitter direction does not correspond to the direction of the minimum signal issued from the receiver.

It is shown in another publication⁽⁶⁾ that the angle error in the determination of the emitter direction is given by the formula:

$$\text{tg } \delta = \frac{1}{2} \text{tg } V \sin 2\alpha$$

where: V = tilt angle of the magnetic field vector with the horizontal plane
 α = accuracy of the air level of the receiver
 δ = horizontal angle error of the emitter direction

The accuracy of the air level of the receiver is about 1'5; consequently, when the emitter is set at a depth of about 12 meters and the receiver at a horizontal distance of 1 meter from the vertical axis emitter, the theoretical error of the vertical position of the emitter is 0.5 cm.

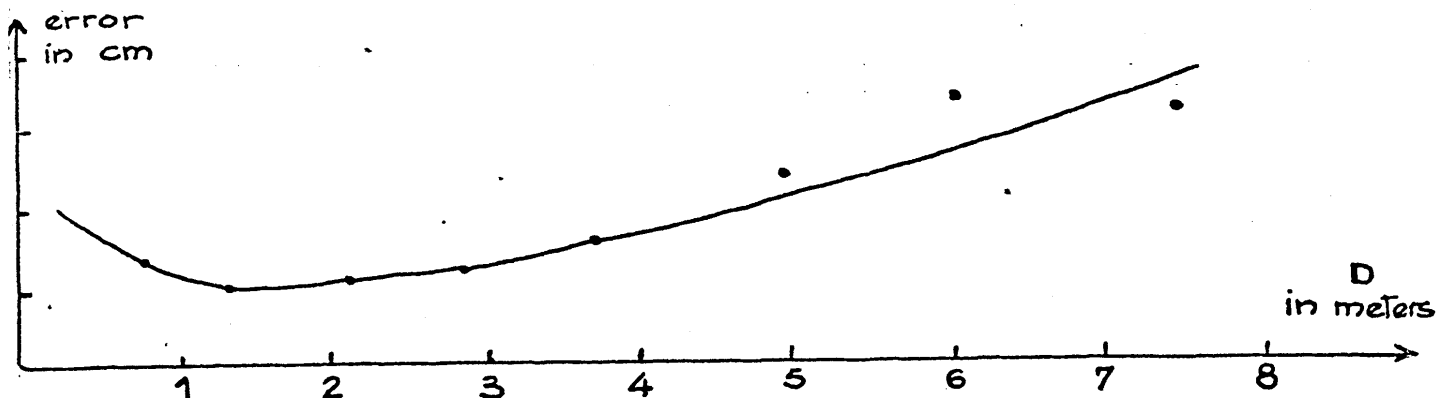


fig.9.

This curve shows that there is an optimum distance D which gives a minimum error. The distance is about 1.5 m.

Conclusions

The experience acquired during these last three years of surveys allows us to say that this method is a fair extension of the traditional survey with a theodolite and permits the reduction in price of the survey by about 20%. But this method is not a substitute for the

traditional survey; in particular, when the ground contains magnetic materials or iron pipes, or when the survey is made under buildings, the theodolite must be used alone. Practically, the survey must be made according to the R.E.P.E. method for distances greater than 16 meters from iron pipes, 8 meters from metallic buildings and 3 meters from any car. However, under certain working conditions, the R.E.P.E. method is the only available, particularly when the galleries are tortuous and their sizes small or when the ceiling is very near the floor.

Acknowledgements

We would like to thank MM. P. Mangez and J. Baudet for their contribution during the realization of these apparatus.

References

- (1) Sinha, A. K., and Bhattacharya, P. K., 1966, Vertical magnetic dipole buried inside a homogeneous earth: Radio Science, v. 1, n. 3.
- (2) Wait, J. R., 1971, Electromagnetic induction technique for locating buried source: I.E.E.E. Trans. Geosci. Electr., v. GE-9, n. 2.
- (3) Wait, J. R., and Spies, K. P., Electromagnetic fields of a small loop buried in a stratified earth: I.E.E.E. Trans. Antennas and Propagation, v. AP-19, n. 5.
- (4) Wait, J. R., 1971 Criteria for locating an oscillating magnetic dipole buried in the earth: Proc. I.E.E.E. (letters), v. 59, n. 6.
- (5) Gabillard, R., Dubus, J. P., and Cauterman, M., 1971, Campagne de detection de carrières souterraines dans la région lilloise par une méthode de prospection électrique: Bull. liaison labo P. et C., v. 54.
- (6) Gabillard, R., Dubus, J. P., Cherpereel, F., Nouveau procédé de levé de plans applicable aux carrières souterraines: Bull. liaison labo P. et C. (à paraître).

FEASIBILITY OF A RADIOCOMMUNICATION IN MINE GALLERIES BY MEANS OF A COAXIAL CABLE HAVING A HIGH COUPLING IMPEDANCE.

By J. FONTAINE, B. DEMOULIN, P. DEGAUQUE and R. GABILLARD
Electronics Department, University of LILLE - 59650 - Villeneuve d'Ascq - FRANCE

To realize a radiowave communication along mine galleries a few kilometers long without repeater, we show that it is possible to use a coaxial cable bearing an important surface transfer impedance like a transmission line with an inductive coupling to the transmitter and the receiver. We determine the electrical and geometrical constants of the cable and the optimal frequency.

INTRODUCTION

To realize a radiowave communication along mine galleries a few kilometers long, it is possible to use different kinds of transmission lines with an inductive coupling to the transmitter and the receiver.

The communication could be established without line amplifier with a two-wires line for frequencies lower than 1MHz. But such a solution requires a very good laying which is not always possible in all the galleries.

An other solution consists of a coaxial cable with spaced tuned slots. This process has been developed by Professor DELOGNE in Belgium mines in the 5-10MHz frequency range. This method gives very good results but the cable is quite expensive.

With the classical slotted coaxial cables it is necessary to use very high frequencies to obtain a good radiation. But the losses are important, and the distances between the repeaters has to be smaller than a few hundred meters.

In this paper, we show that it is possible to use a coaxial cable bearing an important surface transfer impedance. By using the coupled transmission line theory, we determine the electrical and geometrical constants of the cable, and the optimal frequency range.

PROBLEM DESCRIPTION

The transmission line is made of an insulated coaxial cable connected to both ends to its characteristic impedance. It is set in a parallel direction to the gallery at a distance h of the wall (fig.1.).

We have two coupled lines. The first consists of a single wire which is made of the braid outer conductor of the coaxial and of the earth-conductor. This line is adapted and coupled to magnetic transmitter and receiver set near the cable at points A and B. The electrical constants of this first line are :

Z_{c1} = characteristic impedance

$\gamma_1 = \alpha_1 + j\beta_1$ = propagation constant where α_1 is the attenuation factor.

The second line is the coaxial itself with a characteristic impedance Z_{c2} and a propagation constant γ_2 .

The coaxial braid has a coupling impedance Z_t per unit length. Z_t has the following form : $Z_t = jL_T\omega$ where L_T is the transfer inductance of the braid. A part of the transmitted energy on the line 1 can excite the coaxial line by means of the coupling impedance. The other part quickly vanishes by propagating on the single wire line presenting important losses.

The energy propagating in the coaxial has a much lower attenuation for $\alpha_2 \ll \alpha_1$ and can re-induce a current on the line.1. If we call A_1 and A_2 the coupling attenuation between line 1 and 2 and reciprocally, expressed in db, $A\ell_1$ and $A\ell_2$ the attenuations along the first and second lines, expressed in db/m, we can find a length of transmission L such as :

$$A_1 + A\ell_2 \cdot L + A_2 < A\ell_1 \cdot L \quad (1)$$

If so, the communication will get improved by the coupling between the both lines.

On figure.2. we have represented the signal level on the receiver as a function of the distance $AB = x$. A particular point of this curve is the point C which corresponds to the minimum distance L_{\min} to verify the inequality (1). If the receiver sensibility is lower than the level obtained at L_{\min} we see on figure.2. that the communication distance is increased.

THEORETICAL ANALYSIS

We study this problem by means of the theory of coupled lines |1||2|. The following equations of telegraphy could be used as starting point :

$$\begin{pmatrix} \frac{d^2}{dx^2} I_1 \\ \frac{d^2}{dx^2} I_2 \end{pmatrix} = \begin{pmatrix} \gamma_1^2 & Y_1 Z_t \\ Y_2 Z_t & \gamma_2^2 \end{pmatrix} \cdot \begin{pmatrix} I_1 \\ I_2 \end{pmatrix} \quad (2)$$

I_1 and I_2 are the currents along the two lines

Y_1 and Y_2 are the admittances per length unit of lines 1 and 2.

This system solution is :

$$\begin{aligned} I_1 &= k_1 (A_1 e^{\Gamma_1 x} + B_1 e^{-\Gamma_1 x}) - k'_1 (A_2 e^{\Gamma_2 x} + B_2 e^{-\Gamma_2 x}) \\ I_2 &= -k_2 (A_1 e^{\Gamma_1 x} + B_1 e^{-\Gamma_1 x}) + k'_2 (A_2 e^{\Gamma_2 x} + B_2 e^{-\Gamma_2 x}) \end{aligned} \quad (3)$$

with : $k_1 = -Z_t Y_1$

$k_2 = -Z_t Y_2$

$k'_1 = \gamma_1^2 - \Gamma_1^2$

$k'_2 = \gamma_2^2 - \Gamma_2^2$

The constants A_1, B_1, A_2, B_2 could be determined by using the boundary conditions on the ends of lines.

The boundary conditions are obtained in the form of a four linear complex equations system. The system may be solved by means of a computer.

Γ_1^2 and Γ_2^2 are the eigenvalues of the system (2) :

$$\begin{matrix} \Gamma_1 \\ \Gamma_2 \end{matrix} = \left[\frac{1}{2} (\gamma_1^2 + \gamma_2^2) \pm \frac{1}{2} (\gamma_1^2 - \gamma_2^2) \sqrt{1 + \frac{4Z_t^2 \gamma_1 \gamma_2}{(\gamma_1^2 - \gamma_2^2)^2}} \right]^{1/2} \quad (4)$$

If we suppose that $|\gamma_1| \gg |\gamma_2|$ and that the transfer impedance is much smaller than Z_{c1} and Z_{c2} , the expression (4) could be simplified and we finally obtain :

$$\begin{aligned} \Gamma_1 &= \gamma_1 + 0 \left(\frac{Z_T^2}{Z_{c1} Z_{c2}} \frac{\gamma_2}{\gamma_1^2} \right) \\ \Gamma_2 &= \gamma_2 + 0 \left(\frac{Z_T^2}{Z_{c1} Z_{c2}} \frac{\gamma_2}{\gamma_1^2} \right) \end{aligned} \quad (5)$$

The previous conditions are always valid for the low coupled lines that we consider.

DETERMINATION OF COAXIAL CABLE CHARACTERISTICS AND OPTIMAL FREQUENCY

We study the effect of each parameter of the transmission line on the receiving level. It is sufficient to determine the current I_1 on the line 1 as a function of x , (distance AB between the two transmitters) the receiving level being a linear function of I_1 .

We have represented on fig.3. the distribution current $I_1(x)$ for a given frequency $f = 9\text{MHz}$ and for 3 values of Z_T . The other parameters being constant, we observe that the level I_{c1} corresponding to the minimum distance L_{\min} is a linear function of Z_T^2 .

On fig.4. we have studied I_{c1} as a function of the frequency for different values of the permittivity ϵ_{r2} on the coaxial cable. In this study we suppose that the parameters $\alpha_1, \alpha_2, Z_{c1}, Z_{c2}$ are constant. In reality it is not quite exact, particularly for α_1 and α_2 which vary respectively according to the frequency and the square root of the frequency. But we can see on the next figures.5. and .6. that if α_1 and α_2 vary, I_{c1} is not affected if α_1 is much larger than α_2 . Thus we observe that the current on line 1 is all greater as ϵ_{r2} is near 1. For classical values of ϵ_{r2} for braided coaxial cable we observe an optimal frequency of about 7MHz.

On figures.5. and .6. we have represented $I_1(x)$ for different values of α_1 and α_2 . I_1 keeps constant and we notice a region where they are beats between the waves propagated on both lines.

Figure.6. shows that we must choose a ratio $\alpha_1/\alpha_2 > 5$ to use the coupling effect.

To build a coaxial which has good performances for this type of communication we study the current distribution $I_1(x)$ on line 1 for different values of L_T at frequency $f = 7\text{MHz}$ (see fig.7.).

For large values of L_T we take into account an important coupling between both lines. On the curves in fig.7. we can see that there is an optimal transfer inductance $L_T = 40 \cdot 10^{-9}\text{H/m}$ for a communication of one kilometer long.

It is quite evident that it is necessary to determine the geometrical and electrical characteristics of cable to obtain a minimum attenuation factor α_2 in spite of the important value of L_T (for a classical TV coaxial, L_T is of about $0.2 \cdot 10^{-9}\text{H/m}$).

Figure.8. shows the structure of a braided shielding. The transfer inductance of such a braid is given by Krügel^[3] :

$$L_T = \frac{\sigma}{4} \text{tg}^2 \psi \quad (6)$$

where ψ is the angle of braid wire with cable axis

σ is the dispersion factor

$\sigma = 1 - K^2$ where k is the coupling factor of the two half-braids, which behave like two coils wound in the opposite direction. σ is much smaller than 1.

It is very difficult to give an analytical expression for σ . The actual theory of leak transformer is insufficient to take into account all the parameters of the braid in the calculation of σ .

Krügel has shown that σ is an increasing function of ψ and a decreasing function of the coverage ratio for $\psi > 45^\circ$.

R is given by :

$$R = \frac{\text{actual area of braid}}{\text{total surface area}} = 2F - F^2$$

where F is the fill factor, i.e., the ratio of the actual width of one pick to the width of one pick for 100% coverage :

$$F = \frac{a}{b} = \frac{CNd}{2\pi(D+2d)\cos\psi} < 1 \quad (8)$$

C : number of carriers

N : number of braid wires per carrier

d : braid wire (or strand) diameter

D : diameter over cable core

The attenuation factor α_2 of a braided coaxial cable for copper is given by :

$$\alpha_2 = \frac{2.6 \cdot 10^{-9} \sqrt{\epsilon_{r2}}}{\log \frac{D}{D_i}} \left| \frac{K_s}{D_i} + \frac{K_b}{D} \right| \sqrt{f} \text{ db/m} \quad (9)$$

where D_i is the inner conductor diameter

K_s is a factor larger than 1 if the core wire is made of strands (for example $K_s = 1.06$ for 7 strands)

K_b is the braiding factor. It has the following form : ^{|4|}

$$K_b = \frac{1}{F \cdot \cos^2 \psi} = \frac{2\pi(D+2d)}{CNd \cos \psi} \quad (10)$$

According to equations (6) until (10) we see that for a given value of L_T and ψ it is possible to increase C , N and d to obtain an attenuation factor α_2 not too high.

To determine the best ratio D/D_i we have represented on figure.9. the current I_{c1} as a function of Z_{c2} .

We observe a maximum value of I_{c1} for $Z_{c2} = 75\Omega$. If we build a cable having a classical value for the outer diameter of the braid $D+2d = 7,5\text{mm}$, a characteristic impedance $Z_{c2} = 75\Omega$ with $\epsilon_r = 1.5$, $N = 4$, $C = 8$, $d = 0.25\text{mm}$, some measurements have shown us by extrapolating that we can obtain $L_T = 40 \cdot 10^{-9} \text{H/m}$ for an angle of braid $\psi = 60^\circ$.

Then the attenuation factor α_2 has the following form $\alpha_2 = 8 \cdot 10^{-6} \cdot \sqrt{f} \text{ db/m}$.

With this cable we have made the theoretical study of the communication along galleries of mine between the two magnetic transmitters. On figure.10. we have represented $I_1(x)$ for three values of the frequency : $f = 3, 7$ and 20MHz . The attenuation factor of line 1 is evaluated by measurements in coal mine in the South of France. For a single wire line situated at 30cm of the gallery wall, we have :

$$\alpha_1 = 10.4 \cdot 10^{-9} f + 1.74 \cdot 10^{-3} \text{ db/m} \quad (11)$$

The levels R_s corresponding to the receiver sensibility have been represented on figure.10. R_s is proportional to f^2 . We observe on the 3 curves that the communication distance is increased when we use the coaxial cable with a coupling effect. Indeed x_i represents the maximum distance of communication using a single wire line having an attenuation factor α_1 . x'_i is the maximum distance when we use the coaxial cable.

For these three frequencies, we have $x'_i > x_i$ but we notice that 7 MHz is an optimal frequency. $x_2 = 550\text{m}$ and $x'_2 = 1200\text{m}$. There is a ratio 2 between these two distances.

CONCLUSION

With this coaxial cable we have studied, we have the possibility to increase the maximum distance of communication in a ratio greater than 2. An other advantage of this system is that the line could be set careless. Indeed the attenuation factor α_1 of the single wire line made of the cable and the gallery could be important without influence on the communication.

ACKNOWLEDGEMENTS

Thanks are due to C.E.R.C.H.A.R. (Centre d'Etudes et de Recherches des Charbonnages de France) who suggested the investigation.

REFERENCES

- (1) P.I. KUZNETSOV and R.L. STRATONOVICH, The propagation of electromagnetic waves in multiconductor transmission lines, PERGAMON PRESS, 1964
- (2) H. MURATA, S. INAO and H. HONDO, Electromagnetic interference with video transmission cable, 20th International wire and cable symposium proceedings, Atlantic City, N.J., Dec. 2, 1971
- (3) Von L. KRUGEL, Abschirmwirkung von Aussenleitern flexibler Koaxialkabel, Telefunken-Zeitung, Jg 29 (Dezember 56), Heft 114
- (4) J. SPERGEL, Computer aided design of braid parameters for coaxial cable, 20th International wire and cable symposium proceedings, Atlantic City, N.J., Dec.2, 1971

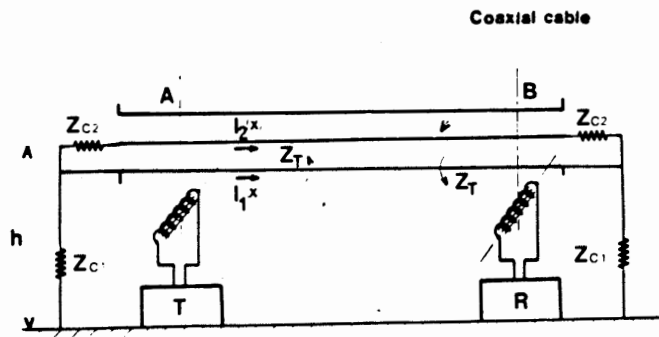


Fig.1

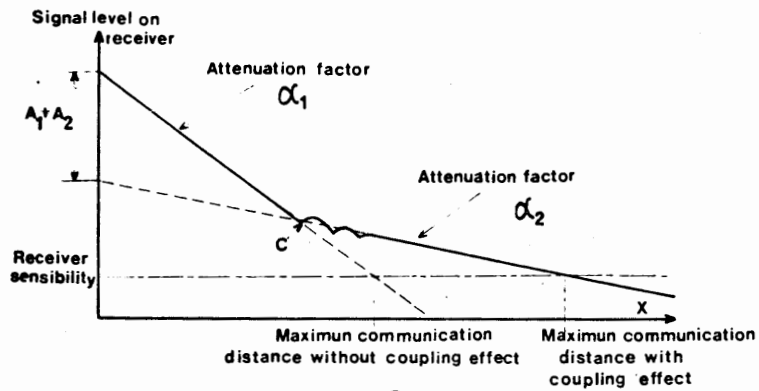


Fig.2

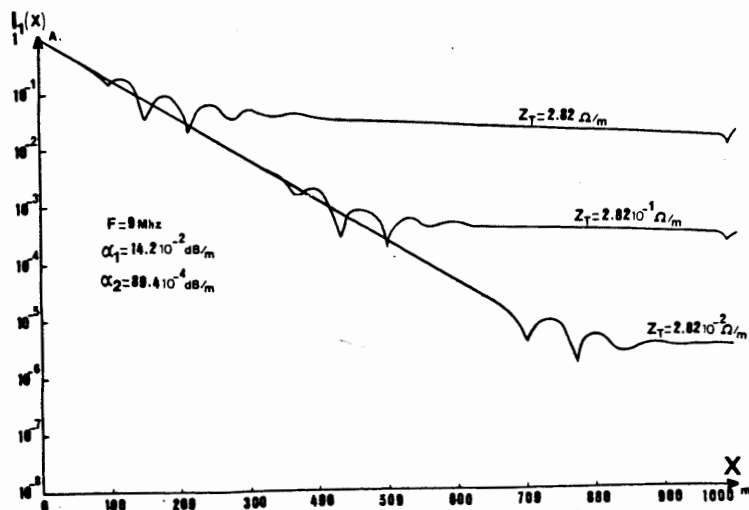
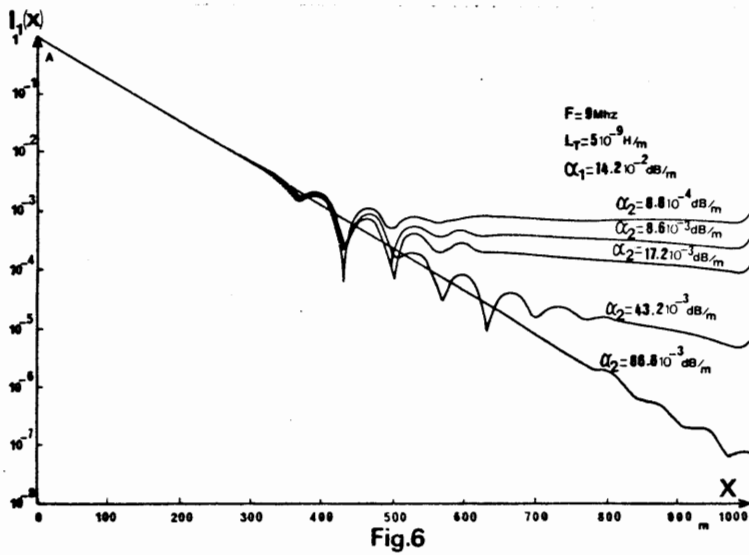
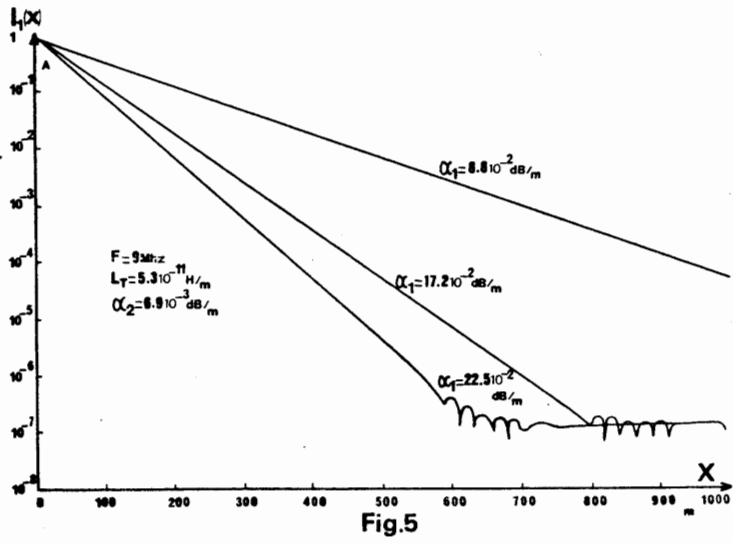
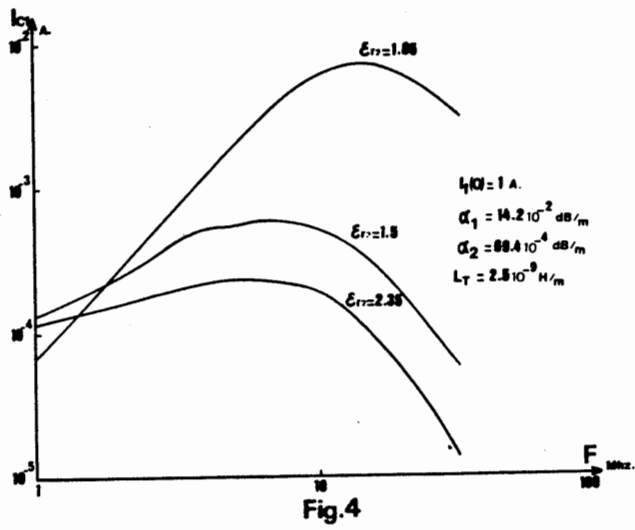
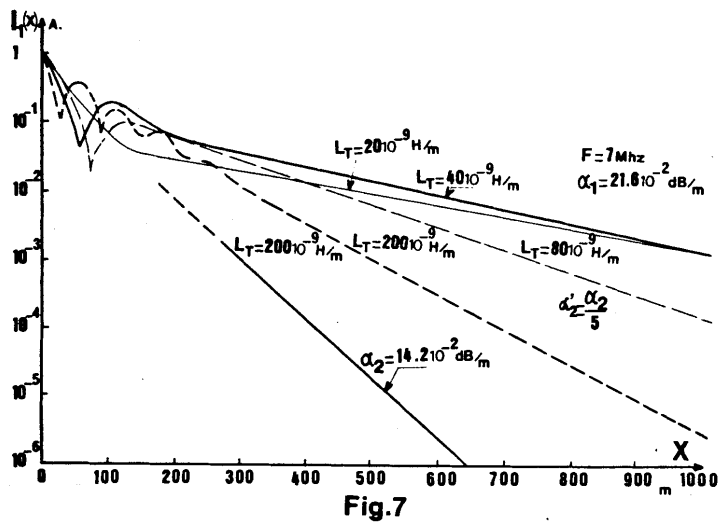


Fig.3





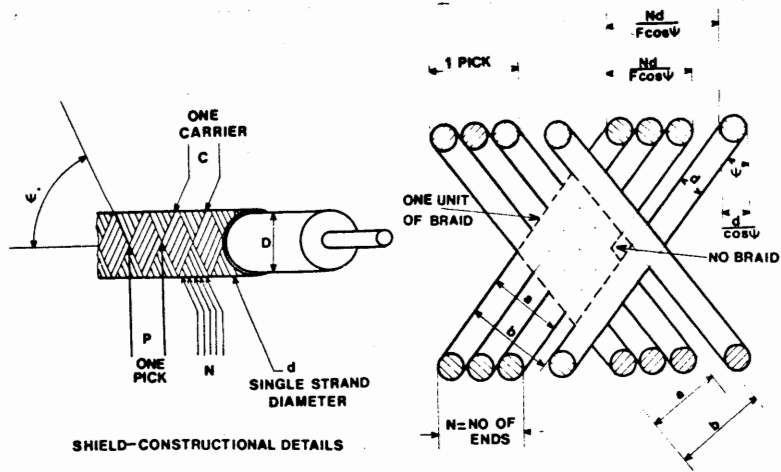
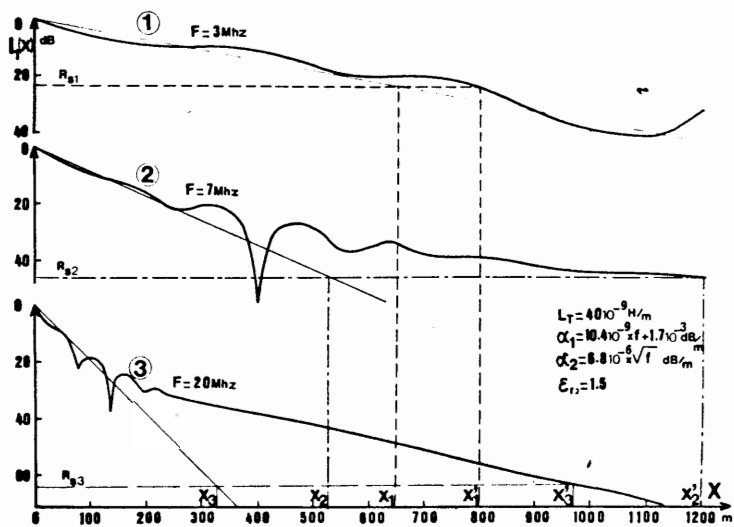
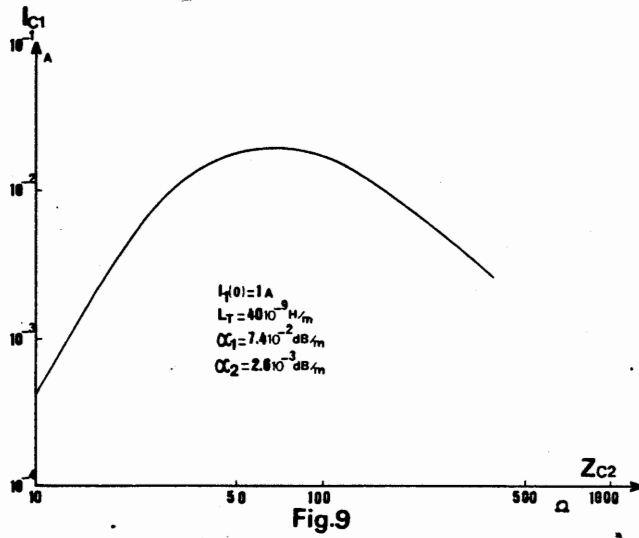


Fig.8



ELECTROMAGNETIC TRANSMISSION AND DETECTION AT DEEP DEPTHS

D. B. Starkey
Acceptance Technology Division 8344
Sandia Laboratories Livermore

Introduction

Investigation into the expressions of the field produced by a loop over a conducting half space or in an infinite conducting half space are well documented. Reasonably complex descriptions of the effects of stratification also are reported. However, a model which must contain all of these complexities because of transmission to depths of 15,000 feet and also include the perturbation of the field by a vertical cylindrical steel casing loses its facility in the field or for quick, accurate approximation to field magnitudes and phase.

This paper describes the results of two field tests to determine the attenuation and phase versus depth and frequency of an electromagnetic wave (induction field). A simple two-layer model is postulated to predict the magnitude and phase of the induced field which does not require sophisticated computing tools. Correlation of the model with experimental results show agreement of most amplitude measurements to within 3 db and most phase measurements to within five degrees. The tests were conducted in a 7400 foot deep well in Nevada and an 11,000 foot deep well in Wyoming which had conductivities ranging from .0025 mhos/m to .25 mhos/m. The surface transmitting dipole had an area of $\sim 10^6$ feet squared and constant frequency signals of 1.5 Hz to 20 Hz were transmitted through the earth utilizing less than 65 watts of power.

Model Description

The magnetic field intensity components generated by a magnetic dipole immersed in an infinite homogeneous medium can be expressed in spherical coordinates as:

$$H_r = \frac{NI (\pi a^2)}{4\pi r^3} [1 + \gamma r] [e^{-\gamma r}] 2 \cos\theta \quad (1)$$

$$H_\theta = \frac{NI (\pi a^2)}{4\pi r^3} [1 + \gamma + \gamma^2 r^2] [e^{-\gamma r}] \sin\theta \quad (2)$$

$$r = (Z^2 + a^2)^{1/2}$$

Z = vertical depth between coaxial loops

where N, I, and (πa^2) are the transmitting antenna turns, current, and effective area, respectively, and r is the range from the loops circumference to the measurement point. The case of interest for these experiments, however, is the special case of coaxial dipoles, i.e., $\theta = 180^\circ$. For this case $H_\theta = 0$ and H_r reduces to:

$$H_r = \frac{NI (\pi a^2)}{2\pi r^3} [1 + \gamma r] [e^{-\gamma r}] \quad (3)$$

It is apparent from the expression for r that dipoles of finite dimensions are being considered. For these tests the radius was either 600 or 1200 feet and the effect of the loop's radius had to be considered.

The complex propagation constant, γ , is expressed in terms of angular frequency, $\omega = 2\pi f$ and the medium properties conductivity, σ , permeability, μ , and permittivity, ϵ . For conducting media, displacement current effects are generally negligible and for the condition $\sigma \gg \omega\epsilon$

$$\gamma \approx (1 + j) \left(\frac{\omega\mu\sigma}{2}\right)^{1/2}$$

where the skin depth δ is the inverse of real part of γ or

$$\delta = (2/\omega\mu\sigma)^{1/2}$$

Although in the actual experiments, there is a half space of air above the ground, the increased complexity of the model including this half space was not considered practical. This appears to be justified in examining the results of the two field experiments.

Media Discontinuity

Because of the depths involved in the experiments, stratification of the media is obvious from the available lithologies. Although consideration was given to characterize the media from a single lumped homogeneous, isotropic region with an average conductivity to n homogeneous, isotropic regions as dictated by the lithology, the end result was to use a two-layer model. The single homogeneous layer appeared impractical when one studied the DC resistivity logs of the experimental wells. Although the resistivity varied over quite a dynamic range, there seemed to be two or three "average" values which fit only a particular depth increment. The n layer model was discarded also because it did not fit the resistivity logs. In addition, because of the wavelengths involved, many thin layers of different conductivity can be ignored because only small phase delays are encountered in a layer, resulting approximately in cancellation of the two reflections.

The resulting two-layer solution is shown below:

$$H_r(Y + X) = H_r(Y) \left(\frac{Y}{Y + X}\right)^3 (1 + \gamma_2 Z_2) (e^{-\gamma_2 Z_2}) \quad (4)$$

where $Y = \text{radius at the interface } (Z_1^2 + a^2)^{1/2}$
 $X = \text{radius below the interface } (Z^2 + a^2)^{1/2}$

$H_r(Y) = \text{magnetic field intensity at interface from Equation 3}$

$\gamma_2 = \text{propagation constant for the second layer}$

$Z_1 = \text{verticle depth from transmitting loop to interface}$

$Z_2 = \text{verticle depth from interface to receiving loop}$

Well Casing Attenuation

Assuming that the resultant field from the above calculations is that which is present at any depth, the attenuation of the magnetic field intensity

by the well casing is calculated by the following relationship described by Shenfeld for infinite long cylinders whose radius is much greater than the cylinder thickness:

$$\frac{\bar{H}_0}{\bar{H}_1} = \cosh(\bar{\gamma}d) + \frac{\mu_0}{2\mu} \gamma \delta r \sinh(\bar{\gamma}d)$$

\bar{H}_0 = magnetic field intensity outside the cylinder

\bar{H}_1 = magnetic field intensity inside the cylinder

$\bar{\gamma}$ = propagation constant for the wall material

δ = skin depth in the wall material

μ = wall material permeability ($200 \mu_0$)

r = cylinder radius

d = cylinder wall thickness

The above expression is said to be valid for the following cases:

1. High or low frequencies (converges to the skin depth solution at high frequencies)
2. Magnetic or non-magnetic wall material
3. Orientation of H_0 is unimportant

Although this expression diverges somewhat from the concept of developing a simple model, it is required at the frequencies of interest (below 20 Hz). Figure 1 is a plot of the attenuation from Shenfeld's relationship and plane wave attenuation from .1 to 10 Hz for a typical casing. It can be seen that even at 10 Hz the plane wave attenuation is ~ 6 db pessimistic relative to Shenfeld's formulation. Multiple casings encountered in some of the testing are handled as a single cylinder whose thickness is equal to the sum of all the casings' thickness.

Receiving Antenna

The receiving antenna is a ferrite loop stick in construction. Assuming that the core "captures" all of flux within the casing and that this flux is uniformly distributed across the internal cross section, the open circuit voltage from the antenna is described as follows:

$$|V| = \omega \mu_0 A_{\text{eff}} |\bar{H}_1|$$

$|\bar{H}_1|$ = magnitude of Shenfeld's internal field intensity
 A_{eff} = effective area of the receiving antenna
 ω = angular frequency
 μ_0 = free space permeability

Since \bar{H}_1 for a given depth and media decreases with frequency and the voltage output has frequency as a multiplier, an optimum frequency is expected. The model (using the Wyoming data below) shows an optimum at ~ 2 Hz at 6000 feet and ~ 1 Hz at 12,000 feet.

Test Apparatus

Figure 2 is a block diagram of the test apparatus used to gather the data for both test series. A square wave oscillator is set at the desired frequency. The phase of this signal relative to that which is the reference for a coherent detector can be selected at either 0 or 45 degrees. The square wave is then filtered and its gain controlled to drive the output of an audio amplifier. The transmitting loop has a .05 ohm resistor in series such that the current in the loop can be determined and the phase shift of the amplifier removed from the phase measurements. The signal received downhole is then amplified by either 130 or 160 db and used as an input to a 1 KHz VCO. This signal is brought uphole on a cable, discriminated, filtered, and fed to the coherent detector. The detector outputs then give a real time indication of the received signal characteristics as follows:

$$V_{\text{received RMS}} = \sqrt{I^2 + Q^2} / \text{Gain}$$
$$\phi_{\text{path}} = \tan^{-1} Q/I - (\text{receiver and transmitter phase})$$

The 3 db bandwidth of the amplifying system was from $\sim .9$ Hz to 30 Hz. The coherent detector's bandwidth was generally left at .025 Hz.

Nevada Test Site and Model Parameters

Figure 3 is a graphic view of the NTS test configuration. A double casing extended to a depth of 940 feet. From this depth to 7410 feet a single casing was present. The model parameters used were:

$$\begin{aligned} \text{Interface Depth: } Z_1 &= 1500 \text{ feet} \\ \text{Layer One: } \sigma &= .0025 \text{ mhos/m} \\ \text{Layer Two: } \sigma &= .01 \text{ mhos/m} \end{aligned}$$

Two transmitting loops were used, each with an area of $\sim 10^6$ feet². One was offset approximately 1200 feet from the well center. The transmitted power (I^2R losses) was varied from 4 to 13 watts with signal-to-noise ratios at 5 Hz varying from 35 to 12 db at 1000 and 7410 feet respectively. The offset antenna was used among other techniques to give assurance that the signal was not propagated down the cable or well casing--since the phase would be different for this case versus through the earth, particularly at the shallow depths. Figures 4, 5, and 6 show the relative strengths of the measured fields as compared to the model predictions.

Wyoming Tests

Figure 7 is a graphic view of the Wyoming test configuration. A triple casing extended to 437 feet. From 437 feet to 8255 feet a double casing existed and below 8255 to 11,000 feet only a single casing was present. The model parameters used were:

$$\begin{aligned} \text{Interface Depth: } &8100 \text{ feet} \\ \text{Layer One: } \sigma &= .05 \text{ mhos/m} \\ \text{Layer Two: } \sigma &= .25 \text{ mhos/m} \end{aligned}$$

One transmitting loop was used with an area of 4×10^6 feet². The transmitter power was varied from 4 to 65 watts with signal-to-noise ratios at 5 Hz varying from 20 db to 2 db at 3500 feet and 11,000 feet respectively. Figures 8, 9, and 10 show the relative strengths of the measured fields.

Discussion of Results

The correlation between calculated and experimental values indicates that the model is extremely accurate. Although the phase plots have been omitted because of space limitations, the two-layer model is also capable of high accuracy in this prediction at all depths also. Only at the shallow depths is the phase prediction high by approximately five degrees. The use of the infinite homogeneous model appears to balance any effects in the field caused by the steel casing.

The amplitude plots show a discontinuity at the location of a change in the number of casings. This fact, plus the use of the offset antenna at NTS, show that the signal is propagating in the medium and not down the casing. Additional calculations yielded a maximum attenuation rate of only .9 db/1000 feet presuming the signals was coupled down the armored cable used to lower the receiving package. Since the actual attenuation rates were much greater, this was also eliminated as a possible coupling link.

Acknowledgements

This work was supported by the United States Atomic Energy Commission Division of Peaceful Nuclear Explosives, Contract Number AT-(29-1)-789.

The author would also like to thank El Paso Natural Gas Company for providing the test well and their capable assistance in the conduction of the Wyoming experiment.

References

1. S. Shenfeld, "Shielding of Cylindrical Tubes", IEEE Transactions on Electromagnetic Compatibility, Volume EMC-10, No. 1, March 1968
2. James R. Wait, "Electromagnetic Fields of Sources in Lossy Media", Antenna Theory: Part II, McGraw-Hill Book Company, 1969

WELL CASING ATTENUATION

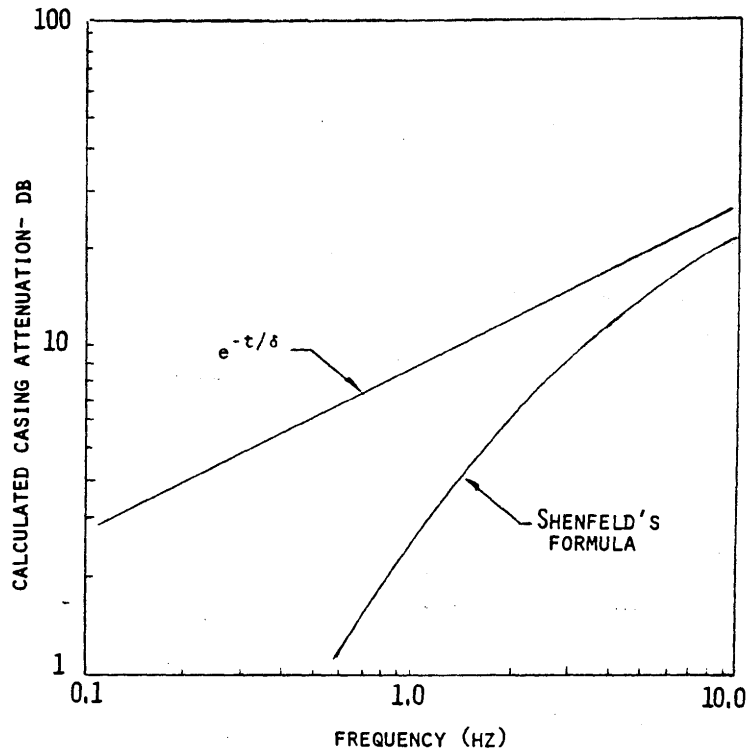
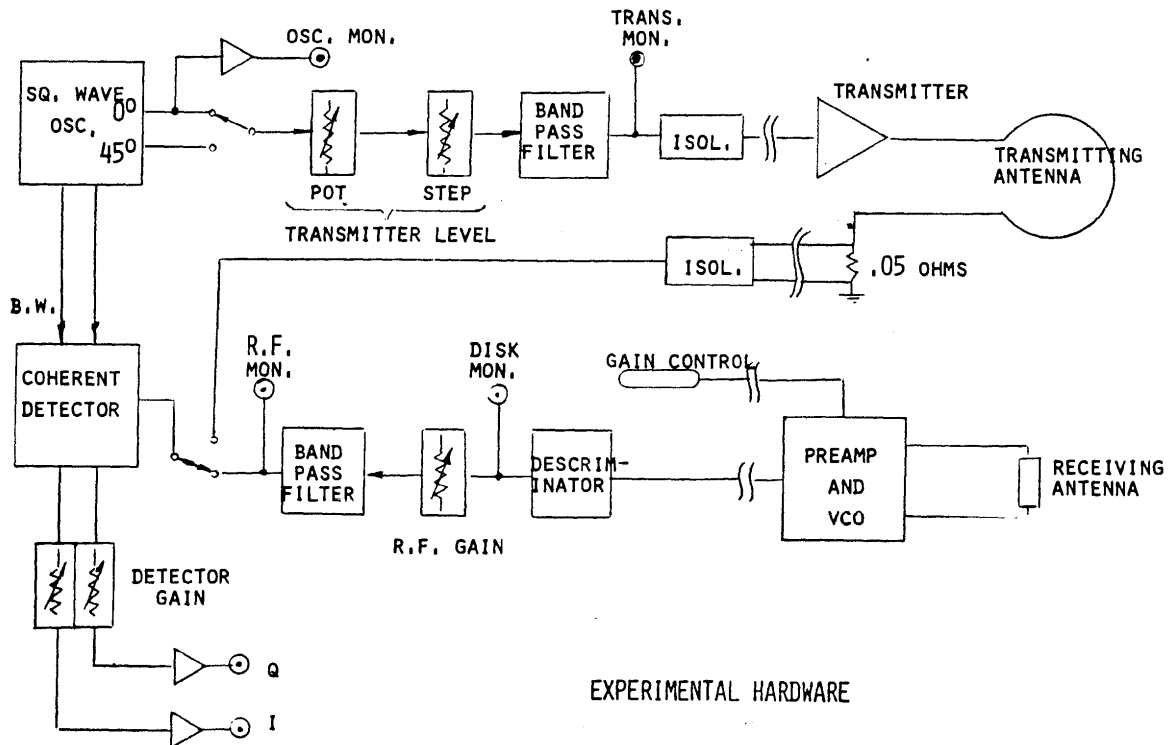


Figure 1



EXPERIMENTAL HARDWARE

Figure 2

NTS TESTS - AREA 20

PAHUTE #1

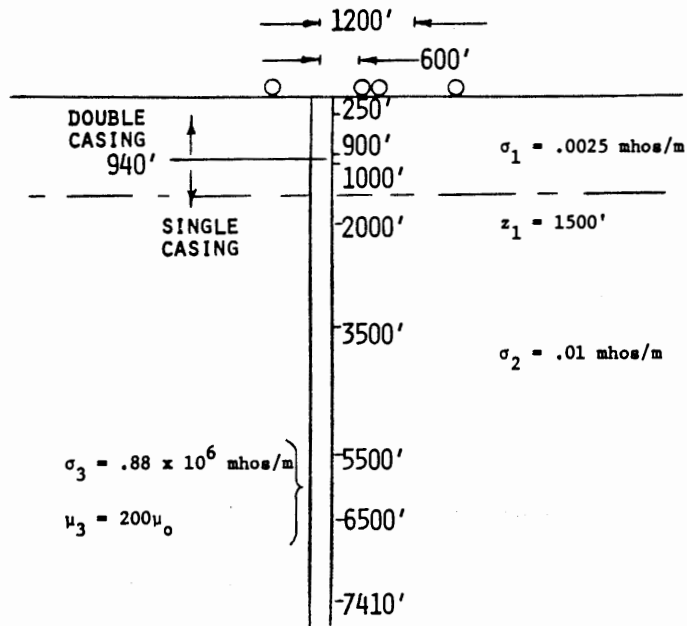


Figure 3

WYOMING TESTS

EP #5

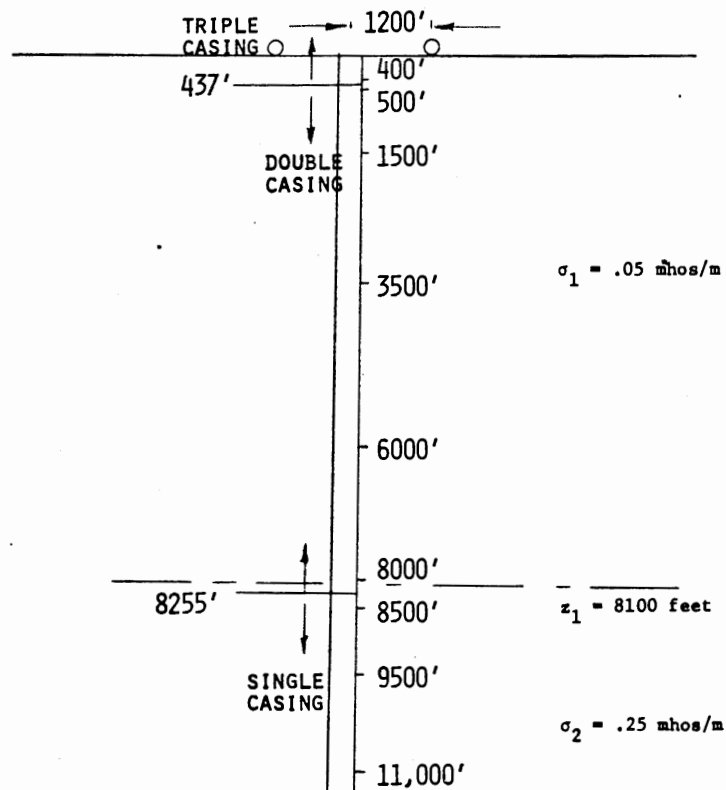
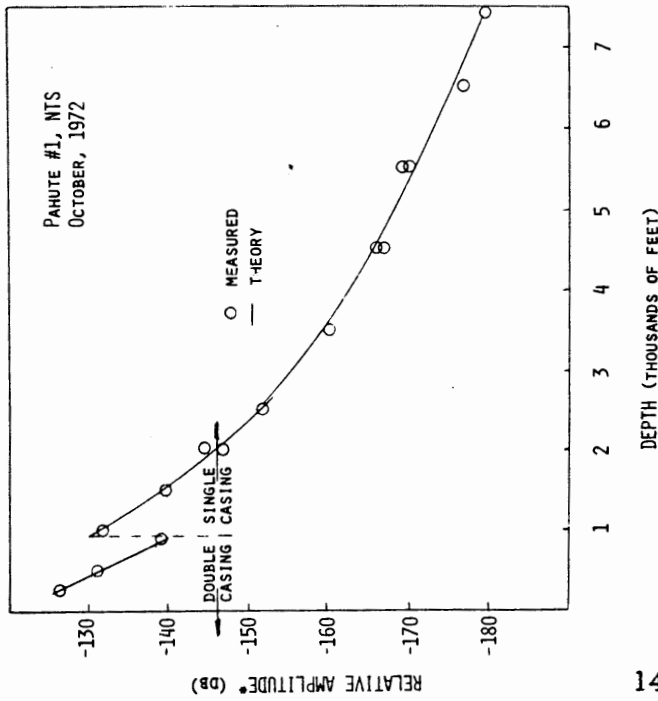


Figure 7

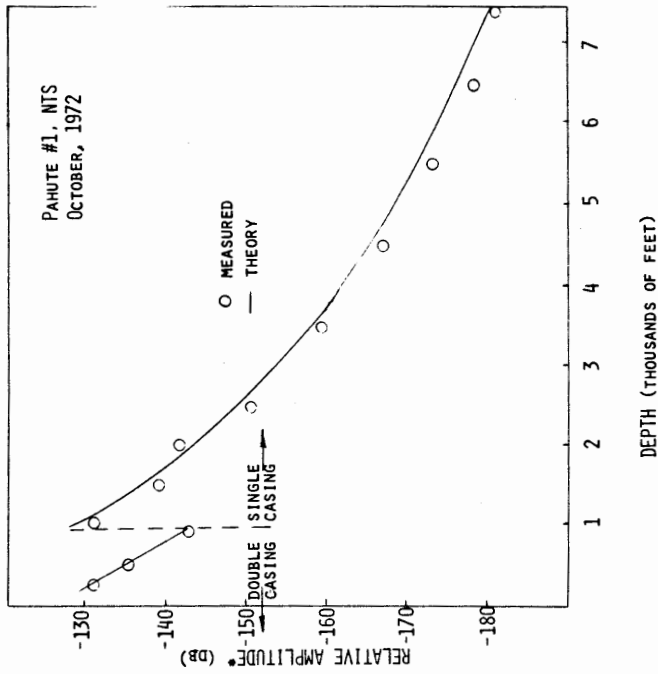


* SIGNALS RELATIVE TO 1 VOLT RMS AT THE RECEIVING ANTENNA FOR 1 AMP RMS IN THE TRANSMITTING LOOP.

MEASURED ATTENUATION RATE: ~4.4 DB/1000 FEET (LAST 3500 FEET)

5 HZ SIGNAL ATTENUATION

Figure 4

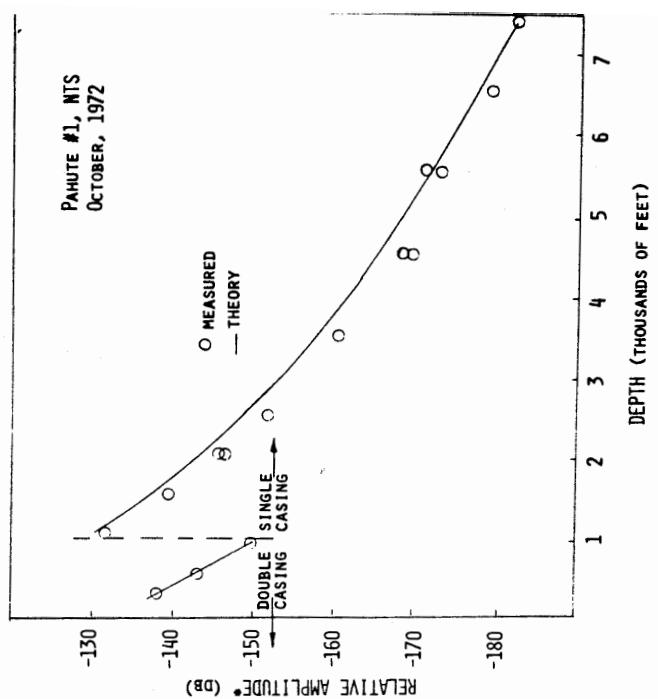


* SIGNALS RELATIVE TO 1 VOLT RMS AT THE RECEIVING ANTENNA FOR 1 AMP RMS IN THE TRANSMITTING LOOP.

MEASURED ATTENUATION RATE: ~4.8 DB/1000 FEET (LAST 3500 FEET)

10 HZ SIGNAL ATTENUATION

Figure 5

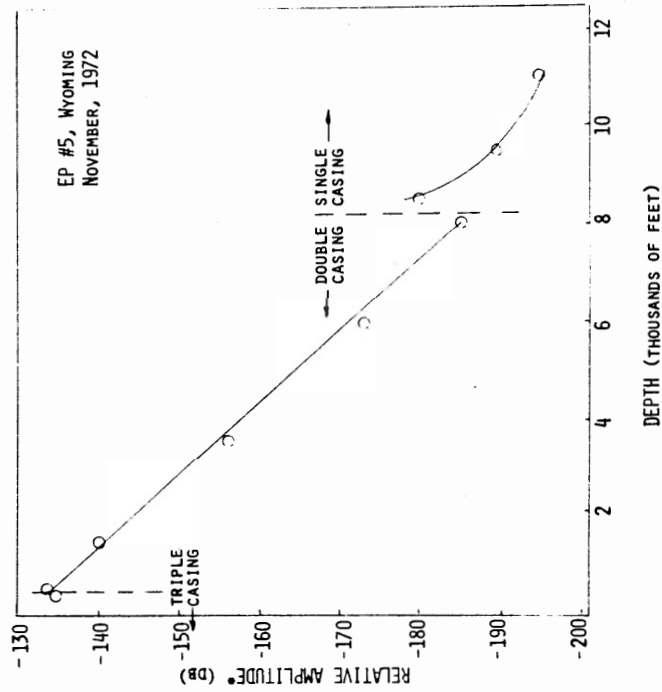


* SIGNALS RELATIVE TO 1 VOLT RMS AT THE RECEIVING ANTENNA FOR 1 AMP RMS IN THE TRANSMITTING LOOP.

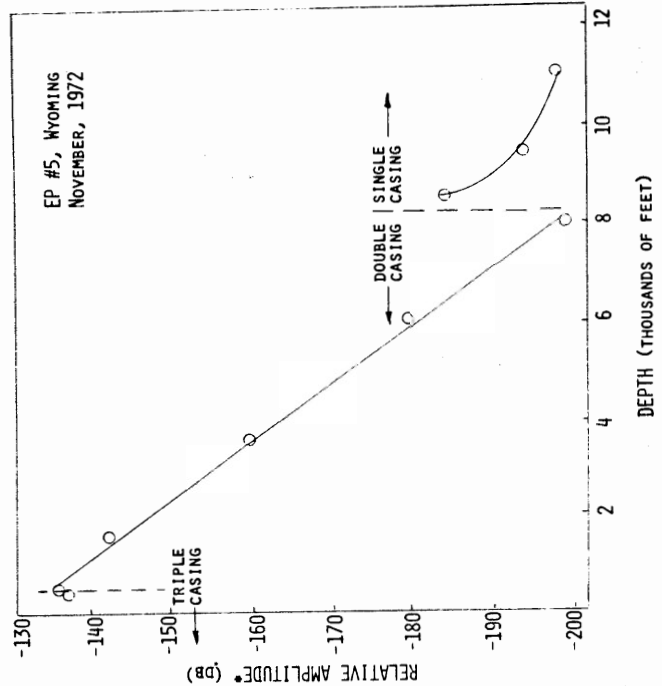
MEASURED ATTENUATION RATE: ~5.1 DB/1000 FEET (LAST 3500 FEET)

20 HZ SIGNAL ATTENUATION

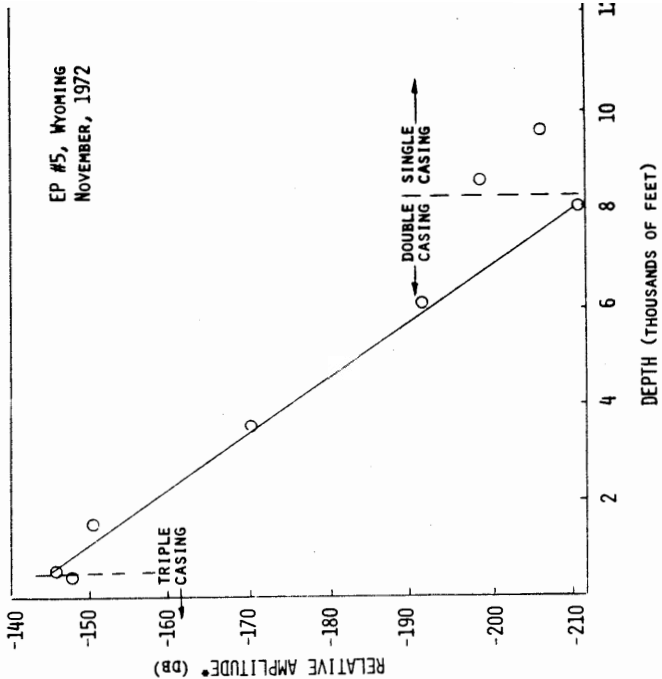
Figure 6



5 Hz SIGNAL ATTENUATION
Figure 8



10 Hz SIGNAL ATTENUATION
Figure 9



20 Hz SIGNAL ATTENUATION
Figure 10

ADMITTANCE AND EFFECTIVE HEIGHT OF BURIED ANTENNAS*

Giorgio Franceschetti
Istituto Elettrotecnico, Universita
via Claudio 21, 80125 Napoli, Italy
Istituto Universitario Navale
via Acton 38, 80137 Napoli, Italy

Abstract

Explicit expressions are presented for the input admittance and effective height of several buried metal antennas, namely: (i) prolate spheroidal; (ii) spherical; (iii) oblate spheroidal; (iv) parallel plate; (v) parallel plate with protruding dielectric in the same plane of the plates; (vi) parallel plate with protruding dielectric in a plane normal to that of the plates (H-shaped antenna).

Expressions are given to several degrees of approximations:
1. The environment is assumed to be homogeneous and infinite and computations are carried out in the zero-frequency limit for cases (i) through (vi). 2. The frequency limitation is partly removed, the antennas being assumed small with respect to the field wavelength in the environment. Computations are carried out for cases (i) through (iii), thus clarifying the limits of approximation 1. 3. The frequency limitation is totally removed for case (ii), thus clarifying the limit of approximation 2.

It is concluded that in all practical situations of "small" antennas approximation 1 is almost always appropriate. Computations were carried out for bare antennas, the extension to insulated ones being, however, straightforward.

Although a rigorous theory of the antenna performance in a realistic semi-infinite conductive medium has not been developed, the results quoted should also be applicable when antennas are a few skin depths below the earth's surface. In particular, for the evaluation of radio-links under up-over-and-down operating conditions, the antennas can be replaced by dipoles of length equal to the effective height.

Since the antenna's parameters are given in analytical form, it is also possible, by using Laplace transform techniques, to compute the transient response of the antenna. The transient is described by pole (short-time behavior) and branch-cut contributions (large time behavior). For these last terms, an asymptotic evaluation is possible,

so obtaining closed form expressions for the response at large observation times, which is closely related to the dispersion characteristic of the environment.

SPECTRUM MEASUREMENTS OF ELECTROMAGNETIC-NOISE IN COAL MINES*

W. D. Bensema and J. W. Adams
National Bureau of Standards

Abstract

A portable, multichannel battery-operated mine-permissible measurement system was developed to measure the rms magnetic-field noise spectrum in the frequency range from 100 Hz to 375 kHz. During each measurement, the entire spectrum is measured simultaneously through the use of time-domain recordings which are later analyzed by Fast Fourier Transform processing. Dynamic ranges of 60 dB in a 125 Hz bandwidth are obtained for spectra covering the range from 100 Hz to 100 kHz. The method also allows a three-dimensional display of the way spectrum occupancy changes with time. Calibration and correction procedures allow absolute field strength measurement with an uncertainty of not more than 3 dB. We feel that further analysis of the system errors will allow this uncertainty to be reduced to less than 1 dB.

Ambient magnetic field noise spectra covering frequencies from 100 Hz to 100 kHz are given for several underground coal mine locations. Examples are also given of magnetic field noise on the surface above the mine, noise in the mine face area, noise radiated by specific equipment, the voltage spectrum found on a 600 V dc trolley wire, and noise picked up simultaneously on loops and on roof support bolts.

I. Introduction

Measurements of the ambient electromagnetic noise present at the receiving terminal must be made in order to design a communication system usable for routine and emergency communications, either operating through the earth or utilizing wire or wireless links within the mine.

Constraints on the experiment made it necessary to rapidly measure electromagnetic noise over most of the spectrum below 300 kHz. Therefore, broadband, analog, real-time recording for later processing was chosen as the means of study, rather than the more usual but slower, narrow band swept-frequency techniques. The chosen method rapidly and continuously records the entire spectrum. The entire spectrum of an event lasting a few seconds, such as an electric locomotive passing by, can be captured quickly on magnetic tape, and later analyzed in great detail.

*Sponsored by U. S. Bureau of Mines

II. Measurement Instrumentation

The system block diagram is shown in Figure 1. Figure 1a shows the field-portable portion of the system. Three data channels were needed to obtain three orthogonal field components at each site. An analog 7-track tape recorder running at 30 inches per second (ips) and weighing 14 kg was used for recording the time series data. Figure 1b shows the laboratory transcription process used to reduce the data bandwidth and transcribe the data to a laboratory-quality analog tape recorder with tape-controlled servo capability. The servo capability accurately controls the tape recorder speed from a stable reference signal recorded on the tape (on a separate channel) at the same time the noise signals were recorded. Figure 1c shows the laboratory digitizing process. During this step, the data bandwidth was further reduced; the tape recorder was run in the tape-controlled servo mode. The digitized data was then processed by a digital computer. The available digitizing instrumentation was not capable of accepting the full bandwidth of the data as recorded. It was therefore necessary to reduce the effective bandwidth of the data by using a slower speed on playback than was used on recording. This process retained all of the original information but traded bandwidth requirements for processing time. A Fast Fourier Transform (FFT) algorithm was used to change the time series data into a frequency series presentation in spectral form. The processed data in its initial form comes from the microfilm plotter and printer, Figure 1d. The FFT routines were developed primarily by L. D. Lewis of the Space Environment Laboratories, National Oceanic and Atmospheric Administration, Boulder, Colorado. Lewis based his algorithm primarily on methods outlined by Welch (1).

III. Typical Coal Mine Spectra

Data were taken in Robena No. 4 Mine, Waynesburg, Pennsylvania. Figure 2 shows a spectrum measured in the face area, about 10 meters behind a continuous mining machine in full operation. The machine was powered by 600 volts dc. For the curve shown, the antenna sensitive axis was oriented for a vertical moment. The field strengths measured were about 39 db above one micro-ampere per meter (39 db $\mu\text{A}/\text{m}$) at 10 kHz and about 0 db $\mu\text{A}/\text{m}$ at 100 kHz. The lower curve shows system noise with the antenna terminals shorted. In addition, the two horizontal antennas recorded mine noise spectra (not shown) that were lower in amplitude by about 10 db at 100 kHz and about 35 db at 10 kHz. Spectra taken in haulageways in the mine tended to show magnetic field strengths typically 60 to 70 db $\mu\text{A}/\text{m}$ out to a few kilohertz, which then dropped off sharply above 8 to 12 kHz. One exception was a spectrum taken near a dc motor-driven hydraulic pump (car pull). This spectrum peaked at 78 db $\mu\text{A}/\text{m}$ at 1000 Hz, dropped to 47 db $\mu\text{A}/\text{m}$ at 10 kHz, and was down to 25 db $\mu\text{A}/\text{m}$ at 30 kHz.

Measurements of voltage between roof support bolts showed the same high spectrum occupancy below approximately 10 kHz. Simultaneous measurements of roof bolt voltage and magnetic field showed that noise events were not necessarily correlated. In one case, a noise burst received on the roof bolts was not received on the loop antennas. This problem needs more investigation.

Simultaneous recordings were made of noise underground and on the surface 30 meters away from a 180 meter deep shaft used for ventilation and power distribution. These measurements showed a coherence between surface and underground signals greater than 0.85 over the frequency range from 250 Hz to 6.8 kHz, with rapidly decreasing coherence above 6.8 kHz.

An approximate cross-check of the rms magnetic field noise at 10 kHz was made using data from the system described in the companion paper "Amplitude Statistics of Electromagnetic Noise in Coal Mines" by M. Kanda and J. Adams. Kanda's system uses a different measurement technique and hence gives an independent value for the rms field level. The cross-check is only approximate in that the two measurements were made with about a 3-hour time separation and a 30 meter spatial separation in the same mine. Operating conditions in the mine were essentially the same. With these differences, agreement was within 10 dB.

IV. Conclusion

Two significant results are reported. First, a powerful measurement technique was developed which clearly shows the simultaneous time and frequency variations of complicated signals. The method of making the spectrum measurements combines the convenience of lightweight, portable instrumentation with the power of a large computer FFT package. A singular advantage of the FFT is the unity probability-of-intercept of signals occurring at any time and at any frequency within the bandwidth covered. One consequence of this is the ability to generate 3-D plots showing how spectrum occupancy changes with time.

The second significant result is a set of electromagnetic spectrum measurements made underground in coal mines. These spectra cover the frequency range from 100 Hz to 320 kHz, and along with those reported by Bensema (2), are the first extensive set of spectral measurements made in an underground coal mine environment.

V. References

1. P. D. Welch, (1967 IEEE Trans. on Audio and Electroacoustics, vol. AU-15, No. 2, pp. 70-73).
2. W. D. Bensema, (1972, Coal Mine ELF Electromagnetic Noise Measurements, NBS Report 10739).

Another reference that may be of interest is:

3. R. B. Blackman and J. W. Tukey (1968 The Measurement of Power Spectra, Dover Publications, Inc., New York).

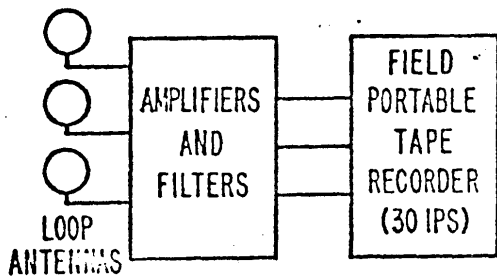


Figure 1a.
Field portable equipment

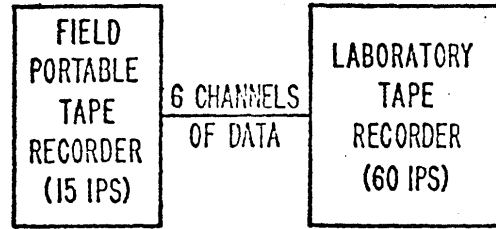


Figure 1b.
Laboratory transcription

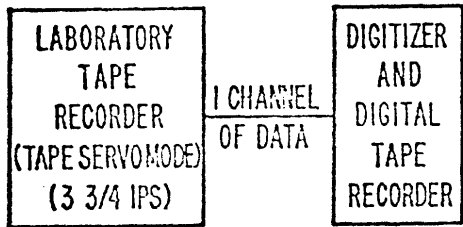


Figure 1c.
Laboratory digitizing

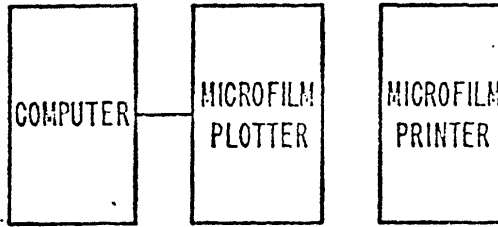


Figure 1d.
Spectral computation, plotting,
and printing

Figure 1. System block diagram showing data processing flow.

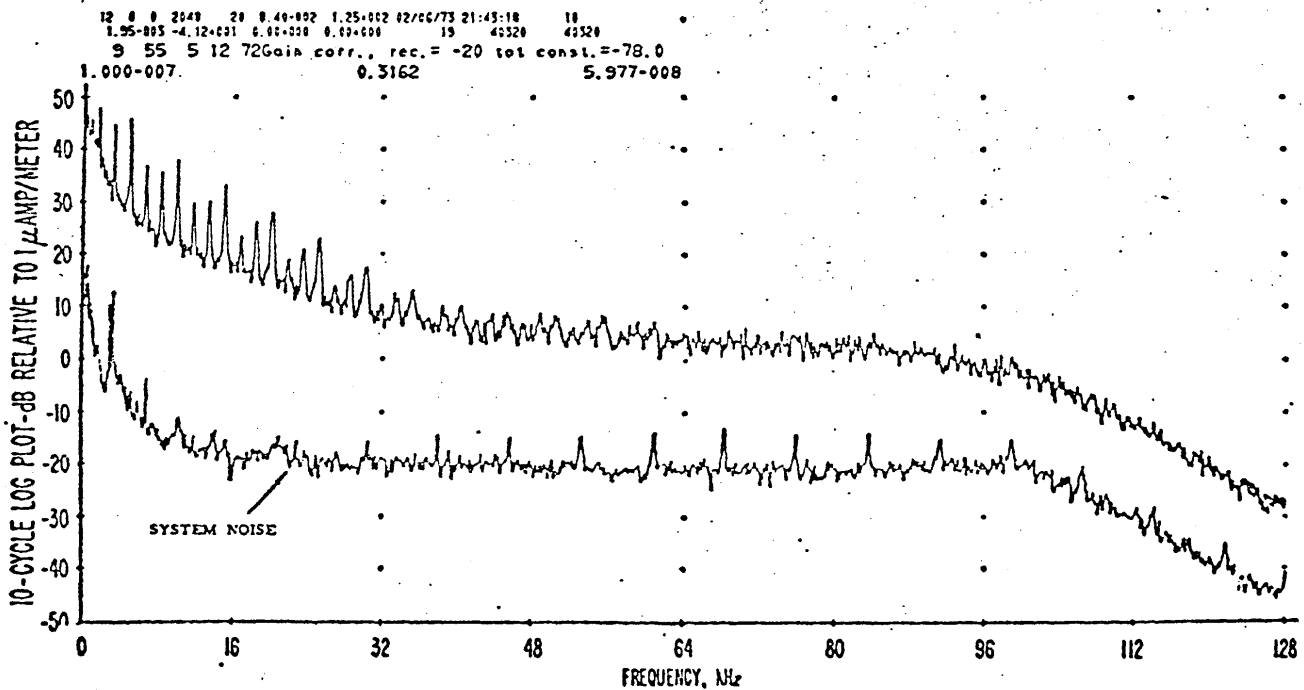


Figure 2. Magnetic field noise measured in Robena Coal Mine face area, 10 meters behind an operating 600 V dc continuous miner. Antenna moment vertical. Do not scale absolute field strengths above 100 kHz. The lower curve shows receiver noise (antenna shorted).

AMPLITUDE STATISTICS OF ELECTROMAGNETIC NOISE IN COAL MINES*

M. Kanda and J.W. Adams
Electromagnetics Division
National Bureau of Standards
Boulder, Colorado

Abstract

A system for measuring amplitude probability distributions (APD's) of electromagnetic noise in coal mines is described and typical APD's from an underground coal mine are presented. The APD is a basic statistic required for the design and analysis of communication systems, especially those intended for use in noisy environments, and where neither overdesign nor underdesign is acceptable. The rms and average field strengths are obtained by integration of the APD, and examples are shown at several frequencies. All field strength levels are given in absolute units. Selected frequencies cover the range from 10 kHz to 32 MHz.

I. Introduction

Ambient electromagnetic (EM) noise often limits radio communications in mines. Therefore, it is necessary to know the detailed statistical characteristics of the interfering noise in order to design optimum performance receivers and effective error-correcting coding schemes. The cumulative amplitude probability distribution (APD) of the received noise envelope is one of the most useful statistical descriptions of the noise process for the design and evaluation of a telecommunication system operating in a noisy environment [1,2].

This paper describes the system used to measure magnetic field noise in a coal mine. The system is an extension of one designed by Matheson [3]. Typical APD's are presented. Figures on Rayleigh graph paper show the fraction of the time that this noise exceeds various levels. This particular Rayleigh graph paper has scales chosen so that Gaussian noise (e.g., thermal noise) plots as a straight line with a slope of $-\frac{1}{2}$. Noise with rapid large changes in amplitude (e.g., impulsive noise) will have a much steeper slope, typically -4 or -5, depending on the receiver bandwidth. The APD's are then integrated to give rms and average values of the field strength, according to the equations

$$H_{\text{avg}} = -\int_0^{\infty} H \, dp(H)$$

*Sponsored by U.S. Bureau of Mines, United States Department of the Interior.

and

$$H_{\text{rms}} = \left(-\int_0^{\infty} H^2 dp(H) \right)^{\frac{1}{2}}$$

where H represents the magnetic field strength of the noise and p is the probability that the measured field strength exceeds the value H. These quantities are also dependent upon the measurement bandwidth, the length of the data run, and possibly other parameters. Finite series are actually used for the numerical integration. The rms and average values so arrived at are identified on each graph.

II. Measurement and Data Processing Instruments

The principal parameter measured was magnetic field strength. The antennas used were electrostatically-shielded loops with impedance transforming baluns. The outputs of the baluns were fed into commercial, battery-powered field strength receivers. The characteristics of the receivers used for our measurements are listed in Table I.

The i-f outputs from the field strength receivers were converted from 455 kHz to 40 kHz using mixers. They were recorded by a portable magnetic tape recorder. The tape speed on record and on playback was 15 inches per second (ips). At this speed, the portable recorder response band was from 100 Hz to 56 kHz at the 2 dB points in the direct recording mode. The dynamic range of the recorder was 48 dB. The tape was then transcribed through another tape recorder whose servo system could take out the flutter and wow introduced by the portable recorder. The data processing system consisted principally of the analog magnetic tape recorder for a playback unit and an instrument which provided a direct digital display of the percentage of the time each of 15 levels, 6 dB apart, were exceeded.

The bandwidth of the whole system was primarily determined by the data processing system and was found to be about 2 kHz. The dynamic range of the whole system, including the recording and the data processing systems, was primarily limited by the magnetic tape recorder to about 45 dB. The system used for recording and data processing is shown in Figure 1.

The calibration of the whole system, including the loop antennas, field strength meters, mixers, magnetic tape recorders, the impedance transforming amplifiers, and the digital counter was performed by immersing the receiving loop antennas in a known field, generated at the NBS field calibration site. Thus all levels of field strength are given in absolute units.

III. Amplitude Statistics of EM Noise in a Coal Mine

Many APD's of magnetic field noise were taken during actual operation of Robena No. 4 Coal Mine, Waynesburg, Pennsylvania, on December 5th and 7th, 1972. The loop antennas were placed about 300 meters from the face area. Three orthogonal components of magnetic fields were measured at eight frequencies ranging from 10 kHz to 32 MHz. Fig. 2 shows a typical APD at 10 kHz underground, and Fig. 3 shows a corresponding APD at the surface above the operating mine. Numerous measurements have shown that although this noise in a mine is strongly time dependent, if the noise is averaged over a period of about 20 minutes, then the resulting values are fairly repeatable from period to period.

The rms and average values result from about 20 minutes of data and are indicated in Fig. 2 and Fig. 3. Rms and average values of noise at selected frequencies from 10 kHz to 32 MHz are shown in Fig. 4.

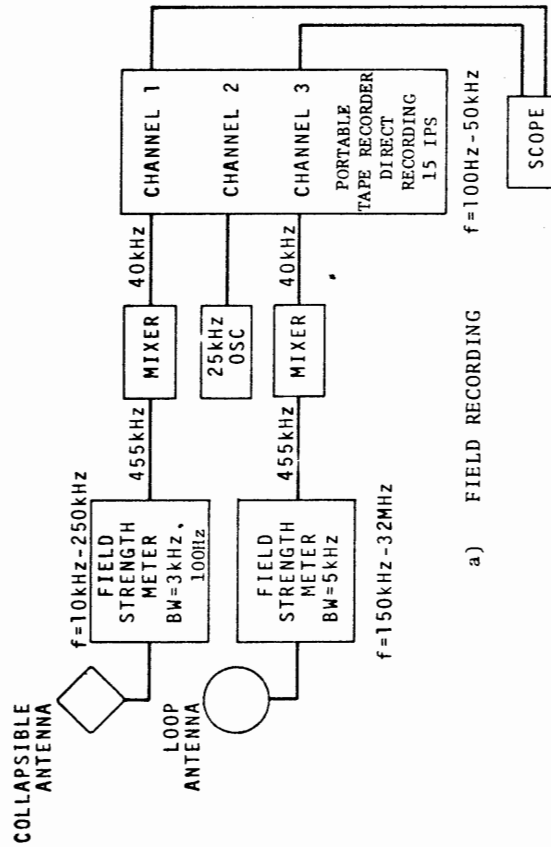
The principal value of the APD curves is that they show statistically how much the magnetic field varies at different times. For instance, at 10 kHz underground, magnetic fields 50 dB above one microampere/meter will be exceeded only .0001 percent of the time, while fields 5 dB above one microampere/meter will be exceeded 99 percent of the time. An rms value of 24 dB above one microampere/meter will be exceeded (in this case) about 36 percent of the time. The surface data show a corresponding rms value of 3 dB above one microampere/meter.

References

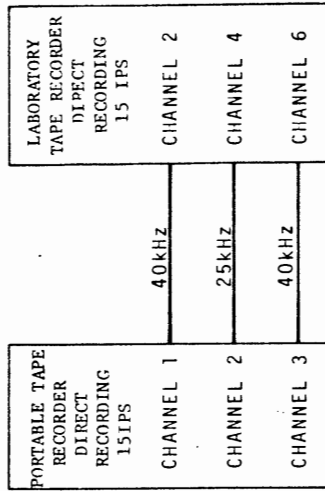
1. W.Q. Crichlow, et al. (1960 NBS Monograph 23).
2. W.I. Thompson, III (1971 DOT Rep. DOT-UMTA-71-3).
3. R.J. Matheson (1970 IEEE Trans. on EMC, EMC-12, p. 151).

Field Strength Meter	A	B
Frequency Coverage	10 kHz - 250 kHz	150 kHz - 32 MHz
IF Bandwidth (Impulsive)	Narrowband 110 Hz Broadband 2.7 kHz	5.0 kHz
Dynamic Range	67 dB	60 dB
Spurious Response Rejection (Image, IF, etc.)	> 50 dB	> 60 dB

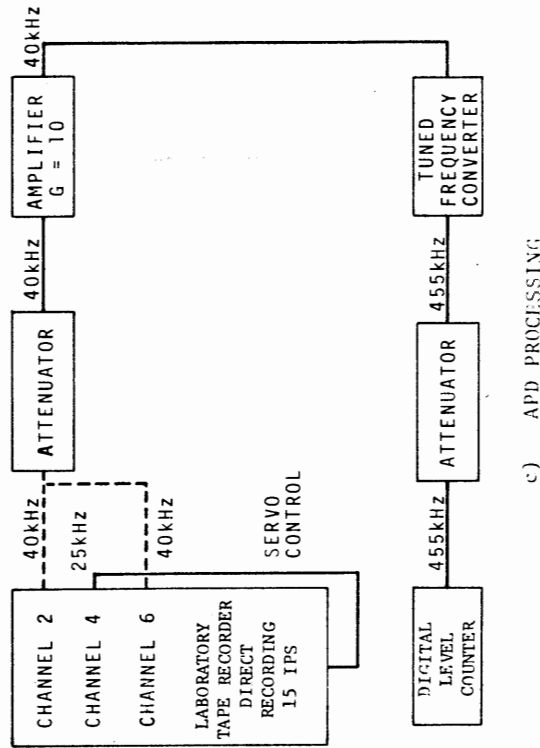
TABLE I CHARACTERISTICS OF THE FIELD INTENSITY RECEIVERS



a) FIELD RECORDING



b) TRANSCRIBING



c) APD PROCESSING

Fig. 1 THE SYSTEM FOR a) FIELD RECORDING, b) TRANSCRIBING, AND c) APD PROCESSING

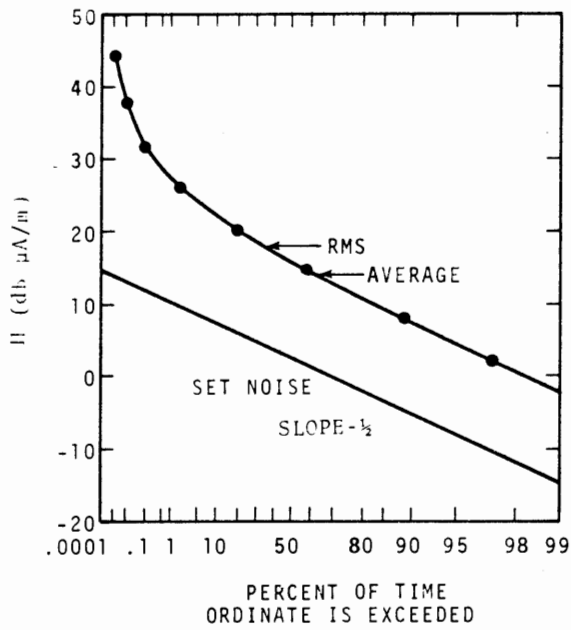


Fig. 2 APD OF FIELD STRENGTH, H, AT 10 kHz (UNDERGROUND)

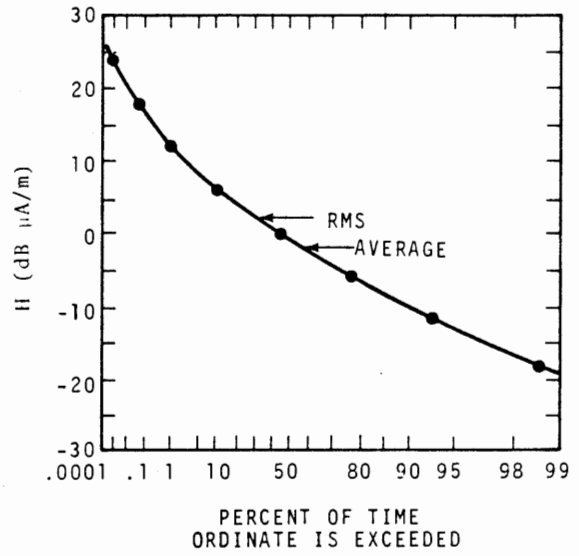


Fig. 3 APD OF FIELD STRENGTH, H, AT 10 kHz (SURFACE)

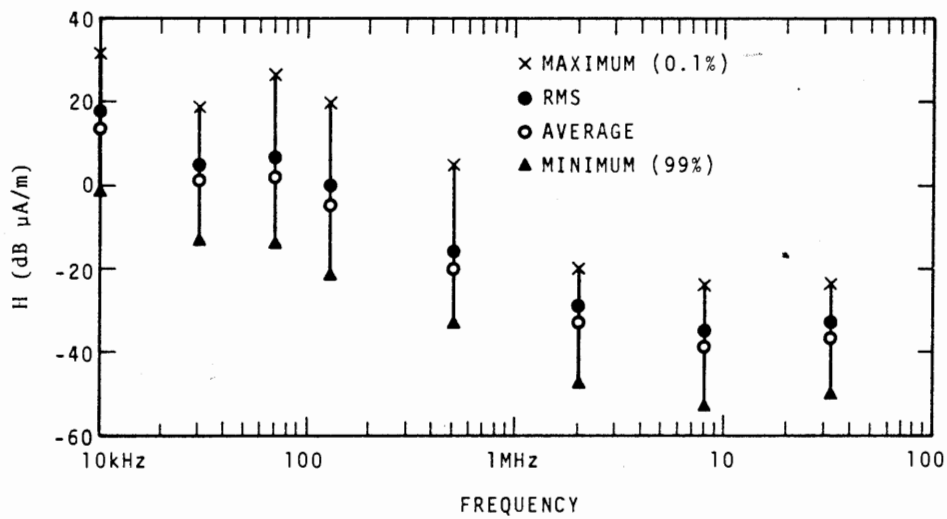


Fig. 4 VARIATION OF FIELD STRENGTH, H (UNDERGROUND)

DESIGN OF AN ELF NOISE PROCESSOR*

by

J. E. Evans and A. S. Griffiths
MIT Lincoln Laboratory, Lexington, Mass.

Abstract

Noise processing experiments with ELF (3 to 300 Hz) atmospheric noise and signals in the 40 to 80 Hz range are described. The primary purpose of the experiments was to record and analyze wideband ELF noise in order to design the noise processing portion of a receiver which minimizes the required transmitter power. The application of appropriate theory and extensive simulations led to a noise processor which consists of the following functions: (1) a compensating (or whitening) filter, (2) a pre-notch filter clipper, (3) notch filters at frequencies of manmade interference (e. g., power lines), (4) a post-notch filter clipper, and (5) a phase-coherent linear matched filter.

The nonlinear processing provides considerable gain relative to a linear receiver (i. e., a receiver consisting only of a matched filter and appropriate whitening filters). It is convenient to measure system performance in terms of an "effective noise level" which is equal to twice the received signal energy divided by the signal to noise ratio at the matched filter output. For example, the highest effective noise levels observed at 45 Hz with the nonlinear processor were about -134, -131 and -137 dB wrt 1 amp/m $\sqrt{\text{Hz}}$ using Saipan, Malta and Norway data, respectively, compared to 1 percent exceedance levels of effective noise for the linear receiver of about -115, 115 and -130 dB wrt 1 amp/m $\sqrt{\text{Hz}}$ respectively.

*This work was sponsored by the Department of the Navy.

EXPERIMENTAL COMPARISON OF BURIED AND ELEVATED ELF TRANSMITTING ANTENNAS

Peter R. Bannister, F. J. Williams, J. R. Katan,
and J. R. Ball

Electromagnetic Systems Department
Naval Underwater Systems Center
New London Laboratory
New London, Connecticut 06320

Abstract

During the last week in March and the first week in April, 1973, the Naval Underwater Systems Center measured the 76 Hz magnetic field strength (in Wisconsin and Texas) produced by both the elevated and (newly installed) buried Wisconsin Test Facility (WTF) north-south (NS) antennas. The principle result obtained from these measurements is that there is no measurable difference in performance between the WTF buried and elevated NS antennas.

Introduction

The U. S. Navy Project SANGUINE Wisconsin Test Facility is located in the Chequamegon National Forest in north-central Wisconsin about 8 km south of the village of Clam Lake. This particular location was chosen because of its low electrical conductivity and sparse population density. This facility was designed to test and demonstrate interference mitigation techniques. It has also been used for ecological studies and as the source for ELF propagation measurements.

The WTF consists of two 14 mile NS antennas (one elevated, the other buried at a depth of approximately one meter) and one 14 mile elevated EW antenna - with the transmitting station at the intersection near the midpoints of the antennas. Each antenna is grounded at both ends. The average direction is 19° E of N for the NS antenna, and 109° E of N for the EW antenna. Although the Wisconsin Test Facility was designed for a maximum current of 540 amps into each antenna, it has been operated to date at only 300 amps, which is about one-third of its power output capacity.

During August of 1972 we measured the effective earth conductivity (σ_e) beneath both elevated antennas of the WTF at 45 and 75 Hz (1). The H/I method was utilized with each WTF antenna alternately employed as the source. (In the H/I induction method, a long insulated wire grounded at both ends is energized by an AC generator at the frequency of interest. The magnitudes of the magnetic fields are

then measured at various distances and angles from the wire (2).) These measurements were performed mainly at distances of 45 to 75 km from the transmitter, in line with and broadside to each WTF antenna. The principal result obtained from these measurements is that the effective conductivity under the EW antenna is greater than that under the NS antenna.

During the last week in March and the first week in April of 1973, we measured the 76 Hz magnetic field strength (in Wisconsin and Texas) produced by both the elevated and (newly installed) buried WTF NS antennas. The main purpose of these measurements was: (a) to compare the buried and elevated NS antennas; and (b) to ascertain the repeatability of the August, 1972 (1) measurements.

Wisconsin Results

During this latest test, measurements were performed at distances (ρ) of 10-70 km from the WTF transmitter -- approximately broadside to the NS antennas. Presented in Figure 1 is a plot of the H_ρ component versus range for the elevated NS antenna. These H_ρ values are normalized to a transmitter current (I) of 300 amperes and azimuth angle (ϕ) of 90° (i. e., directly broadside to the antenna). The solid line in Figure 1 was derived (1, 3) by assuming an effective conductivity under the NS antenna of 2.2×10^{-4} mhos/m. This is the value that was measured during the August, 1972 test (1). From this curve it is observed that the theoretical and experimental values of H_ρ are in excellent agreement for measurement distances greater than 26 km. Thus, the repeatability of the August, 1972 measurements is excellent.

It has been shown (4) that for the homogeneous isotropic earth case, the measurement distance must be greater than seven skin depths ($\delta \sim 500/\sqrt{f\sigma}$, where f is the frequency in Hertz and σ is the uniform earth conductivity) in order for the H_ρ component to be inversely proportional to $\sqrt{\sigma}$. Referring to Figure 1, we see that the measurements taken at ranges less than 26 km are grossly different east and west of the NS antenna. Since 26 km is approximately seven effective earth skin depths ($\delta_e \sim 500/\sqrt{f\sigma_e}$ meters) at 76 Hz, it appears that the $7\delta_e$ criterion is also valid for the geoelectrically complex WTF area. (It should be noted that Wait (5) has recently shown that -- for certain two-layered earth conditions -- even the $7\delta_e$ measurement distance is too close for determining σ_e).

Presented in Figure 2 is a plot of the H_ρ component versus range for the buried NS antenna at 76 Hz. The H_ρ values are

normalized to $I = 300$ amperes and $\phi = 90^\circ$. These measurements were taken at distances of 36-71 km from the WTF transmitter, approximately broadside to the buried NS antenna. They were repeated at each of the 35 sites. The solid line in Figure 2 was derived (1,3) by assuming an effective conductivity under the buried NS antenna of 2.2×10^{-4} mhos/m (i.e., the same σ_e as measured under the elevated NS antenna). From this curve it is observed that the theoretical and experimental values are in excellent agreement. Thus, within the experimental accuracy of the measurements (± 0.1 db), there is no difference (in produced field strength) between the buried and elevated WTF NS antennas. There is also no difference in the pattern of these two antennas ($\pm 1^\circ$).

Texas Measurements

During the period extending from mid-March through early April, 1973, the Naval Underwater Systems Center performed a conductivity survey of the Llano Uplift area of Texas using the wave impedance measurement technique (with the WTF NS antenna as the transmission source). An additional task, the far field comparison of the WTF elevated and buried NS antennas, was performed during the first week in April in Kingsland, Texas. This far field site ($\rho \sim 1.85$ Mm) is approximately in line (i.e., $\phi = 0^\circ$) with the WTF NS antennas. The measurement period was divided into two segments (1030 - 1430 GMT and 1530 - 2330 GMT) during which the elevated and buried NS antennas were utilized. (The first two hours (1030 - 1230 GMT) were not used for the buried versus elevated comparison as this period coincided with Texas sunrise.) At 1430 GMT each day, the transmitter was switched from the buried to elevated antenna (or vice-versa).

The measured daily averages for the H_ϕ magnetic field strength component are presented in Figure 3. It should be noted that some of the atmospheric noise estimates taken during this period were upper bounds to the noise (i.e., these noise estimates are suspected to be contaminated with 60 Hz). Therefore some of the 80% confidence intervals (computed for each of the daily averages) may be too large.

Receiver integration times of 30 minutes per sample were employed for the majority of these measurements resulting in 36 samples for the buried NS antenna and 34 for the elevated. Referring to Figure 3, we see that the six day H_ϕ average is -142.6 ± 0.5 dBAm for the buried NS antenna and -143.2 ± 0.6 dBAm for the elevated NS antenna. Since these confidence intervals overlap, there is no discernible difference between the buried and elevated NS antennas.

(The buried antenna appears to be slightly better although not enough data exists to make it statistically significant.)

Conclusions

The principal results obtained from these two different range measurements are:

1. There is no difference in performance between the WTF buried and elevated NS antennas (within the experimental accuracy of the measurements).
2. The NUSC August, 1972 WTF effective earth conductivity measurements are repeatable, and
3. The measurement distance must be greater than seven effective skin depths in order for the H_p component to be inversely proportional to $\sqrt{\sigma_e}$.

It should be noted that Lincoln Laboratory personnel measured in Norway during the same time period. Their results (6) also indicate that there is no measurable difference in performance between the WTF buried and elevated NS antennas.

References

1. Bannister, P. R., and F. J. Williams, "Results of the August, 1972 Wisconsin Test Facility Effective Earth Conductivity Measurements," (to be published in Journal of Geophysical Research).
2. F. C. Frischknecht, "Electrical Methods in Geophysical Prospecting," Pergamon Press, Oxford, 1966, Chapters IV and VI.
3. Bannister, P. R., "The Image Theory Quasi-Static Magnetic Fields of a Finite Length Horizontal Electric Antenna Located Near the Earth's Surface," NUSC Tech. Report 1011, 4 June, 1969.
4. Bannister, P. R., "Quasi-Static Fields of Dipole Antennas at the Earth's Surface," Radio Science, vol. 1 (New Series), no. 11, p. 1321 - 1330, November, 1966.
5. Wait, J. R., "Note on the Surface Impedance and Wave Tilt for a Line Source - Excited Two-Layer Earth," (Private Communication, April, 1973).

6. White, D. P. (Private Communication, April, 1973).

Figure 1. H_g vs. S - elevated NS antenna, 76 Hz

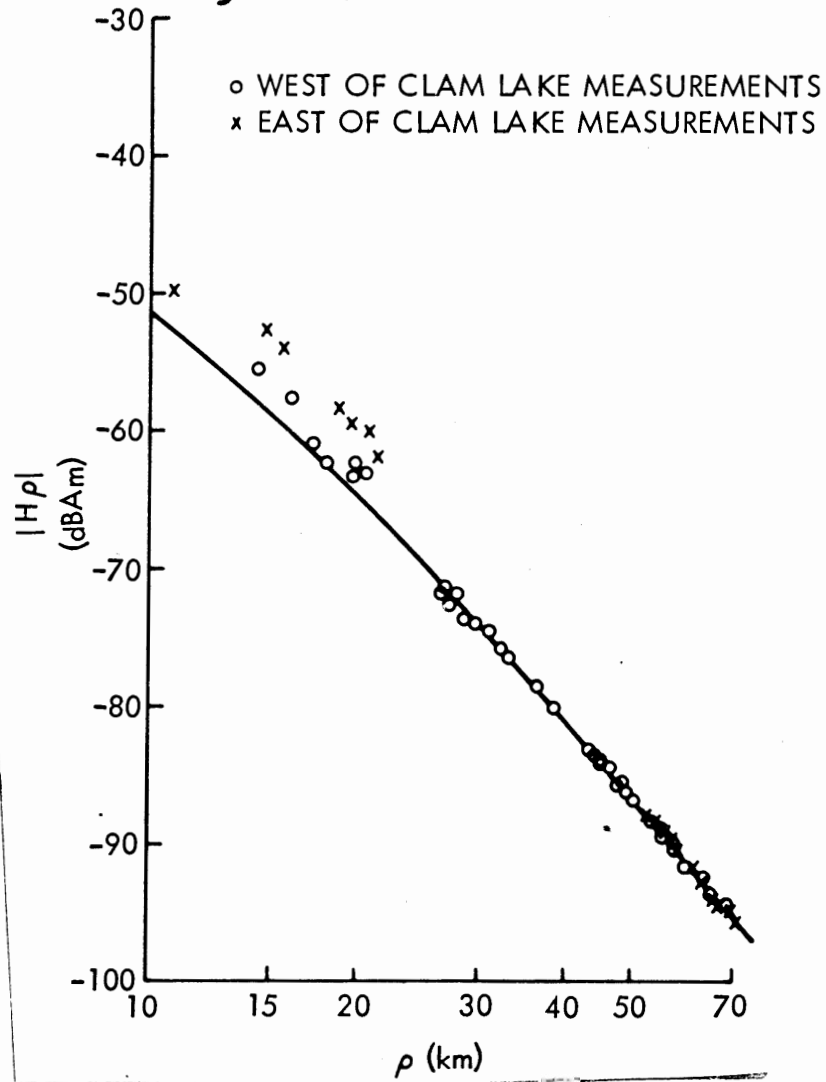


Figure 2. H_ρ vs. ρ - buried NS antenna, 76 Hz

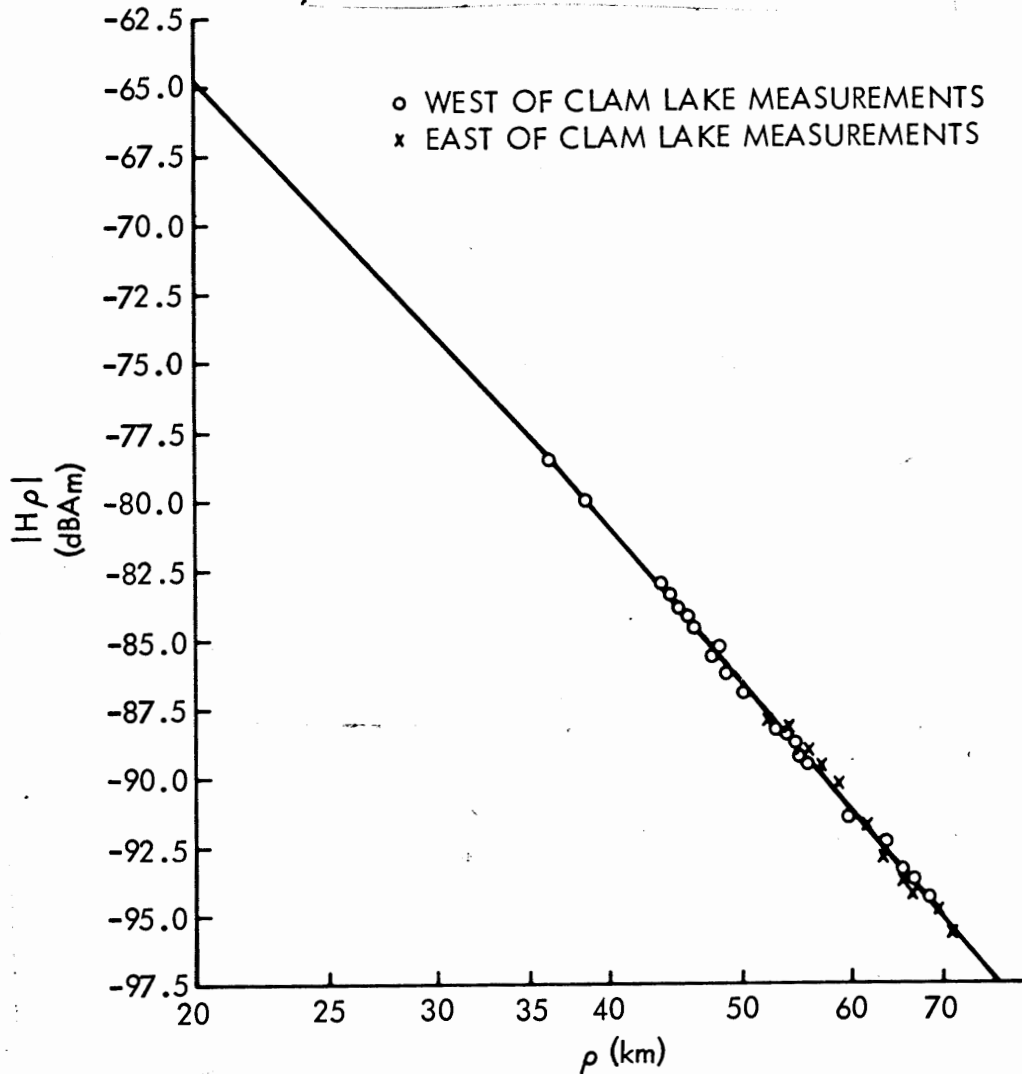
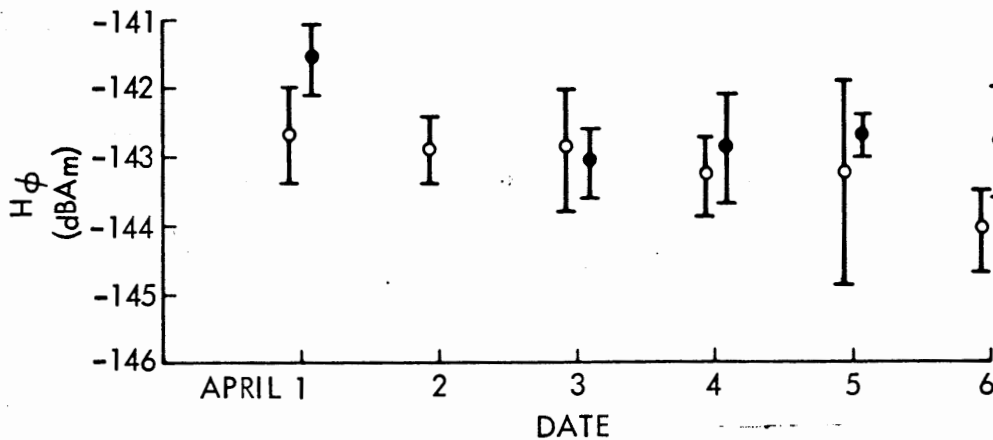


Figure 3. TEXAS H_ϕ daily averages

o ELEVATED ANTENNA • BURIED ANTENNA Δ SIX-DAY AVERAGE



AN UNDERGROUND ELECTROMAGNETIC SOUNDER EXPERIMENT

by

Lambert Dolphin, Jr., Robert Bollen, and George Oetzel
Radio Physics Laboratory, Stanford Research Institute
Menlo Park, California

Abstract

An electromagnetic sounder developed for an archaeological application in Egypt has been successfully tested in a California dolomite mine. Chambers in the mine 100 to 130 feet from the surface gave intense, well-defined echoes consistent with an average attenuation coefficient of 0.6 dB/m and a relative dielectric constant of 11. By moving the transmitter and receiver units on the hillside above the underground chambers, various characteristics of the propagation could be observed such as dispersion, chamber aspect sensitivity and cross section. The transmitted pulse was one to one-and-a-half radio-frequency cycles long at a peak power of 0.2 MW. Frequencies employed were 16 to 50 MHz. The light weight, highly portable, battery-powered equipment is potentially suited to other underground sounding applications.

SUMMARY REPORT ON ELECTROMAGNETIC NOISE MEASUREMENT PROGRAM

John W. Adams
National Bureau of Standards
Boulder, Colorado 80302

The present status of the National Bureau of Standards program is that many magnetic tapes of analog data have been recorded in four major mines. Each mine uses different types of equipment. In addition, some surface measurements of noise have been made at two additional mines.

Two types of recordings have been made: (1) broadband measurements for spectral plots and (2) narrowband measurements for amplitude probability density (APD) plots. Only data from one mine (Robena #4) has been processed and was presented at this workshop.

The short-term goals are: (1) finish processing data from the other mines, (2) establish or reduce measurement system uncertainties, (3) put Robena report into final form for distribution, and (4) hold a review to determine what has been done, to distribute and to interpret the preliminary data, and to determine what still needs to be done.

Long-term goals are: (1) complete final reports on each of the mine trips, (2) establish techniques for predicting noise in mines already visited and establish uncertainty bounds for these predictions, and (3) establish techniques for predicting noise in mines that have not been visited (but that use similar equipment to those visited) and also establish uncertainty bounds for these predictions.

Specific factors or formats to be presented include:

(A) For underground broadband measurements:

1. 300 Hz to 100 kHz spectral plots
2. 300 Hz to 384 kHz spectral plots
3. 300 Hz to 192 kHz spectral plots
4. 300 Hz to 6kHz (subject to change to 3 or 12 kHz) spectral plots

(B) For surface broadband measurements:

1. 300 Hz to 6 kHz (or 12 kHz) spectral plots
2. 300 Hz to 3 kHz spectral plots

(C) For underground narrowband measurements:

1. APD plots at 12 frequencies from 10 kHz to 32 mHz of magnetic field strength
2. R.M.S. and average values will be calculated based on time averaging for these plots

(D) Sample spectral measurements of:

1. Roof-bolt voltages
2. Trolley wire-to-rail voltages
3. Phone line currents

Future efforts will be decided after data processing is completed.

Possible tasks are:

- (1) Measurements in an all-AC mine
- (2) Measurements in some typical hard-rock mines
- (3) spectral measurements below 300 Hz (requested by Arnie Farstad)
- (4) Time statistical presentations from existing data
- (5) Development of noise prediction techniques and uncertainty bounds
- (6) Determine technique for using copies of analog noise tapes for system tests.

SUMMARY REPORT OF ELECTROMAGNETIC LOCATION TECHNIQUES

WORKING GROUP

Arnold J. Farstad, Group Chairman
Westinghouse Georesearch Laboratory

1.0 INTRODUCTION

The Location Group conversed in the Petroleum Room of the Green Center with the purpose of addressing the following list of topics in light of the Bureau of Mines' requirements for detecting and locating trapped miners by electromagnetic methods. These topics include: Noise, Sources, Antennas (transmit and receive), the Propagation Medium, Signal Processing, Optimum Frequency, Receivers, Pulse vs. CW Techniques, Passive Location Techniques, and Obstacles. Practical constraints such as equipment size, weight and power requirements, cost and intrinsic safety were kept in mind during these discussions. It was emphasized that in-mine equipment must be inexpensive, rugged, simple and lightweight. Otherwise, the mine operators probably would not buy it nor would the miners be able to effectively use it.

Present techniques for experimentally detecting and locating trapped miners were discussed, along with techniques to improve their location accuracy. Analytical, numerical, and scale modelling methods were considered as a means of giving further insight into measurement anomalies caused by terrain variations, conductivity contrasts, and obstacles.

After discussion of these topics, conclusions were drawn and existing problem areas were identified. These problem areas were addressed in developing guidelines for future efforts. Following the discussion period, the Chairman gave a summary of the Location Group report and comments were solicited from the entire group.

2.0 GROUP DISCUSSION HIGHLIGHTS

2.1 Noise

W. Bensema asked the group whether the noise data provided by NBS was adequate. It was determined that for location systems analysis, the most important form of noise data was the frequency spectra of vertical and horizontal magnetic fields on the surface, and the answer to his question was affirmative. Drs. Wait and Frischknecht pointed out the difficulty in accurately measuring the true vertical magnetic field since these measurements are heavily influenced by the loop setting and the local geology. Nevertheless, these measurements are important since the same perturbations would also affect a receiving loop oriented to receive the vertical magnetic field. Dr. Rankin pointed

out that the magnetic noise fields pass through a null somewhere between 0.2 Hz and 5 Hz, that this frequency range may have merit in deep mine detection problems.

2.2 Sources

Sources that have been used most extensively and successfully to date in mine location problems are vertical magnetic dipoles (VMD) consisting of single turn and multiple turn loops of wire powered by a source of AC current. The advantages and disadvantages of using a horizontal magnetic dipole (HMD) as an alternate to the vertical dipole were discussed. The main advantage in using the HMD is that the null field is the vertical magnetic field (H_z) and that a greater resolution of the null plane may be realizable due to a lower H_z background noise. However, the main disadvantages in using a horizontal magnetic dipole source is that only one null plane in H_z is produced by a single HMD source and that additional information is needed to resolve the null point location. Furthermore, there are practical constraints on how large an area can be realized in an HMD configuration and how difficult it would be for a miner to implement in an actual emergency.

2.3 Antennas

Transmitting antennas that have been successful in location exercises for the Bureau of Mines have consisted of single turn and multiple turn loops deployed on the mine floor usually in intersections or around coal pillars. These antennas have produced adequate signals for detection and location at mine depths as great as 1650 feet. However, it was pointed out that these antenna configurations are not possible in most metal mines because of the random mine tunnel construction (following the ore veins) and the relatively narrow width of the walls. Consequently, it may become necessary to revert to long wire antennas tied to roof bolts or large area loops if closed paths are available. Since metal mines are normally deeper than coal mines, the increased moments of these large antennas may be required anyway to produce detectable signals on the surface.

The possibility of using ferrite core transmitting antennas was also discussed. In view of Dr. Gabillard's success with these antennas, it was decided that they warrant further investigation for location purposes.

The relative advantages of using air core and ferrite core receiving antennas were also discussed. Ferrite core antennas are more compact but are not as stable as air core loops. Since much of the experimental work for the Bureau of Mines entails the measurement of absolute field strength profiles, it was concluded that for the present time, air core loops are more desirable.

Other forms of receiving antennas that were discussed were a dual coil system for field gradient measurements and a broadband gradiometer for ultra low frequencies. Some preliminary work has been done by Westinghouse on the dual coil system but it is yet too early to evaluate the results.

2.4 Propagation Medium

In discussing the propagation medium, the general consensus among the members of this group was that the half space/plane earth was well understood. Simple extensions of the plane earth theory, such as hill slope corrections, have proven useful in refining the location accuracy of the measured results. Cylindrical and spherical models have also been developed to account for terrain anomalies but have not been fully evaluated with respect to experimental results. The request was made by Drs. Wait and Lewis that careful documentation of actual field environments including anomalies in the propagation media be made and forwarded to those investigators developing analytical models to further guide them in producing realistic models. Dr. Geyer suggested that analysis of dipping bed conductivity contrasts be investigated to determine their effect on location accuracy.

Analysis of the effects of arbitrary terrain variations in the media were also discussed. Dr. Frischknecht proposed a three-dimensional scale modelling approach to the terrain problem while Dr. Greenfield suggested a two-dimensional numerical analysis technique. It was felt that both of these techniques would enhance our understanding of the effects of terrain on location accuracy although Dr. Wait expressed reservations on the two-dimensional analysis.

Techniques for experimentally determining the apparent conductivity of the medium are well understood and measurement results can be used directly in predicting field strengths when one knows the transmitted moment and the overburden depth.

2.5 Signal Processing/Receiving

In existing EM location receivers, signal processing is straight-

forward and consists merely of narrowband amplification of an AC signal transmitted from an underground dipole. It was pointed out that for mines appreciably deeper than 1500 feet, it will probably be necessary to use some sort of synchronous detection scheme with expanded integration time to obtain signal to noise ratios suitable for detection and location from existing levels of transmitted moment. Dick Myers suggested the possible use of ambient 60 Hz fields as a common synchronizing source for both transmitter and receiver.

2.6 Optimum Frequency

Although it has been demonstrated that frequencies between 900-3000 Hz are ideally suited to uplink detection and location in most coal mines, the optimum frequency will no doubt be shifted downward when considering their use in deeper and more conductive metal mines. When discussing the range of lower frequencies available, it was suggested by Dr. Frischknecht that we look into the use of magnetometers and broadband gradiometers as field sensors. Dr. Rankin suggested that if ultra low frequencies are used, we should take advantage of the low background noise region between 0.2 Hz and 5 Hz.

2.7 Pulse vs. CW

Source location by waveshape analysis of underground transmitted pulses has been proposed by Dr. Wait. Analytically, these techniques contain diagnostic information not found in simple CW transmissions. However, in light of intrinsic safety requirements, the technique was not considered practical for use in coal mines. Consequently, the Bureau of Mines has pursued the CW approach and with a relative measure of success. However, this is not to say that the pulse technique will not be feasible in hardrock mines where the intrinsic safety limitation no longer exists. Pending the outcome of future CW tests in hardrock mines, the question of pulse vs. CW should be temporarily deferred.

2.8 Passive Location

The passive location technique (also proposed by Dr. Wait) is one which enables a miner to modulate a secondary source in the mine by opening and closing a large coil of wire and by doing so, have a recognizable effect on the impedance of the transmitting loop. Initial investigations into the practicality of this scheme have been somewhat pessimistic in light of realistic parameters of noise, conductivity,

and overburden depth. However, it has been suggested that the potential use of this scheme be investigated more thoroughly to decide once and for all whether it is practical. The advantages of such a scheme are quite obvious in that no power is required on the part of the trapped miner.

2.9 Obstacles

It has been shown that obstacles appearing in the mine overburden have a distorting effect on uplink field patterns especially if they occur near the observer location. Dr. Wait suggested that obstacles of primary importance are cylinders and longitudinal conductors. These geometric figures can be used to model buried pipelines and cables and analytical results are available to study their effects. Dr. Wait pointed out that someone should conduct a study to identify what information would be most useful in improving overall location accuracy.

3.0 MAJOR CONCLUSIONS

The uplink detection problem has been solved for the vast majority of coal mines in the United States.

Location techniques (uncorrected) are generally accurate to better than 10% of overburden depth.

The half space/plane earth theory is well understood; however, more work is needed on analyzing terrain anomalies and near surface conductivity anomalies to obtain more refined correction factors for the data.

The detection problem has not been solved for extremely deep hardrock mines; however, removal of intrinsic safety limitations will facilitate this problem. Also it may be necessary to lower frequency, use long wire antennas or coherent receivers to get satisfactory results in these mines.

Noise data of primary importance to location problems are the spectral information on the three component magnetic fields at the surface.

4.0 RECOMMENDATIONS FOR FUTURE WORK

Based on the workshop discussions, the following review session

and a later informal session of the location group, the following recommendations for future work are given in descending order of priority. The primary emphasis is on signal detection above deep mines and the secondary emphasis is upon refining location accuracy obtained using existing techniques.

The relative level of effort and the time required to achieve the desired goals are roughly estimated and are indicated by the following:

<u>Level of Effort</u>		<u>Time Duration</u>
High	(H)	Short Term (ST)
Medium	(M)	Long Term (LT)
Low	(L)	

1. Optimize frequency for propagation in deep mines and for minimum influence from anomalies. (H, ST)
2. Investigate alternate detection techniques such as magnetometer, gradiometer, multiple coil systems and coherent detection for use in deep mines. (M, LT)
3. Increase understanding of anomalous location results, i. e.,
 - arbitrary terrain effects (scale modelling) (L, ST)
 - arbitrary terrain effects (numerical techniques) (M, LT)
 - effects of long cylinders and longitudinal conductors (rapid analytical methods). (M, ST)
 - geometric terrain effects (spherical/cylindrical). (M, ST)
4. Investigate alternate transmitter techniques: (L, LT)
 - Ferrite loop source vs. air core loop.
 - Pulse type transmitter for metal mines.
 - Hand crank power source.
5. Predict performance of passive detection technique. (L, ST)

SUMMARY REPORT OF UPLINK AND DOWNLINK COMMUNICATIONS

WORKING GROUP

Robert L. Lagace, Group Chairman
Arthur D. Little Inc.

	PAGE
I. OVERVIEW	180
II. BRIEF DESCRIPTION OF THE FOUR PROMISING SYSTEMS	181
A. Uplink-Data	181
B. Downlink-Voice	181
C. Sidelink-Call Alert Coded Page	181
D. Sidelink-Roof Bolt Voice Page	182
III. PRESENT STATUS AND RECOMMENDED FUTURE WORK	182
A. Uplink Data System	183
1. Overview	183
a. Nominal Mines	183
b. Deep Mines	184
c. Equipment	184
2. The Channel-Transmission Loss	184
a. Loops	185
b. Parasitic Structures	185
c. Grounded Wires	185
3. The Channel-Noise	186
a. Past Data	186
b. NBS Mine Noise Measurements	186
c. Whistler and Geomagnetic Data	187
d. Data Utilization	187
4. The Source-Message, Coding, Modulation, Operating Frequency	188
5. The Receiver-Sensor, Demodulation/Decoding, Special Processing	188
B. Downlink Voice System	189
1. Overview	189
a. Experience to Date	189
b. Future Developments	190
c. Deep Mines	190
2. The Channel-Transmission Loss	191
a. Long Wire Antennas	191
b. Parasitic Structures	192
3. The Channel-Noise	193
4. The Source-Message, Coding, Modulation, Operating Frequency	193
5. The Receiver-Sensor, Demodulation/Decoding, Special Processing	194
a. Downlink	194
b. Uplink	195
C. Sidelink Call Alert Coded Page System	195
1. Overview	195
2. The Channel-Transmission Loss	196
a. Loops	196
b. Parasitic Structures	197
c. Roof Bolts	197
3. The Channel-Noise	198
4,5. The Source and Receiver	198
D. Sidelink Roof Bolt Voice Page System	198
1. Overview	198
2. The Channel-Transmission Loss	199
a. Finite Wire Antenna Terminated by Roof Bolts	199
b. Parasitic Structures	200
3. The Channel-Noise	200
4,5. The Source and Receiver	201

I. OVERVIEW

The attention of this group was focussed on four through-the-earth communication systems that are presently of high interest to the U.S. Bureau of Mines; four systems for providing operational/emergency communications on the working sections of coal mines, indeed up to the very face of the section. The systems are: uplink-data, downlink-voice, sidelink-call alert coded page, sidelink-roof bolt voice page. Each of these systems makes use of the mine overburden as the signal transmission medium, as opposed to the guiding wires, cables, and tunnels treated by the operational communications working group. Each of these systems satisfies one or more of the Bureau's objectives for mine communications systems; namely

- reliable links for monitoring the mine environment under both operational and emergency conditions.
- reliable links for communicating with miners during emergencies.
- special links for increasing the efficiency of day-to-day operations of the mine.

Each of these systems has been successfully demonstrated on a limited experimental basis, and prototypes of all these systems are installed and operating in the USBM experimental mine in Bruceton, Pa. Each of these systems must now be optimized regarding its performance, and engineered for practical routine application to the working sections of actual operating coal mines, particularly those of the room and pillar type.

This optimization and engineering must take place subject to the principal constraints listed by Howard E. Parkinson in his Workshop paper entitled, "Objectives and Constraints of Through-the-Earth Electromagnetic Communications Systems" and enumerated below.

- Depth of Mine Overburden
- Overburden Conductivity
- Electromagnetic Noise In and Above Mines
- Limited In-Mine Electrical Energy (Stationary or Man Carried) During an Emergency
- Intrinsic Safety for In-Mine Equipment
- Practical and Rugged Equipment for Use Under Both Operational/
Emergency Conditions
- Severe Weight Limitations for Man Carried Equipment
- Reasonably Low Costs Especially for Man Carried Equipment

Part II of this paper provides a brief description of each system, while Part III summarizes the present status of developments related to these systems and some recommendations for future work needed to advance these systems to the practical application stage.

II. BRIEF DESCRIPTION OF THE FOUR PROMISING SYSTEMS

A. Uplink-Data

This is a vertical through-the-earth narrow band data channel for monitoring important parameters of the mine environment under operational and emergency conditions, and for receiving coded messages or replies from miners during an emergency. Operating ranges compatible with 1,000 foot deep mines with $\sigma = 10^{-2}$ mho/m overburden are required. The in-mine transmitter would be located at a key place on the section, such as the loading point, where the present mine pager phone is also terminated. The surface receiver would have to be located in the vicinity of the point directly above the in-mine transmitter, primarily because of the inherent power limitations imposed on an in-mine transmitter during an emergency. This location requirement for the surface receiver may pose a difficulty for some mines with regard to surface access rights over advancing sections, and therefore may restrain such uplink communications to emergency situations during which mobile equipment can be temporarily installed over the known location of the in-mine transmitter. During normal mine operations, the mine environmental data could be monitored by means of a carrier channel over the mine pager phone line.

The limited in-mine transmitter power available during an emergency and the electromagnetic noise levels present on the surface have led to the conclusion that uplink transmission of baseband voice is not a practical goal. Therefore it has been deleted as a requirement until practical, voice bandwidth compression techniques or other types of signal processing become available to change this conclusion.

B. Downlink-Voice

This is a vertical through-the-earth voice channel for transmitting messages, during a mine emergency, to miners carrying a small emergency voice receiver, preferably built into their helmets. As in the case of the uplink receiver, difficulties regarding surface access rights over advancing sections may require a mobile surface transmitter installation that is temporarily installed only during emergencies. However, since the transmitter power available on the surface is much greater than that underground during an emergency, the downlink allows greater operational flexibility in communicating with moving miners, and may reduce the surface access rights problem somewhat, because of the potentially greater coverage area of each surface transmitter. As in the uplink case, operating ranges compatible with 1,000 foot deep mines with $\sigma = 10^{-2}$ mho/m overburden are required.

C. Sidelink-Call Alert Coded Page

This is a horizontal through-the-earth narrow band channel for transmitting a call alert paging signal to key individuals roving on a working section during normal mine operations, to notify them that they are wanted on the mine pager phone. The transmitter, activated by a signal sent over the mine phone line, would be somewhat centrally located near the section loading point as in the uplink system, and conceivably could be integrated with the uplink equipment if desired. The receivers would be carried by the miner, preferably in his helmet as in the case of the emergency voice receiver for the downlink system. In fact the Bureau's present desire is to have this emergency voice receiver serve a dual role, for key supervisory and maintenance people, by also operating as a

narrowband call alert receiver under normal operating conditions. Such a call alert system would extend mine phone paging to roving individuals right up to the working face, thereby increasing both safety and operational efficiency. This would require operating ranges on the order of 400 to 800 feet in overburdens of $\sigma = 10^{-2}$ mho/m in order to cover a typical 600 by 600 foot section, depending on the location of the transmitter.

D. Sidelink-Roof Bolt Voice Page

This is a horizontal through-the-earth voice channel for transmitting a more comprehensive voice message or page, as opposed to a simple call alert, to key individuals roving on a working section during normal operating conditions. As in the call alert system the transmitter could also be located at the section loading point, thereby requiring the same operating range as the call alert system. However it most likely would not share equipment with an uplink system as a call alert system might. Being a voice bandwidth system for use under operational conditions when electromagnetic noise levels are high, particularly in the audio band, a significantly higher operating frequency than that possible for a narrowband call alert or uplink system is favored. The receiver for the roof bolt paging system is presently conceived as a pocket-sized unit, but other packages such as a helmet mounted unit are not excluded.

III. PRESENT STATUS AND RECOMMENDED FUTURE WORK

To arrive at a design that is at least acceptable, if not optimum, regarding performance and practicality for any of the above communication systems, one usually must first determine how each of the major elements comprising the system influence its performance, and then use them so as to get the desired results. An often indispensable aid to this process, particularly when design information for one or more of the major system elements is missing, is to put together a breadboard system based on existing related hardware and try it out. Several of the above through-the-earth systems have evolved, with beneficial results, from the latter approach. Concurrently, some of the previously missing design information on transmission loss and noise has been accumulated. Therefore, it will now be possible to better optimize each of these systems by quantitative analysis and comparison of alternative designs.

No papers evaluating or describing any of the above through-the-earth systems were presented during the Workshop. However, several papers treating two major system elements, channel transmission loss and noise, were given. These and some past work by the attendees of this working group provided the basis for the group's findings and recommendations. We grouped the system elements as follows:

- o The Source: its message, modulation or coding, transmitter, and operating frequency.
- o The Channel: its transmission loss for each antenna type, and its noise characteristics.
- o The Receiver: its pick up sensor, demodulation/decoding, and special processing for signal to noise improvement.

These elements were then discussed in the context of each of the four systems to the level of detail that was possible under the circumstances. The order of treatment for each system will be Channel, Source, and Receiver, which mainly reflects the emphasis of this Workshop's charter and papers. Progress made to date in the Channel area should now allow more emphasis to be placed on overall system design and analysis, thereby calling greater attention to the Source and Receiver areas.

In the discussions below, that for the uplink system is somewhat longer than the others, because certain elements that have common application to several of the systems are first introduced in the uplink treatment.

A. Uplink Data System

This section treats the principal narrowband data uplink application. The more difficult, less practical uplink voice application is treated briefly in the downlink voice section.

1. Overview

To date the combination of overburden transmission loss and available surface noise data have identified the frequency band below 5 kHz as the most favorable for practical narrow band uplink data systems intended for coal mines with overburden depths of up to 1,000 feet and conductivity of $\sigma = 10^{-2}$ mho/m. Though shallower mines allow a somewhat higher frequency limit, and more conductive ($\sigma = 10^{-1}$ mho/m) or deeper mine overburdens demand a significantly lower frequency limit, the under 5 kHz limit should cover most coal mine situations.

a. Nominal Mines

Signal to noise analyses performed by Westinghouse Georesearch Laboratory (WGL) support this under 5 kHz conclusion for 10^{-2} mho/m overburdens, while also identifying the frequency band between 500 Hz to 3 kHz as a distinctly optimum one for narrowband systems. The WGL analyses were based on Wait/WGL transmission loss curves for loop transmitters and broadband atmospheric noise data (under 10 kHz) taken by WGL in Colorado. Signal to noise analyses performed by Arthur D. Little, Inc. (ADL) reach a similar under 5 kHz overall conclusion, but do not reveal the presence of an optimum frequency band as distinct as the one by WGL. The ADL analyses were based on the same transmission loss curves of Wait/WGL, but different broadband noise data, namely surface atmospheric noise data (under 300 Hz) taken by MIT Lincoln Laboratory (LL) in Florida and early WGL and National Bureau of Standards (NBS) surface noise data (under 10 kHz) taken over four Western coal mines. The differences in the results of the two analyses, regarding the presence or absence of a clearly optimum frequency band between 500-3000 Hz for $\sigma = 10^{-2}$ mho/m overburdens (based on broadband noise levels) should be easily resolved when the large amount of noise data recently taken over coal mines by NBS soon becomes available. However, WGL and NBS field experiences have revealed a potentially more serious noise problem that may tend to favor use of frequencies between 1-5 kHz over coal mines, namely the extremely strong harmonics of 60 Hz and 360 Hz caused by the mine power conversion equipment, harmonic levels that are high enough in some cases to interfere with even narrowband systems operating between the harmonics.

b. Deep Mines

For mines with overburdens deeper than 1,000 feet (such as hardrock mines) or conductivities greater than 10^{-2} mho/m, it is generally agreed that operating frequencies will definitely be forced downward to perhaps 500 Hz or 100 Hz. In some extremely deep hardrock mines that approach 10,000 feet, lower frequencies yet may be needed if direct transmission to the surface is required. The favorable downlink signal transmission test results to depths of 11,000 feet achieved with under 100 watts by Sandia Laboratories, using Develco, Inc. equipment at frequencies below 20 Hz, should be carefully evaluated and exploited if such depths become important to the Bureau. However, it should be kept in mind that such a downlink transmission test has the advantages of power and large antenna size on the surface, and a relatively noise free underground receiver, which is the converse of the mine uplink problem.

c. Equipment

An experimental prototype uplink data monitoring system has been built by WGL for the Bureau. It operates at designated frequencies between 3-5 kHz, utilizes PCM/FSK modulation, a loop transmitter antenna, and is presently installed in the Bureau's experimental mine in Bruceton, Pa. Similar experimental equipment that illustrates the feasibility of uplink data transmission, even with limited available power, has also been built by WGL for miner location applications. An example is the keyed CW electromagnetic transmitter for miner location which utilizes a one turn, 360 foot periphery loop and the miner's 4-volt cap lamp battery to generate a magnetic moment of about 2,000 ampere-meters² at 2 kHz. Detection ranges in excess of 1,000 feet have been obtained at several mine sites using this and similar units, as reported during this Workshop. It should be noted that the approximately 80 foot overburden at the USBM experimental mine is not considered by the Bureau as being typical of that found over operating mines.

A multichannel uplink data system of practical design suited for installation and test in an operating coal mine with up to 1,000 feet of overburden will soon be needed. The basic monitoring requirements of the in-mine station are now being formulated, so that an overall uplink data communication system can then be designed and optimized for the operating conditions of this mine.

2. The Channel-Transmission Loss

a. Loops

Uplink communications to date have primarily utilized loop source antennas of vertically oriented magnetic moment. These have consisted typically of one turn loops (up to 500 foot periphery) wrapped around one or two coal pillars; and less frequently a smaller one turn loop (up to 100 foot periphery) placed in an entry. Such loops have been preferred over long wire antennas for in-mine installations because of their lower input resistance, fixed impedance characteristics over time, and convenience of installation and maintenance in the adverse mine environment. The primarily vertical magnetic fields produced by vertical axis loops can also offer a signal to noise advantage on the surface in some cases, depending on the sources of the noise, i.e. natural or man-made.

The theoretical results of Wait and ITS, regarding the field strengths expected on the surface from infinitesimal loops of moment NIA placed in homogeneous and layered conducting overburdens, are well established and have been found to be in good agreement with experimental data obtained by WGL and Colorado School of Mines (CSM) at several mine sites. For the large overburden depths of interest and sizes of corresponding loops required, the simplifying infinitesimal loop assumptions apply. Furthermore it has been shown by Wait and ITS that typical conducting obstacles, such as pipes, and inhomogeneities found in the transmission path to the surface should produce only small effects on the resultant magnetic field seen at the surface for the under 5 kHz band of interest. WGL and ITS have also shown that the effects of surface topography on the resultant surface field are also small. Consequently these effects can largely be ignored for communications applications, as opposed to location applications where some of the effects can take on greater importance in some cases.

Therefore it was concluded that no new theoretical derivations were required on uplink transmission loss for loop transmitters; but that appropriate curves, tables, nomographs, etc., based on the available theoretical results should be prepared, as an aid to uplink systems designers who desire to apply the theory to typical mine overburdens. Included in these design aids should be curves that show the additional amount of signal loss suffered as the horizontal displacement between surface and in-mine loops is increased. This will help determine the surface coverage obtainable from a single in-mine loop.

b. Parasitic Structures

All of the above results apply for cases in which no large closed loops of wire, cable, or steel roof mesh are close enough to the finite, relatively large, in-mine transmitter loops to allow significant currents to be induced in these parasitic structures, which in turn might reduce the effective strength or field of the transmit loops. The likelihood of encountering parasitic structures on working sections is high, but the degree to which they could adversely affect system performance, has not been ascertained. Since this may be a potential problem to both the uplink data system and the call alert page system to be discussed below, the practical influence of such structures needs to be assessed. However, until that is done, uplink or call alert system transmit loops should be installed away from such structures as steel roof mesh, trolley lines, and probably power cables, since the effects of their presence will decrease with increasing separation.

c. Grounded Wires

Lastly, should there be a renewed interest in comparing the performance of a loop source uplink system with that for a grounded finite straight wire source that utilizes a wire terminated by a roof bolt ground rod at each end, ITS has derived expressions and curves for the magnetic field produced on the surface by such a buried finite wire source. The results apply to the case of the wire inclined at an arbitrary tilt angle to the horizontal in a homogeneous overburden. They show that small tilt angles made by the wire with a flat or hilly surface do not influence the magnitude of the surface field.

3. The Channel-Noise

a. Past Data

Up until this year very little good noise data pertinent to coal mine environments, underground or on the surface, were available for making comprehensive systems analyses or optimizing uplink or downlink system designs. With respect to noise levels on the surface, the ELF noise measurements made by Lincoln Laboratory for the Navy were the most useful below 300 Hz, even though not taken over coal mines, but in Florida and other parts of the world. Between 300 Hz and 5 kHz the surface noise data were even more sparse, consisting of limited atmospheric noise measurements taken by WGL in Colorado, and limited noise measurements conducted by NBS and WGL at a few coal mines.

These surface data were not considered adequate, because it was suspected that the predominant sources of both broadband and discrete frequency noise on the surface over coal mines would be man-made, since mines were such large power consumers and/or located near industrialized areas. Though broadband atmospheric noise would probably play an important role, broadband noise levels produced on the surface by the mine equipment, and by poorly maintained rural high voltage power lines, were viewed as having a potentially greater influence at a local mine site, except in the case of local thunderstorms. More importantly, even less data were available on the in-mine noise environment for the design of downlink and in-mine systems.

b. NBS Mine Noise Measurements

Therefore, during this past year, NBS conducted a major noise measurement effort for the Bureau of Mines in an attempt to characterize in a practical manner the electromagnetic noise environment in and above several "representative" coal mines. Data has been taken at a 600 volt all DC coal mine; a coal mine with 300 VDC rail haulage and shuttle cars, and AC face machinery and belt haulage; a 300 volt DC longwall mine with AC haulage; and a hardrock AC mine with diesel haulage. The measurements encompass operating and quiet conditions for different machines, locations, power centers and boreholes, in working sections, haulageways and on the surface. Some of these noise data have already been processed and made available, with the remainder to become available within the next six months.

In-mine measurements have included wideband recordings from 100 Hz to 300 kHz of three magnetic field components, and of voltages on telephone lines, trolley lines, and roof bolts; from which noise power spectra are being generated. In addition, narrowband (2 kHz) spot frequency recordings were made at eight frequencies covering the 10 kHz to 32 MHz band, of three magnetic field components; from which noise amplitude probability distributions (APD's) are being generated. On the surface, only the components of magnetic field are required, but over a more restricted frequency range, because of the lower frequencies required for uplink systems. The surface wideband recordings for generating spectra cover 100 Hz to 10 kHz, while the narrowband spot frequency recordings for generating APD's cover four frequencies in the 10 kHz to 150 kHz band.

The preliminary results now available from these NBS noise measurements indicate that high levels of discrete frequency noise at harmonics of 60 Hz and 360 Hz predominate over broadband spectrum levels below about 10 kHz, both in

the mine and on the surface, with the broadband noise predominating above about 15 kHz, and the levels of both noise types decreasing with increasing frequency. Furthermore, the discrete frequency surface noise levels are highly correlated with in-mine levels below about 7 kHz, the degree of correlation falling off rapidly above 7 kHz. Noise levels also have a strong dependence on distance from power cables, and can vary over dynamic ranges in excess of 60 dB.

c. Whistler and Geomagnetic Data

A representative from Develco, Inc. stated that "mountains" of atmospheric noise data had been taken some years ago in the 1-30 kHz frequency band by Stanford Research Institute with regard to its whistler work. Though some of this data might possibly be useful for the under 5 kHz band of interest, he was also of the opinion that the data had not been analyzed in a form convenient to the uplink application, and that in any case, access to and subsequent understanding of this old data might involve much more difficulty than any potential benefits would justify.

A representative from University of Alberta claimed the presence of a minimum in the geomagnetic noise spectrum between 0.2-8 Hz, with 5 Hz perhaps being the most favorable frequency. Though there was some uncertainty regarding the level of this noise minimum among the Workshop participants, this claim should be checked out, since it might be worth considering for very deep mines. A book by Campbell and Matsushita was given as a reference.

d. Data Utilization

It was concluded that the NBS noise data taken to date at six coal mines and one hard rock mine, together with the planned NBS measurements at an all AC coal mine and another hard rock mine, when added to past atmospheric noise data taken below 10 kHz, should provide a substantial data base from which the design and optimization of mine communications systems can proceed in an orderly manner. Therefore, it was concluded that no new noise measurements over and above that already planned by NBS were required at this time.

In the under 5 kHz frequency band presently of interest to uplink data systems noise, power spectra and dubs of selected NBS tape recordings of the surface noise will be made available to system designers. Surface data up to 10 kHz will also be available if needed. The uplink system designers will need data on the levels of both discrete frequency and broadband noise components: broadband spectrum levels (and amplitude statistics if possible) for optimizing the coding, modulation, and receiver processing for narrowband data uplink; and discrete component levels for estimating likely levels of out-of-band interference, and ways to combat them by choice of operating frequencies and/or receiver signal processing techniques.

To better estimate these noise levels, particularly the broadband noise levels between discrete harmonic components, it was recommended that NBS provide expanded frequency scale spectra, covering only the 0-5 kHz band per spectrum plot, as opposed to the more compressed plots presently being prepared. Spectra for vertical and horizontal magnetic field components on the surface under both operational and "quieter" emergency conditions will be required. Note: these 0-5 kHz expanded spectra will be required not only for

the surface noise data, but also for the underground data for use in the design of call-alert and baseband-voice-downlink communications for mine sections. Though not discussed in the working group, amplitude statistics for the broad-band levels between harmonics may also be required.

For deep mine applications that may require operating frequencies in the vicinity of 100 Hz and below, the present NBS mine noise data down to 100 Hz and the LL atmospheric noise data down to about 3 Hz may be adequate for designing such systems. The need for additional noise measurements at these low frequencies should be carefully evaluated and justified before embarking on such a measurement program, because of the increased measurement difficulties encountered at these frequencies.

4. The Source - Message, Coding, Modulation, Operating Frequency.

The group agreed that firm conclusions regarding preferred techniques for coding, modulation, and operating frequency for a data uplink were premature, and could only be reached after a detailed overall systems analysis. Such an analysis would need to consider such things as the actual data message requirements, the bandwidth and power available, the transmission loss, characteristics of the noise, etc. Though the frequency band between 1-5 kHz is currently favored, based on past noise data, even this should be re-evaluated in the light of the new and more comprehensive NBS mine noise data.

The present WGL transmitters used for miner location utilize a CW signal that is simply keyed on and off with a ten to one duty cycle, to keep it simple, conserve cap lamp battery life, and to help distinguish it from adjacent power line harmonics. Operating frequencies are located between the harmonics of 60 Hz in the 1-3 kHz band. The present WGL uplink data system installed in the Bureau's experimental mine utilizes PCM/FSK to transmit the monitored data, and operates at select channel frequencies in the 3400 to 4500 Hz band, also placed between 60 Hz harmonics. The location transmitter is described in a Workshop paper, whereas the present experimental uplink data system is described in WGL reports. The specific results obtained with these systems should be reviewed as an aid to future designs.

As mentioned earlier, the data requirements and subsequent systems design have not yet been formulated for the uplink data system that will soon be developed for installation in an operating mine. This system design should benefit from the additional noise data and field experience now available.

5. The Receiver - Sensor, Demodulation/Decoding, Special Processing

As for the source, firm overall conclusions could not be reached, but several suggestions were made. An electrostatically shielded and balanced air core loop was recommended as a sensor. Notch filters were suggested to reduce interference from strong harmonics adjacent to the channel frequency.

The present WGL location receiver utilizes several stages of bandpass filtering to obtain a resultant bandwidth of 6 Hz. Notches as described above apparently have not yet been required at the mine sites visited to date. The present WGL uplink data system utilizes a phase-locked-loop FSK detector prior to decoding. Neither system was discussed.

Lastly, MIT Lincoln Laboratory (LL) has done extensive signal design and non-linear receiver processing work aimed at optimizing ELF secure narrow-band data communications (for the Navy Sanguine program) in the face of highly impulsive ELF atmospheric noise, and occasional discrete power line components. Reductions in required signal power of 10-20 dB have been reported, depending on the level of man-made discrete frequency interference, which apparently makes the techniques less effective. LL has been cooperative in the past by making its noise data and instrumentation information available to the Bureau and its contractors; and by recently offering suggestions regarding computer simulation of receiver design configurations for testing performance in the presence of environmental noise. This work should be reviewed to see if it can be applied to the mine problem in a practical and economic manner, particularly in those cases where transmitter power is at a premium and the noise environment severe. This work has recently been reported in the open literature, and more extensively in LL Technical Reports which are available from LL.

B. Downlink Voice System

1. Overview

a. Experience to Date

The objective of a downlink emergency voice system is to provide coverage of as large an area as possible to mobile miners during an emergency, in mines with nominal overburden characteristics of conductivity $\sigma = 10^{-2}$ mho/m and depths to 1,000 feet; and to do this with as few antennas on the surface as possible within practical limits. This being the case, the overburden transmission loss, the "quiet-mine" noise data available to date, and the greater space and power available on the surface, have favored direct transmission of 500-3,000 Hz baseband voice signals by means of grounded long wire antennas on the surface. Under relatively "quiet" emergency conditions, the present system designed by WGL with a transmitter capacity of 200 watts, has successfully transmitted intelligible voice messages to miners carrying simple manpack receivers to depths of about 1,000 feet. Mine overburdens of low conductivity will of course extend this usable range, while deeper or more conductive overburdens will quickly deteriorate performance or require significantly more power.

The success experienced under emergency conditions led to speculation that such a downlink voice system could have some beneficial operational applications as well, if the surface transmitter power and manpack receiver processing demands did not become excessive. However system performance was discovered to be even more dramatically affected by the in-mine operational noise environment than by the depth and conductivity. Namely, the noise levels severely deteriorated message intelligibility and usable range, demanding greatly increased power to maintain performance. This behavior is predicted by system analyses by both ADL and WGL, using early NBS and WGL in-mine noise data, and has been confirmed several times in operating mines by WGL. The deterioration occurs mainly because of the high levels of 60 Hz and 360 Hz harmonics produced by the mine machinery and DC power conversion equipment, and less often by the broadband impulsive noise near arcing trolleys, levels that can vary over a dynamic range in excess of 60 dB depending on location and machinery operating cycles. By applying simple corrective measures such as varying the orientation of the manpack receiver antenna for minimum noise pickup, which can be an operational incon-

venience, and by severely attenuating the large 360 Hz harmonic component by filtering in the manpack receiver, WGL was able to obtain some improvement in performance; but not enough to make it a dependable and practical system under mine operational conditions.

b. Future Developments

The above experience under operational conditions, when combined with the problems associated with gaining surface access rights over advancing coal mine sections (for the installation of long wire antennas, perhaps several thousand feet in length, or smaller loops, which have to be moved more often) make it very unlikely that the permanent surface installations required for operational applications will be a practical possibility in the near future. Thus in the near term, downlink voice will remain an emergency condition mobile system; thereby keeping the communication problem closer to the one originally treated by WGL, but with some added features.

The emphasis for future efforts on this system should probably be in the development of a reliable, compact, dual purpose receiver to be carried by a miner, preferably integrated into his helmet and operated from the cap lamp battery, as described by H. Parkinson in his paper. It will function as a downlink baseband voice receiver under emergency conditions, and as a call alert page receiver under operational conditions for key mining personnel, as mentioned in Section II. Though the present surface transmitter is apparently adequate to handle several emergency conditions, it too will probably need to be redesigned and optimized: for truly mobile utilization in the sense of being easily transportable by backpack or helicopter to the desired spots above the mine; for compatibility with the new dual purpose miner carried receivers to be developed; and for the mine emergency noise conditions likely to be prevailing. Since the downlink voice transmitter will have to be transported to and installed at selected locations above the mine after an emergency has occurred, the mine or section of interest will most likely be in a nearly power-down noise condition with only essential, lower-powered, electrical equipment such as pumps, fans, etc. in operation.

c. Deep Mines

The above applies to the nominal coal mine conditions specified. The deep hardrock mine situation is a vastly more difficult one as described in the uplink section, requiring frequencies down to 500 Hz and possibly 100 Hz and below even for narrowband data applications. Therefore, unless practical and economical techniques for dramatically compressing the bandwidth required for intelligible voice transmission become available, downlink voice to deep mines on the order of 10,000 feet will not be practically feasible under any noise conditions.

2. The Channel-Transmission Loss

a. Long Wire Antennas

Downlink communications to date have primarily utilized grounded, horizontal long wire source antennas on the surface, which reportedly give good coverage in the mine to a strip of width about equal to the depth of the mine under the wire, and sometimes wider, depending on the depth and available transmitter power. Antenna lengths have typically ranged from a low of about 1,500 feet up to greater than a mile, WGL field experience indicating that a length greater than about three times the mine depth being adequate to assume infinitely long wire behavior for the transmission loss. In the mine, the wire's magnetic field is primarily horizontal, with a gradually increasing vertical component as one moves away from the wire in a perpendicular direction; as opposed to the field of a surface loop which has primarily a vertical component. In those cases where the position of the miner or communication station is relatively well known and fixed, a large one turn loop, like that for the uplink, placed over the miner's position can offer a performance advantage as well as one of convenience, depending on the orientation of the miner's receive loop and the direction of the maximum noise component in the mine.

Grounding of the long-wire antenna has been accomplished by means of four or more ground rods at each end of the wire, with special care being taken to ensure good connections by the use of mud and copious amounts of rock salt. In this manner, total resistance values between about 50 and 100 ohms can be achieved for the long wire antenna; however, maintaining these values over long periods of time can sometimes be a problem.

To establish values of average overburden conductivity for estimating system operating ranges at different mine sites, the well established dipole-dipole measurement technique has been used extensively, and found to give results that agree reasonably well with system test results in most cases over coal mines.

The theoretical results of Wait and ITS, regarding the magnetic fields expected underground from infinitely long, insulated wire sources, placed on the surface of homogeneous and layered conducting overburdens, are well established and have been found to be generally in good agreement with experimental data obtained by WGL and CSM at several mine sites. Similar results have been obtained for surface loops. However WGL field experiences have also revealed a somewhat greater tendency for occasional experimental deviations, from predicted field strength values for the long wire antennas. A possible cause cited for this behavior was the presence of long conductors such as power cables, trolley wires, or rails in the mine, or large inhomogenieties in the overburden. This bears some further investigation.

A constant current assumption is used throughout these derivations. This has been shown to be valid for the frequencies of interest provided the conductors are insulated, which they are in practical applications of interest. The Navy experience in particular, with the huge Sanguine transmit antenna, provides good testimony to the validity of this constant current assumption.

ITS and Wait have also derived expressions and curves for the underground magnetic and electric fields produced by finite, grounded, insulated wire antennas on the surface of a homogeneous, unlayered half space, and for the converse situation of the surface fields from buried finite grounded wires. These cases are more closely related to actual field installations. Both analyses reveal that a finite grounded wire can be treated as an infinitesimal dipole when the observation distance, or depth, is more than about twice the cable length; and treated as an infinitely long wire when the observation distance is less than about one quarter of the cable length, this latter behavior having been experimentally observed at several mines by WGL. In between these depths neither approximation is good, the exact curves or analytical formulation being required. Examination of these curves also indicates only slight departure from infinitely long wire field values for distances up to half the length of the wire, and a reduction from infinite wire field values of only about 3 to 6 dB up to distances, or depths, equal to the length of the wire. The degree to which this behavior changes as the observation point moves toward and beyond the end of the wire was not discussed, but should be obtainable from the analysis. These results will be quite useful for determining minimum practical lengths for surface and underground antenna installations, and as a means for understanding observed experimental behavior.

It was concluded that no new theoretical derivations were needed for loops or infinitely long wire sources on the surface for downlink transmission loss, but as in the uplink case, appropriate practical curves, tables, nomographs, etc. be prepared based on the above results for homogeneous and layered overburdens. Similar curves, nomographs, etc. are needed of the magnetic and electric fields for the finite wire cases treated by ITS. As in the uplink case, curves should be included that depict the increase in signal loss with horizontal in-mine movement away from the long wire, finite wire, and loop positions on the surface, in order to determine in-mine coverage areas.

The effects of a layered overburden on the fields of finite grounded wires have not been treated yet. If it is concluded that layering is likely to influence the downlink field behavior in a significant manner, this case should also be treated by analysis and corresponding practical application curves produced. A summary assessment of the importance of layering to the fields produced by the other sources would also be desirable. Lastly, new and better ways of quickly making good, and long lasting, ground terminations in different ground covers should receive some attention.

b. Parasitic Structures

Long wire and loop antennas deployed on the surface are not as likely as in-mine installations to encounter parasitic structures in their immediate vicinity, unless they have to be deployed in and across the streets of a town, or perhaps directly over a gas pipe or under power lines in rural areas. In the first case the complexity of the parasitic structure configuration will probably defy analytical treatment, and what is perhaps more needed is a practical strategy for choice of antenna type and its deployment, based on present knowledge. In the second instance, Wait and ITS have examined cases of long wire sources parallel to buried conducting non-insulated cylinders.

These results should be examined for their potential application to the gas pipe structure. However, since the effects of such structures generally decrease with increasing distance and orientation angle, perhaps a practical solution to this potential problem is again a deployment strategy for minimum effect, when the presence of this conductor is known and flexibility in antenna deployment is available.

In the section and haulage ways at the receiving end of the downlink, metal structures in the vicinity of the man-carried receiving antennas may play a more important role in altering or providing a shielding effect to underground fields, and, may account for some of the lower than predicted levels experienced by WGL in a few instances. Prime suspects for these infrequently reported anomalies could be closed loops made by two or more vehicle trolley poles across the trolley-track transmission line, say in the vicinity of the section loading point, or steel mesh used for roof support in the entries of some mines. The effects of these structures should be estimated using approximate methods, to see if they, as opposed to large unknown conducting anomalies in the overburden, could account for the significantly reduced horizontal field strength levels observed.

3. The Channel-Noise

As concluded during the workshop and discussed in the downlink overview section, it can be assumed for the purpose of system design and optimization that the mine or mine sections will be in a non-operational, power-down, condition during the operation of the downlink emergency voice system. All major mining and haulage equipment will be turned off, only minor equipment such as pumps, fans, etc., may be left on.

The in-mine wideband noise recordings made by NBS should provide a more than adequate data base from which to optimize the design of the downlink baseband voice system. Expanded frequency-scale power spectra covering the 0-5 kHz band, and depicting discrete frequency and broadband noise levels of both horizontal and vertical components of the magnetic field intensity will be needed. Dubs of selected noise tape recordings are also desired for testing receiver processing techniques and overall system performance in the laboratory. Of particular interest will be data during quiet times and locations on the sections and haulageways, that characterize the emergency power down conditions. Consultation with Bureau of Mines and NBS staff will no doubt be helpful if not necessary in the selection of measurement conditions and data that typify this condition.

4. The Source-Message, Coding, Modulation, Operating Frequency

The source topic was given only brief treatment by the group. It was noted that performance calculations by ADL using early NBS and WGL mine noise data indicate that intelligible downlink baseband voice reception is possible to 1,000 feet in 10^{-2} mho/m overburdens, with under 50 watts of average power under low noise mine conditions. This kind of performance is supported by WGL experience in the field. Indeed, even as little as 5 watts may be required under some highly favorable non-operational conditions. (These reasonable average power requirements can climb to prohibitive levels above 10 kilowatts under operational conditions in DC mines.)

The emphasis for the downlink voice system has remained on the direct transmission of baseband voice signals through-the-earth, particularly under the relatively favorable emergency power-down noise condition. Under this condition, the high-level harmonics of 60 Hz, and particularly those of 360 Hz, will be greatly reduced. Updated performance and overall systems analysis calculations based on the more comprehensive mine noise data recently taken by NBS will help to verify (or deny) the desirability of this frequency band of operation, and better establish the required power levels. These noise data should also help identify transmitter signal conditioning techniques and receiver signal and/or noise processing techniques that can be used to reduce the power, size, and weight required for the mobile, emergency surface transmitter.

The use of pre-emphasized and/or clipped speech upon transmission were suggested for consideration as ways to reduce the peak power requirements of the transmitter, while sacrificing only little intelligibility for the same average speech power transmitted. Means of significantly reducing the bandwidth needed (by more than an order of magnitude) to transmit voice intelligibly have been claimed in the literature. Since such reductions would correspondingly reduce transmitter power, these reported methods should also be investigated.

An alternative method for improving mine communications was also recommended by the group as perhaps a long-term goal for the mining equipment suppliers. Namely, the effective suppression of electrical noise at its source in the equipment whenever practically possible, by means of improved designs and/or addition of special noise suppression equipment.

5. The Receiver-Sensor, Demodulation/Decoding, Special Processing

a. Downlink

As for the source, only brief consideration was given to this topic. A helmet mounted loop antenna design is desired, together with a similarly mounted compact dual-purpose receiver, as mentioned in the system description section. The call-alert function of the receiver will be discussed later.

Use of notch filtering to reduce the interfering effects of high-level harmonics of 60 Hz and 360 Hz, thereby reducing required transmitter power, was the principal suggestion. Such filters have been successfully applied in France, and reference material on these applications will be forwarded to the Bureau of Mines by representatives of the University of Lille. Dramatic improvements in voice reception in the face of harmonic interference have also been demonstrated by ADL in the laboratory, with a breadboard design of a simple electronic commutator-type filter that is particularly suited to rejecting harmonic signals. The French and ADL reported results should be reviewed, together with other reported notch filter work. They should be reviewed for their effectiveness against the mine emergency condition harmonic interference; and for their practical application to a compact helmet mounted receiver, should the measured harmonic levels warrant the use of notch filtering under emergency power-down conditions. In regard to this latter point, it may be necessary to evaluate the effect of pure or complex "tones" of noise,

such as those created by harmonics of 60 Hz and 360 Hz, on the intelligibility of received speech. The effect of direct audio noise in the mine environment (which will probably be low under emergency conditions) should also receive brief consideration along with that of the overall speech sound level to be delivered to the miner.

b. Uplink

Performance calculations, similar to those for the downlink discussed above have also been performed by ADL for a baseband voice uplink using a multiturn 100-foot periphery loop transmit antenna instead of a long wire. The results indicate that, except under the most favorable conditions of depth (300 feet) and the quietest of surface noise conditions, the levels of transmitter power, voltage, and current required are well in excess of those demanded by intrinsic safety, long operating life, and practical size and weight for an in-mine emergency unit. These uplink transmitter requirements for voice should be reconfirmed, along with those for the downlink voice system, in light of the more comprehensive NBS mine noise data now available and the larger in-mine loop antennas being considered. However, it appears that an uplink voice system that can operate from available emergency power will continue to remain impractical until an economic and practical way is found to significantly reduce the bandwidth required to transmit intelligible speech.

C. Sidelink Call Alert Coded Page System

1. Overview

The call alert system is a recent by-product of the success experienced with the experimental electromagnetic CW transmitter developed by WGL for locating miners trapped beneath overburdens of 10^{-2} mho/m conductivity to depths of 1,000 feet. As mentioned previously, the location transmitter is intrinsically safe, operates from a miner's 4-volt cap lamp battery into a one-turn loop placed in an entry or wrapped around a coal pillar, and generates a periodically interrupted CW signal in the 1-3 kHz band. This signal is detectable on the surface above the miner and is suitable for locating the miner's horizontal position. The development of this location transmitter has now progressed to where an improved preproduction prototype unit is being manufactured by Collins Radio Co. in limited quantities for testing in some operating mines.

Since the horizontal ranges desired for the call alert system described in section II are commensurate with the vertical ranges obtained for miner location, the Bureau is presently giving high priority to the development of a call alert page system centered around an adapted version of the WGL location transmitter. As presently conceived, this paging transmitter will be activated by means of a carrier signal sent over the mine phone line from the surface to the desired section. The call alert transmitter will be connected to a loop wrapped around a coal pillar, perhaps at the section loading point, and will transmit a single frequency tone (perhaps simply coded) to a compact, dual-purpose, helmet-mounted receiver worn by the individual being paged to the section's mine phone. Under low noise emergency conditions, this receiver will

be operable in a baseband voice mode for downlink message reception. Under high noise operational conditions, it will operate in a narrowband call alert mode, receiving a prearranged CW paging signal spaced between the strong 60 Hz harmonics usually present under these conditions.

A first generation experimental call alert system has been built from existing hardware by WGL, and installed in the Bureau's experimental mine to demonstrate concept feasibility in a non-operational environment. Though the operating frequencies of the present experimental unit are in the 1-3 kHz band, to take advantage of the frequencies available with the present location transmitter, an overall system analysis for an operational noise environment may reveal a more effective operating frequency.

Overall system requirements are presently being formulated by the Bureau. These will form the basis for subsequent systems analysis and optimization of designs that can be converted into practical, intrinsically-safe hardware for day-to-day use in operating mines.

2. The Channel-Transmission Loss

a. Loops

In-mine call alert paging is a sidelink application utilizing two essentially coplanar loops, while miner location is an uplink application utilizing two essentially coaxial loops. Examination of Wait's theoretical coupling curves for infinitesimal loops buried in homogeneous overburdens reveals that the operating range for a horizontal coplanar geometry is reduced by only about 20% over the range for a vertical coaxial geometry, for ranges in the vicinity of three skin depths. This operating range is reduced even less at greater distances. Vertical ranges in excess of 1,000 feet have been obtained with the location transmitter. At 2 kHz (the center of the 1-3 kHz operating band of the location transmitter), the three skin depth range is 1,100 feet, which gives rise to a potential sidelink operating range of 900 feet. This 900 foot range is in excess of the 400 to 800 foot range needed for call alert coverage of the typical 600 by 600 foot section mentioned in section II. The above range conclusions are, of course, based on equal noise conditions for each case. Since the noise environment will likely be more severe for the in-mine, operational, call alert application, its effect on operating range and transmitter/receiver design has to be determined.

At the under 5 kHz frequencies of present interest for the call alert system, the theoretical work of Wait/ITS has shown that the effects of layering (such as that found above and below coal seams) and air-filled cavities (such as tunnels in coal seams) should not be significant for loops, and therefore can largely be ignored for communications applications. Similarly, the infinitesimal loop theoretical results should be adequate for making performance predictions, particularly at the desired range limits, for mine sections free of parasitic influences. At ranges close to the loop installation, the infinitesimal loop results will tend to overestimate signal strengths somewhat. This discrepancy will become important primarily when treating potential coupling to nearby parasitic structures, as discussed below. Therefore, curves, tables, nomographs should be prepared for the vertical magnetic

field component in the plane of the transmit loop, based on the available theoretical results for coplanar infinitesimal loops. These can be used temporarily for making preliminary performance predictions until more information is forthcoming on the effects of the conductors prevalent in mine sections.

b. Parasitic Structures

Mine sections typically contain many conductors, such as trolley wires and rails, fixed and trailing power cables, roof bolts, and sometimes steel roof-supported mesh, that can affect the strength and orientation of magnetic fields. Therefore, a series of limited signal strength measurements should be conducted in operational mine sections, and in other mine locations that are relatively conductor-free. These simple experiments are needed; to verify whether the homogeneous-overburden coplanar loop results can be applied with confidence to operational sections, and to formulate practical design guides for operational sections. Preliminary results from field measurements taken by ADL in the Bureau's experimental mine indicate that significant departures from the theoretical results can in fact occur.

In parallel with the above field measurements, corresponding theoretical analyses are needed to predict the degree to which the direction and strength of the magnetic fields produced in the tunnels, by finite loops wrapped around coal pillars, will be affected by the above mentioned conductors in working sections of the mines. Of particular interest will be the effects caused by trailing and fixed power cables, roof bolts, and trolley wire/rail structures, which appear manageable analytically. The potential problems caused by heavy metal mesh occasionally used for roof support were acknowledged, but assigned a lower priority for analytical treatment, because of the infrequent use of this mesh and perceived analytical difficulties.

ITS has done some investigation of the currents induced in a thin, infinitely long, cylindrical conductor by a nearby infinitesimal loop transmitter. This work reportedly is easily extendable; to include the effects of the magnetic field produced by this induced current, and to include the effects produced by a finite loop source. The utility of this approach should be investigated, and pursued if found applicable.

ITS has also examined the influence of buried spherical and prolate spheroidal conducting objects on the fields produced by infinitesimal loop sources. Though originally done in connection with the miner location problem, the results can be applied to the call alert application, to estimate the likely field effects produced by machinery and shuttle cars. For the frequencies, sizes, geometries, and distances of interest, these objects will not significantly alter the magnitude of the fields, but mainly their direction somewhat in the immediate vicinity of the objects. No further investigations of this area were recommended.

c. Roof Bolts

If a finite wire terminated by roof bolts is shown to be a favorable transmit antenna for the roof bolt paging system, a suggestion was made that it also be considered for use in the call alert system.

3. The Channel-Noise

Since this is a narrowband operational system for mine sections, the in-mine wideband noise recordings made by NBS should provide an adequate data base. Of particular interest will be expanded frequency-scale power spectra showing levels of discrete and broadband noise covering the 0-5 kHz band; and representing data taken primarily on working sections in the vicinity of face machinery and power cables and conversion equipment, under representative operating conditions. Vertical field components of the noise will be more important for this application. Dubs of select recordings will also be desirable as mentioned previously. Although frequencies below 5 kHz are presently favored, data can and should be examined above 5 kHz for this system.

4,5. The Source and Receiver

Only little attention was devoted to this topic, with the group agreeing that a definition of system requirements and an overall system analysis were needed to identify the most favorable and practical system design approaches. However, a few brief comments were made.

The transmitted call alert signal could be a single tone, keyed on and off with a fixed duty cycle, as in the present experimental unit. For a single page signal per section, the simple, single tone system now used in the experimental unit could be adequate. For several pages addressable to different individuals per section, some means of coding the single tone, or use of multiple tones would be needed. The most favorable coding method from practical and noise immunity standpoints needs to be determined.

On the receiving end, it was noted that notch filters may be needed to minimize interference from 60 Hz harmonics adjacent to the signal frequency. The most practical and effective noise processing techniques suited to a compact, helmet-mounted receiver need to be determined.

As mentioned in section II, this system could conceivably share equipment with an uplink data station also located on the mine section.

D. Sidelink Roof Bolt Voice Page

1. Overview

The roof bolt voice paging system is a system conceived and recently developed by the Bureau for transmitting voice messages to key individuals carrying small pocket pagers on working sections under operational conditions. A prototype, using readily available commercial equipment, is presently installed in the Bureau's experimental mine to demonstrate its feasibility in a non-operational environment. The system concept developed as a result of some successful in-mine experiments performed by the Pittsburgh Mining and Safety Research Center; whereby a 20-watt trolley phone 88 kHz FM transmitter was connected to two roof bolts approximately 50 to 100 feet apart in an operating mine, and its voice transmission then received at distances up to about 600 feet away with a small pocket pager utilizing a ferrite loop stick antenna.

Limited field experience to date indicates that operating ranges commensurate with the 400 to 600 feet required to provide section coverage may be achievable, under operational conditions, with an operating frequency in the vicinity of 100 kHz. At this point in time a more quantitative understanding of the transmission loss and what affects it is needed; in order to determine the most favorable operating frequency, to develop practical guidelines for tailoring installations and estimating performance in different mines, and to eventually develop an improved system.

2. The Channel-Transmission Loss

a. Finite Wire Antennas Terminated by Roof Bolts

The finite wire antenna in this case is an insulated wire that runs along the roof of a tunnel and is terminated at each end by attachment to a roof bolt. Field experience to date has found the total termination impedance for such roof bolt pairs, separated by 50 to 200 feet, to fall in the range of 120 to 50 ohms resistive. Theoretical curves and supporting experimental data are needed, to adequately describe the behavior of the magnetic fields produced in the tunnels throughout a section in which such a finite wire transmitter is located.

The theoretical work of Wait and ITS on finite wire antennas buried in homogeneous overburdens, described in sections IIA2c and IIB2a, should be particularly useful in this regard and for estimating system coverage areas in mine sections. Though the present results are for the electric and magnetic fields produced on the surface from such buried antennas, ITS maintains that the desired field strengths in the coal seam tunnels can be easily obtained from its present buried-finite-wire analysis. This case of interest corresponds to receiver locations below, but in the immediate vicinity of, the plane of the finite wire.

Frequencies presently being investigated for this voice page application range from 10 kHz to 300 kHz, with present experimental systems operating around 100 kHz. Although the frequencies in the upper part of this band are higher than originally anticipated for buried finite wire applications, ITS believes that its present analysis should apply.

Therefore, it was concluded that the ITS theoretical analysis of the fields from buried finite wires should be used to determine the desired magnetic fields in the coal seam, in the 1-300 kHz band; and to prepare appropriate practical curves, tables, etc. for use by system designers. In addition, since the overburden is usually layered above and below coal seams, and since layers of varying conductivity can potentially influence the fields from finite wire antennas more than those from finite loops, a theoretical analysis to determine the effects of a simple, representative, layered model should be performed.

The non-conducting volumes created by the grid of tunnels in the coal seam were considered too difficult for exact analytical treatment at this stage; and in fact may not create significant effects on the magnetic fields in the tunnels, because the tunnels are relatively narrow and the currents can still flow without much alteration through the wider coal pillars.

Collins Radio and Spectra Associates are also reported to have performed theoretical analyses of the fields from buried wires, for the infinitely long and infinitesimally small cases. This work should also be reviewed, compared with the ITS results, and utilized if applicable.

Collins Radio has also conducted some limited measurements of the magnetic fields produced by 52 feet long, finite wire roof bolt antennas in an operating mine. Three field components were measured at three distances between 300 and 700 feet away from the finite wire, in both the broadside and axial directions, and at five frequencies in the 1-50 kHz band. Though these measurements do not fully characterize the expected transmission loss behavior, the data serve as a good starting point for comparisons with theory and establishing practical design guidelines. More measurements are needed, covering a greater range of distance, frequency, and roof bolt spacing, and particularly in mine working sections.

b. Parasitic Structures

As in the case of the call alert system, a roof bolt system installed in a working section can be expected to encounter many conducting parasitic structures that may alter the directions and magnitudes of the signal magnetic fields. These effects may even be magnified for finite wire systems operating at the higher frequencies anticipated. Indeed, some limited field measurements taken at 88 kHz by ADL, for a roof bolt antenna installation in the Bureau's experimental mine, indicate an extremely high variability in the levels of the measured vertical field component at comparable ranges from the roof bolt antenna. Therefore, and for the same reasons given for the call alert system, a similar experimental and theoretical effort is recommended to resolve the issues concerning the effects of parasitic conducting structures found in representative working sections of operating mines.

3. The Channel-Noise

Since the roof bolt system is a voice paging system for use under operational conditions, its operating frequency will most likely be above about 10 kHz, where the operational noise levels decrease to more tolerable levels. Present consideration is being focussed on the 10 kHz to 300 kHz band. The present experimental system operates at 88 and 100 kHz, but since these frequencies are already utilized by mine trolley wire carrier systems, alternative non-interfering frequencies are also desirable.

As for the other systems, the recently obtained NBS in-mine noise data should serve as a more than adequate data base for systems analysis and optimization in the 10 kHz to 300 kHz band. From the wideband tape recordings, power spectra for horizontal and vertical magnetic field components will be available, depicting discrete and broadband noise levels over the frequency range from 0-100 kHz and 0-300 kHz. In addition, noise amplitude probability distributions and rms levels will be available from the narrowband (2 kHz) spot frequency noise recordings, at eight frequencies over the 10 kHz to 32 MHz band, four of which fall below 300 kHz. Appropriate dubs of selected tape recordings for both types of noise measurement

should also be available. Detailed reports documenting these measurements and data will soon be published by NBS.

4,5. The Source and Receiver

The present experimental system is designed around a commercially available 20 watt, mine trolley wire phone transmitter that employs conventional FM modulation and an industrial pocket pager FM receiver that operate at a carrier frequency of either 88 or 100 kHz. Lack of time prevented discussion of the overall system by the group, but it was concluded that the degree to which this system can or should be optimized or otherwise improved with regard to performance, practicality, intrinsic safety, etc. will eventually be determined by the system requirements and a subsequent system analysis.

SUMMARY REPORT OF OPERATIONAL COMMUNICATIONS

WORKING GROUP

Martyn F. Roetter, Group Chairman
Arthur D. Little, Inc.

I. SUMMARY

The work of the operational communication systems' group dealt with a range of communication needs and functions within mines, primarily along haulageways, to and within sections up to the working face itself, and in mine shafts. A mixture of communication techniques and hardware is needed to satisfy this variety of communication needs within the differing environments encountered in U.S. mines. Substantial progress, both experimental and theoretical, has been made in recent years towards developing alternative communication systems suitable for use in mines which are based on "guided" waves, including wire-less (waveguide-like propagation in mine tunnels) and wire-based systems (leaky coaxial cables or wires). Major priorities identified for further work needed to confirm (or deny) the applicability, and refine the operational specifications of promising communication systems for mine use include:

Short-Term Projects

- o Cost/performance analyses of promising leaky coaxial cable and UHF radio communication systems which require further data from:

- Experimental investigation under U.S. mine conditions of the performance of potentially applicable leaky coaxial cable communication systems developed in Europe (France, Belgium, and the U.K).
- Cost estimates on these coaxial cable communication systems.
- Measurements of UHF radio propagation in low-coal mines.
- Investigation of the influence of obstacles (e.g. shuttle cars and section machinery) in the entries on UHF radio propagation in mines.

- o Investigation of the problems of transmitter and receiver coupling and termination matching associated with the two-way propagation of low frequency radio waves in hoist shafts.

Longer-Term Projects

i.e. of lesser urgency or where less information is currently available.

- o Investigation of techniques for coupling UHF radio to leaky coaxial cable communication systems.

- o Delineation of the role of, and needed interfaces for, operational communication capability related to emergency, paging and monitoring functions.

II. OPERATIONAL COMMUNICATIONS FUNCTIONS

The communication functions under discussion in this report are primarily:

- o Two-way communication along main haulageways up to 4-5 miles long, to vehicles and to maintenance personnel.

- o Two-way communication in sections up to working faces; all entries near the working face should be covered, but possibly only a limited proportion of those at or near main haulageways. Communication with roving personnel at up to 3,000 feet away from main haulageways must be established. More than one kind of working face must be dealt with, i.e. room and pillar (predominant in the U.S.) and longwall.

- o Two-way communication in mine hoist shafts (on the order of 10,000 feet long).

Two distinctive categories of communication are involved, the first depending upon a base station, and the other dealing with direct mobile-to-mobile communication.

Although not discussed in detail, it is recognized that the communication systems designed to fulfil these purposes may interface with other communication systems such as trolley phone, as well as play a role in assuring some emergency, paging (call alert), and one-way monitoring communication functions.

III. ENVIRONMENTAL CONSTRAINTS

The primary constraints recognized as affecting the communication systems under consideration are:

- o Daily utility of equipment
- o Intrinsic safety
- o Ruggedness and resistance to harsh mine environment
- o Available power
- o Weight and size limitations
- o Cost limitations

The electromagnetic noise environment at the frequencies typically proposed or employed (a few MHz up to 1 GHz) appears not to be a significant factor in determining communication system performance. A possible exception to this rule or slightly less clear-cut situation may prevail in the case of low frequency (LF) radio propagation proposed for communication in mine shafts (at frequencies of a few tens of kilohertz).

IV. OPERATIONAL COMMUNICATIONS SYSTEMS

Several alternative communication systems are in principle technically capable of satisfying the communication needs just described. A tentative conclusion in the light of our present state of knowledge is that communication along haulageways may be efficiently provided by one or more of the proposed leaky coaxial cable systems discussed later. However, leaky coaxial cable systems seem incapable of providing communications capability at more than 10 to 20 meters lateral distance from the cable. Thus in order to provide wide area communications coverage within the network of tunnels in a coal mine section, it would be necessary to string cables along most of them. The cost and practical obstacles to stringing all this cable in a continually changing section geography favor the application of UHF radio for wide area communications within a section. There is both theoretical and experimental evidence to indicate that UHF radio is capable of providing this function.

Coaxial cable, radio, and low frequency TEM radio wave transmission in the shaft are all potential candidates for providing communication in a mine shaft. No single one of these communication techniques has yet been identified as being especially advantageous in this application.

The communication techniques discussed fall under the general description of "guided" waves and comprise:

- o Wire-less (UHF frequencies)

- o Wire-based
 - Coaxial cable with periodic radiative structures (INIEX/Delogne)
 - Coaxial cable with high surface transfer impedance (braid outer conductor)
 - Coaxial cable with repeaters
 - Wire pairs
 - Single wire (including LF radio propagation in mine hoist shafts)

It is also recognized that power-line carrier communication techniques are potentially attractive for some of the communication applications under consideration; it is worthwhile to investigate power line carrier systems further, however, no serious evaluation of them was made in this workshop. Power line carrier systems are already used along the trolleyway in some mines.

In the following, promising communication systems are identified and their current state of development described. Problems and areas where additional data or further theoretical understanding are needed are listed, and priorities for future development work are suggested.

A. UHF Radio (U.S.)

1. State-of-the-Art

Marked progress has recently been made in understanding the characteristics and capabilities of UHF radio wave propagation along coal mine tunnels. Measurements taken in mines by Collins Radio indicate that effective communication can be provided throughout most of a typical U.S. coal mine section by UHF radio. A theoretical analysis carried out by Arthur D. Little, Inc. (ADL) staff based upon the hypothesis of waveguide propagation is in agreement with the Collins measurements in several important respects. The theoretical model is believed to reflect the basic structure of UHF radio wave propagation in coal mine tunnels, although it is presently not intended to give accurate signal loss estimates around corners when either the transmitter or receiver is near the corner (less than 50-100 feet). In those cases the model's loss asymptotes will over estimate the loss.

During the workshop an apparent violation of the reciprocity theorem was discovered in an application of the ADL theory to extend Collins Radio's data for a determination of the extent of coverage provided by UHF communication within a section. This apparent violation is believed to result from an application of the ADL model in a region where it is invalid, namely in the corner loss situation just mentioned. The reciprocity theorem must be respected, and a refinement of the model is needed to predict transmission loss around a corner when either the transmitter or receiver is nearby the corner. Collins Radio has re-evaluated the section coverage predicted for UHF radio which can be deduced from their data and extrapolated by the ADL theory, assuming the reciprocity theorem holds. The results of this computation are attached; they are very encouraging.

Leaky coaxial cable communication systems operating between 2-20 MHz appear incapable of providing communication along cross-cuts in which they are not strung, and hence appear both costly and unlikely of implementation for communication in the grid of many tunnels which constitute a section. UHF radio is likely to be more effective in this situation of areal rather than essentially linear or tubular communication coverage. In summary,

both theoretical and experimental results obtained to date warrant further development of UHF radio techniques for providing practical communications in coal mine sections.

2. Future Development Programs

(a) Short-Term

No measurements have yet been taken of UHF radio wave propagation in low-coal mines, which constitute a significant fraction of U.S. coal mining activity. These measurements are needed to determine if the different geometry of low-coal as against high-coal mine tunnels permits practical communication of UHF.

Additionally information is needed on the influence of obstacles in entries and tunnels on UHF radio wave propagation. In a coal mine "obstacles" such as section machinery and shuttle cars are inherently present. Some of these obstacles can block the major portion of an entry and may wipe out effective communication to various areas of the mine section as they move around. Multipath propagation effects may help in overcoming this problem; at any rate, data are urgently needed.

Less urgently, it would be revealing to obtain UHF propagation data of higher frequencies (above 1 GHz) where critical tests of the ADL theory, including the selection of the optimum operating frequency, would be possible. In practical terms these measurements are not, as already mentioned, of the highest urgency, as the use of a frequency above 1 GHz for mobile UHF radio is improbable since it would entail significantly more expensive (because non-standard equipment). Standard UHF frequencies for mobile communication are in the 450 MHz band, and the 960 MHz band soon to be opened by the FCC. It may additionally be noted that the FCC may not in any case approve non-standard UHF frequencies for underground mobile communication, even though in principle, use of non-standard frequencies is acceptable for underground use as long as no leakage to the surface occurs. The basis for this attitude may be explained by the ease with which mobile, as against fixed communications gear, may be taken out of the mine for personal use.

The Bureau of Mines should also delineate clearly the alternatives and practical considerations associated with the placing of the UHF transmitter (and possibly repeaters) to provide the best communication coverage within a section, taking account of its continually changing features.

(b) Long-Term

A future scenario may be envisaged in which a leaky coaxial cable communication system is in use along mine haulageways, whereas UHF radio provides communication up to working faces. In this situation the effective exploitation of all the advantages of these two communication techniques would be enhanced by the ability to couple them together. The techniques, costs, and performance of methods practicable to accomplish this coupling should be investigated.

B. Leaky Coaxial Cable Communication Systems (Europe)

1. State-of-the-Art

Three major classes of coaxial cable communication systems designed for use in mines have been reported as being in various stages of development in Europe.

(a) INIEX/Delogne system (Belgium) employing regularly spaced radiating devices.

Much experimental and theoretical investigation of this system has been performed including trials at the Bruceton, Pa. experimental mine of the USBM. The optimum operational frequency is believed to fall in the range of 2-20 MHz. Prototype installations are on order in Belgium, at a price of about \$2500/km. Firm production sales prices are not yet available. The INIEX/Delogne scheme appears potentially suitable for application in U.S. mines, although several uncertainties regarding performance/cost trade-offs in typical U.S. mine environments still have to be resolved, as discussed below. These uncertainties are connected in particular with the restraint in U.S. mines, in contrast to Europe, of having to install the cable close to the rib with consequent increases in attenuation, over a more central location in the tunnel, and with the influences on performance of dirt and water on the cable and on the radiative devices.

(b) Coaxial cable with high surface transfer impedance -- specially designed "leaky" braid outer conductor (France).

Theoretical investigations carried out at the University of Lille in France indicate that effective communication along several miles of mine haulageway may be achieved by use of a coaxial cable whose braid outer conductor is designed for "optimum" leakage of radiation. Experimental investigations of this scheme in a French mine are planned to be carried out in a few months' time. The optimum operational frequency is believed to be between 5-10 MHz.

Similar uncertainties exist with regard to the effects of dirt, water, and proximity to the walls of the tunnel on the performance of the proposed French scheme in U.S. mine environments, as were mentioned in the context of the Belgian cable system.

(c) Coaxial Cable with Repeaters (U.K.)

It has been reported that coaxial cable communication systems incorporating repeaters are being tested experimentally in the U.K. At this workshop little information on the cost and performance of this system was available. Additional uncertainties in the performance and cost evaluation of this system are introduced by questions associated with the reliability and maintainability of the repeaters that can realistically be expected in a mine environment.

2. Future Development Programs

(a) Short-Term

Progress achieved in Europe in the development of the coaxial cable communication systems mentioned above should be carefully and continually monitored and evaluated. In particular, cost estimates and further operating performance data should be obtained as soon as possible.

Nevertheless, European results, while valuable and to date encouraging, cannot be directly applied to the different environment of U.S. mines. In particular it appears impossible to install communication cables in U.S. mines in the locations recommended by European researchers. Specifically cables will have to be installed close to the ribs or walls of tunnels. Accordingly different attenuation rates, and correspondingly different optimum operating frequencies or trade-offs between the rate of "leakage" of power and total communication system length may prevail than in the European situation. Experimental investigations in U.S. mines with the proposed European coaxial cable systems are required before their applicability in this country can be definitively confirmed or denied, and if confirmed, operational specifications written (frequency, design of radiative structure or "leaky" outer conductor, and so forth).

(b) Long-Term

As was discussed in the section on UHF radio, techniques for coupling coaxial cable systems to UHF radio communication should be investigated.

C. Simple Wire Systems (Europe)

1. Wire Pairs

The technical feasibility of communication via waves propagated along wire pairs is well established, and the coupling between and characteristics of the unbalanced and balanced modes of propagation are well understood. However the sensitivity and lack of resistance of simple wire pairs to the deleterious effects of the mine environment (dirt, water, rough handling) tend to rule them out as practical implementations of in-mine communication systems.

2. Single Wire

A single wire communication system is impractical as a solution to a mines' operational communication needs along haulageways or in sections, although a similar type of communication system operating in the low frequency (LF) range holds promise for use in mine shafts.

D. Low Frequency Radio in a Hoist Shaft (U.S.)

1. State-of-the-Art

Theoretical investigations at ADL have analyzed the propagation of LF radio waves in deep (10,000 feet) hoist shafts in which the hoist cable is the only metal conductor present. Propagation losses of approximately 2dB over 10,000 feet at frequencies near 50 kHz have been computed. This is a very encouraging result.

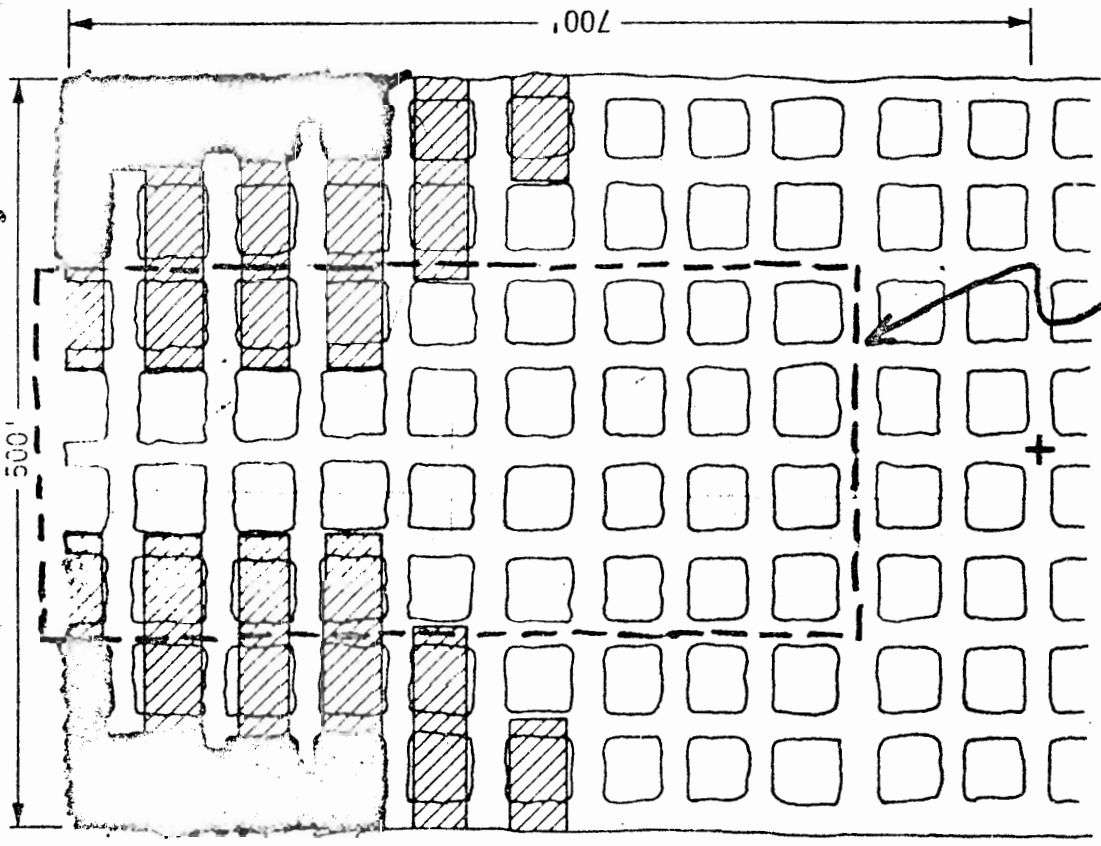
2. Future Development Programs

(a) Short-Term

Two difficulties with respect to LF propagation in hoist shafts have been identified. Firstly, the large penetration of the wave into the rock outer conductor may present a problem with regard to coupling the transmitter or receiver to the transmission line with a minimum of insertion loss. The amount of the insertion loss that can be tolerated has not yet been specified; it may be quite large, in view of the remarkably low transmission losses calculated. The coupling problem merits attention to determine, for example, how closely to the theoretical distribution of the vertical component of current density, in the fundamental propagation mode, should the actual driving current be distributed.

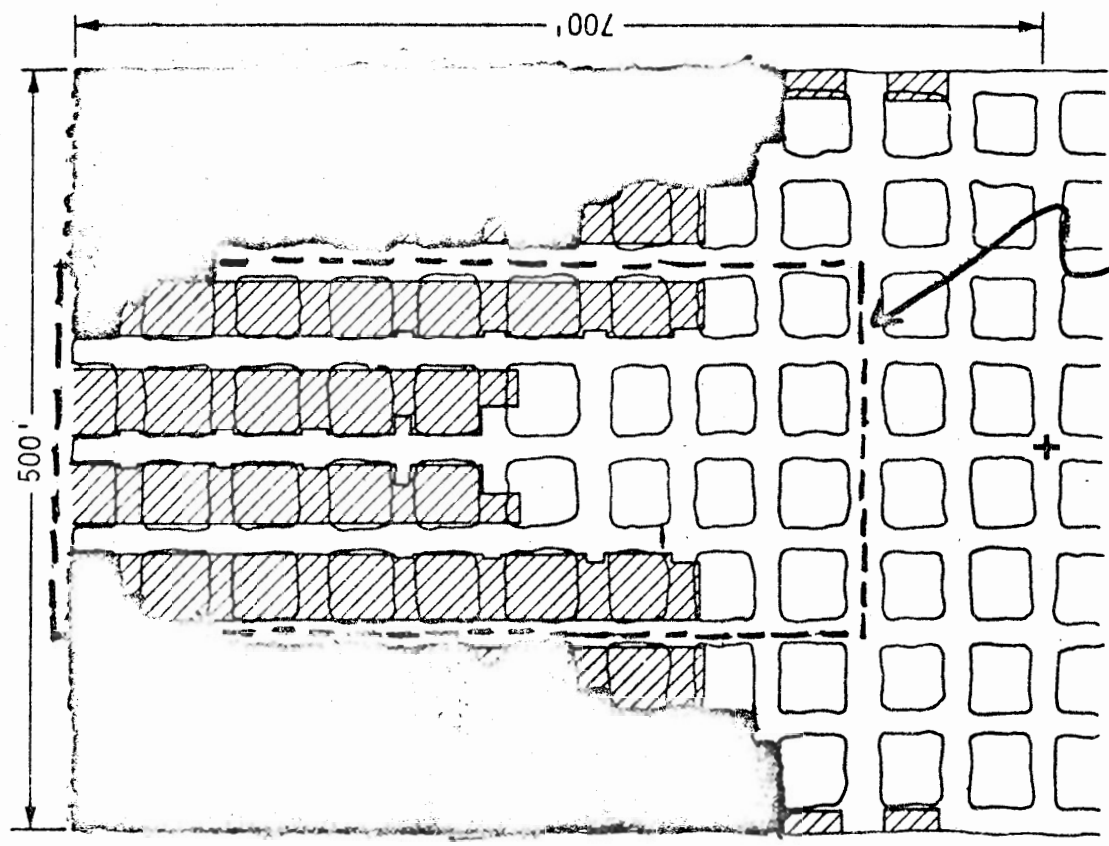
Secondly, in order to minimize reflections, both ends of the hoist cable-shaft transmission system must be terminated in approximately the characteristic impedance of the transmission line. Further work is needed to resolve the question of how, how well, and how expensively matching terminations may be provided.

DARK REGIONS INDICATE ARE NOT COVERED BY UHF RADIO (Ignore diagonal lines)



1000 MHZ
 20 W FIXED STATION PAGING
 HORIZONTAL POLARIZATION
 155 DB BASIC TRANSMISSION LOSS

REGION COVERED BY TEST DATA



1000 MHZ
 1 W PORTABLE TALK BACK
 HORIZONTAL POLARIZATION
 142 DB BASIC TRANSMISSION LOSS

REGION COVERED BY TEST DATA

PREDICTED COVERAGE OF MINE SECTION BY UHF RADIO

LIST OF ATTENDEES

Adams, John W.
NBS, 272 55 NBS
Boulder, Colo. 80302

Allen, J. W.
Westinghouse Georesearch
8401 Baseline Rd.
Boulder, Colo. 80302

Anderson, Dean T.
Collins Radio
5200 C. Ave., N.E.
Cedar Rapids, Iowa 52406

Badgley, Peter C.
Office of Naval Research
Code 410
Arlington, Virginia 22217

Ball, Larry
Westinghouse Georesearch Lab.
8401 Baseline Rd.
Boulder, Colo. 80302

Bannister, Peter R.
Naval Underwater Systems Center
New London, Conn. 06320

Bensema, W. D.
Nat. Bureau of Standards
Boulder, Colo. 80302

Binger, Kenneth B.
Collins Radio Co.
M.S. 107 153
Cedar Rapids, Iowa 52406

Bollen, Robert
Stanford Research Inst.
333 Ravenswood Ave.
Menlo, California 94025

Burr, John F.
Lee Eng. Consol.
200 Hidden Valley Rd.
McMurray, Pa. 15317

Caffey, Thurlow
Sandia Lab.
Box 5800
Albuquerque, New Mexico 87115

Degauque, Pierre
Electronics Dept.
University of LILLE - 59650
Villeneuve d'Ascq, France

Dobroski, Harry
U.S. Bureau of Mines
4800 Forbes Ave.
Pittsburgh, Pa. 15213

Dolphin, Lambert
Stanford Research Inst.
333 Ravenswood Ave.
Menlo Park, California 94025

Donaldson, Paul
Colo. School of Mines
40 Prospector Village
Golden, Colo. 80401

Dowling, Forrest L.
Office of Naval Research
536 S. Clark St.
Chicago, Illinois 60605

Emslie, A. G.
Arthur D. Little, Inc.
15 Acorn Park
Cambridge, Mass. 02140

Farstad, Arnold J.
Westinghouse Georesearch Lab.
8401 Baseline Rd.
Boulder, Colo. 80302

Fisher, Carl, Jr.
Westinghouse Georesearch Lab.
8401 Baseline Rd.
Boulder, Colo. 80302

Frischknecht, Frank C.
U.S. Geological Survey
Bldg. 25, Denver Federal Center
Denver, Colo. 80215

Gabillard, Robert
Electronics Dept.
University of LILLE - 59650
Villeneuve d'Ascq, France

Galbraith, Lee
Sandia Laboratory
Box 5800
Albuquerque, New Mexico 87115

Geyer, Richard G.
Consultant
3973 Baumberger Rd.
Stow, Ohio 44224

Gianzero, Stan
Schlumberger Research
Ridgefield, Conn.

Goddard, Arthur E.
Collins Radio Co.
M.S. 108 185
Cedar Rapids, Iowa 52406

Greenfield, Roy
Penn State University
University Park, Pa.

Halford, Donald
National Bureau of Standards
NBS 272.60
Boulder, Colo. 80302

Havener, Robert E.
Mine Safety Appliances Co.
Pittsburgh, Pa. 15213

Hill, David A.
Office of Telecommunications
Institute of Telecommunication Sciences
Boulder, Colo. 80302

Hooker, Vering E.
U.S. Bureau of Mines
Bldg. 20, Denver Federal Center
Denver, Colo. 80215

Howard, Allen Q., Jr.
U.S. Dept. of Commerce
Inst. of Telecommunication Sciences
Boulder, Colo. 80302

Humphreys, Larry D.
Sandia Laboratory
Box 969
Livermore, California 94550

Jones, F. W.
Univ. of Alberta
Dept. of Physics
Edmonton 7, Alberta
Canada

Kanda, M.
U.S. Dept. of Commerce
National Bureau of Standards
27260 NBS
Boulder, Colo. 80302

Lagace, Robert L.
Arthur D. Little Inc.
15 Acorn Park
Cambridge, Mass. 02140

Lewis, Richard L.
University of Colorado
6390 Jay Rd.
Boulder, Colorado 80302

Liegeois, Robert M.
INIEX
Rue Du Chera
B 4000, Liege
Belgium

Linfield, Robert F.
Westinghouse Georesearch Lab.
8401 Baseline Rd.
Boulder, Colo. 80302

Moffatt, David L.
ElectroScience Laboratory
Dept. of Electrical Engineering
Ohio State University
Columbus, Ohio 43212

Morgan, Robert R.
7805 W. Hampden Ave.
Denver, Colo. 80215

Murphy, John N.
U.S. Bureau of Mines
4800 Forbes Ave.
Pittsburgh, Pa. 15213

Murray, John C.
Colo. School of Mines
Rural Route Box 721A
Golden, Colo. 80401

Myers, Richard
U.S. Bureau of Mines
Bldg. 20, Denver Federal Center
Denver, Colo. 80215

Nasiatka, Thomas M.
U.S. Bureau of Mines
9472 Shouse Dr.
Vienna, Virginia 22180

Olsen, Robert G.
Westinghouse Georesearch Lab.
8401 Baseline Rd.
Boulder, Colo. 80302

Parra, Jorge O.
Colo. School of Mines
66 Prospector Village
Golden, Colorado 80401

Powell, James
U.S. Bureau of Mines
4800 Forbes Ave.
Pittsburgh, Pa. 15213

Rankin, David
University of Alberta
Dept. of Physics
Edmonton 7, Alberta
Canada

Roetter, Martyn F.
Arthur D. Little Inc.
15 Acorn Park
Cambridge, Mass. 02140

Ruskey, Frank
U.S. Bureau of Mines
Bldg. 20, Denver Federal Center
Denver, Colo. 80215

Sacks, Ken
U.S. Bureau of Mines
4800 Forbes Ave.
Pittsburgh, Pa. 15213

Smith, Robert L.
Develco
530 Logue Ave.
Mountain View, California 94040

Starkey, Donald B.
Sandia Laboratory
P. O. Box 969
Livermore, California 94550

Stout, William N.
Collins Radio Co.
5225 Cave N.E.
Cedar Rapids, Iowa 52406

Tibbetts, Benton
U.S. Bureau of Mines
Bldg. 20, Denver Federal Center
Denver, Colo. 80215

Tockey, Robert
Sandia Laboratory
Box 969
Livermore, California 94550

Utter, Stephen
U.S. Bureau of Mines
Bldg. 20, Denver Federal Center
Denver, Colo. 80215

Wait, James R.
U.S. Dept. of Commerce
NOAA
Inst. of Telecommunication Sciences
Boulder, Colo. 80302

Aldridge, M. Dayne
West Virginia University
Dept. of Electrical Eng.
Morgantown, West Virginia